DEVELOPING A PIV5-BASED RESPIRATORY SYNCYTIAL VIRUS VACCINE

by

SHANNON IRENE PHAN

(Under the Direction of Biao He)

ABSTRACT

Human respiratory syncytial virus (RSV) is the leading cause of severe respiratory disease and hospitalizations in infants and young children. It also causes significant morbidity and mortality in elderly and immunocompromised populations. Despite 50 years of effort, no licensed vaccine exists. Parainfluenza virus 5 (PIV5), a paramyxovirus that causes no known human illness, has been used as a platform for vector-based vaccine development. We hypothesized that PIV5 could be used as a vector to develop RSV vaccines. We generated vaccine candidates expressing either the fusion (F) or attachment (G) proteins of RSV and evaluated them in various pre-clinical animal models. When tested in rodents and nonhuman primates, the vaccines were safe, immunogenic, and protective against RSV infection. The vaccines were also stable after multiple passages *in vitro* and a single passage *in vivo*. We sought to improve on the original F-expressing candidate by modifying the PIV5 vector, by modifying the F antigen, or by changing the position of the F gene insertion in the PIV5 genome. We found that changing the position of the F gene insertion resulted in an improved vaccine candidate that was effective when administered intranasally or subcutaneously. These

results suggest that PIV5 presents an attractive platform for developing vector-based vaccines against RSV infection.

INDEX WORDS: Respiratory syncytial virus; Viral vectored vaccine; PIV5

DEVELOPING A PIV5-BASED RESPIRATORY SYNCYTIAL VIRUS VACCINE

by

SHANNON IRENE PHAN

BA, University of California, Berkeley, 2008

A Dissertation Submitted to the Graduate Faculty of The University of Georgia in Partial Fulfillment of the Requirements for the Degree

DOCTOR OF PHILOSOPHY

ATHENS, GEORGIA

2016

DEVELOPING A PIV5-BASED RESPIRATORY SYNCYTIAL VIRUS VACCINE

by

SHANNON IRENE PHAN

Major Professor:	Biao He
Committee:	Kaori Sakamoto
	Vincent J. Starai
	Michael N. Teng
	Ralph A. Tripp

Electronic Version Approved:

Suzanne Barbour
Dean of the Graduate School
The University of Georgia
August 2016

ACKNOWLEDGEMENTS

I would like to thank my major advisor, Biao He, my committee, my family, and friends for all of their support throughout my graduate career. I would not have been able to do it without you. A piece of my Ph.D. belongs to each of you.

TABLE OF CONTENTS

APPENDICES

LIST OF TABLES

Page

LIST OF FIGURES

Page

CHAPTER 1

INTRODUCTION

Human respiratory syncytial virus is the leading cause of pediatric respiratory infection and hospitalizations (1). Since re-infection with RSV can occur throughout life, it is also a significant cause of morbidity and mortality in aged and immune-compromised populations (2). Despite efforts over the last several decades, no licensed vaccine exists. Parainfluenza virus 5 (PIV5) has been used in our lab to develop several vaccine candidates against a variety of pathogens. PIV5 has shown to be a promising vector, as it is safe, efficacious, and is able to overcome pre-existing host immunity (3–9). Therefore, the long-term goal of our studies is to develop a potential vaccine candidate against RSV using PIV5 as a vector. The fusion (RSV-F) and attachment (RSV-G) proteins of RSV are known to play important roles in inducing protective immune responses against RSV infection (10, 11). Therefore, we hypothesize that using PIV5 to express RSV-F or RSV-G will enable us to generate a safe and efficacious vaccine candidate. The rationale for these studies is that successful completion will not only help advance the field of RSV vaccine research, but the results will also further our understanding of the immune responses elicited by PIV5 when used as a vector. We will examine the following specific aims:

Specific aim 1: To develop vaccine candidates against human RSV using parainfluenza virus 5 (PIV5) as a vector to express RSV surface glycoproteins. The working hypothesis is that PIV5-expressing RSV-F or RSV-G will be able to elicit RSV

antigen-specific humoral responses and provide protection against RSV infection in various animal models.

***Specific aim 1a*:** To evaluate the efficacies of PIV5 expressing RSV-F or RSV-G as vaccines to prevent RSV infection in mice.

***Specific aim 1b*:** To evaluate the efficacies of the above vaccines in cotton rats, a more relevant model for RSV vaccine evaluation.

***Specific aim 1c*:** To examine the replication and evaluate the efficacies of the above vaccines in RSV-experienced and RSV-naïve non-human primates.

Specific aim 1d: To determine the sequence stability of the vaccine candidates *in vitro* and *in vivo*. In light of earlier studies involving the serial passage of PIV5 expressing EGFP, the working hypothesis is that the PIV5 expressing RSV-F or RSV-G will remain stable through *in vitro* and *in vivo* passage.

Specific aim 2: To improve the rPIV5-RSV-F vaccine candidate by engineering RSV-F to be more immunogenic and/or by modifying the PIV5 vector to enhance RSV-F presentation. The working hypothesis is that deleting the SH gene from the PIV5 backbone and/or expressing pre-fusion mutants of RSV-F will improve the current vaccine candidate by enhancing apoptosis and by eliciting highly neutralizing antibodies, respectively (6, 12, 13).

References

1. **Nair H**, **Nokes DJ**, **Gessner BD**, **Dherani M**, **Madhi S a.**, **Singleton RJ**, **O'Brien KL**, **Roca A**, **Wright PF**, **Bruce N**, **Chandran A**, **Theodoratou E**, **Sutanto A**, **Sedyaningsih ER**, **Ngama M**, **Munywoki PK**, **Kartasasmita C**, **Simões EA**, **Rudan I**, **Weber MW**, **Campbell H**. 2010. Global burden of acute lower respiratory infections due to respiratory syncytial virus in young children: a systematic review and meta-analysis. Lancet **375**:1545–1555.

2. **Falsey AR**, **Hennessey PA**, **Formica MA**, **Cox C**, **Walsh EE**. 2005. Respiratory syncytial virus infection in elderly and high-risk adults. N. Engl. J. Med. **352**:1749–59.

3. **Tompkins SM**, **Lin Y**, **Leser GP**, **Kramer KA**, **Haas DL**, **Howerth EW**, **Xu J**, **Kennett MJ**, **Durbin RK**, **Durbin JE**, **Tripp R**, **Lamb RA**, **He B**. 2007. Recombinant parainfluenza virus 5 (PIV5) expressing the influenza A virus hemagglutinin provides immunity in mice to influenza A virus challenge. Virology **362**:139–50.

4. **Mooney A**, **Li Z**, **Gabbard JD**, **He B**, **Tompkins SM**. 2012. Recombinant PIV5 vaccine encoding the influenza hemagglutinin protects against H5N1 highly pathogenic avian influenza virus infection when delivered intranasally or intramuscularly. J. Virol. **Epub ahead of print**.

5. **Li Z**, **Mooney AJ**, **Gabbard JD**, **Gao X**, **Xu P**, **Place RJ**, **Hogan RJ**, **Tompkins SM**, **He B**. 2013. Recombinant Parainfluenza Virus 5 Expressing Hemagglutinin of Influenza A Virus H5N1 Protected Mice against Lethal Highly Pathogenic Avian Influenza Virus H5N1 Challenge. J. Virol., 2012/10/19 ed. **87**:354–362.

6. **Li Z**, **Gabbard JD**, **Mooney A**, **Chen Z**, **Tompkins SM**, **He B**. 2013. Efficacy of parainfluenza virus 5 mutants expressing hemagglutinin from H5N1 influenza A virus in mice. J. Virol. **87**:9604–9.

7. **Li Z**, **Gabbard J**, **Johnson S**, **Dlugolenski D**, **Phan S**, **Tompkins M**, **He B**. 2015. Efficacy of a parainfluenza virus 5 (PIV5)-based H7N9 vaccine in mice and guinea pigs: antibody titer towards HA was not a good indicator for protection. PLoS One In Press.

8. **Chen Z**, **Zhou M**, **Gao X**, **Zhang G**, **Ren G**, **Gnanadurai CW**, **Fu ZF**, **He B**. 2012. A novel rabies vaccine based on a recombinant parainfluenza virus 5 expressing rabies virus glycoprotein. J. Virol., 2012/12/28 ed.

9. **Chen Z**, **Xu P**, **Salyards GW**, **Harvey SB**, **Rada B**, **Fu ZF**, **He B**. 2012. Evaluating a PIV5-based vaccine in a host with pre-existing immunity against PIV5. PLoS One **In Press**.

10. **Connors M**, **Collins PL**, **Firestone CY**, **Murphy BR**. 1991. Respiratory syncytial virus (RSV) F, G, M2 (22K), and N proteins each induce resistance to RSV

challenge, but resistance induced by M2 and N proteins is relatively short-lived. J. Virol. **65**:1634–1637.

11. **Connors M**, **Kulkarni a B**, **Firestone CY**, **Holmes KL**, **Morse HC**, **Sotnikov a V**, **Murphy BR**. 1992. Pulmonary histopathology induced by respiratory syncytial virus (RSV) challenge of formalin-inactivated RSV-immunized BALB/c mice is abrogated by depletion of $CD4^+$ T cells. J. Virol. **66**:7444–51.

12. **Lin Y**, **Bright AC**, **Rothermel TA**, **He B**. 2003. Induction of apoptosis by paramyxovirus simian virus 5 lacking a small hydrophobic gene. J. Virol. **77**:3371–83.

13. **McLellan JS**, **Chen M**, **Joyce MG**, **Sastry M**, **Stewart-Jones GBE**, **Yang Y**, **Zhang B**, **Chen L**, **Srivatsan S**, **Zheng A**, **Zhou T**, **Graepel KW**, **Kumar A**, **Moin S**, **Boyington JC**, **Chuang G-Y**, **Soto C**, **Baxa U**, **Bakker AQ**, **Spits H**, **Beaumont T**, **Zheng Z**, **Xia N**, **Ko S-Y**, **Todd J-P**, **Rao S**, **Graham BS**, **Kwong PD**. 2013. Structure-based design of a fusion glycoprotein vaccine for respiratory syncytial virus. Science **342**:592–8.

CHAPTER 2

LITERATURE REVIEW

RSV Classification and History

Human RSV (RSV) is an enveloped, non-segmented negative-sense RNA virus with a genome of approximately 15,200 nucleotides. It belongs to the order *Mononegavirales,* family *Paramyxoviridae,* subfamily *Pneumovirinae,* and genus *Pneumovirus*. RSV is a prototypical Pneumovirus that has counterparts that infect other animal species (e.g. bovine RSV (bRSV), ovine RSV (oRSV) and pneumovirus of rodents that infect other animal species (1). RSV was first isolated in 1956 from a colony of chimpanzees with coryza and identified as chimpanzee coryza agent (2). That same year, the virus was recovered from two children, one with pneumonia and the other with croup (3, 4). The virus was renamed respiratory syncytial virus due to its ability to promote the formation of syncytia in infected tissue culture cells (3). Etiological studies performed during the 1960s demonstrated a prominent association between lower respiratory tract illness and isolation of RSV from affected children, providing evidence that RSV is a major cause of childhood respiratory disease (4–9). Studies of RSV infection among seropositive children and adults showed that symptoms of re-infection are generally milder, but that primary infection fails to provide long-lasting immunity (8–10).

RSV strains are subdivided into two distinct antigenic groups, A and B. Early *in vitro* neutralization studies showed that monoclonal antibodies raised against the F, G,

and N proteins of RSV Long, A2, and CH-18537 strains demonstrated virus-binding patterns that could be categorized into three groups, two of which were similar (11). Mufson et al. developed antibodies against the F, G, M, N, and P proteins of the Long strain and found that they reacted with different clinical isolates in two distinct patterns, leading to the designation of A and B subgroups. The RSV Long and A2 strains belong to subgroup A, while CH-18537 belongs to subgroup B. The variation between the A and B subgroups were attributed to differences in the G protein (12). Johnson et al. determined the nucleotide and amino acid sequences of G mRNAs from the Long and CH-18537 strains and compared them to the A2 strain. The Long and A2 strains share 94% amino acid identity, while CH-18537 only shares 53% amino acid identity with A2 (13). Further sequencing studies of the variable region of G of clinical isolates revealed distinct clades, designated GA1 to GA5 for group A and GA1 to GA7 for group B (14). Subsequent studies identified two additional clades for the A subgroup (15). Studies associating disease severity with different subgroups have yielded conflicting results. Some groups have reported that subgroup A viruses cause more severe RSV disease, while others have reported that there is no correlation between subgroup and disease severity (16–18).

RSV Virion Structure and Morphology

The RSV virion structure is pleomorphic when propagated in cell lines (19–21). Cryo-electron tomography has shown the presence of three virus morphologies: spherical, filamentous, and asymmetric (20, 21). The spheres range from 100 nm to 1 μm in diameter. The filaments are 70-190 nm wide and up to 10 μm in length (20, 22).

Filtration studies have shown that the filamentous viral particles are the predominant infectious form of RSV (19).

Inside the particle, the single-stranded RNA (ssRNA) genome is encapsidated within the nucleocapsid. The nucleocapsid associates with proteins that comprise the RNA-dependent RNA polymerase (RdRp). The viral envelope surrounds these components and contains glycoproteins that protrude from the virus surface. The matrix layer lines the interior of the viral envelope, providing structure to the particle (1).

RSV Genome and Proteins

The RSV genome contains 10 genes in the following order: (3') NS1-NS2-N-P-M-SH-F-G-M2-L (5') (23). These genes encode 11 proteins, with M2 encoding the proteins M2-1 and M2-2 (24). Nonstructural proteins 1 and 2 (NS1 and NS2) are involved in suppressing host type I and type III interferon (IFN) responses and promoting anti-apoptotic pathways in the cell (25–29). The nucleoprotein (N) encapsidates the RNA genome and protects it from degradation by host proteins. N, along with the phosphoprotein (P) and large polymerase (L) protein, form the minimum unit required for RNA replication (23). M2-1 is a processivity factor that prevents the premature termination of RNA transcription (30, 31). M2-2 is involved in switching RNA synthesis between transcription and replication (24). The M (matrix) protein lines the inside of the virus envelope and is important in virus packaging and budding. The F glycoprotein mediates fusion between the viral membrane and the host cell, as well fusion between the membranes of infected cells. Unlike other paramyxoviruses, expression of F alone is sufficient to mediate fusion and does not require the involvement of G, the attachment protein (32). G is the heavily glycosylated surface protein involved in virus attachment

to host cells. It contains two hypervariable mucin-like regions that are poorly conserved between different virus strains. It also has a conserved central region that contains a CX3C motif, which plays a role in cytokine mimicry and immune evasion (33). The short hydrophobic (SH) protein has viroporin-like properties and is able to downregulate apoptosis as well as TNF-α signaling (34, 35).

RSV Entry and Replication Cycle

RSV attachment to the host cell is mediated by both G and F (36). Following attachment, the virus has been shown to enter the cell by multiple mechanisms. Srinivaskamur et al. found that RSV fused directly with the target membrane, much like other paramyxoviruses (37). However, studies by Kolokoltsov et al. showed RSV entered via clathrin-mediated endocytosis (38). San-Juan-Vergara et al. demonstrated RSV entry by a two-step mechanism in which hemifusion occurs at cholesterol-rich plasma membrane domains followed by endocytosis and fusion in endosomes (39). A more recent study by Krzyzaniak et al. showed RSV is internalized by macropinosomes and penetrates the cell prior to fusion with endolysosomal compartments (40). The precise mechanism of RSV entry remains unclear.

Following entry, the processes of RSV gene expression and genome replication are similar to those of other non-segmented negative-strand RNA viruses (41). The genome is transcribed by the RdRp to generate capped, methylated, and polyadenylated subgenomic mRNAs. These mRNAs are translated by host cell machinery to produce the viral proteins. The genome is also transcribed to produce the positive-sense antigenomic RNA, which is used as the template for producing more negative-sense, genomic RNA. The RdRp initiates transcription and replication at promoter sequences located at the 3’

ends of the genomic and antigenomic RNAs. The leader (Le) sequence at the 3' end of the genomic RNA controls the initiation of mRNA transcription. The trailer (Tr) sequence at the 3' end of the controls synthesis of the antigenome (42). Once a sufficient amount of viral genome and proteins have been produced, the genome is packaged into the virion and buds out of the cell in a process largely coordinated by M.

PIV5 Classification and History

Parainfluenza virus 5 (PIV5) is a member of the order *Mononegavirales*, family *Paramyxoviridae*, subfamily *Paramyxovirinae,* and genus *Rubulavirus* (1). It was first discovered in 1956 as a contaminant in rhesus monkey primary kidney cell cultures and named simian virus 5 (SV5) (43). However, later epidemiological studies suggested that SV5 was not of simian origin. Wild-caught monkeys with no evidence of SV5 exposure seroconverted in captivity, suggesting that infection occurred during transit or through human contact (44–46). There was also evidence that SV5 naturally infects humans (46, 47). However, these results have been confounded by the possibility that SV5 could have been a contaminant in the cells used for virus isolation. Furthermore, since SV5-specific antibodies cross-react with those of other paramyxoviruses viruses in hemadsorption assays, early serological tests of SV5 immune status may not be reliable (48, 49). However, with data strongly suggesting that SV5 was of non-simian origin, the name was changed to PIV5 in 2009 (1).

No human disease has been reliably attributed to PIV5 infection. Goswami et al. reported the presence of antibodies against PIV5 in the cerebrospinal fluid (CSF) of multiple sclerosis (MS) patients, suggesting a possible link between the virus and the disease (50). This link was later dismissed. Vankdvik and Norrby were unable to

confirm that PIV5 was a major immunogen in the CSF of MS patients and attributed Goswami et al.'s findings to cross-reacting antibodies against other paramyxoviruses (51). Furthermore, antibodies against PIV5 have been detected in the CSF of patients with a variety of neurological disorders, showing that it is not likely the etiological agent of MS (52). Cohn et al. found that both MS patients and healthy individuals had positive proliferative T-cell responses to PIV5, further confirming that the virus does not cause MS (53). The results from this study also suggest that the human population has been widely exposed to PIV5 with no apparent disease.

PIV5 has also been isolated from a variety of other animals. It has been associated with kennel cough in dogs, but experimental infection of dogs with PIV5 does not cause kennel cough (54–56). PIV5 has been found in cows, cats, hamsters, and pigs, but the host range of the virus is still unclear (43, 44, 46, 57).

PIV5 Genome Organization and Proteins

The PIV5 genome contains 7 genes that encode 8 proteins. The genes follow the order: (3') NP-P/V-M-F-SH-HN-L (5'). NP encapsidates the RNA genome and forms a helical nucleocapsid structure that protects the genome from degradation by cellular nucleases. The P mRNA is generated from the P/V gene by the insertion of two nontemplated guanine residues into the transcript via RNA editing. The P protein does not have enzymatic activity, but serves as a cofactor for the viral polymerase to regulate transcription and replication. NP, P, and L (large polymerase protein) together form the RdRp (1). Faithful transcription of the P/V gene results in expression of the V protein, which plays an important role in counteracting the host antiviral responses (58). The matrix (M) protein coordinates the viral budding process and provides structure to the

virion. The fusion protein (F), hemagglutinin-neuraminidase protein (HN), and small hydrophobic protein (SH) are envelope proteins. F is a surface glycoprotein that mediates the fusion of viral and host cell membranes. HN mediates attachment via sialic acid receptors on the cell surface and also cleaves them, preventing virus aggregation at the cell membrane during budding. HN also activates F to promote membrane fusion (1). The small hydrophobic protein (SH) has anti-apoptotic activity, and deleting SH from PIV5 induces apoptosis in L929 cells through a TNF-α-dependent extrinsic mechanism (59).

PIV5 as a Vaccine Vector

Development of a reverse genetics system for PIV5 has enabled researchers to engineer it to express foreign genes and use it as a vector for vaccines. Given the anti-PIV5 immunity in humans, anti-vector immunity may be a problem. Our recent studies indicate that pre-existing immunity to PIV5 does not negatively affect immunogenicity of a PIV5-based vaccine in dogs, demonstrating that pre-existing anti-PIV5 immunity is not a concern for using PIV5 as a vector (60). This result is consistent with the report that neutralizing antibodies against PIV5 do not prevent PIV5 infection in mice (61). The genome structure of PIV5 is also stable, in contrast to positive strand RNA viruses such as poliovirus (62). Recombinant PIV5 expressing GFP has been generated, and the GFP gene was maintained for more than 10 generations (the duration of the experiment) (63). PIV5 can be grown to $8x10^8$ PFU/ml, demonstrating its potential as a cost-effective, safe vaccine vector that is amenable to mass production.

PIV5 has been used as a platform for developing vector-based vaccines against other viruses. A single-dose immunization of PIV5 expressing the rabies virus

glycoprotein G protects mice against lethal rabies virus challenge (64). Additionally, a single-dose inoculation of as little as 10^3 PFU of PIV5 expressing H5 hemagglutinin (HA) protects against lethal H5N1 challenge in mice (65). Also, PIV5 expressing the NP protein of influenza virus (PIV5-NP) provides broad protection against different subtypes of influenza viruses (66). Immunization with PIV5-NP is more efficacious than immunization with either adenovirus (AdV) or vaccinia virus (VV)-based vectors expressing NP. In the best result reported to date, a single inoculation of 10^{10} virus particles of replication-deficient AdV-NP conferred only 80% protection of mice from lethal H1N1 challenge and the mice lost close to 30% of body weight (67). There is no report of a successful single inoculation of AdV-NP against H5N1 challenge in mice. MVA, a modified vaccinia virus-Ankara strain containing a deletion in the late genes, has been used extensively as a vaccine vector. However, MVA expressing NP did not provide immunity against lethal influenza virus challenge (68). Together, these results demonstrate that PIV5 has the potential to be an effective vaccine vector. Importantly, intranasal administration of PIV5 is effective for eliciting robust mucosal immune responses (65), and thus ideal for vaccinating against respiratory pathogens.

RSV Transmission and Symptoms

RSV is spread by large droplet or fomite transmission. The onset of illness typically occurs three to five days after infection. Primary infection is usually symptomatic, with upper respiratory symptoms including coughing, sneezing, sore throat, rhinorrhea, and nasal congestion. These symptoms can be accompanied by fever and otitis media. RSV infection can also cause lower respiratory tract illness, such as bronchiolitis and pneumonia. Wheezing may be present during acute infection, and

airway hyperreactivity may be observed later in life. Symptoms of repeat infection are generally milder than those observed during primary infection (23).

RSV Pathogenesis

Disease associated with RSV infection is due to a combination of damage caused by the virus as well as the host immune response. Tissue culture models of RSV infection have demonstrated that the virus is not especially cytopathic, as it does not cause widespread tissue destruction (69, 70). Infection is generally restricted to the ciliated superficial cells of the respiratory tract (69). Pathologic changes include necrosis of ciliated cells, influx of inflammatory cells, and excessive mucus production. The accumulation of cell debris, inflammatory infiltrates, and mucus obstructs the bronchioles and alveoli. In patients with pneumonia, the interalveolar walls thicken and the alveoli fill with fluid. Interestingly, syncytia formation *in vivo* has only been observed on occasion (23).

In humans, RSV infection triggers the infiltration of many immune cells, with neutrophils being the most abundant cell type (71). The neutrophil response precedes the peak $CD8^+$ T-cell response (which occurs during convalescence), suggesting that some of the disease caused during acute infection is possibly neutrophil-mediated (72). However, studies in murine models have demonstrated the involvement of both $CD8^+$ and $CD4^+$ T-cells in both viral clearance and disease. In depletion studies of T lymphocytes in mice, Graham et al. observed a dominant role of $CD8^+$ T-cells in contributing to disease (73). However, in light of the results from the Lukens et al. study, the role of $CD8^+$ T-cells in pathogenesis is unclear. Th2 biasing of the $CD4^+$ T-cell response is also thought to contribute to disease, as Th2-like immune responses lead to increased mucus production

and wheezing, hallmarks of RSV infection. Furthermore, a positive correlation has been observed between increased IL-4 production and RSV disease severity (74). Despite this evidence, there have been mixed reports of Th1 and Th2-biased immune responses in infants with severe RSV infection. Furthermore, since neonates are born with a Th2 bias, it is possible that the Th2 response is due to the status of the infant immune system, and not the virus (75).

RSV Immunobiology

RSV innate immunity

Toll-like receptors. Innate immunity is important in eliciting the early defense against RSV infection. RSV possesses pathogen-associated molecular patterns (PAMPs) that are recognized by pattern recognition receptors (PRRs). RSV is known to stimulate Toll-like receptors (TLRs), RIG-I-like receptors (RLRs), and nucleotide oligomerization domain (NOD)-like receptors (NLRs) on immune cells and in tissues.

TLR2 is expressed on the surface of immune cells as a heterodimer in complex with TLR1 or TLR6. TLR2 typically recognizes lipoproteins and lipoteichoic acid from bacteria but can also be stimulated by RSV (76, 77). RSV infection triggers TLR2/6 signaling on leukocytes and induces the production of TNF-α, IL-6, CCL2, and CCL5. It also promotes neutrophil trafficking and dendritic cell activation in the lung. Mice deficient in TLR2 or TLR6 are less able to control RSV replication, indicating that these TLRs play an important role in innate immunity against RSV.

TLR3 is an intracellular receptor that recognizes double-stranded (dsRNA) (76). While RSV is a single-stranded RNA virus, dsRNA intermediates are formed during its replication cycle (78). Following stimulation, TLR3 signals through TRIF to induce the

activation of NF-κB and the production of type I IFNs (76). Groskreutz et al. found that RSV infection of A549 cells and primary human tracheobronchial epithelial cells increased TLR3 and protein kinase R (PKR) expression, leading to NF-κB activation and IL-8 production. Interestingly, TLR3 expression was only detectable on the cell surface following RSV infection, sensitizing cells to repeat dsRNA exposure. These results suggest a possible mechanism for airway hyperresponsiveness that is observed in RSV patients after infection. TLR3 expression during RSV infection is also important for IP-10/CXCL10 and CCL5 production, two chemokines that have been previously reported to correlate with disease severity (78).

TLR4, a surface receptor essential for lipopolysaccharide (LPS) recognition, is also known to play a role in RSV recognition (76, 79). RSV interacts with TLR4, with CD14 acting as a co-receptor, and activates NF-κB *in vivo* (79, 80). The early innate response occurs independent of virus replication shortly after infection and is dependent on TLR4 activation. The later response requires virus replication but is TLR4-independent (80). TLR4 signaling is important for RSV immunity, as TLR4-deficient mice have reduced NK cell and $CD4^+$ T-cell recruitment to the lung during RSV infection. These mice also demonstrate reduced NK cell function, decreased IL-12 production, and delayed viral clearance (81). TLR4/CD14 signaling is also important for the production of the pro-inflammatory cytokines IL-6 and IL-8 in epithelial cells (82).

The clinical significance of TLR4 signaling in humans is unclear. Awomoyi et al. reported that polymorphisms (SNPs) encoding N299G or T399I substitutions in the TLR4 ectodomain correlate with symptomatic RSV infection in high-risk infants. These substitutions have been previously associated with decreased TLR4 responsiveness and

increased susceptibility to bacterial infections (83). Conversely, increased TLR4 expression on blood monocytes isolated from infants has been linked with increased RSV disease severity (84). Still, other groups have reported that there is no correlation between TLR4 expression and RSV disease (85, 86). Thus, while RSV interacts with TLR4 to trigger innate immune responses, the clinical significance of the interaction is unclear.

TLR7, an endosomal TLR that detects ssRNA, is also known to play a role in innate immunity against RSV. Stimulation of TLR7 leads to the production of type I IFNs and inflammatory cytokines (87). RSV infection in TLR7-deficient mice results in increased inflammation and mucus production. These mice also have increased levels of IL-4, IL-13, and IL-17, and their dendritic cells display reduced IL-12 production and increased IL-23 production. These results suggest that TLR7 is important for RSV immunity, and its absence leads to a dysregulated Th17-like T-cell response that leads to enhanced mucus production.

Rig-I-like receptors. Retinoic acid-inducible gene I-like receptors (RLRs) are a family of cytoplasmic RNA helicases that detect viral RNA (88). RIG-I is one member of this family known to be important in RSV innate immunity. RSV infection of A549 cells stimulates RIG-I signaling within 12 hours and activates the NF-κB and IRF-3 pathways, leading to the early production of IFN-β, IP-10/CXCL10, CCL5, and ISG15. RIG-I signaling also regulates TLR3 induction through the production of IFN-β (89). The viral protein NS2 is able to inhibit both the RIG-I and TLR3 pathways. NS2 binds to the N-terminus of the caspase activation and recruitment (CARD) domain of RIG-I, inhibiting its interaction with the downstream effector, mitochondrial antiviral signaling

protein (MAVS). This blocks the activation of NF-κB and IRF-3, and the subsequent production of type I IFNs and inflammatory cytokines (88).

RSV adaptive immunity

Immunity against RSV infection is mostly attributed to neutralizing antibodies. The F and G proteins are the major viral antigens capable of eliciting the production of neutralizing antibodies (90, 91). Animal studies involving passive transfer of serum antibodies or the administration of monoclonal antibodies have demonstrated protective roles against RSV infection (92–94). Studies in humans have shown an inverse correlation between neutralizing antibody titers and risk of infection (95). Furthermore, the administration of the commercial monoclonal antibody, Synagis (palivizumab), is used to prevent severe infection in high risk populations, such as premature infants (96). Since serum antibodies enter the respiratory tract by passive transudation, a relatively high level of serum neutralizing antibodies is required to confer protection (approximately 1:380 for a 99% reduction in virus in the lower respiratory tract and 1:3500 in the upper respiratory tract based on the cotton rat model) (94). Secretory IgA is also known to play a protective role against RSV infection, but the protection is not as long-lived (97, 98).

While antibodies are important for preventing infection, T-cell responses to RSV are important for viral clearance. Murine studies have shown that both $CD4^+$ and $CD8^+$ T-cells responses are required for complete viral clearance (73). $CD8^+$ T-cells recruited to the site of infection secrete cytokines and induce lysis of infected cells. IFN-γ has been shown to be particularly important, as the adoptive transfer of $CD8^+$ T-cells deficient in IFN- γ production fail to protect against RSV challenge (99). The secretion

of perforin and granzymes, or the upregulation of Fas ligand induce the apoptosis of infected target cells. The role of T-cells in protection against RSV is especially apparent in individuals with T-cell deficiencies, as they experience prolonged virus shedding (100). However, as was previously discussed, both of these T-cell subsets, while protective, have also been implicated as contributors to RSV disease.

At-Risk Populations

It has been previously mentioned that the major at-risk populations for RSV infection are infants, the elderly, and the immunocompromised. These groups have immunological differences that have implications for developing vaccine candidates.

Infants

Infants are at risk for infection due to immunological immaturity, as well as inherent differences in immunity due to the transition from the *in utero* environment to the outside. Infants have dampened innate immune responses. For example, neonatal neutrophils have impaired chemotactic and killing capabilities. Antigen-presenting cells (APCs) also display impaired chemotaxis, phagocytic function, and expression of co-stimulatory molecules. Infants tend to produce different cytokine profiles in response to infection compared with adults, which may be a consequence of biased TLR stimulation. They have reduced production of pro-inflammatory cytokines, such as TNF-α, IL-12, and IFN-γ, in response to LPS. Their production of IL-10, IL-6, and IL-23 tends to be higher than in adults. This bias from Th1-type cytokines towards Th2/Th17-type cytokines is thought to contribute to disease susceptibility, but may be necessary for survival *in utero* (101).

In terms of adaptive immunity, $CD4^+$ T-cell responses in infants tend to be lower and more Th2-biased. This pattern along with sub-optimal APC function contribute to sub-optimal $CD8^+$ T-cell responses. Humoral responses after primary infection tend to be lower in magnitude and short-lived, but get boosted with repeat exposure to RSV, suggesting immunological immaturity. B-cells in infants express lower levels of CD40, CD80, and CD86 costimulatory molecules, making them less responsive to signals from other immune cells. Low expression of CD21 supports the production of memory B-cells but suppresses the development of antibody-producing plasma cells, therefore suppressing antibody production (102). Maternal antibodies transferred through the placenta provide immune protection but wane within the first three months of life. Maternal antibodies can also suppress primary antibody responses in the infant (103). All of these factors together (blunted innate and adaptive responses, along with Th2-biasing) enhance infant susceptibility to RSV infection.

Immunocompromised

Depending on nature of their underlying condition, immunocompromised individuals are more susceptible to RSV infection for many reasons. HIV-positive patients have impaired virus clearance due to T-cell deficiency and can shed virus for months, whereas healthy individuals shed virus for a few weeks. Hematopoietic stem cell transplant patients are most susceptible to RSV infection, especially prior to engraftment, because their immune systems have been globally depleted. Organ transplant patients are not just susceptible to RSV infection due to immunosuppressive therapy, but RSV infection has also been associated with organ rejection (23). In patients with chronic

obstructive pulmonary disorder (COPD), RSV infection and the resulting inflammation can exacerbate COPD symptoms and further impair breathing (104).

Elderly

Elderly adults are a particularly high-risk population due to immune senescence. Similar to infants, aged adults have defects in innate immunity. Neutrophil chemotaxis and killing capabilities are impaired. Dendritic cells have reduced phagocytic capabilities as well. Whereas infants have normal TLR expression levels but defects in TLR stimulation, elderly individuals have decreased TLR expression and function. These defects in innate immunity impact the first-line response to RSV infection.

Reduced T-cell function is a hallmark of immune senescence. Cytotoxic T-cell function is diminished. Long-lived $CD4^+$ T-cells in the peripheral compartment develop defects in forming immunological synapses, T-cell receptor signaling, and proliferation. These defects result in reduced B-cell help and antibody production. With aging also comes a shift from Th1 to Th2-type responses. Th17 responses are also upregulated in response to increased production of IL-6. Serum IgG levels against RSV seem to remain relatively stable even with aging. Thus, elderly individuals are more likely to have trouble clearing RSV infection due to reduced T-cell function (15).

Target Groups for Vaccination

Target groups for vaccination can be divided into four categories: children less than six months old, children more than six months old, elderly adults, and pregnant women. Each group has different underlying immunological factors and vaccination goals that need to be achieved.

Children less than six months of age should be vaccinated with the goal of preventing serious complications caused by RSV infection. These children comprise the most susceptible population and have the highest hospitalization rates of any of the target groups (105). Vaccinating this group is particularly challenging because the presence of maternal antibodies can suppress the infant's immune response to vaccination (103, 106). Factors associated with immunological immaturity will also impact vaccine efficacy (75). Lastly, since many of these children have not yet been primed with live RSV infection, they are at risk for vaccine-induced enhanced disease. The best vaccines for this group will be live attenuated vaccines or live vectored vaccines.

Children who are more than six months old are less likely to have serious RSV-associated complications than younger infants, but they should still be vaccinated with the purpose of preventing serious complications and reducing RSV transmission to close contacts. These infants will still be immunologically immature, but maternal antibodies levels should wane significantly by six months of age (103). Like younger infants, the best vaccination approach for this group is likely live attenuated or vectored vaccines.

Vaccinating pregnant women or women of childbearing age is another viable strategy to protect infants from RSV infection. It has been shown that newborns with higher maternal antibody titers are less likely to develop serious RSV disease, and children become more susceptible as maternal antibody levels wane (107). Vaccinating mothers will boost antibody titers and increase passive protection to the fetus. Ideally, these passive antibodies will protect the newborns until they are immunologically more mature and can mount better immune responses to vaccination. Pregnant women and women of childbearing age will likely have pre-existing antibodies against RSV, so the

ideal vaccine candidate should safely boost these antibodies to high enough levels to protect the fetus. Subunit vaccines will likely be the best vaccination strategy for this population.

Elderly individuals should be vaccinated because there is significant RSV-associated morbidity and mortality in this population. The goal of vaccinating this group is to prevent serious respiratory complications and to reduce transmission. Elderly individuals have pre-existing antibodies against RSV and have complicating factors associated with immune senescence. Therefore, these individuals should be immunized with either live vectored vaccines or with adjuvanted subunit vaccines to boost neutralizing antibody titers.

Vaccine Antigens

Fusion protein

The respiratory syncytial virus fusion protein (RSV-F) is a surface glycoprotein that mediates virus-cell fusion and cell-cell fusion. It is incorporated into the viral particle and is expressed on the surface of infected cells upon infection. RSV-F is a type I transmembrane protein that is synthesized as the inactive precursor F0. F0 is glycosylated as it passes through the Golgi network and is then proteolytically cleaved by furin-like proteases before being presented on the cell surface as disulfide-linked F1 and F2 subunits. Cleavage of F0 releases a 27-amino acid peptide called pep27 that has tachykinin activity and is believed to be immunomodulatory (108).

RSV-F exists in a meta-stable, pre-fusion conformation on the virion surface and on the surface of infected cells. Triggering events induce dramatic structural rearrangements, in which the hydrophobic fusion peptide inserts into the target

membrane, and the protein folds into a highly stable, post-fusion conformation. The energy released during this process is believed to drive the fusion of the two opposing membranes (109).

Since RSV-F exists in multiple conformations, the exposed antigenic sites differ depending on the protein conformation. Studies using monoclonal antibodies against RSV-F have enabled researchers to identify several distinct antigenic sites. Sites I and IV exist on the post-fusion conformation and are associated with neutralizing activity (110–112). Site II is also exposed on both the pre-fusion and post-fusion conformations, and is the target of the highly neutralizing antibodies, palivizumab and motavizumab (113, 114). Recent studies have shown that the most potent neutralizing antibodies are directed against antigenic site φ, which exists on the pre-fusion conformation of F (115–117). These discoveries have spurred interest in developing RSV structure-based vaccines and therapeutics.

Attachment protein

The major glycoprotein of RSV (RSV-G) is a heavily glycosylated surface glycoprotein that mediates virus attachment to the host cell. It is a type II transmembrane protein that also has a secreted form that is translated from an alternative start codon in the N-terminus of the open reading frame (1). RSV-G is not required for RSV replication, but the RSVΔG virus exhibits growth defects in HEp-2 cells and *in vivo*. *In vitro*, RSV-G attaches to glycosaminoglycans (GAGs) on the cell surface, but likely uses other receptors *in vivo* (33, 118). The protein has two mucin-like hypervariable regions that flank a central conserved region. The central conserved region contains a cysteine-rich CX3C motif that binds CX3CR1 receptors on leukocytes and mimics fractalkine

(33). This chemokine mimicry reduces leukocyte trafficking in the mouse lung, leading to dampened innate and adaptive immune responses (119). RSV-G also interacts with the C-type lectin, DC-SIGN, but DC-SIGN is not a functional receptor. RSV-G binding to DC-SIGN decreases dendritic cell activation via ERK1/ERK2-mediated pathways (120). Antibodies against RSV-G do not efficiently neutralize virus infectivity, but can inhibit RSV-G-host interactions and block the immunomodulatory effects.

Small hydrophobic protein

The small hydrophobic protein of RSV (SH) has also been examined as a vaccine antigen. RSV-SH is a weakly immunogenic viral surface antigen that has a pentameric structure with putative viroporin function. It is not required for RSV replication. It is believed that antibodies against SH are non-neutralizing but can mediate protection against RSV infection through an antibody-dependent cellular cytotoxic (ADCC) or an antibody-dependent cellular phagocytic (ADCP) mechanism (121).

Vaccine History

Formalin-inactivated RSV vaccine

In the 1960s, a formalin-inactivated, alum-precipitated RSV vaccine (FI-RSV) was developed and tested in children. The vaccine regimen consisted of three immunizations. During the following RSV season, the vaccine not only failed to protect against RSV infection, but it also enhanced disease in many of the vaccinees. Of the 31 infants vaccinated, 25 children required hospitalization and two died. In contrast, only one child out of 40 in the control group required hospitalization (122). Incidence of enhanced disease diminished as children grew older, but was observed in vaccinees up to 37 months old at the time of vaccination (123).

Examination of lung tissue from the children who died showed extensive pulmonary inflammation. Airways were also obstructed with epithelial cell debris and cellular infiltrates consisting of mononuclear cells, neutrophils, and eosinophils. Fibrin deposition was also observed. However, these signs of enhanced disease were complicated by the fact that these children also had bacterial co-infections (124). There have been several proposed immune mechanisms explaining why enhanced disease occurred in the FI-RSV-vaccinated children.

Poorly neutralizing antibodies fail to neutralize virus and facilitate the formation of immune complexes, potentiating disease. One possible factor was that the process of formalin-inactivation altered the immunogenic epitopes of RSV F and G, eliciting the production of antibodies that bound viral antigen, but were non-neutralizing. Cotton rats immunized with FI-RSV developed enhanced disease upon RSV challenge, and despite developing high F and G-specific antibody titers measured by ELISA, their neutralizing antibody levels were 1/20th of those of cotton rats who were infected with RSV. It was believed that formalin was responsible for enhancing disease, as live virus or virus heated in the absence of formalin did not potentiate disease in cotton rats (125). Similarly, examination of sera from infants enrolled in the FI-RSV vaccine trial showed that those who received the FI-RSV developed high antibody titers when measured by ELISA, but these antibodies were less neutralizing than the antibodies of infants who were infected with RSV (126, 127). Poorly neutralizing antibodies fail to protect against RSV infection, and high levels of non-neutralizing antibodies have been associated with the deposition of immune complexes and disease potentiation (128).

Poor TLR stimulation leads to aberrant affinity maturation. The antigen disruption mechanism does not explain how cotton rats immunized with purified protein have been reported to show signs of enhanced disease (129). Another potential mechanism for FI vaccine failure was that poor TLR stimulation led to poor B-cell activation, which in turn led to the production of antibodies with low avidity for RSV. While low avidity antibody responses may be sufficient for protection against some viruses, it seems as though protection against RSV requires the production of high-avidity antibodies. RSV infection stimulates the engagement of TLRs 2, 3, 4, and 7, while non-replicating, UV-inactivated RSV only weakly stimulates a subset of these TLRs, such as TLR4. Delgado et al. found that the production of high-avidity antibodies against RSV requires sufficient TLR activation and B-cell activation. Exogenous TLR agonists boost TLR stimulation and can help non-replicating vaccines enhance the production of high-avidity antibodies (130). Thus, the production of poorly neutralizing antibodies can be attributed to poor TLR stimulation in addition to antigen disruption by formalin treatment.

Aberrant $CD4^+$, $CD8^+$, and Treg T-cell responses lead to enhanced disease. T-cell responses against RSV infection are important in virus clearance. However, vaccine-enhanced disease upon challenge has been attributed to aberrant T-cell responses, as antibodies alone are not sufficient to cause this effect (129). FI-RSV-immunized mice show reduced pulmonary lesions when depleted of $CD4^+$ T-cells prior to challenge, suggesting that $CD4^+$ T-cell responses contribute to enhanced disease. FI-RSV-immunized mice also have low levels of cytotoxic T-cells compared to RSV-infected mice, demonstrating that FI-RSV vaccination also skews $CD8^+$ T-cell responses

(131). This is further reinforced by studies in which priming a $CD8^+$ T cell response in FI-RSV-vaccinated mice abrogates pulmonary eosinophilia after RSV challenge (132). Increased infiltration of $CD4^+$ T-cells into the lung and impaired recruitment of Treg cells has also been attributed to enhanced disease. Compared to RSV-infected mice, FI-RSV-vaccinated mice have a significant increase in $CD4^+$ T-cell infiltration accompanied by low numbers of Treg cells upon challenge. Supplementing these mice with the chemokine ligands CCL17 and CCL22 recruits airway Tregs and helps reduce CD+ T-cell recruitment, as well as weight loss associated with enhanced disease (133).

Addition of carbonyl groups on proteins boost Th2 responses. Enhanced disease induced by FI-RSV vaccination has been associated with enhanced IL-4, IL-5, and IL-13 production and tissue eosinophilia, all characteristics of a poorly-protective, Th2-biased immune response (134–136). The association between FI vaccine candidates and enhanced disease is not unique to RSV, as the effect has also been observed with FI measles virus (MeV), human parainfluenza virus 3 (HPIV3), and human metapneumovirus (HMPV) (137–139). Moghaddam et al. have proposed a mechanism in which the addition of reactive carbonyl groups to proteins through formalin treatment induces a Th2-biased immune response upon immunization. In their study, they re-created the FI-RSV vaccine candidate used in the human trials and either reduced it with $NaBH_3CN$ or left it unreduced. Mice that received unreduced FI-RSV developed increased disease and weight loss upon RSV challenge, accompanied by elevated levels of IL-5 and IgG1 antibodies, all signatures of Th2 responses and vaccine-enhanced disease. Mice that received the reduced formulation did not show any of these signs

(140). Thus, it is possible that the carbonyl modifications on antigens are responsible for biasing the immune response towards a Th2 response.

In the years since the FI-RSV vaccine trial, a number of RSV vaccine candidates have been developed using various approaches, as described below.

Live attenuated vaccine candidates

A live attenuated vaccine candidate, cpts248/404, was generated by cold passaging RSV in tissue culture and performing chemical mutagenesis (141). It was immunogenic and well-tolerated in children six months of age and older, but under-attenuated and poorly immunogenic in one to two-month-old infants. These infants experienced upper respiratory infections and rises in serum and mucosal IgA, but no increase in neutralizing antibody titers (142).

The development of a reverse genetics system for RSV allowed groups to engineer live attenuated candidates with defined mutations, short passage histories, and increased genetic stability. The candidate rcp248/404/1030ΔSH was developed to further attenuate cpts248/404. The growth of this candidate was 10 times more restricted in seronegative children and well-tolerated in one to two-month-old infants. However, it was only moderately immunogenic. Furthermore, recovery of rcp248/404/1030ΔSH isolates from vaccinees showed phenotypic instability. Over 33% of the isolates had a one to two degree increase in temperature sensitivity, which was associated with the loss of the 248 or 1030 mutations (143).

MEDI-559 was a stabilized version of rcp248/404/1030ΔSH that contained changes in the codon encoding the 248 mutation to decrease the chance of reversion to the wild-type sequence. This candidate underwent phase I/II clinical trials in which it

was tested in five to 23-month-old infants. MEDI-559 was highly immunogenic with a 95% seroresponse rate, but there was an increased number of medically-attended lower respiratory tract infections in vaccinees (144). Another version of MEDI-559 was developed in order to further improve genetic stability and delete the NS2 gene to reduce type I IFN antagonism. The RSVΔNS2Δ1313I1314L candidate had similar replication levels in chimpanzees compared to MED-559 and is being prepared for testing in clinical trials (145–147).

The most recently tested live attenuated RSV candidate is ΔM2-2, which contains a deletion of most of the M2-2 open reading frame. The M2-2 protein acts as a switch between mRNA synthesis during early infection and genomic RNA synthesis later in the cycle. This mutant exhibits decreased genomic RNA replication, but increased mRNA transcription and increased antigen production (24). When tested in seronegative chimpanzees, ΔM2-2 was highly restricted in the upper respiratory tract and undetectable in the lower respiratory tract. Serum neutralizing antibody titers were slightly lower than those induced by wild-type RSV infection, but the animals were still protected against RSV challenge (148). The candidate has also been tested in healthy adults, seropositive children, and seronegative children. Healthy adults and seropositive children did not shed the vaccine virus, suggesting that it is highly attenuated in these groups. Seronegative children shed the vaccine virus, but shedding was more restricted when compared to rcp248/404/1030/ΔSH. There was a 95% seroresponse rate in seronegative vaccinees and no evidence of increased illness. During the following RSV season, 30% of the seronegative vaccinees had increases in serum neutralizing antibody titers without

medically attended respiratory illness, suggesting that vaccination with ΔM2-2 induced a memory response upon infection with circulating RSV (149).

Live attenuated RSV vaccine candidates have the advantage of containing all or most of the RSV antigens to elicit broad humoral and cell-mediated immune responses. A major hurdle of developing these vaccine candidates is striking a balance between attenuation, immunogenicity, and stability. Furthermore, use of these candidates is largely limited to seronegative populations, as RSV-experienced groups have antibodies that neutralize the vaccine. Similarly, maternally-derived antibodies in infants pose a problem because these antibodies can also neutralize live-attenuated vaccines. Despite this, several candidates have been developed and tested in clinical trials with promising results.

Vectored vaccine candidates

Vectored RSV vaccines have the advantage of expressing defined RSV antigens in replicating systems while avoiding challenges associated with residual RSV pathogenicity. Vectors are also able to induce immunity in a manner that is distinct from wild-type RSV infection, which only confers short-lived protection. Ideally, vectored vaccines can be used in RSV seropositive as well as seronegative populations because the vector should be safe but still robustly express RSV antigens in the human host.

Vesicular stomatitis virus-based candidates. Vesicular stomatitis virus (VSV) has been used as a vector to express RSV-F or RSV-G because it infects a wide variety of cells and has shown to be a promising vector for developing vaccines against measles and influenza viruses (150). However, VSV is a neurotropic virus that raises concerns about safety. Candidates expressing RSV-F and RSV-G have been developed using both wild-

type VSV and VSVΔG, the latter of which lacks the VSV attachment protein that mediates VSV neurotropism. All four candidates induced the production of RSV-specific IgG in mice, but serum neutralizing antibody titers were low or undetectable. The VSVΔG-RSV-G candidate failed to protect mice against challenge. Mice vaccinated with the other three candidates had no detectable challenge virus in the lungs. All animals immunized with the vaccine candidates had significant pulmonary inflammation, lymphocyte infiltration, and damage to the bronchial epithelium. However, since there was no RSV-primed and RSV-challenged group for comparison, it is unclear whether the level of inflammation observed in vaccinated animals was in fact enhanced. Further studies are warranted to examine the suitability of a VSV-based RSV vaccine (151).

Vaccinia virus-based vaccine candidates. The modified vaccinia virus Ankara (MVA) vector was generated by passaging a vaccinia virus Ankara strain over 570 times in chicken fibroblast embryo cells, resulting in a virus that replicates efficiently in avian cells but replicates poorly in humans and cannot produce infectious progeny (152). This vector was engineered to express RSV-F, RSV-G, or both, and the candidates were evaluated in several animal models. The different studies produced mixed results. Wyatt et al. found that MVA-RSV-F and MVA-RSV-G protected mice against RSV challenge when administered intranasally or intramuscularly. MVA-RSV-G immunization fully protected the lower respiratory tract and provided a 2 $\log_{10}$ reduction of challenge virus in the upper respiratory tract. MVA-RSV-F completely protected both upper and lower respiratory tracts. MVA-RSV-FG boosted IgG titers in mice previously immunized with cpts248/404, suggesting that it could be used to boost immunity in seropositive populations. Unfortunately, serum neutralizing antibody titers and post-challenge lung

inflammation were not examined in this study (153). Olzewska et al. found that mice, immunized with MVA-F or MVA-G intraperitoneally, cleared challenge virus more rapidly than control mice. However, these mice lost weight similar to the FI-RSV immunized mice and had signs of enhanced disease (154). The inconsistencies between the two mouse studies may be explained by the use of different vaccine doses and different routes of administration. When MVA-F and MVA-FG were evaluated in seronegative calves, the vaccine candidates protected against lower respiratory bRSV infection with no evidence of enhanced disease (155). This study had the advantage of testing vaccine efficacy against RSV infection in a natural host. Interestingly, when MVA-F and MVA-G were tested in seronegative infant rhesus macaques, they induced very low levels of serum neutralizing antibodies and did not protect against RSV challenge (156). Given the inconsistent results of the various MVA-RSV vaccine studies, more studies are required to determine whether these candidates are efficacious and whether they cause enhanced disease.

Newcastle disease virus-based vaccine. A Newcastle disease virus (NDV) vectored RSV vaccine was developed by using the lentogenic Hitchner B1 NDV strain to express RSV-F. When tested in both interferon-α receptor knockout ($IFNAR^{-/-}$) and BALB/c mice, the vaccine candidate only decreased RSV lung titers by 1 $\log_{10}$ in both mouse models (157).

Sendai virus-based vaccines. Sendai virus (SeV), a murine virus closely related to human parainfluenza virus 1 (HPIV1), has been explored as a vector for an RSV vaccine. HPIV1 is a major cause of croup in children, and a chimeric vaccine against both HPIV1 and RSV is of significant interest. Intranasal infection of African green

monkeys with SeV fully protects against HPIV1 infection, making it an attractive xenogeneic vaccine candidate (158). Cotton rats intranasally immunized with recombinant SeV expressing RSV-F develop both humoral and cell-mediated immune responses against RSV and are protected against lower respiratory tract RSV/A and RSV/B infection (159). Sendai virus expressing RSV-G also protects cotton rats against challenge with a homologous RSV/A strain, but combining with SeV-RSV-F does not appear to improve efficacy of the F-expressing candidate (159, 160). African green monkeys immunized with SeV-RSV-F develop partial upper respiratory tract and complete lower respiratory tract protection against RSV infection. SeV-RSV-F also confers protection in a cotton rat maternal antibody model. Cotton rats passively administered RSV-neutralizing antibodies and then vaccinated with SeV-RSV-F are protected against RSV challenge three months later. These results suggest that infants with maternal antibodies against RSV can still be immunized with this vaccine candidate (161). One drawback of using SeV as a vector, however, is that pre-existing immunity against HPIV1 significantly impacts vaccine efficacy. HPIV1-seropositive adults do not shed SeV when experimentally infected, suggesting that the virus may be too highly attenuated to be used as a vaccine vector in this population (162).

Human parainfluenza virus 3-based vaccine. MEDI-534 is a chimeric, recombinant vaccine consisting of a bovine parainfluenza virus 3 (bPIV3) backbone engineered to express the human PIV3 (hPIV3) fusion protein, hPIV3 hemagglutinin-neuraminidase (HN), and RSV fusion protein (F). In a Phase 1 study conducted in seronegative children of ages 6 to 24 months, all subjects seroconverted in response to hPIV3, but only 50% seroresponded to RSV (163). Sequence analysis of post-

vaccination nasal wash samples showed mutations in the poly A sequence downstream of the bPIV3 nucleocapsid gene (N) as well as in the F open reading frame. These variant subpopulations existed at low levels in the administered vaccine, and the mutations were implicated in the down-regulation of F expression and subsequent reduction in the antibody response against F (164).

Subunit and particulate vaccine candidates

Numerous subunit and particulate-based RSV vaccine candidates have been developed using a variety of approaches. Unlike replicating vaccines, these candidates do not pose immediate safety concerns in children and elderly or immunocompromised adults. However, non-replicating vaccines raise concerns regarding enhanced disease in infants upon natural exposure to RSV. These candidates also encounter challenges with immunogenicity and often require co-administration with an adjuvant.

BBG2nA. One subunit vaccine, BBG2Na, is an RSV-G-based candidate that has been tested extensively in animals and humans. The vaccine consists of the central conserved region of RSV-G (G2Na) fused to the C-terminus of the albumin-binding region of streptococcal protein G (BB). Fusion of the RSV-G subunit to the streptococcal protein G increases the *in vivo* half-life of the antigen. When administered with alum, BBG2Na induced high RSV-specific IgG antibody titers but low neutralizing antibody titers in mice and cotton rats. Both the upper and lower respiratory tracts of mice were protected from RSV challenge, but only the lower respiratory tracts of cotton rats were protected (165). Intramuscular immunization of infant cynomolgus macaques induced the production of RSV-specific IgG, but no neutralizing antibody titers. Two out of four immunized monkeys also developed IL-13-producing T-cell responses, raising concerns

about RSV disease potentiation. The vaccine did not reduce RSV loads in the bronchoalveolar lavage (BAL) fluid when measured by qRT-PCR (166). The lack of vaccine efficacy in infant macaques was attributed to immunological immaturity in these animals, but the results of the study still warranted concerns about vaccine safety.

When initially evaluated in healthy adult volunteers, BBG2Na was well-tolerated and immunogenic. All of the vaccinees had at least a two-fold increase in G2Na-specific IgG titers, and 71% had at least a two-fold increase in serum neutralizing antibody titers (167). However, vaccine failed to advance when two healthy young adults in a phase II clinical trial developed type III sensitivity reactions (purpura) after vaccination (168). Therefore, while BBG2Na appeared somewhat promising in small animal models, concerns regarding its safety ultimately caused it to fail.

RSV particulate vaccines. The company, Novavax, Inc., has developed an RSV-F-based particulate vaccine. The RSV-F protein has been engineered to contain mutations in furin cleavage site II and a 10 amino-acid deletion in the fusion domain. When expressed in Sf9 insect cells using a baculovirus vector, the purified recombinant F protein assembles into 40-nm particles that consist of multiple F trimers in a post-fusion or intermediate post-activation conformation. Intramuscular vaccination of cotton rats with different doses of the F particles elicited the production of neutralizing antibody titers, which increased 3.5 to 18-fold with the addition of alum adjuvant. Some of these antibodies were specific for RSV-F antigenic site II, as they were able to inhibit palivizumab binding in a competitive ELISA. The vaccine candidate completely protected the lungs against RSV infection with no evidence of enhanced disease (169).

A phase I clinical trial conducted in healthy adults demonstrated that the F particle vaccine is safe and immunogenic. Seropositive 18 to 49 year-old adults were intramuscularly immunized two times with various doses of particles with or without alum. The vaccine was well-tolerated with no evidence of adverse events. The vaccinees had 7 to 19-fold increases in F-specific IgG titers but only 2 to 4-fold increases in neutralizing antibody titers. The authors attributed the modest increases in neutralizing antibody titers to the limitations of the assay. Spiking serum samples with clinically relevant amounts of palivizumab only induced modest rises in neutralizing antibody titers, suggesting that the antibody titers could still be protective. Overall, the phase I study demonstrated that F particles are safe in healthy adults and capable of eliciting modest increases in neutralizing antibody titers (170). A phase II clinical trial has recently been completed in women of child-bearing age to explore the possibility of maternal immunization. A phase III clinical trial testing the vaccine in elderly adults is also underway.

An RSV-G polypeptide-based nanoparticle vaccine has recently been developed. The engineered nanoparticle is produced using layer-by-layer fabrication and is loaded with RSV-G polypeptides spanning the conserved CX3C chemokine motif. Immunization with this conserved chemokine motif can induce the production of antibodies that cross-neutralize both RSV A and B strains (171). Mice subcutaneously immunized with the nanoparticles develop RSV-specific IgG antibody titers as well neutralizing antibodies. These antibodies prevent RSV-G from binding to the CX3CR1 receptor, which inhibits the virus's ability to block leukocyte trafficking (172). The immunized mice are completely protected against RSV challenge, have reduced RSV-

associated lung inflammation, and do not show signs of enhanced disease (173). These results suggest that the RSV-G-based nanoparticle vaccine can protect against RSV infection and disease by interfering with the RSV-G and CX3CR1 interaction.

Animal Models

No single animal model fully recapitulates RSV disease in humans. The most common animal models have been rodents and nonhuman primates, but there is increasing interest in using cognate host-pneumovirus models. Since different animal species model different aspects of RSV disease pathogenesis, it important to consider what characteristics of human disease will be examined and to choose the most relevant and practical model based on these considerations.

Mice

Mice are the most popular animal model for RSV infection. They are less expensive than many other models, and a wide variety of reagents are available to facilitate research. Furthermore, inbred strains allow for researchers to control for genetic background and reduce animal-to-animal variability. Different mouse strains show different levels of susceptibility to RSV infection, with up to a 100-fold difference between the most and least permissive mouse strains. BALB/c mice are commonly used for RSV research and are considered moderately permissive to infection (174).

RSV infection in mice displays some similarities to infection in humans. Lung function studies in mice have shown that RSV infection increases breathing rate and airway hyperresponsiveness (175, 176). RSV infection in mice also induces the production of pro-inflammatory cytokines and chemokines such as TNF-α, IL-6, IFN-γ, RANTES/CCL5, and MIP-1α. In histology studies, high doses of RSV induce exhibit

peribronchiolar and perivascular infiltration of lymphocytes and macrophages, sometimes accompanied by interstitial pneumonia (177, 178).

There are also significant limitations associated with the mouse model. Mice are only semi-permissive to RSV infection, and age-dependent susceptibility to RSV infection in mice does not match that in humans. Older mice, specifically those more than 15 weeks old, are more susceptible to RSV infection than neonatal mice. Mice also have differences in innate and adaptive signaling, such as differences in TLR expression and differences in leukocyte subsets (179). RSV infection in humans induces pulmonary recruitment of mostly neutrophils, some lymphocytes, and few eosinophils, while mouse lung infiltrates mostly consist of lymphocytes (178, 180). There are also key anatomical differences in the mouse lung, such as less airway branching and fewer bronchioles that can contribute to discrepancies observed between human and mouse RSV infection (181). Despite these drawbacks, many immunological insights have been gained from using the mouse model of RSV infection. Almost all of the immunology studies done examining FI-RSV-mediated enhanced disease have been performed in mice, furthering our understanding of this aspect of disease pathogenesis.

Cotton Rats

Cotton rats (*Sigmodon hispidus*) have been a standard model for evaluating RSV vaccines, antivirals, and therapeutics. Cotton rats are more than 100-fold more permissive to RSV infection than mice, and data obtained from this model has been used to advance immunoprophylactic antibodies, such as RespiGam and Synagis, to clinical trials (182). This model is also able to recapitulate some of the hallmarks of RSV infection such as inflammation and cellular infiltration in the lungs. Histopathologic

changes include mild bronchitis and epithelial cell sloughing (183). The inflammatory infiltrates consist of mostly lymphocytes and neutrophils (182). Cotton rats have also been able to recapitulate FI-RSV-associated enhanced disease. Animals that have been primed and boosted with FI-RSV show signs of enhanced disease upon infection with RSV along with a Th2-type immune response, similar to what was observed in children who were vaccinated with the FI-RSV vaccine (125).

The cotton rat model of RSV infection has a number of drawbacks. Cotton rats do not exhibit clinical signs of RSV infection and do not accurately reflect age-dependent susceptibility (183). Furthermore, the limited availability of species-specific reagents has made immunological studies challenging. The pool of reagents has expanded considerably over the past decade, however, making cotton rats an increasingly useful model (182).

Nonhuman primates

Chimpanzees are genetically the most closely related animal models to humans. RSV was originally isolated from chimpanzees with coryza (2). Animals experimentally infected with RSV develop of signs of upper respiratory disease, such as rhinorrhea, sneezing, and coughing (184). Chimpanzees do not commonly develop lower respiratory tract RSV disease, but there was one documented case of fatal bronchopneumonia in a captive chimpanzee that was non-experimentally infected with RSV. This animal had evidence of pulmonary neutrophilic inflammation and edema (185). Despite these advantages, the monetary costs along with ethical and logistical complications involved with working with chimpanzees, make them an impractical model for RSV research.

The African green monkey model has been used extensively for preclinical testing of RSV vaccines and therapeutics. They are more permissive to RSV infection than cotton rats and are able to mirror FI-RSV-associated enhanced disease. However, they still do not develop clinical signs of disease despite being genetically more related to humans (186, 187).

Ovine and bovine models

The perinatal lamb model of RSV infection has been explored by a number of groups due to the many similarities it shares with human RSV infection. The ovine lungs are more similar to those of humans in terms of branching, cellular organization, and alveologenesis. Pre-term and full-term lambs are susceptible to ovine, bovine, and human RSV infection. They demonstrate age-dependent susceptibility to infection, as younger lambs tend to exhibit more severe disease than older lambs. Lambs also develop symptoms similar to humans, including fever, wheezing, and malaise. RSV infection in this model induces bronchiolitis and injury to the pulmonary epithelia. Inflammatory infiltrates consist mostly of neutrophils (188). Furthermore, post-infection epithelial remodeling alters the pulmonary microenvironment and leads to airway hyperreactivity (189), all hallmarks of human RSV infection.

The bovine RSV (bRSV) infection model in calves offers many of the same advantages as the ovine model. Calves also have similar pulmonary architecture, age-dependent susceptibility, and symptomatic upper and lower respiratory tract RSV infection. BRSV infection in calves causes fever, nasal discharge, wheezing, and reduced activity. Histopathological changes include bronchiolitis and interstitial pneumonia.

This model is advantageous because calves are a natural host for bRSV, so disease pathogenesis can be studied in a cognate host-pathogen model (190).

Ovine and bovine models of RSV infection have similar drawbacks. Like other non-mouse models, the limited availability of reagents translates to limitations on the types of immunological studies that can be performed. The size of the animals requires a large amount space, and the high incidence of bacterial co-infections requires fastidious housing conditions (188, 190). Despite complicating factors, the ovine and bovine RSV infection models are promising and warrant further study.

References

1. **Fields BN**, **Knipe DM**, **Howley PM**. 2015. Fields virology. Wolters Kluwer Health/Lippincott Williams & Wilkins, Philadelphia.

2. **Blount RE**, **Morris JA**, **Savage RE**. 1956. Recovery of cytopathogenic agent from chimpanzees with coryza. Proc Soc Exp Biol Med **92**:544–549.

3. **Chanock R**, **Roizman B**, **Myers R**. 1957. Recovery from infants with respiratory illness of a virus related to chimpanzee coryza agent (CCA). I. Isolation, properties and characterization. Am J Hyg **66**:281–90.

4. **Chanock R**, **Finberg L**. 1957. Recovery from infants with respiratory illness of a virus related to chimpanzee coryza agent (CCA). II. Epidemiologic aspects of infection in infants and young children. Am J Hyg **66**:291–300.

5. **Beem M**, **Wright FH**, **Hamre D**, **Egerer R**, **Oehme M**. 1960. Association of the Chimpanzee Coryza Agent with Acute Respiratory Disease in Children. N Engl J Med **263**:523–530.

6. **Parrott RH**, **Vargosko AJ**, **Kim HW**, **Cumming C**, **Turner H**, **Huebner RJ**, **Chanock RM**. 1961. Respiratory syncytial virus. II. Serologic studies over a 34-month period of children with bronchiolitis, pneumonia, and minor respiratory diseases. JAMA **176**:653–7.

7. **Mcclelland L**, **Hilleman MR**, **Hamparian V V**, **Ketler A**, **Reilly CM**, **Cornfield D**, **Stokes J**. 1961. Studies of acute respiratory illnesses caused by respiratory syncytial virus. 2. Epidemiology and assessment of importance. N Engl J Med **264**:1169–75.

8. **Kapikian AZ**, **Bell JA**, **Mastrota FM**, **Johnson KM**, **Huebner RJ**, **Chanock RM**. 1961. An outbreak of febrile illness and pneumonia associated with respiratory syncytial virus infection. Am J Hyg **74**:234–48.

9. **Chanock RM**, **Parrott RH**, **Vargosko AJ**, **Kapikian AZ**, **Knight V**, **Johnson KM**. 1962. Acute respiratory diseases of viral etiology. IV. Respiratory syncytial virus. Am J Public Health Nations Health **52**:918–25.

10. **Kravetz HM**, **Knight V**, **Chanock RM**, **Morris JA**, **Johnson KM**, **Rifkind D**, **Utz JP**. 1961. Respiratory syncytial virus. III. Production of illness and clinical observations in adult volunteers. JAMA **176**:657–63.

11. **Anderson LJ**, **Hierholzer JC**, **Bingham PG**, **Stone YO**. 1985. Microneutralization test for respiratory syncytial virus based on an enzyme immunoassay. J Clin Microbiol **22**:1050–2.

12. **Mufson MA**, **Orvell C**, **Rafnar B**, **Norrby E**. 1985. Two distinct subtypes of human respiratory syncytial virus. J Gen Virol **66 (Pt 10**:2111–24.

13. **Johnson PR**, **Spriggs MK**, **Olmsted R a**, **Collins PL**. 1987. The G glycoprotein of human respiratory syncytial viruses of subgroups A and B: extensive sequence divergence between antigenically related proteins. Proc Natl Acad Sci U S A **84**:5625–5629.

14. **Peret TC**, **Hall CB**, **Schnabel KC**, **Golub JA**, **Anderson LJ**. 1998. Circulation patterns of genetically distinct group A and B strains of human respiratory syncytial virus in a community. J Gen Virol **79 (Pt 9)**:2221–9.

15. **Graham BS**, **Anderson LJ**. 2013. Challenges and opportunities for respiratory syncytial virus vaccines. Curr Top Microbiol Immunol **372**:391–404.

16. **Hall CB**, **Walsh EE**, **Schnabel KC**, **Long CE**, **McConnochie KM**, **Hildreth SW**, **Anderson LJ**. 1990. Occurrence of Groups A and B of Respiratory Syncytial Virus over 15 Years: Associated Epidemiologic and Clinical Characteristics in Hospitalized and Ambulatory Children. J Infect Dis **162**:1283–1290.

17. **Martinello RA**, **Chen MD**, **Weibel C**, **Kahn JS**. 2002. Correlation between respiratory syncytial virus genotype and severity of illness. J Infect Dis **186**:839–42.

18. **Gilca R**, **De Serres G**, **Tremblay M**, **Vachon M-L**, **Leblanc E**, **Bergeron MG**, **Dery P**, **Boivin G**. 2006. Distribution and clinical impact of human respiratory syncytial virus genotypes in hospitalized children over 2 winter seasons. J Infect Dis **193**:54–8.

19. **Roberts SR**, **Compans RW**, **Wertz GW**. 1995. Respiratory syncytial virus matures at the apical surfaces of polarized epithelial cells. J Virol **69**:2667–2673.

20. **Liljeroos L**, **Krzyzaniak MA**, **Helenius A**, **Butcher SJ**. 2013. Architecture of respiratory syncytial virus revealed by electron cryotomography. Proc Natl Acad Sci U S A **110**:11133–11138.

21. **Kiss G**, **Holl JM**, **Williams GM**, **Alonas E**, **Vanover D**, **Lifland AW**, **Gudheti M**, **Guerrero-Ferreira RC**, **Nair V**, **Yi H**, **Graham BS**, **Santangelo PJ**, **Wright ER**. 2014. Structural analysis of respiratory syncytial virus reveals the position of M2-1 between the matrix protein and the ribonucleoprotein complex. J Virol **88**:7602–7617.

22. **Bächi T**, **Howe C**. 1973. Morphogenesis and ultrastructure of respiratory syncytial virus. J Virol **12**:1173–80.

23. **Lamb R**, **Kolakofsky D**. 2001. Paramyxoviridae: The viruses and their replication, p. . *In* Knipe, D, Howley, P (eds.), Fields Virology4th Editio. Lippincott, Williams, and Wilkins, Philadelphia.

24. **Bermingham A**, **Collins PL**. 1999. The M2-2 protein of human respiratory syncytial virus is a regulatory factor involved in the balance between RNA replication and transcription. Proc Natl Acad Sci U S A **96**:11259–64.

25. **Spann KM**, **Tran K-C**, **Chi B**, **Rabin RL**, **Collins PL**. 2004. Suppression of the Induction of Alpha, Beta, and Gamma Interferons by the NS1 and NS2 Proteins of Human Respiratory Syncytial Virus in Human Epithelial Cells and Macrophages. J Virol **78**:4363–4369.

26. **Ramaswamy M**, **Shi L**, **Monick MM**, **Hunninghake GW**, **Look DC**. 2004. Specific Inhibition of Type I Interferon Signal Transduction by Respiratory Syncytial Virus. Am J Respir Cell Mol Biol **30**:893–900.

27. **Ramaswamy M**, **Shi L**, **Varga SM**, **Barik S**, **Behlke MA**, **Look DC**. 2006. Respiratory syncytial virus nonstructural protein 2 specifically inhibits type I interferon signal transduction. Virology **344**:328–39.

28. **Elliott J**, **Lynch OT**, **Suessmuth Y**, **Qian P**, **Boyd CR**, **Burrows JF**, **Buick R**, **Stevenson NJ**, **Touzelet O**, **Gadina M**, **Power UF**, **Johnston JA**. 2007. Respiratory syncytial virus NS1 protein degrades STAT2 by using the Elongin-Cullin E3 ligase. J Virol **81**:3428–36.

29. **Bitko V**, **Shulyayeva O**, **Mazumder B**, **Musiyenko A**, **Ramaswamy M**, **Look DC**, **Barik S**. 2007. Nonstructural proteins of respiratory syncytial virus suppress premature apoptosis by an NF-kappaB-dependent, interferon-independent mechanism and facilitate virus growth. J Virol **81**:1786–95.

30. **Collins PL**, **Hill MG**, **Cristina J**, **Grosfeld H**. 1996. Transcription elongation factor of respiratory syncytial virus, a nonsegmented negative-strand RNA virus. Proc Natl Acad Sci **93**:81–85.

31. **Fearns R**, **Collins PL**. 1999. Role of the M2-1 transcription antitermination protein of respiratory syncytial virus in sequential transcription. J Virol **73**:5852–64.

32. **Heminway BR**, **Yu Y**, **Tanaka Y**, **Perrine KG**, **Gustafson E**, **Bernstein JM**, **Galinski MS**. 1994. Analysis of respiratory syncytial virus F, G, and SH proteins in cell fusion. Virology **200**:801–5.

33. **Tripp RA**, **Jones LP**, **Haynes LM**, **Zheng H**, **Murphy PM**, **Anderson LJ**. 2001. CX3C chemokine mimicry by respiratory syncytial virus G glycoprotein. Nat Immunol **2**:732–738.

34. **Gonzalez ME**, **Carrasco L**. 2003. Viroporins. FEBS Lett **552**:28–34.

35. **Fuentes S**, **Tran KC**, **Luthra P**, **Teng MN**, **He B**. 2007. Function of the respiratory syncytial virus small hydrophobic protein. J Virol **81**:8361–6.

36. **Techaarpornkul S**, **Collins PL**, **Peeples ME**. 2002. Respiratory syncytial virus with the fusion protein as its only viral glycoprotein is less dependent on cellular glycosaminoglycans for attachment than complete virus. Virology **294**:296–304.

37. **Srinivasakumar N**, **Ogra PL**, **Flanagan TD**. 1991. Characteristics of fusion of respiratory syncytial virus with HEp-2 cells as measured by R18 fluorescence dequenching assay. J Virol **65**:4063–4069.

38. **Kolokoltsov AA**, **Deniger D**, **Fleming EH**, **Roberts NJJ**, **Karpilow JM**, **Davey RA**. 2007. Small interfering RNA profiling reveals key role of clathrin-mediated endocytosis and early endosome formation for infection by respiratory syncytial virus. J Virol **81**:7786–7800.

39. **San-Juan-Vergara H**, **Sampayo-Escobar V**, **Reyes N**, **Cha B**, **Pacheco-Lugo L**, **Wong T**, **Peeples ME**, **Collins PL**, **Castano ME**, **Mohapatra SS**. 2012. Cholesterol-rich microdomains as docking platforms for respiratory syncytial virus in normal human bronchial epithelial cells. J Virol **86**:1832–1843.

40. **Krzyzaniak MA**, **Zumstein MT**, **Gerez JA**, **Picotti P**, **Helenius A**. 2013. Host cell entry of respiratory syncytial virus involves macropinocytosis followed by proteolytic activation of the F protein. PLoS Pathog **9**:e1003309.

41. **Whelan S**, **Goldman N**. 2004. Estimating the frequency of events that cause multiple-nucleotide changes. Genetics **167**:2027–2043.

42. **Mink MA**, **Stec DS**, **Collins PL**. 1991. Nucleotide sequences of the 3' leader and 5' trailer regions of human respiratory syncytial virus genomic RNA. Virology **185**:615–624.

43. **Hull RN**, **Minner JR**, **SMITH JW**. 1956. New viral agents recovered from tissue cultures of monkey kidney cells. I. Origin and properties of cytopathogenic agents S.V.1, S.V.2, S.V.4, S.V.5, S.V.6, S.V.11, S.V.12 and S.V.15. Am J Hyg **63**:204–15.

44. **Tribe GW**. 1966. An investigation of the incidence, epidemiology and control of Simian virus 5. Br J Exp Pathol **47**:472–479.

45. **Atoynatan T**, **Hsiung GD**. 1969. Epidemiologic studies of latent virus infections in captive monkeys and baboons. II. Serologic evidence of myxovirus infections with special reference to SV5. Am J Epidemiol **89**:472–479.

46. **Hsiung GD**. 1972. Parainfluenza-5 virus. Infection of man and animal. Prog Med Virol Fortschritte der medizinischen Virusforschung Progrès en Virol médicale **14**:241–74.

47. **Goswami KKA**, **Lange LS**, **Mitchell DN**, **Cameron KR**, **Russell WC**. 1984. Does simian virus 5 infect humans. J Gen Virol **65**:1295–1303.

48. **Randall RE**, **Young DF**. 1988. Comparison between parainfluenza virus type 2 and simian virus 5: monoclonal antibodies reveal major antigenic differences. J Gen Virol **69 (Pt 8)**:2051–2060.

49. **Tsurudome M**, **Nishio M**, **Komada H**, **Bando H**, **Ito Y**. 1989. Extensive antigenic diversity among human parainfluenza type 2 virus isolates and immunological relationships among paramyxoviruses revealed by monoclonal antibodies. Virology **171**:38–48.

50. **Goswami KK**, **Randall RE**, **Lange LS**, **Russell WC**. 1987. Antibodies against the paramyxovirus SV5 in the cerebrospinal fluids of some multiple sclerosis patients. Nature, 1987/05/21 ed. **327**:244–247.

51. **Vandvik B**, **Norrby E**. 1989. Paramyxovirus SV5 and multiple sclerosis. Nature **338**:769–71.

52. **McLean BN**, **Thompson EJ**. 1989. Antibodies against the paramyxovirus SV5 are not specific for cerebrospinal fluid from multiple sclerosis patients. J Neurol Sci **92**:261–6.

53. **Cohn ML**, **Robinson ED**, **Thomas D**, **Faerber M**, **Carey S**, **Sawyer R**, **Goswami KK**, **Johnson AH**, **Richert JR**. 1996. T cell responses to the paramyxovirus simian virus 5: studies in multiple sclerosis and normal populations. Pathobiology **64**:131–5.

54. **Cornwell HJ**, **McCandlish IA**, **Thompson H**, **Laird HM**, **Wright NG**. 1976. Isolation of parainfluenza virus SV5 from dogs with respiratory disease. Vet Rec **98**:301–2.

55. **Rosenberg FJ**, **Lief FS**, **Todd JD**, **Reif JS**. 1971. Studies of canine respiratory viruses. I. Experimental infection of dogs with an SV5-like canine parainfluenza agent. Am J Epidemiol **94**:147–165.

56. **McCandlish IA**, **Thompson H**, **Cornwell HJ**, **Wright NG**. 1978. A study of dogs with kennel cough. Vet Rec **102**:293–301.

57. **Goswami KK**, **Cameron KR**, **Russell WC**, **Lange LS**, **Mitchell DN**. 1984. Evidence for the persistence of paramyxoviruses in human bone marrows. J Gen Virol **65 (Pt 11**:1881–8.

58. **Didcock L**, **Young DF**, **Goodbourn S**, **Randall RE**. 1999. The V protein of simian virus 5 inhibits interferon signalling by targeting STAT1 for proteasome-mediated degradation. J Virol **73**:9928–33.

59. **Lin Y**, **Bright AC**, **Rothermel TA**, **He B**. 2003. Induction of apoptosis by paramyxovirus simian virus 5 lacking a small hydrophobic gene. J Virol **77**:3371–83.

60. **Chen Z**, **Xu P**, **Salyards GW**, **Harvey SB**, **Rada B**, **Fu ZF**, **He B**. 2012. Evaluating a Parainfluenza Virus 5-Based Vaccine in a Host with Pre-Existing Immunity against Parainfluenza Virus 5. PLoS One **7**:e50144.

61. **Young DF**, **Randall RE**, **Hoyle JA**, **Souberbielle BE**. 1990. Clearance of a persistent paramyxovirus infection is mediated by cellular immune responses but not by serum-neutralizing antibody. J Virol **64**:5403–5411.

62. **Mueller S**, **Wimmer E**. 1998. Expression of foreign proteins by poliovirus polyprotein fusion: analysis of genetic stability reveals rapid deletions and formation of cardioviruslike open reading frames. J Virol, 1998/01/07 ed. **72**:20–31.

63. **He B**, **Paterson RG**, **Ward CD**, **Lamb RA**. 1997. Recovery of infectious SV5 from cloned DNA and expression of a foreign gene. Virology **237**:249–260.

64. **Chen Z**, **Zhou M**, **Gao X**, **Zhang G**, **Ren G**, **Gnanadurai CW**, **Fu ZF**, **He B**. 2012. A Novel Rabies Vaccine Based on a Recombinant Parainfluenza Virus 5 Expressing Rabies Virus Glycoprotein. J Virol **87**:2986–2993.

65. **Li Z**, **Mooney AJ**, **Gabbard JD**, **Gao X**, **Xu P**, **Place RJ**, **Hogan RJ**, **Tompkins SM**, **He B**. 2013. Recombinant Parainfluenza Virus 5 Expressing Hemagglutinin of Influenza A Virus H5N1 Protected Mice against Lethal Highly Pathogenic Avian Influenza Virus H5N1 Challenge. J Virol, 2012/10/19 ed. **87**:354–362.

66. **Li Z**, **Gabbard JD**, **Mooney A**, **Gao X**, **Chen Z**, **Place RJ**, **Tompkins SM**, **He B**. 2013. Single-dose vaccination of a recombinant parainfluenza virus 5 expressing NP from H5N1 virus provides broad immunity against influenza A viruses. J Virol **87**:5985–93.

67. **Price GE**, **Soboleski MR**, **Lo CY**, **Misplon JA**, **Quirion MR**, **Houser K V**, **Pearce MB**, **Pappas C**, **Tumpey TM**, **Epstein SL**. 2010. Single-dose mucosal immunization with a candidate universal influenza vaccine provides rapid protection from virulent H5N1, H3N2 and H1N1 viruses. PLoS One, 2010/10/27 ed. **5**:e13162.

68. **Lawson CM**, **Bennink JR**, **Restifo NP**, **Yewdell JW**, **Murphy BR**. 1994. Primary pulmonary cytotoxic T lymphocytes induced by immunization with a vaccinia virus recombinant expressing influenza A virus nucleoprotein peptide do not protect mice against challenge. J Virol, 1994/06/01 ed. **68**:3505–3511.

69. **Zhang L**, **Peeples ME**, **Boucher RC**, **Collins PL**, **Pickles RJ**. 2002. Respiratory Syncytial Virus Infection of Human Airway Epithelial Cells Is Polarized, Specific to Ciliated Cells, and without Obvious Cytopathology. J Virol **76**:5654–5666.

70. **Wright PF**, **Ikizler MR**, **Gonzales RA**, **Carroll KN**, **Johnson JE**, **Werkhaven JA**. 2005. Growth of respiratory syncytial virus in primary epithelial cells from the human respiratory tract. J Virol **79**:8651–4.

71. **Everard ML**, **Swarbrick A**, **Wrightham M**, **McIntyre J**, **Dunkley C**, **James PD**, **Sewell HF**, **Milner AD**. 1994. Analysis of cells obtained by bronchial lavage of infants with respiratory syncytial virus infection. Arch Dis Child **71**:428–32.

72. **Lukens M V**, **van de Pol AC**, **Coenjaerts FEJ**, **Jansen NJG**, **Kamp VM**, **Kimpen JLL**, **Rossen JWA**, **Ulfman LH**, **Tacke CEA**, **Viveen MC**, **Koenderman L**, **Wolfs TFW**, **van Bleek GM**. 2010. A systemic neutrophil response precedes robust CD8(+) T-cell activation during natural respiratory syncytial virus infection in infants. J Virol **84**:2374–83.

73. **Graham BS**, **Bunton LA**, **Wright PF**, **Karzon DT**. 1991. Role of T lymphocyte subsets in the pathogenesis of primary infection and rechallenge with respiratory syncytial virus in mice. J Clin Invest **88**:1026–33.

74. **Miyairi I**, **DeVincenzo JP**. 2008. Human genetic factors and respiratory syncytial virus disease severity. Clin Microbiol Rev.

75. **Wood N**, **Siegrist C-A**. 2011. Neonatal immunization: where do we stand? Curr Opin Infect Dis **24**:190–5.

76. **Takeda K**, **Akira S**. 2005. Toll-like receptors in innate immunity. Int Immunol **17**:1–14.

77. **Murawski MR**, **Bowen GN**, **Cerny AM**, **Anderson LJ**, **Haynes LM**, **Tripp RA**, **Kurt-Jones EA**, **Finberg RW**. 2009. Respiratory syncytial virus activates innate immunity through Toll-like receptor 2. J Virol **83**:1492–500.

78. **Rudd BD**, **Burstein E**, **Duckett CS**, **Li X**, **Lukacs NW**. 2005. Differential role for TLR3 in respiratory syncytial virus-induced chemokine expression. J Virol **79**:3350–7.

79. **Kurt-Jones EA**, **Popova L**, **Kwinn L**, **Haynes LM**, **Jones LP**, **Tripp RA**, **Walsh EE**, **Freeman MW**, **Golenbock DT**, **Anderson LJ**, **Finberg RW**. 2000. Pattern recognition receptors TLR4 and CD14 mediate response to respiratory syncytial virus. Nat Immunol **1**:398–401.

80. **Haeberle HA**, **Takizawa R**, **Casola A**, **Brasier AR**, **Dieterich H-J**, **Van Rooijen N**, **Gatalica Z**, **Garofalo RP**. 2002. Respiratory syncytial virus-induced activation of nuclear factor-kappaB in the lung involves alveolar macrophages and toll-like receptor 4-dependent pathways. J Infect Dis **186**:1199–206.

81. **Haynes LM**, **Moore DD**, **Kurt-Jones EA**, **Finberg RW**, **Anderson LJ**, **Tripp RA**. 2001. Involvement of toll-like receptor 4 in innate immunity to respiratory syncytial virus. J Virol **75**:10730–7.

82. **Numata M**, **Chu HW**, **Dakhama A**, **Voelker DR**. 2010. Pulmonary surfactant phosphatidylglycerol inhibits respiratory syncytial virus–induced inflammation and infection. Proc Natl Acad Sci U S A **107**:320–325.

83. **Awomoyi AA**, **Rallabhandi P**, **Pollin TI**, **Lorenz E**, **Sztein MB**, **Boukhvalova MS**, **Hemming VG**, **Blanco JCG**, **Vogel SN**. 2007. Association of TLR4 polymorphisms with symptomatic respiratory syncytial virus infection in high-risk infants and young children. J Immunol **179**:3171–7.

84. **Gagro A**, **Tominac M**, **Krsulović-Hresić V**, **Baće A**, **Matić M**, **Drazenović V**, **Mlinarić-Galinović G**, **Kosor E**, **Gotovac K**, **Bolanca I**, **Batinica S**, **Rabatić S**. 2004. Increased Toll-like receptor 4 expression in infants with respiratory syncytial virus bronchiolitis. Clin Exp Immunol **135**:267–72.

85. **Ehl S**, **Bischoff R**, **Ostler T**, **Vallbracht S**, **Schulte-Monting J**, **Poltorak A**, **Freudenberg M**. 2004. The role of Toll-like receptor 4 versus interleukin-12 in immunity to respiratory syncytial virus. Eur J Immunol **34**:1146–1153.

86. **Douville RN**, **Lissitsyn Y**, **Hirschfeld AF**, **Becker AB**, **Kozyrskyj AL**, **Liem J**, **Bastien N**, **Li Y**, **Victor RE**, **Sekhon M**, **Turvey SE**, **HayGlass KT**. 2010. TLR4 Asp299Gly and Thr399Ile polymorphisms: no impact on human immune responsiveness to LPS or respiratory syncytial virus. PLoS One **5**:e12087.

87. **Kawai T**, **Akira S**. 2006. TLR signaling. Cell Death Differ **13**:816–25.

88. **Loo Y-M**, **Gale M**. 2011. Immune signaling by RIG-I-like receptors. Immunity **34**:680–92.

89. **Liu P**, **Jamaluddin M**, **Li K**, **Garofalo RP**, **Casola A**, **Brasier AR**. 2007. Retinoic acid-inducible gene I mediates early antiviral response and Toll-like receptor 3 expression in respiratory syncytial virus-infected airway epithelial cells. J Virol **81**:1401–11.

90. **Connors M**, **Collins PL**, **Firestone CY**, **Murphy BR**. 1991. Respiratory syncytial virus (RSV) F, G, M2 (22K), and N proteins each induce resistance to RSV challenge, but resistance induced by M2 and N proteins is relatively short-lived. J Virol **65**:1634–1637.

91. **Connors M**, **Kulkarni AB**, **Collins PL**, **Firestone CY**, **Holmes KL**, **Morse HC**, **Murphy BR**. 1992. Resistance to respiratory syncytial virus (RSV) challenge induced by infection with a vaccinia virus recombinant expressing the RSV M2 protein (Vac-M2) is mediated by $CD8^+$ T cells, while that induced by Vac-F or Vac-G recombinants is mediated by antibodie. J Virol **66**:1277–81.

92. **Taylor G**, **Stott EJ**, **Bew M**, **Fernie BF**, **Cote PJ**, **Collins a P**, **Hughes M**, **Jebbett J**. 1984. Monoclonal antibodies protect against respiratory syncytial virus infection in mice. Immunology **52**:137–42.

93. **Walsh EE**, **Schlesinger JJ**, **Brandriss MW**. 1984. Protection from respiratory syncytial virus infection in cotton rats by passive transfer of monoclonal antibodies. Infect Immun **43**:756–8.

94. **Prince GA**, **Horswood RL**, **Chanock RM**. 1985. Quantitative aspects of passive immunity to respiratory syncytial virus infection in infant cotton rats. J Virol **55**:517–20.

95. **Glezen WP**, **Taber LH**, **Frank AL**, **Kasel JA**. 1986. Risk of primary infection and reinfection with respiratory syncytial virus. Am J Dis Child **140**:543–6.

96. **Malley R**, **DeVincenzo J**, **Ramilo O**, **Dennehy PH**, **Meissner HC**, **Gruber WC**, **Sanchez PJ**, **Jafri H**, **Balsley J**, **Carlin D**, **Buckingham S**, **Vernacchio L**, **Ambrosino DM**. 1998. Reduction of respiratory syncytial virus (RSV) in tracheal aspirates in intubated infants by use of humanized monoclonal antibody to RSV F protein. J Infect Dis **178**:1555–61.

97. **Weltzin R**, **Hsu SA**, **Mittler ES**, **Georgakopoulos K**, **Monath TP**. 1994. Intranasal monoclonal immunoglobulin A against respiratory syncytial virus protects against upper and lower respiratory tract infections in mice. Antimicrob Agents Chemother **38**:2785–2791.

98. **Domachowske JB**, **Rosenberg HF**. 1999. Respiratory syncytial virus infection: immune response, immunopathogenesis, and treatment. Clin Microbiol Rev **12**:298–309.

99. **Ostler T**, **Davidson W**, **Ehl S**. 2002. Virus clearance and immunopathology by CD8(+) T cells during infection with respiratory syncytial virus are mediated by IFN-gamma. Eur J Immunol **32**:2117–23.

100. **Hall CB**, **Powell KR**, **MacDonald NE**, **Gala CL**, **Menegus ME**, **Suffin SC**, **Cohen HJ**. 1986. Respiratory syncytial viral infection in children with compromised immune function. N Engl J Med **315**:77–81.

101. **Levy O**. 2007. Innate immunity of the newborn: basic mechanisms and clinical correlates. Nat Rev Immunol **7**:379–90.

102. **Siegrist C-A**, **Aspinall R**. 2009. B-cell responses to vaccination at the extremes of age. Nat Rev Immunol **9**:185–94.

103. **Siegrist CA**. 2003. Mechanisms by which maternal antibodies influence infant vaccine responses: review of hypotheses and definition of main determinants. Vaccine **21**:3406–12.

104. **Mehta J**, **Walsh EE**, **Mahadevia PJ**, **Falsey AR**. 2013. Risk factors for respiratory syncytial virus illness among patients with chronic obstructive pulmonary disease. COPD **10**:293–9.

105. **Anderson LJ**, **Dormitzer PR**, **Nokes DJ**, **Rappuoli R**, **Roca A**, **Graham BS**. 2013. Strategic priorities for respiratory syncytial virus (RSV) vaccine development. Vaccine **31 Suppl 2**:B209–15.

106. **Crowe JE**. 2001. Influence of maternal antibodies on neonatal immunization against respiratory viruses. Clin Infect Dis **33**:1720–7.

107. **Ogilvie MM**, **Santhire Vathenen A**, **Radford M**, **Codd J**, **Key S**. 1981. Maternal antibody and respiratory syncytial virus infection in infancy. J Med Virol **7**:263–271.

108. **Zimmer G**, **Budz L**, **Herrler G**. 2001. Proteolytic activation of respiratory syncytial virus fusion protein. Cleavage at two furin consensus sequences. J Biol Chem **276**:31642–50.

109. **Dutch RE**, **Jardetzky TS**, **Lamb RA**. 2000. Virus membrane fusion proteins: biological machines that undergo a metamorphosis. Biosci Rep **20**:597–612.

110. **Arbiza J**, **Taylor G**, **López JA**, **Furze J**, **Wyld S**, **Whyte P**, **Stott EJ**, **Wertz G**, **Sullender W**, **Trudel M**. 1992. Characterization of two antigenic sites recognized by neutralizing monoclonal antibodies directed against the fusion glycoprotein of human respiratory syncytial virus. J Gen Virol **73 (Pt 9)**:2225–34.

111. **López JA**, **Bustos R**, **Orvell C**, **Berois M**, **Arbiza J**, **García-Barreno B**, **Melero JA**. 1998. Antigenic structure of human respiratory syncytial virus fusion glycoprotein. J Virol **72**:6922–8.

112. **López JA**, **Peñas C**, **García-Barreno B**, **Melero JA**, **Portela A**. 1990. Location of a highly conserved neutralizing epitope in the F glycoprotein of human respiratory syncytial virus. J Virol **64**:927–30.

113. **McLellan JS**, **Yang Y**, **Graham BS**, **Kwong PD**. 2011. Structure of respiratory syncytial virus fusion glycoprotein in the postfusion conformation reveals preservation of neutralizing epitopes. J Virol **85**:7788–96.

114. **Swanson KA**, **Settembre EC**, **Shaw CA**, **Dey AK**, **Rappuoli R**, **Mandl CW**, **Dormitzer PR**, **Carfi A**. 2011. Structural basis for immunization with postfusion respiratory syncytial virus fusion F glycoprotein (RSV F) to elicit high neutralizing antibody titers. Proc Natl Acad Sci U S A **108**:9619–24.

115. **Magro M**, **Mas V**, **Chappell K**, **Vázquez M**, **Cano O**, **Luque D**, **Terrón MC**, **Melero JA**, **Palomo C**. 2012. Neutralizing antibodies against the preactive form of respiratory syncytial virus fusion protein offer unique possibilities for clinical intervention. Proc Natl Acad Sci U S A **109**:3089–94.

116. **McLellan JS**, **Chen M**, **Leung S**, **Graepel KW**, **Du X**, **Yang Y**, **Zhou T**, **Baxa U**, **Yasuda E**, **Beaumont T**, **Kumar A**, **Modjarrad K**, **Zheng Z**, **Zhao M**, **Xia N**, **Kwong PD**, **Graham BS**. 2013. Structure of RSV fusion glycoprotein trimer bound to a prefusion-specific neutralizing antibody. Science **340**:1113–7.

117. **McLellan JS**, **Chen M**, **Joyce MG**, **Sastry M**, **Stewart-Jones GBE**, **Yang Y**, **Zhang B**, **Chen L**, **Srivatsan S**, **Zheng A**, **Zhou T**, **Graepel KW**, **Kumar A**,

Moin S, **Boyington JC**, **Chuang G-Y**, **Soto C**, **Baxa U**, **Bakker AQ**, **Spits H**, **Beaumont T**, **Zheng Z**, **Xia N**, **Ko S-Y**, **Todd J-P**, **Rao S**, **Graham BS**, **Kwong PD**. 2013. Structure-based design of a fusion glycoprotein vaccine for respiratory syncytial virus. Science **342**:592–8.

118. **Johnson SM**, **McNally BA**, **Ioannidis I**, **Flano E**, **Teng MN**, **Oomens AG**, **Walsh EE**, **Peeples ME**. 2015. Respiratory Syncytial Virus Uses CX3CR1 as a Receptor on Primary Human Airway Epithelial Cultures. PLoS Pathog **11**:e1005318.

119. **Harcourt JL**, **Karron RA**, **Tripp RA**. 2004. Anti-G protein antibody responses to respiratory syncytial virus infection or vaccination are associated with inhibition of G protein CX3C-CX3CR1 binding and leukocyte chemotaxis. J Infect Dis **190**:1936–1940.

120. **Johnson TR**, **McLellan JS**, **Graham BS**. 2012. Respiratory syncytial virus glycoprotein G interacts with DC-SIGN and L-SIGN to activate ERK1 and ERK2. J Virol **86**:1339–47.

121. **Schepens B**, **Sedeyn K**, **Vande Ginste L**, **De Baets S**, **Schotsaert M**, **Roose K**, **Houspie L**, **Van Ranst M**, **Gilbert B**, **van Rooijen N**, **Fiers W**, **Piedra P**, **Saelens X**. 2014. Protection and mechanism of action of a novel human respiratory syncytial virus vaccine candidate based on the extracellular domain of small hydrophobic protein. EMBO Mol Med **6**:1436–54.

122. **Kim HW**, **Canchola JG**, **Brandt CD**, **Pyles G**, **Chanock RM**, **Jensen K**, **Parrott RH**. 1969. Respiratory syncytial virus disease in infants despite prior administration of antigenic inactivated vaccine. Am J Epidemiol **89**:422–434.

123. **Fulginiti VA**, **Eller JJ**, **Sieber OF**, **Joyner JW**, **Minamitani M**, **Meiklejohn G**. 1969. Respiratory virus immunization. I. A field trial of two inactivated respiratory virus vaccines; an aqueous trivalent parainfluenza virus vaccine and an alum-precipitated respiratory syncytial virus vaccine. Am J Epidemiol **89**:435–48.

124. **Chin J**, **Magoeetn RL**, **Shearer L a NN**, **Schleble JH**, **Lennette EH**. 1969. Sociated With Bronchiolitis and Pneumonia **89**:449–463.

125. **Prince G a**, **Jenson a B**, **Hemming VG**, **Murphy BR**, **Walsh EE**, **Horswood RL**, **Chanock RM**. 1986. Enhancement of respiratory syncytial virus pulmonary pathology in cotton rats by prior intramuscular inoculation of formalin-inactiva ted virus. J Virol **57**:721–8.

126. **Murphy BR**, **Prince GA**, **Walsh EE**, **Kim HW**, **Parrott RH**, **Hemming VG**, **Rodriguez WJ**, **Chanock RM**. 1986. Dissociation between serum neutralizing and glycoprotein antibody responses of infants and children who received inactivated respiratory syncytial virus vaccine. J Clin Microbiol **24**:197–202.

127. **Murphy BR**, **Walsh EE**. 1988. Formalin-inactivated respiratory syncytial virus vaccine induces antibodies to the fusion glycoprotein that are deficient in fusion-inhibiting activity. J Clin Microbiol **26**:1595–7.

128. **Polack FP**, **Teng MN**, **Collins PL**, **Prince GA**, **Exner M**, **Regele H**, **Lirman DD**, **Rabold R**, **Hoffman SJ**, **Karp CL**, **Kleeberger SR**, **Wills-Karp M**, **Karron RA**. 2002. A role for immune complexes in enhanced respiratory syncytial virus disease. J Exp Med **196**:859–65.

129. **Connors M**, **Collins PL**, **Firestone CY**, **Sotnikov A V**, **Waitze A**, **Davis AR**, **Hung PP**, **Chanock RM**, **Murphy BR**. 1992. Cotton rats previously immunized with a chimeric RSV FG glycoprotein develop enhanced pulmonary pathology when infected with RSV, a phenomenon not encountered following immunization with vaccinia--RSV recombinants or RSV. Vaccine **10**:475–84.

130. **Delgado MF**, **Coviello S**, **Monsalvo a C**, **Melendi G a**, **Hernandez JZ**, **Batalle JP**, **Diaz L**, **Trento A**, **Chang H-Y**, **Mitzner W**, **Ravetch J**, **Melero J a**, **Irusta PM**, **Polack FP**. 2009. Lack of antibody affinity maturation due to poor Toll-like receptor stimulation leads to enhanced respiratory syncytial virus disease. Nat Med **15**:34–41.

131. **Connors M**, **Kulkarni a B**, **Firestone CY**, **Holmes KL**, **Morse HC**, **Sotnikov a V**, **Murphy BR**. 1992. Pulmonary histopathology induced by respiratory syncytial virus (RSV) challenge of formalin-inactivated RSV-immunized BALB/c mice is abrogated by depletion of $CD4^+$ T cells. J Virol **66**:7444–51.

132. **Olson MR**, **Varga SM**. 2007. CD8 T cells inhibit respiratory syncytial virus (RSV) vaccine-enhanced disease. J Immunol **179**:5415–24.

133. **Loebbermann J**, **Durant L**, **Thornton H**, **Johansson C**, **Openshaw PJ**. 2013. Defective immunoregulation in RSV vaccine-augmented viral lung disease restored by selective chemoattraction of regulatory T cells. Proc Natl Acad Sci U S A **110**:2987–92.

134. **Waris M**, **Tsou C**, **Erdman D**. 1996. Respiratory Syncytial Virus Infection in BALB/c mice previously immunized with formalin-inactivated virus induces enhanced pulmonary inflammatory response with a predominant Th2-like cytokine pattern. J Virol **70**:2852–2860.

135. **Openshaw PJ**, **Culley FJ**, **Olszewska W**. 2001. Immunopathogenesis of vaccine-enhanced RSV disease. Vaccine **20 Suppl 1**:S27–31.

136. **De Swart RL**, **Kuiken T**, **Timmerman HH**, **van Amerongen G**, **Van Den Hoogen BG**, **Vos HW**, **Neijens HJ**, **Andeweg AC**, **Osterhaus ADME**. 2002. Immunization of macaques with formalin-inactivated respiratory syncytial virus (RSV) induces interleukin-13-associated hypersensitivity to subsequent RSV infection. J Virol **76**:11561–9.

137. **Fulginiti VA**, **Eller JJ**, **Downie AW**, **Kempe CH**. 1967. Altered reactivity to measles virus. Atypical measles in children previously immunized with inactivated measles virus vaccines. JAMA **202**:1075–80.

138. **Henrickson KJ**. 2003. Parainfluenza viruses. Clin Microbiol Rev **16**:242–64.

139. **de Swart RL**, **van den Hoogen BG**, **Kuiken T**, **Herfst S**, **van Amerongen G**, **Yüksel S**, **Sprong L**, **Osterhaus ADME**. 2007. Immunization of macaques with formalin-inactivated human metapneumovirus induces hypersensitivity to hMPV infection. Vaccine **25**:8518–28.

140. **Moghaddam A**, **Olszewska W**, **Wang B**, **Tregoning JS**, **Helson R**, **Sattentau QJ**, **Openshaw PJM**. 2006. A potential molecular mechanism for hypersensitivity caused by formalin-inactivated vaccines. Nat Med **12**:905–7.

141. **CROWEJR J**, **BUI P**, **DAVIS A**, **CHANOCK R**, **MURPHY B**. 1994. A further attenuated derivative of a cold-passaged temperature-sensitive mutant of human respiratory syncytial virus retains immunogenicity and protective efficacy against wild-type challenge in seronegative chimpanzees. Vaccine **12**:783–790.

142. **Wright PF**, **Karron RA**, **Belshe RB**, **Thompson J**, **Crowe JE**, **Boyce TG**, **Halburnt LL**, **Reed GW**, **Whitehead SS**, **Anderson EL**, **Wittek AE**, **Casey R**, **Eichelberger M**, **Thumar B**, **Randolph VB**, **Udem SA**, **Chanock RM**, **Murphy BR**. 2000. Evaluation of a live, cold-passaged, temperature-sensitive, respiratory syncytial virus vaccine candidate in infancy. J Infect Dis **182**:1331–42.

143. **Karron RA**, **Wright PF**, **Belshe RB**, **Thumar B**, **Casey R**, **Newman F**, **Polack FP**, **Randolph VB**, **Deatly A**, **Hackell J**, **Gruber W**, **Murphy BR**, **Collins PL**. 2005. Identification of a recombinant live attenuated respiratory syncytial virus vaccine candidate that is highly attenuated in infants. J Infect Dis **191**:1093–1104.

144. **Malkin E**, **Yogev R**, **Abughali N**, **Sliman J**, **Wang CK**, **Zuo F**, **Yang C-F**, **Eickhoff M**, **Esser MT**, **Tang RS**, **Dubovsky F**. 2013. Safety and immunogenicity of a live attenuated RSV vaccine in healthy RSV-seronegative children 5 to 24 months of age. PLoS One **8**:e77104.

145. **Luongo C**, **Yang L**, **Winter CC**, **Spann KM**, **Murphy BR**, **Collins PL**, **Buchholz UJ**. 2009. Codon stabilization analysis of the “248” temperature sensitive mutation for increased phenotypic stability of respiratory syncytial virus vaccine candidates. Vaccine **27**:5667–5676.

146. **Luongo C**, **Winter CC**, **Collins PL**, **Buchholz UJ**. 2012. Increased Genetic and Phenotypic Stability of a Promising Live-Attenuated Respiratory Syncytial Virus Vaccine Candidate by Reverse Genetics. J Virol **86**:10792–10804.

147. **Luongo C**, **Winter CC**, **Collins PL**, **Buchholz UJ**. 2013. Respiratory Syncytial Virus Modified by Deletions of the NS2 Gene and Amino Acid S1313 of the L Polymerase Protein Is a Temperature-Sensitive, Live-Attenuated Vaccine

Candidate That Is Phenotypically Stable at Physiological Temperature. J Virol **87** :1985–1996.

148. **Teng MN**, **Whitehead SS**, **Bermingham A**, **St. Claire M**, **Elkins WR**, **Murphy BR**, **Collins PL**. 2000. Recombinant Respiratory Syncytial Virus That Does Not Express the NS1 or M2-2 Protein Is Highly Attenuated and Immunogenic in Chimpanzees. J Virol **74**:9317–9321.

149. **Karron RA**, **Luongo C**, **Thumar B**, **Loehr KM**, **Englund JA**, **Collins PL**, **Buchholz UJ**. 2015. A gene deletion that up-regulates viral gene expression yields an attenuated RSV vaccine with improved antibody responses in children. Sci Transl Med **7**:312ra175–312ra175.

150. **Kahn JS**, **Schnell MJ**, **Buonocore L**, **Rose JK**. 1999. Recombinant vesicular stomatitis virus expressing respiratory syncytial virus (RSV) glycoproteins: RSV fusion protein can mediate infection and cell fusion. Virology **254**:81–91.

151. **Kahn JS**, **Roberts A**, **Weibel C**, **Buonocore L**, **Rose JK**. 2001. Replication-competent or attenuated, nonpropagating vesicular stomatitis viruses expressing respiratory syncytial virus (RSV) antigens protect mice against RSV challenge. J Virol **75**:11079–11087.

152. **Blanchard TJ**, **Alcami A**, **Andrea P**, **Smith GL**. 1998. Modified vaccinia virus Ankara undergoes limited replication in human cells and lacks several immunomodulatory proteins: implications for use as a human vaccine. J Gen Virol **79 (Pt 5)**:1159–1167.

153. **Wyatt LS**, **Whitehead SS**, **Venanzi KA**, **Murphy BR**, **Moss B**. 1999. Priming and boosting immunity to respiratory syncytial virus by recombinant replication-defective vaccinia virus MVA. Vaccine **18**:392–397.

154. **Openshaw PJM**, **Culley FJ**, **Olszewska W**. 2001. Immunopathogenesis of vaccine-enhanced RSV disease. Vaccine **20**:S27–S31.

155. **Antonis AFG**, **van der Most RG**, **Suezer Y**, **Stockhofe-Zurwieden N**, **Daus F**, **Sutter G**, **Schrijver RS**. 2007. Vaccination with recombinant modified vaccinia virus Ankara expressing bovine respiratory syncytial virus (bRSV) proteins protects calves against RSV challenge. Vaccine **25**:4818–27.

156. **de Waal L**, **Wyatt LS**, **Yüksel S**, **van Amerongen G**, **Moss B**, **Niesters HGM**, **Osterhaus ADME**, **de Swart RL**. 2004. Vaccination of infant macaques with a recombinant modified vaccinia virus Ankara expressing the respiratory syncytial virus F and G genes does not predispose for immunopathology. Vaccine **22**:923–6.

157. **Martinez-Sobrido L**, **Gitiban N**, **Fernandez-Sesma A**, **Cros J**, **Mertz SE**, **Jewell NA**, **Hammond S**, **Flano E**, **Durbin RK**, **García-Sastre A**, **Durbin JE**. 2006. Protection against respiratory syncytial virus by a recombinant Newcastle disease virus vector. J Virol **80**:1130–9.

158. **Hurwitz JL**, **Soike KF**, **Sangster MY**, **Portner A**, **Sealy RE**, **Dawson DH**, **Coleclough C**. 1997. Intranasal Sendai virus vaccine protects African green monkeys from infection with human parainfluenza virus-type one. Vaccine **15**:533–540.

159. **Zhan X**, **Hurwitz JL**, **Krishnamurthy S**, **Takimoto T**, **Boyd K**, **Scroggs RA**, **Surman S**, **Portner A**, **Slobod KS**. 2007. Respiratory syncytial virus (RSV) fusion protein expressed by recombinant Sendai virus elicits B-cell and T-cell responses in cotton rats and confers protection against RSV subtypes A and B. Vaccine **25**:8782–8793.

160. **Takimoto T**, **Hurwitz JL**, **Coleclough C**, **Prouser C**, **Krishnamurthy S**, **Zhan X**, **Boyd K**, **Scroggs RA**, **Brown B**, **Nagai Y**, **Portner A**, **Slobod KS**. 2004. Recombinant Sendai virus expressing the G glycoprotein of respiratory syncytial virus (RSV) elicits immune protection against RSV. J Virol **78**:6043–6047.

161. **Jones BG**, **Sealy RE**, **Surman SL**, **Portner A**, **Russell CJ**, **Slobod KS**, **Dormitzer PR**, **DeVincenzo J**, **Hurwitz JL**. 2014. Sendai virus-based RSV vaccine protects against RSV challenge in an in vivo maternal antibody model. Vaccine **32**:3264–73.

162. **Slobod KS**, **Shenep JL**, **Luján-Zilbermann J**, **Allison K**, **Brown B**, **Scroggs RA**, **Portner A**, **Coleclough C**, **Hurwitz JL**. 2004. Safety and immunogenicity of intranasal murine parainfluenza virus type 1 (Sendai virus) in healthy human adults. Vaccine **22**:3182–3186.

163. **Bernstein DI**, **Malkin E**, **Abughali N**, **Falloon J**, **Yi T**, **Dubovsky F**. 2012. Phase 1 study of the safety and immunogenicity of a live, attenuated respiratory syncytial virus and parainfluenza virus type 3 vaccine in seronegative children. Pediatr Infect Dis J **31**:109–14.

164. **Yang CF**, **Wang CK**, **Malkin E**, **Schickli JH**, **Shambaugh C**, **Zuo F**, **Galinski MS**, **Dubovsky F**, **Tang RS**. 2013. Implication of respiratory syncytial virus (RSV) F transgene sequence heterogeneity observed in Phase 1 evaluation of MEDI-534, a live attenuated parainfluenza type 3 vectored RSV vaccine. Vaccine **31**:2822–2827.

165. **Power UF**, **Plotnicky-Gilquin H**, **Huss T**, **Robert A**, **Trudel M**, **Ståhl S**, **Uhlén M**, **Nguyen TN**, **Binz H**. 1997. Induction of protective immunity in rodents by vaccination with a prokaryotically expressed recombinant fusion protein containing a respiratory syncytial virus G protein fragment. Virology **230**:155–66.

166. **De Waal L**, **Power UF**, **Yüksel S**, **van Amerongen G**, **Nguyen TN**, **Niesters HGM**, **de Swart RL**, **Osterhaus ADME**. 2004. Evaluation of BBG2Na in infant macaques: specific immune responses after vaccination and RSV challenge. Vaccine **22**:915–22.

167. **Power UF**, **Nguyen TN**, **Rietveld E**, **de Swart RL**, **Groen J**, **Osterhaus AD**, **de Groot R**, **Corvaia N**, **Beck A**, **Bouveret-Le-Cam N**, **Bonnefoy JY**. 2001. Safety and immunogenicity of a novel recombinant subunit respiratory syncytial virus vaccine (BBG2Na) in healthy young adults. J Infect Dis **184**:1456–60.

168. **Durbin AP**, **Karron RA**. 2003. Progress in the development of respiratory syncytial virus and parainfluenza virus vaccines. Clin Infect Dis **37**:1668–77.

169. **Smith G**, **Raghunandan R**, **Wu Y**, **Liu Y**, **Massare M**, **Nathan M**, **Zhou B**, **Lu H**, **Boddapati S**, **Li J**, **Flyer D**, **Glenn G**. 2012. Respiratory syncytial virus fusion glycoprotein expressed in insect cells form protein nanoparticles that induce protective immunity in cotton rats. PLoS One **7**:e50852.

170. **Glenn GM**, **Smith G**, **Fries L**, **Raghunandan R**, **Lu H**, **Zhou B**, **Thomas DN**, **Hickman SP**, **Kpamegan E**, **Boddapati S**, **Piedra PA**. 2013. Safety and immunogenicity of a Sf9 insect cell-derived respiratory syncytial virus fusion protein nanoparticle vaccine. Vaccine **31**:524–32.

171. **Choi Y**, **Mason CS**, **Jones LP**, **Crabtree J**, **Jorquera P a**, **Tripp R a**. 2012. Antibodies to the central conserved region of respiratory syncytial virus (RSV) G protein block RSV G protein CX3C-CX3CR1 binding and cross-neutralize RSV A and B strains. Viral Immunol **25**:193–203.

172. **Jorquera PA**, **Oakley KE**, **Powell TJ**, **Palath N**, **Boyd JG**, **Tripp RA**. 2015. Layer-By-Layer Nanoparticle Vaccines Carrying the G Protein CX3C Motif Protect against RSV Infection and Disease. Vaccines **3**:829–49.

173. **Jorquera P a**, **Choi Y**, **Oakley KE**, **Powell TJ**, **Boyd JG**, **Palath N**, **Haynes LM**, **Anderson LJ**, **Tripp R a**. 2013. Nanoparticle Vaccines Encompassing the Respiratory Syncytial Virus (RSV) G Protein CX3C Chemokine Motif Induce Robust Immunity Protecting from Challenge and Disease. PLoS One **8**:e74905.

174. **Prince GA**, **Horswood RL**, **Berndt J**, **Suffin SC**, **Chanock RM**. 1979. Respiratory syncytial virus infection in inbred mice. Infect Immun **26**:764–766.

175. **Jafri HS**, **Chavez-Bueno S**, **Mejias A**, **Gomez AM**, **Rios AM**, **Nassi SS**, **Yusuf M**, **Kapur P**, **Hardy RD**, **Hatfield J**, **Rogers BB**, **Krisher K**, **Ramilo O**. 2004. Respiratory syncytial virus induces pneumonia, cytokine response, airway obstruction, and chronic inflammatory infiltrates associated with long-term airway hyperresponsiveness in mice. J Infect Dis **189**:1856–1865.

176. **van Schaik SM**, **Enhorning G**, **Vargas I**, **Welliver RC**. 1998. Respiratory syncytial virus affects pulmonary function in BALB/c mice. J Infect Dis **177**:269–276.

177. **Graham BS**, **Perkins MD**, **Wright PF**, **Karzon DT**. 1988. Primary respiratory syncytial virus infection in mice. J Med Virol **26**:153–62.

178. **Taylor G**, **Stott EJ**, **Hughes M**, **Collins AP**. 1984. Respiratory syncytial virus infection in mice. Infect Immun **43**:649–655.

179. **Mestas J**, **Hughes CCW**. 2004. Of mice and not men: differences between mouse and human immunology. J Immunol **172**:2731–8.

180. **Everard ML**, **Swarbrick A**, **Wrightham M**, **McIntyre J**, **Dunkley C**, **James PD**, **Sewell HF**, **Milner AD**. 1994. Analysis of cells obtained by bronchial lavage of infants with respiratory syncytial virus infection. Arch Dis Child **71**:428–432.

181. **Irvin CG**, **Bates JH**. 2003. Measuring the lung function in the mouse: the challenge of size. Respir Res. BioMed Central.

182. **Boukhvalova MS**, **Prince GA**, **Blanco JCG**. 2009. The cotton rat model of respiratory viral infections. Biologicals **37**:152–9.

183. **Prince GA**, **Jenson a B**, **Horswood RL**, **Camargo E**, **Chanock RM**. 1978. The pathogenesis of respiratory syncytial virus infection in cotton rats. Am J Pathol **93**:771–91.

184. **Belshe RB**, **Richardson LS**, **London WT**, **Sly DL**, **Lorfeld JH**, **Camargo E**, **Prevar DA**, **Chanock RM**. 1977. Experimental respiratory syncytial virus infection of four species of primates. J Med Virol **1**:157–162.

185. **Clarke CJ**, **Watt NJ**, **Meredith A**, **McIntyre N**, **Burns SM**. 1994. Respiratory syncytial virus-associated bronchopneumonia in a young chimpanzee. J Comp Pathol **110**:207–212.

186. **Byrd LG**, **Prince GA**. 1997. Animal models of respiratory syncytial virus infection. Clin Infect Dis **25**:1363–8.

187. **Bem R a**, **Domachowske JB**, **Rosenberg HF**. 2011. Animal models of human respiratory syncytial virus disease. Am J Physiol Lung Cell Mol Physiol **301**:L148–56.

188. **Derscheid RJ**, **Ackermann MR**. 2012. Perinatal lamb model of respiratory syncytial virus (RSV) infection. Viruses **4**:2359–78.

189. **You D**, **Becnel D**, **Wang K**, **Ripple M**, **Daly M**, **Cormier SA**. 2006. Exposure of neonates to respiratory syncytial virus is critical in determining subsequent airway response in adults. Respir Res **7**:107.

190. **Taylor G**. 2013. Bovine model of respiratory syncytial virus infection. Curr Top Microbiol Immunol **372**:327–45.

CHAPTER 3

A RESPIRATORY SYNCYTIAL VIRUS (RSV) VACCINE BASED ON PARAINFLUENZA VIRUS 5[1]

[1]Phan S.I., Chen Z., Xu P., Li Z., Gao X., Foster S.L., Teng M.N., Tripp R.A., Sakamoto K., He B. 2014. *Vaccine*. 32:3050–3057. Reprinted here with permission of the publisher.

Abstract

Human respiratory syncytial virus (RSV) is a leading cause of severe respiratory disease and hospitalizations in infants and young children. It also causes significant morbidity and mortality in elderly and immune compromised individuals. No licensed vaccine currently exists. Parainfluenza virus 5 (PIV5) is a paramyxovirus that causes no known human illness and has been used as a platform for vector-based vaccine development. To evaluate the efficacy of PIV5 as a RSV vaccine vector, we generated two recombinant PIV5 viruses - one expressing the fusion (F) protein and the other expressing the attachment glycoprotein (G) of RSV strain A2 (RSV A2). The vaccine strains were used separately for single-dose vaccinations in BALB/c mice. The results showed that both vaccines induced RSV antigen-specific antibody responses, with IgG2a/IgG1 ratios similar to those seen in wild-type RSV A2 infection. After challenging the vaccinated mice with RSV A2, histopathology of lung sections showed that the vaccines did not exacerbate lung lesions relative to RSV A2-immunized mice. Importantly, both F and G vaccines induced protective immunity. Therefore, PIV5 presents an attractive platform for vector-based vaccines against RSV infection.

Introduction

Respiratory syncytial virus (RSV) is the most important cause of pediatric respiratory virus infection, and is a major cause of morbidity and mortality among infants, immune compromised individuals, and the elderly (1). In the early 1960s, vaccination of infants with a formalin-inactivated RSV vaccine not only failed to protect against RSV disease during the following RSV season, but some vaccinees developed enhanced disease upon natural infection, resulting in increased rates of severe pneumonia and two deaths (2). In the intervening years, a number of different approaches have been evaluated, including subunit vaccines, vectored vaccines, and live attenuated vaccines. However, there remains no licensed RSV vaccine. Therefore, there is a pressing need for a safe and effective vaccine for RSV.

Parainfluenza virus 5 (PIV5), a negative-sense, non-segmented, single-stranded RNA virus, is a good viral vector for vaccine development. PIV5 is safe, as it infects a large number of mammals without being associated with any disease except canine kennel cough (3-7). Humans have been exposed to PIV5 (8-10), likely due to the wide use of kennel cough vaccines containing live PIV5, which dogs can shed after vaccination (11). Given anti-PIV5 immunity in humans, anti-vector immunity may be a problem. Our recent studies indicate that pre-existing immunity to PIV5 does not negatively affect immunogenicity of a PIV5-based vaccine in dogs, demonstrating that pre-existing immunity is not a concern for using PIV5 as a vector (12). This result is consistent with the report that neutralizing antibodies against PIV5 do not prevent PIV5 infection in mice (13).

PIV5 has been used as a platform for developing vector-based vaccines against other viruses. A single-dose immunization of PIV5 expressing the rabies virus glycoprotein G protects mice against lethal rabies virus challenge (14). Additionally, a single-dose inoculation of PIV5 expressing hemagglutinin (HA) or the NP protein of influenza virus protects against lethal H5N1 challenge in mice (15, 16). Importantly, intranasal administration of PIV5 is effective for eliciting robust mucosal immune responses (17), and is therefore ideal for vaccinating against respiratory pathogens.

Since an anti-RSV-F monoclonal antibody has been used to control RSV infection, it may be possible to develop an RSV vaccine by targeting RSV-F. Although several studies have implicated the G protein in RSV disease pathogenesis (18-21), prophylactic or therapeutic treatment with a monoclonal antibody (mAb 131-2G) specific to RSV-G mediates virus clearance, and decreases leukocyte trafficking and IFN-γ production in the lungs of RSV-infected mice (22-26). In this study, we have tested the efficacies of recombinant PIV5 expressing RSV-F (rPIV5-RSV-F) or RSV-G (rPIV5-RSV-G) as potential vaccines in mice.

Materials and Methods

Cells and viruses

BSR-T7 cells were maintained in Dulbecco's modified Eagle medium (DMEM) containing 10% fetal bovine serum (FBS), 10% tryptose phosphate broth (TPB), 100 IU/mL penicillin, 100 μg/mL streptomycin (1% P/S; Mediatech Inc., Manassas, VA), and 400 μg/mL G418 sulfate (Mediatech, Inc.). MDBK, BHK21, and Vero cells were maintained in the same media without TPB or G418.

To construct the plasmids for rescuing rPIV5-RSV-F or rPIV5-RSV-G, the coding sequence of the green fluorescent protein (GFP) gene in the BH311 plasmid (27), containing GFP between HN and L of the full-length PIV5 genome, was replaced with the RSV-F or RSV-G gene, respectively. rPIV5-RSV-F and rPIV5-RSV-G were rescued as described previously (28). PIV5, rPIV5-RSV-F, and rPIV5-RSV-G were grown in in MDBK cells as described previously (27). RSV A2 and rA2-Luc (RSV A2 expressing *Renilla* luciferase) were grown in Vero cells as previously described (29).

Immunoprecipitation and Western blots

Immunoprecipitation (IP) was performed as previously described (30). A549 cells were infected with rPIV5-RSV-F or RSV A2 in 6-cm dishes. After 18 to 20 hours, the cells were starved and metabolically labeled with ^{35}S-Met and ^{35}S-Cys for 3 hours. The cells were lysed with whole-cell extraction buffer (WCEB; 50 mM Tris-HCl [pH 8], 280 mM NaCl, 0.5% NP-40, 0.2 mM EDTA, 2 mM EGTA, 10% glycerol) (31) and immunoprecipitated with anti-RSV-F antibody. The IP products were resolved on a 10% SDS-PAGE gel and visualized using a Typhoon 9700 Phosphorimager (GE Healthcare Life Sciences, Piscataway, NJ).

To examine RSV-G protein expression, rPIV5-RSV-G-infected MDBK cells and RSV A2-infected A549 cells were lysed with WCEB. The lysates were processed and resolved by SDS-PAGE as described before. The proteins were transferred onto a polyvinylidene difluoride (PVDF) membrane and detected using mouse anti-RSV-G antibody (1:2,000 dilution) as previously described (14).

Recombinant PIV5 growth curves and plaque assays

Six-well plates of Vero cells were infected with rPIV5-RSV-F, rPIV5-RSV-G, or PIV5 at a MOI = 5 or 0.01. One hundred μL samples of supernatant were collected at 0, 24, 48, 72, 96, and 120 hours post-infection. Virus was quantified by plaque assay as described in Chen et al. (14).

Immunization of mice

All animal experiments were performed according to the protocols approved by the Institutional Animal Care and Use Committee at the University of Georgia. Six to eight week-old female BALB/c mice (Harlan Laboratories, Indianapolis, IN) were anesthetized by intraperitoneal injection of 200 μL of 2, 2, 2-tribromoethanol in tert-amyl alcohol (Avertin). Immunization was performed by intranasal administration of 10^6 PFU of rPIV5-RSV-F, rPIV5-RSV-G, or RSV A2 in a 50 μL volume. Negative controls were treated intranasally with 50 μL of PBS.

Three weeks post-immunization, blood was collected via the tail vein for serological analysis. Four weeks post-immunization, all mice were challenged intranasally with 10^6 PFU of RSV A2 in a 50 μL volume. Four days later, lungs were collected from 5 mice per group to assess viral burden. The lungs of the other 5 mice in each group were perfused with 10% formalin solution and submitted for histology. To detect neutralizing antibody titers, mice were immunized as described above and terminally bled 4 weeks post-immunization.

ELISAs measuring total RSV antigen-specific IgG, IgG1 and IgG2a

RSV-F and RSV-G-specific serum antibody titers were measured by ELISA. Immulon® 2HB 96-well microtiter plates were coated with 100 μL of purified RSV-F or

G protein at 1 μg/ml in PBS (29) and incubated overnight at 4°C. Two-fold serial dilutions of serum were made in blocking buffer (5% nonfat dry milk, 0.5% BSA in wash buffer; KPL, Inc., Gaithersburg, MD). One hundred μL of each dilution was transferred to the plates and incubated for one hour at room temperature. After aspirating the samples, the plates were washed three times with wash buffer. Secondary antibody was diluted 1:1,000 [alkaline phosphatase-labeled goat anti-mouse IgG (KPL, Inc.) or horseradish-peroxidase-labeled goat anti-IgG1 or IgG2a (SouthernBiotech, Birmingham, AL)] in blocking buffer. One hundred μL of diluted secondary antibody was added to each well, and the plates were incubated for one hour at room temperature. After aspiration, the plates were washed and developed with 100 μL of pNpp substrate or SureBlue Reserve TMB substrate (KPL, Inc.) at room temperature. The OD was read at 405 nm or 450 nm using a BioTek Epoch microplate reader. The endpoint antibody titer was defined as the highest serum dilution at which the OD was greater than two standard deviations above the mean OD of the naïve serum.

Neutralizing antibody assay

Two-fold serial dilutions of serum were made starting at a 1:10 dilution with Opti-MEM supplemented with 1% BSA and 5% guinea pig complement (Sigma-Aldrich, St. Louis, MO). The diluted serum was incubated with 100 $TCID_{50}$ of RSV A2 expressing *Renilla* luciferase (rA2-Rluc) for one hour at 37°C, 5% CO_2 (32). The serum and virus mixture was transferred to confluent monolayers of Vero cells in 96-well plates and incubated for 18 hours at 37°C, 5% CO_2. The cells were then lysed with 70 μL/well of *Renilla* lysis buffer for 20 minutes while shaking on an orbital shaker. The lysates were transferred to V-bottom plates and clarified by centrifugation at 2000 x g for 5

minutes. Forty μL of clarified lysate was transferred to Costar® white 96-well assay plates (Corning, Inc., Corning, NY) and read using a GloMax® 96 microplate luminometer (Promega). Neutralizing antibody titers were reported as the highest serum dilution at which the luminescence measurement was lower than that of 50 $TCID_{50}$ of rA2-Rluc based on a standard curve. Cells treated with 100 $TCID_{50}$ of UV-inactivated rA2-Luc were the negative control.

Titration of RSV from mouse lungs

Mouse lungs were harvested aseptically into gentleMACS M tubes (Miltenyi Biotec Inc., Auburn, CA) containing 3 mL of Opti-MEM with 1% BSA and stored on ice. Lungs were homogenized at 4°C using the Protein_01 program of a gentleMACS Dissociator (Miltenyi Biotec Inc.) and then centrifuged at 3000 x g for 10 minutes. RSV titers in the supernatants were determined using plaque assay as described in Johnson et al., except the media was 0.8% methylcellulose in Opti-MEM with 2% FBS, 1% P/S (33).

Histology

Four days post-challenge, the lungs from the mice were perfused with 1 mL of 10% formalin and then immersed in 10% formalin for at least 24 hours. The formalin-fixed lungs were transferred to 70% ethanol, embedded in paraffin wax, sectioned, and stained with hematoxylin and eosin. A pathologist scored the sections in a group-blind fashion for perivascular cuffing, interstitial pneumonia, bronchiolitis, alveolitis, vasculitis and pleuritis. The lesions were scored on a scale of 0 to 4, with 0 indicating no lesions and 4 indicating severe lesions.

Statistical analysis

Statistical analysis was performed using GraphPad Prism software version 5.04 for Windows (GraphPad Software, La Jolla, CA). Analysis of variance (ANOVA) and Tukey multiple comparison tests were used to analyze total serum IgG, IgG1 or IgG2a antibody titers and lung viral loads. Unpaired, two-tailed t-test was used to analyze neutralizing antibody titers. Histology data was analyzed using the Kruskal-Wallis test.

Results

Construction and characterization of recombinant PIV5-based RSV vaccine viruses

RSV-F and RSV-G genes from RSV A2 were cloned into a plasmid containing the PIV5 backbone. The genes were inserted in between the HN and L genes, and the viruses were rescued by methods previously described (Fig. 3.1A) (28). RSV-F expression in rPIV5-RSV-F-infected cells was confirmed by immunoprecipitation with an RSV-F-specific monoclonal antibody (Fig. 3.1B). Expression of RSV-G in rPIV5-RSV-G-infected cells was shown by Western blot using an RSV-G-specific monoclonal antibody (Fig. 3.1C). RSV-G expressed in rPIV5-RSV-G-infected cells displayed both wild-type size and glycosylation pattern.

Single-step and multi-step growth rates of rPIV5-RSV-F, rPIV5-RSV-G, and PIV5 were compared. In the single-step growth curve, both rPIV5-RSV-F and rPIV5-RSV-G displayed slightly delayed growth kinetics at 24 hours compared to PIV5, and grew to similar, though slightly decreased, titers by 48 hours (Fig. 3.1D). This growth delay was also evident in the multi-step growth curve at 24 hours, but both the rPIV5-RSV-F and rPIV5-RSV-G grew to titers similar to PIV5 by 48 hours (Fig. 3.1E). Therefore, growth kinetics of the rPIV5-RSV-F and rPIV5-RSV-G were similar to that of

PIV5, although with a slight delay at early time points and a slight decrease in final viral titer.

Immunization with recombinant PIV5-based RSV vaccine viruses induces RSV antigen-specific antibody responses

Total serum IgG antibody titers to RSV were measured 21 days post-vaccination. Mice immunized with rPIV5-RSV-F developed F-specific serum IgG antibodies, although to a lesser degree (~ 2-fold lower) than RSV A2-immunized mice (Fig. 3.2A and 3.2B). Interestingly, mice vaccinated with rPIV5-RSV-G developed G-specific antibody titers slightly higher (~ 2-fold) than those seen in mice immunized with RSV A2 (Fig. 3.2C and 3.2D). Mice treated with PBS had no detectable RSV-specific antibodies (Fig. 3.2A-D).

Immunization with the recombinant vaccine viruses induced RSV antigen-specific IgG2a/IgG1 antibody ratios similar to those observed in RSV A2-immunized mice. Overall, RSV-F-specific IgG1 and IgG2a titers were lower in rPIV5-RSV-F-immunized mice compared to the RSV A2-immunized mice (Fig. 3.3A). RSV-G-specific IgG1 and IgG2a titers in rPIV5-RSV-G and RSV A2-immunized mice were similar (Fig. 3.3B). Mean RSV-F-specific IgG2a/IgG1 ratios in rPIV5-RSV-F and RSV A2-vaccinated groups were 13 and 5, respectively, with no significant difference between the two groups (Fig. 3.3C). Mean RSV-G-specific IgG2a/IgG1 ratios of groups vaccinated with rPIV5-RSV-G or RSV A2 were 0.49 and 0.48, respectively (Fig. 3.3D). The IgG2a/IgG1 ratios induced by the rPIV5 vaccine candidates did not differ significantly from those observed in RSV A2 infection, which is known to generate balanced IgG2a/IgG1 responses.

Immunization with rPIV5-RSV-F generates RSV-neutralizing antibodies

A complement-enhanced microneutralization assay was performed to determine if serum antibodies induced by immunization were able to neutralize RSV A2 expressing *Renilla* luciferase (rA2-Rluc) *in vitro*. By 28 days post-immunization, mice immunized with rPIV5-RSV-F or RSV A2 generated neutralizing antibodies against rA2-Rluc. The antibody titers of the rPIV5-RSV-F-immunized group did not differ significantly from the titers of the RSV A2-immunized group. No neutralizing activity was detected in the sera of rPIV5-RSV-G-immunized mice (Fig. 3.4).

Recombinant PIV5-based RSV vaccine viruses induce protective immunity in the mouse lung

Four days post-challenge, RSV A2 titers were measured in the lungs to assess the efficacy of the recombinant vaccine viruses in reducing viral burden. Mice vaccinated with either rPIV5-RSV-F or rPIV5-RSV-G had no detectable challenge virus in the lungs. In the RSV A2-immunized group, one mouse had a viral titer of 90 PFU/lung, while all other mice in the group had no detectable virus. Mice with PBS had an average viral titer of $4.5x10^3$ PFU/lung (Fig. 3.5). Therefore, immunization with the vaccine candidates induced potent immunity against RSV A2 challenge.

Mice immunized with recombinant PIV5-based RSV vaccine viruses or RSV A2 display similar lung lesions

Lung histology was performed to determine if immunization with the recombinant vaccine viruses affected RSV-induced lung pathology. At low magnification, tissue from mice vaccinated with RSV A2 or the rPIV5 viruses showed similar levels of inflammatory infiltrates 4 days post-challenge. Lung tissue from the mock-vaccinated

mice was the least inflamed (Fig. 3.6A-D), suggesting that vaccinated animals had likely generated immune responses to RSV challenge.

At high magnification, the inflammation in the mice vaccinated with RSV A2 or the recombinant vaccine viruses was characterized most prominently by perivascular cuffing (Fig. .3.7A and 3.7B). The leukocytes surrounding the pulmonary blood vessels consisted of mostly lymphocytes and macrophages, with few neutrophils and eosinophils. Mild-to-moderate interstitial pneumonia (Fig. 3.7A and 3.9C) and little-to-no bronchiolitis (Fig. 3.7A and 3.7D) was observed in all groups. Tissue sections were also scored for alveolitis, pleuritis, and vasculitis (Fig. 3.7E-G). There were no significant differences in the histopathology scores of mice vaccinated with the recombinant vaccine viruses relative to the RSV A2-vaccinated controls.

Discussion

The most advanced area of investigation for RSV vaccine candidates is live attenuated viruses. These viruses have several benefits: 1) enhanced RSV disease has not been observed either after natural infection or vaccination with live attenuated viruses (34-36); 2) live attenuated RSV vaccines induce balanced immune responses that more closely match natural immunity compared with subunit or inactivated vaccines (37, 38); 3) intranasal vaccination with live attenuated viruses should induce better local immunity compared with intramuscular injection of subunit vaccines. Live attenuated RSV vaccines have been in development for several decades, using a combination of cold passage (*cp*) and chemical mutagenesis to induce temperature sensitivity (*ts*). A number of *cpts* RSV vaccine candidates have been tested clinically. The *cpts* 248/404 candidate was sufficiently attenuated in adults and sero-negative children and tested in 1 to 3-

month-old infants. However, *cpts* 248/404 caused nasal congestion in these infants, an unacceptable adverse effect (34).

More recently, the advent of reverse genetics systems for RSV, whereby infectious virus is derived from cDNAs, has allowed the development of live attenuated RSV vaccine candidates encoding specific combinations of attenuating mutations and deletions of nonessential viral genes. RSV lacking NS2 (rA2ΔNS2) was tested in clinical trials as a vaccine for the elderly, since it was less attenuated in chimpanzees than *cpts* 248/404. It was shown to be over-attenuated in adults but under-attenuated in children, a contraindication for testing in infants (39).

Subunit and other synthetic vaccines have shown only moderate immunogenicity in clinical trials, even with the development of newer adjuvant regimens. Vectored vaccines expressing RSV F and/or G have been generated based on paramyxoviruses, such as Sendai virus (SeV), Newcastle disease virus (NDV), and a chimeric recombinant bovine parainfluenza virus 3 (PIV3) expressing human PIV3 F/HN and RSV-F (MEDI-534). Sendai virus expressing RSV-F or G protected the lower respiratory tract (LRT) of cotton rats against RSV infection. SeV-RSV-F also conferred LRT protection in African green monkeys (41). Immunization of mice with NDV expressing RSV-F was only modestly effective, reducing RSV burden in lungs by approximately 1 $\log_{10}$ (40). MEDI-534 was attenuated and safe in clinical trials, but it was only minimally immunogenic in adults and children (42). Furthermore, the vaccine candidate genome was unstable, with mutations observed *in vivo* and *in vitro* (43, 44). Thus, while many RSV vaccine candidates have been researched extensively, an important public health gap remains for RSV disease prevention.

This work demonstrated that PIV5-based RSV vaccine candidates provide a promising alternative for RSV vaccine development. Single-dose immunization with rPIV5-RSV-F or rPIV5-RSV-G induced potent immunity against RSV challenge in mice. Importantly, the recombinant vaccine viruses did not exacerbate lung lesions relative to the RSV A2-immunized controls. Natural infection with RSV does not lead to enhanced disease upon reinfection, in contrast to immunization with formalin-inactivated RSV (45). Inflammation in the lung tissue of mice immunized with the vaccine candidates was likely due to the induction of host immunity in response to RSV challenge.

Serum neutralizing antibodies were generated in rPIV5-RSV-F-immunized mice, suggesting that the vaccine candidate induces a functional, systemic humoral response against RSV. Immunization with rPIV5-RSV-G did not generate neutralizing antibodies, but reduced viral burden in the lungs. The mechanism is unclear, but rPIV5-RSV-G immunization may generate protective antibodies that are non-neutralizing *in vitro*. In the case of the RSV-G subunit vaccine candidate, BBG2Na, passively transferred serum from immunized mice reduced lung viral burden in recipient mice at dilutions negative for neutralizing activity (46). Other groups have also shown that neutralizing activities of RSV-G or RSV-F-specific antibodies *in vitro* do not necessarily correlate with lung protection *in vivo* (47-49).

In summary, PIV5 is safe, stable, efficacious, cost-effective to produce, and overcomes pre-existing anti-vector immunity. In this work, we have shown that PIV5-based RSV vaccine candidates have the potential to be an effective RSV vaccine, providing an additional option for RSV vaccine development.

Acknowledgements

We appreciate the helpful discussion and technical assistance from all members of Biao He's laboratory. This work was partially supported by grants from the National Institute of Allergy and Infectious Disease (R01AI070847) to B.H. and (R01AI081977) to M.N.T.

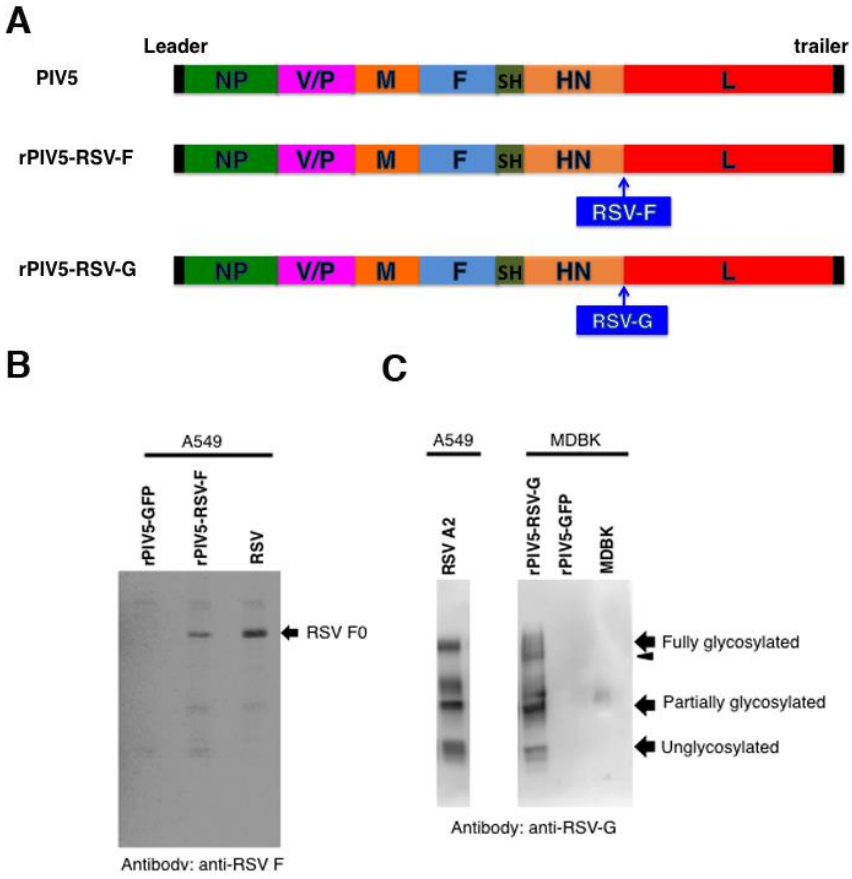
A
Leader
trailer
PIV5
NP
V/P
M
F
SH
HN
L
rPIV5-RSV-F
RSV-F
rPIV5-RSV-G
RSV-G
B
A549
rPIV5-GFP
rPIV5-RSV-F
RSV
RSV F0
Antibody: anti-RSV F
C
A549
MDBK
RSV A2
rPIV5-RSV-G
rPIV5-GFP
MDBK
Fully glycosylated
Partially glycosylated
Unglycosylated
Antibody: anti-RSV-G
D
1.00E+08
1.00E+07
1.00E+06
1.00E+05
1.00E+04
1.00E+03
1.00E+02
1.00E+01
1.00E+00
0
24
48
72
96
120
Time (hours)
PIV5
rPIV5-RSV-F
rPIV5-RSV-G
Limit of Detection
E
1.00E+08
1.00E+07
1.00E+06
1.00E+05
1.00E+04
1.00E+03
1.00E+02
1.00E+01
1.00E+00
0
24
48
72
96
120
Time (hours)
PIV5
rPIV5-RSV-F
rPIV5-RSV-G
Limit of Detection

Figure 3.1. Generation of rPIV5-RSV-F and rPIV5-RSV-G. (A) Schematic of rPIV5-RSV-F and rPIV5-RSV-G. NP, nucleoprotein; V, V protein; P, phosphoprotein; M, matrix protein; F, fusion protein; SH, small hydrophobic protein; HN, hemagglutinin-neuraminidase protein; L, RNA-dependent RNA polymerase; RSV-F, respiratory syncytial virus fusion protein; RSV-G, respiratory syncytial virus G attachment glycoprotein. (B) RSV-F expression in rPIV5-RSV-F-infected A549 cells was detected by immunoprecipitation. rPIV5-RSV-F-infected cells were starved and labeled with ^{35}S-Met and ^{35}S-Cys at 18 to 20 hours post-infection. Proteins from cell lysate were immunoprecipitated with mouse anti-RSV-F antibody, and expression was visualized by ^{35}S incorporation. Lysate from RSV A2-infected A549 cells was the positive control. Lysate from rPIV5-GFP-infected A549 cells was the negative control. (C) Detection of RSV-G expression by Western blot. MDBK cells were infected with rPIV5-RSV-G, and lysate was immunoblotted with mouse anti-RSV-G antibody. Lysate from RSV A2-infected A549 cells was the positive control. Lysate from rPIV5-GFP-infected MDBK cells was the negative control. (D) Single-cycle growth curves of rPIV5-RSV-F and rPIV5-RSV-G in Vero cells. Vero cells were infected at a MOI = 5. Aliquots of cell culture supernatant were collected at 24-hour intervals for 120 hours. (E) Multi-cycle growth curves of rPIV5-RSV-F and rPIV5-RSV-G in Vero cells. Vero cells were infected at a MOI = 0.01. Aliquots of cell culture supernatant were collected at 24-hour intervals for 120 hours. Plaque assays were performed in BHK21 cells to determine the virus titer at each time point. Growth curve samples were assayed in duplicate. Error bars represent the standard error of the mean.

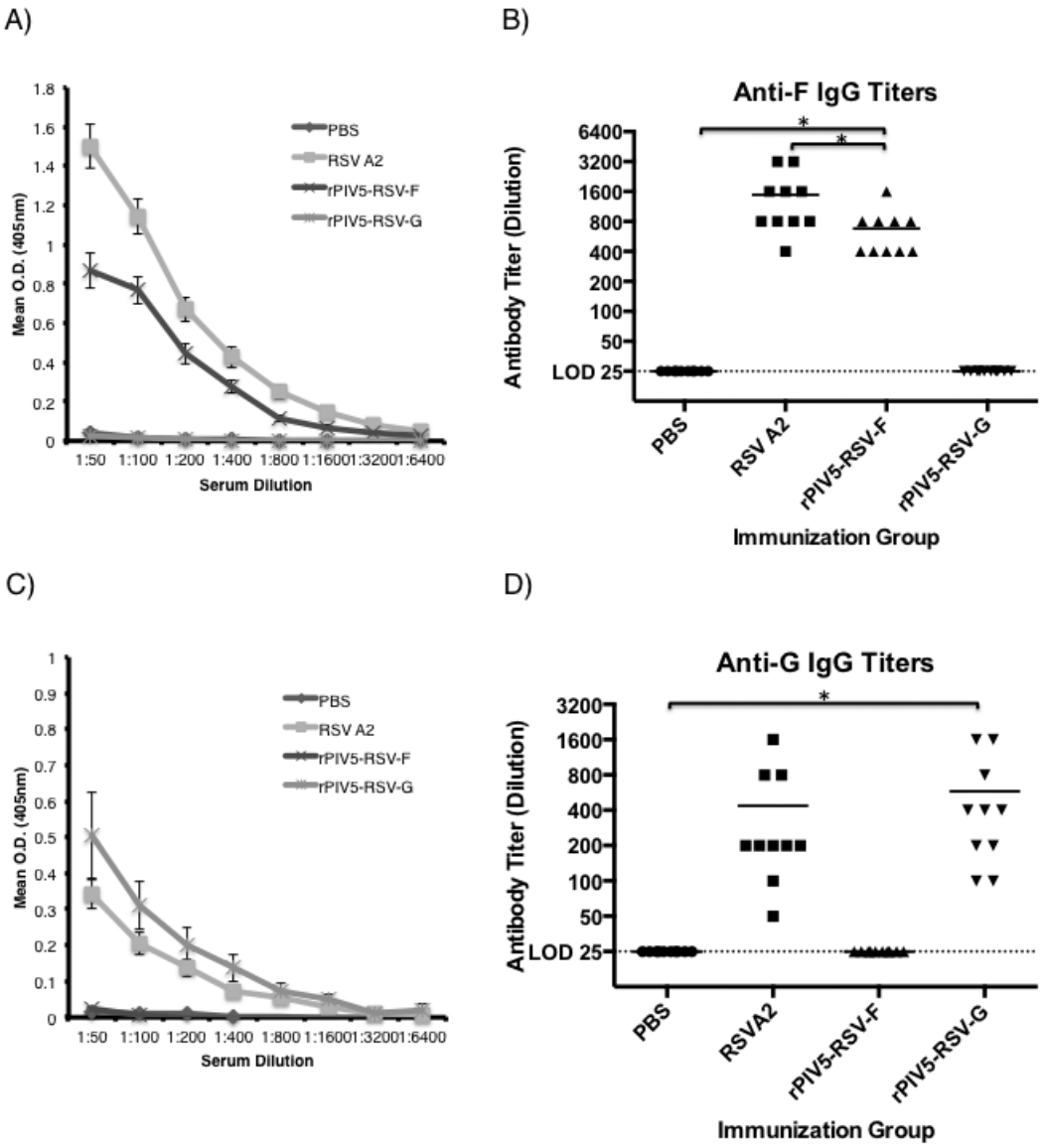

Figure 3.2. Immunization with rPIV5-RSV-F and rPIV5-RSV-G induces RSV antigen-specific IgG antibody responses in mice. Naïve BALB/c mice were treated with PBS or immunized intranasally with 10^6 PFU of rPIV5-RSV-F, rPIV5-RSV-G, or RSV A2. Sera were collected at 3 weeks post-immunization. (A) Anti-RSV-F IgG antibody curves were generated by ELISA using serially-diluted sera. (B) RSV-F-specific IgG antibody endpoint titers were determined based on the values in (A). (C) Anti-RSV-G IgG antibody curves were generated by ELISA. (D) RSV-G-specific IgG antibody endpoint

titers were determined based on the values in (C). Serum IgG was detected in (A) and (C) using goat anti-mouse IgG antibody conjugated to alkaline phosphatase. Each group consisted of 10 mice. Error bars in (A) and (C) represent standard error of the mean. Horizontal lines in (B and D) represent the mean antibody titer of each group. Statistical significance was determined by ANOVA and Tukey multiple comparison tests. *, $P < 0.05$. LOD, limit of detection.

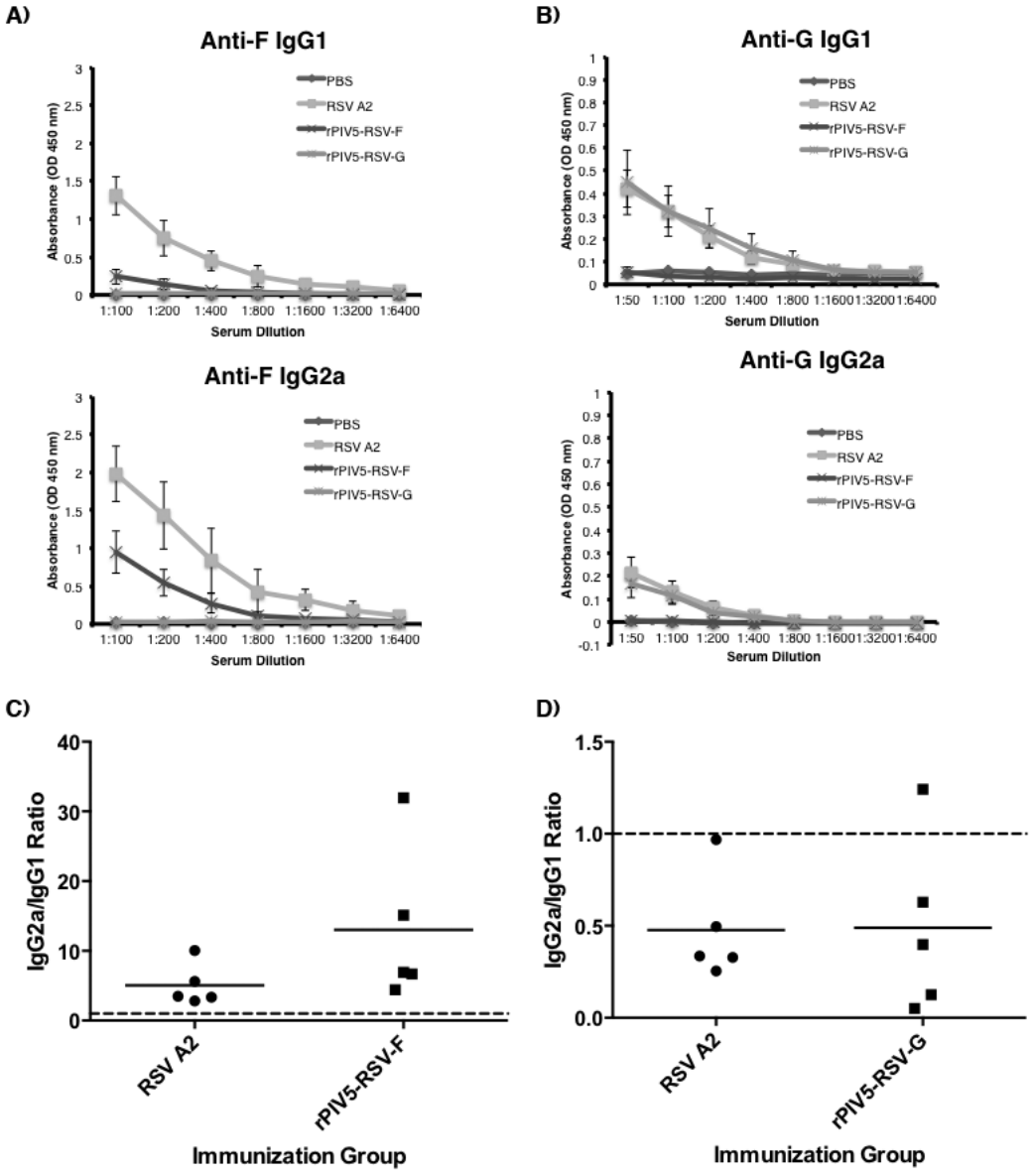

Figure 3.3. Immunization with rPIV5-RSV-F and rPIV5-RSV-G induce IgG1 and IgG2a antibody responses similar to RSV A2 infection. Naïve BALB/c mice were treated with PBS or immunized intranasally with 10^6 PFU of rPIV5-RSV-F, rPIV5-RSV-G, or RSV A2. Sera were collected 3 weeks post-immunization. (A, B) RSV-F (A) and RSV-G-specific (B) IgG1 and IgG2a antibody curves were generated by ELISA using isotype-specific secondary antibodies conjugated to HRP. (C, D) RSV-F (C) and RSV-G-specific (D) IgG2a/IgG1 ratios were calculated using values in (A) and (B), respectively. IgG1 and IgG2a antibodies in the sera were quantified using standard curves to generate IgG2a/IgG1 ratios. Each group consisted of 5 mice. Solid horizontal lines represent the mean of each group. Dotted horizontal lines indicate a ratio of 1.

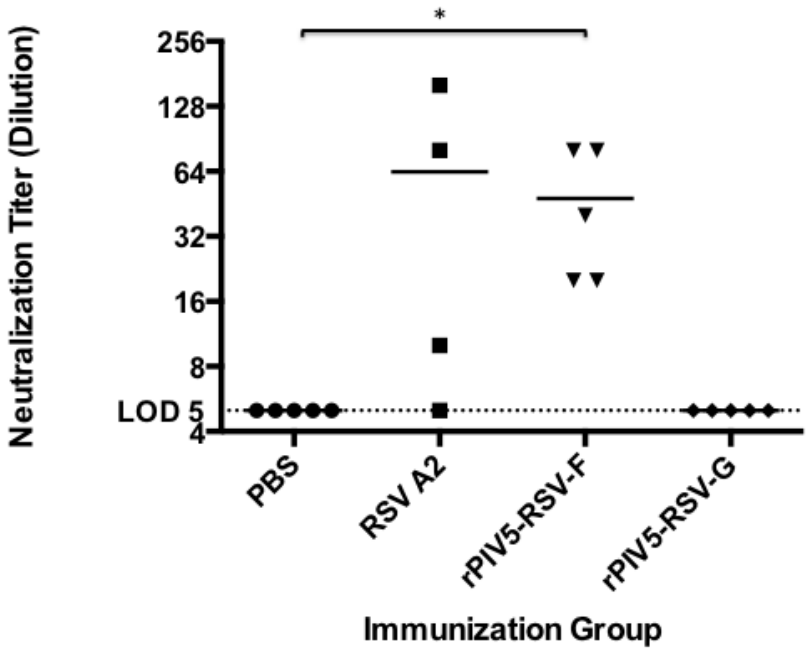

Figure 3.4. Immunization with rPIV5-RSV-F generates RSV-neutralizing antibodies. Naïve BALB/c mice were treated with PBS or immunized intranasally with 10^6 PFU of rPIV5-RSV-F, rPIV5-RSV-G, or RSV A2. At 4 weeks post-immunization, sera were collected and tested for RSV-neutralizing activity using a microneutralization assay. Neutralizing antibody titers were defined as the highest dilution of sera at which the luminescence measurement of the sample was less than that of 50 $TCID_{50}$ of rA2-Rluc using a standard curve. Each group consisted of 4 to 5 mice. All samples were assayed in duplicate. Horizontal lines represent the mean antibody titer of each group. Statistical significance was determined by unpaired, two-tailed t-test. *, $P < 0.05$. LOD, limit of detection.

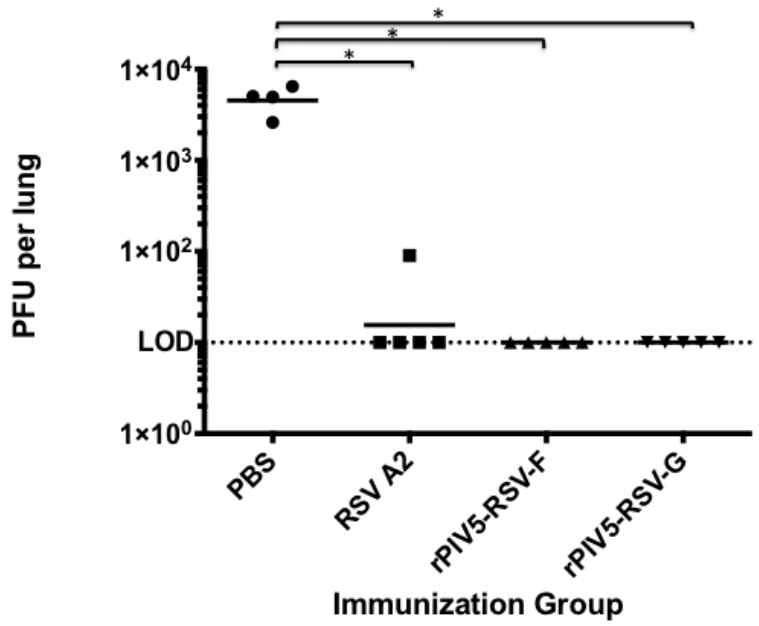

Figure 3.5. Immunization with rPIV5-RSV-F and rPIV5-RSV-G generates protective immunity against RSV A2 challenge. Naïve BALB/c mice were treated with PBS or immunized intranasally with 10^6 PFU of rPIV5-RSV-F, rPIV5-RSV-G, or RSV A2. At 4 weeks post-immunization, mice were challenged with 10^6 PFU of RSV A2. At 4 days post-challenge, lungs were harvested and viral load was determined by plaque assay in Vero cells. Each group consisted of 5 mice. Solid horizontal lines represent the geometric mean of each group. Statistical significance was determined by ANOVA and Tukey multiple comparison tests. *, $P < 0.05$. LOD, limit of detection.

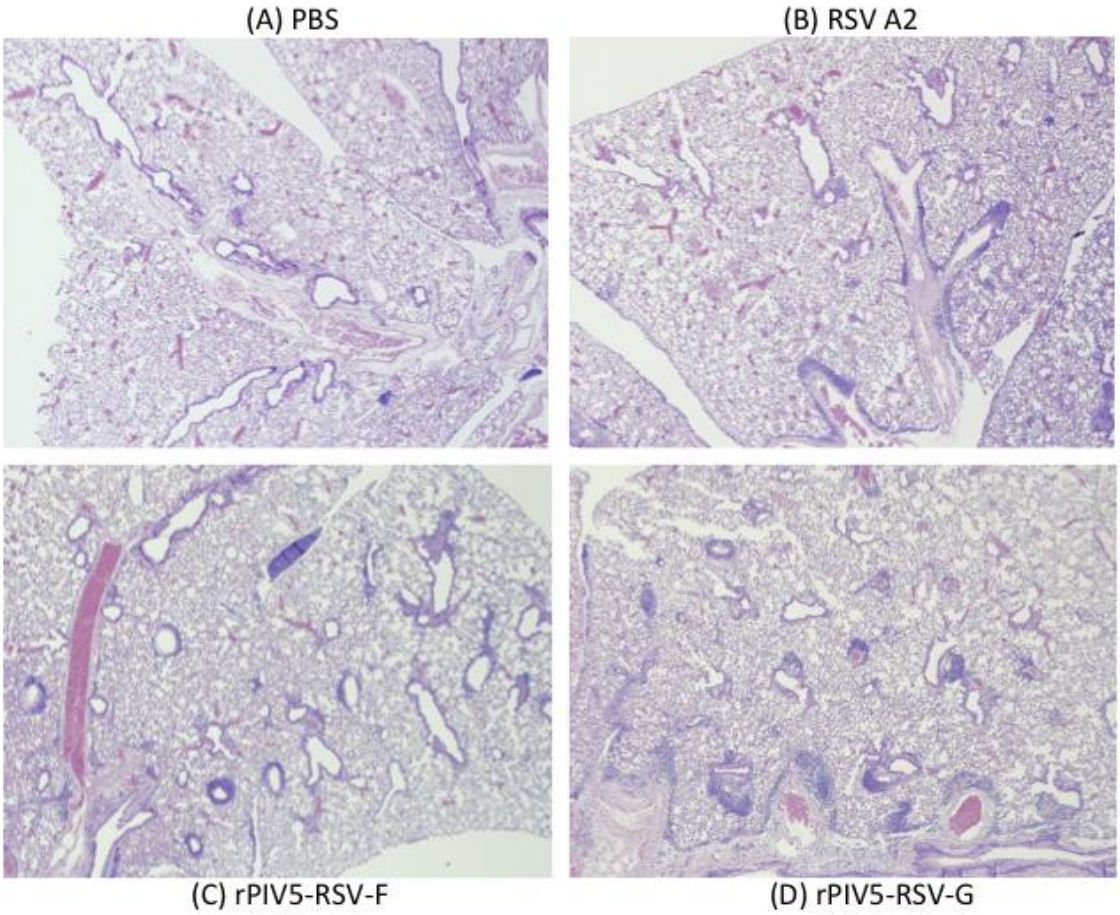

Figure 3.6. Low-magnification images of post-challenge lung lesions in mice treated with PBS or immunized with RSV A2, rPIV5-RSV-F or rPIV5-RSV-G. BALB/c mice were treated with PBS or immunized intranasally with 10^6 PFU of rPIV5-RSV-F, rPIV5-RSV-G, or RSV A2. Four weeks after immunization, mice were challenged with 10^6 PFU of RSV A2. At 4 days post-challenge, lungs were harvested and fixed with 10% formalin. Lung sections were stained with hematoxylin and eosin. Images were taken at 4x magnification. (A) Lung section from a mouse treated with PBS. (B) Lung section from a RSV A2-immunized mouse. (C) Lung section from a rPIV5-RSV-F-immunized mouse. (D) Lung section from a rPIV5-RSV-G-immunized mouse.

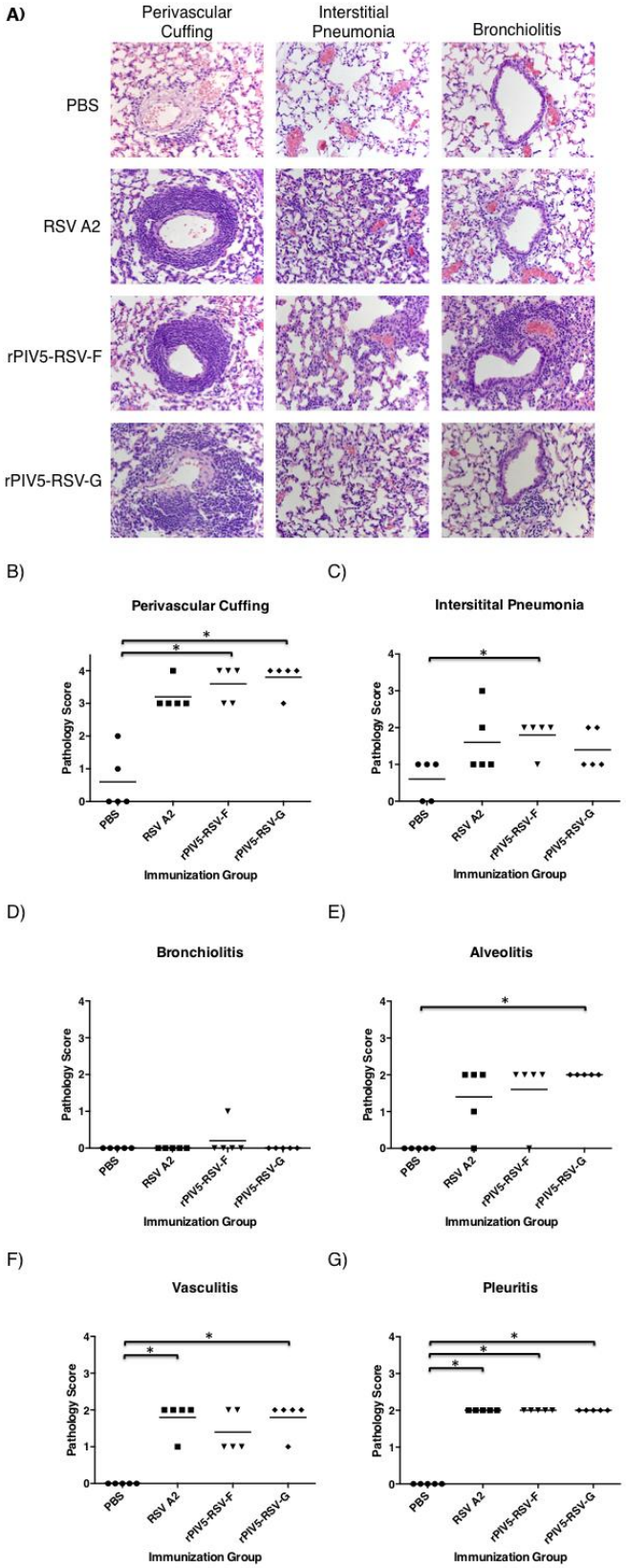
A)
Perivascular Cuffing
Interstitial Pneumonia
Bronchiolitis
PBS
RSV A2
rPIV5-RSV-F
rPIV5-RSV-G
B)
Perivascular Cuffing
C)
Intersititial Pneumonia
D)
Bronchiolitis
E)
Alveolitis
F)
Vasculitis
G)
Pleuritis
Pathology Score
Immunization Group
PBS
RSV A2
rPIV5-RSV-F
rPIV5-RSV-G

Figure 3.7. High-magnification images of post-challenge lung lesions in mice treated with PBS or immunized RSV A2, rPIV5-RSV-F or rPIV5-RSV-G. BALB/c mice were treated with PBS or immunized intranasally with 10^6 PFU of rPIV5-RSV-F, rPIV5-RSV-G, or RSV A2. Four weeks after immunization, mice were challenged with 10^6 PFU of RSV A2. Four days after challenge, lungs were harvested and fixed with 10% formalin. Lung sections were stained with hematoxylin and eosin. (A) Images in the far-left column show perivascular cuffing. Images in the middle column show interstitial pneumonia. Images in the far-right column show bronchiolitis. Each image is from a representative mouse in each group. Images of lung lesions were taken at 40x magnification. (B-G) Lung sections were scored in a group-blind fashion on a scale of 0 to 4 for perivascular cuffing (B), interstitial pneumonia (C), bronchiolitis (D), alveolitis (E), vasculitis (F), and pleuritis (G). Each group consisted of 5 mice. Horizontal lines represent the mean of each group. Statistical significance was determined using the Kruskal-Wallis test. *, $P < 0.05$.

References

1. **Collins PL, Chanock RM, Murphy BR. Respiratory syncytial virus. In: Knipe DM, Howley PM**, editors. Fields Virology. Fourth ed. Philadelphia: Lippincott, Williams and Wilkins; 2001. p. 1443-85.

2. **Kim HW, Canchola JG, Brandt CD, Pyles G, Chanock RM, Jensen K, et al.** Respiratory syncytial virus disease in infants despite prior administration of antigenic inactivated vaccine. Am J Epidemiol. 1969;89:422-34.
3. **Binn LN, Eddy GA, Lazar EC, Helms J, Murnane T.** Viruses recovered from laboratory dogs with respiratory disease. Proc Soc Exp Biol Med. 1967;126:140-5.
4. **Rosenberg FJ, Lief FS, Todd JD, Reif JS.** Studies of canine respiratory viruses. I. Experimental infection of dogs with an SV5-like canine parainfluenza agent. Am J Epidemiol. 1971;94:147-65.

5. **Cornwell HJ, McCandlish IA, Thompson H, Laird HM, Wright NG.** Isolation of parainfluenza virus SV5 from dogs with respiratory disease. Vet Rec. 1976;98:301-2.

6. **McCandlish IA, Thompson H, Cornwell HJ, Wright NG.** A study of dogs with kennel cough. Vet Rec. 1978;102:293-301.

7. **Azetaka M, Konishi S. Kennel cough complex: confirmation and analysis of the outbreak in Japan.** Nippon Juigaku Zasshi. 1988;50:851-8.

8. **Goswami KKA, Lange LS, Mitchell DN, Cameron KR, Russell WC. Does simian virus 5 infect humans.** J Gen Virol. 1984;65:1295-303.

9. **Goswami KK, Randall RE, Lange LS, Russell WC. Antibodies against the paramyxovirus SV5 in the cerebrospinal fluids of some multiple sclerosis patients.** Nature. 1987;327:244-7.

10. **Chen Z, Xu P, Salyards GW, Harvey SB, Rada B, Fu ZF, et al.** Evaluating a Parainfluenza Virus 5-Based Vaccine in a Host with Pre-Existing Immunity against Parainfluenza Virus 5. PLoS One. 2012;7:e50144.

11. **Chladek DW, Williams JM, Gerber DL, Harris LL, Murdock FM.** Canine parainfluenza-Bordetella bronchiseptica vaccine immunogenicity. Am J Vet Res. 1981;42:266-70.

12. **Young DF, Randall RE, Hoyle JA, Souberbielle BE.** Clearance of a persistent paramyxovirus infection is mediated by cellular immune responses but not by serum-neutralizing antibody. J Virol. 1990;64:5403-11.

13. **Chen Z, Zhou M, Gao X, Zhang G, Ren G, Gnanadurai CW, et al.** A novel rabies vaccine based on a recombinant parainfluenza virus 5 expressing rabies virus glycoprotein. Journal of virology. 2012.

14. **Li Z, Mooney AJ, Gabbard JD, Gao X, Xu P, Place RJ, et al.** Recombinant Parainfluenza Virus 5 Expressing Hemagglutinin of Influenza A Virus H5N1 Protected Mice against Lethal Highly Pathogenic Avian Influenza Virus H5N1 Challenge. Journal of virology. 2013;87:354-62.

15. **Li Z, Gabbard JD, Mooney A, Gao X, Chen Z, Place RJ, et al.** SIngle Dose Vaccination of A Recombinant Parainfluenza Virus 5 Expressing NP from H5N1 Provides Broad Immunity Against Influenza A VIruses. Journal of Virology. 2013;87.

16. **Mooney A, Li Z, Gabbard JD, He B, Tompkins SM.** Recombinant PIV5 vaccine encoding the influenza hemagglutinin protects against H5N1 highly pathogenic avian influenza virus infection when delivered intranasally or intramuscularly. J Virol. 2012;Epub ahead of print.

17. **Collins PL, Melero JA.** Progress in understanding and controlling respiratory syncytial virus: still crazy after all these years. Virus research. 2011;162:80-99.

18. **Castilow EM, Olson MR, Varga SM.** Understanding respiratory syncytial virus (RSV) vaccine-enhanced disease. Immunologic research. 2007;39:225-39.
19. Hurwitz JL. Respiratory syncytial virus vaccine development. Expert review of vaccines. 2011;10:1415-33.

20. **Tripp RA, Jones LP, Haynes LM, Zheng H, Murphy PM, Anderson LJ.** CX3C chemokine mimicry by respiratory syncytial virus G glycoprotein. Nature immunology. 2001;2:732-8.

21. **Choi Y, Mason CS, Jones LP, Crabtree J, Jorquera PA, Tripp RA.** Antibodies to the central conserved region of respiratory syncytial virus (RSV) G protein block RSV G protein CX3C-CX3CR1 binding and cross-neutralize RSV A and B strains. Viral immunology. 2012;25:193-203.

22. **Zhang W, Choi Y, Haynes LM, Harcourt JL, Anderson LJ, Jones LP, et al.** Vaccination to induce antibodies blocking the CX3C-CX3CR1 interaction of respiratory syncytial virus G protein reduces pulmonary inflammation and virus replication in mice. Journal of virology. 2010;84:1148-57.

23. **Harcourt JL, Karron RA, Tripp RA.** Anti-G protein antibody responses to respiratory syncytial virus infection or vaccination are associated with inhibition of G protein CX3C-CX3CR1 binding and leukocyte chemotaxis. The Journal of infectious diseases. 2004;190:1936-40.

24. **Haynes LM, Caidi H, Radu GU, Miao C, Harcourt JL, Tripp RA, et al.** Therapeutic monoclonal antibody treatment targeting respiratory syncytial virus (RSV) G protein mediates viral clearance and reduces the pathogenesis of RSV infection in BALB/c mice. The Journal of infectious diseases. 2009;200:439-47.

25. **Radu GU, Caidi H, Miao C, Tripp RA, Anderson LJ, Haynes LM.** Prophylactic treatment with a G glycoprotein monoclonal antibody reduces pulmonary inflammation in respiratory syncytial virus (RSV)-challenged naive and formalin-inactivated RSV-immunized BALB/c mice. Journal of virology. 2010;84:9632-6.

26. **He B, Paterson RG, Ward CD, Lamb RA.** Recovery of infectious SV5 from cloned DNA and expression of a foreign gene. Virology. 1997;237:249-60.

27. Sun D, Luthra P, Li Z, He B. PLK1 down-regulates parainfluenza virus 5 gene expression. PLoS Pathog. 2009;5:e1000525.

28. **Tripp RA, Jones LP, Haynes LM, Zheng H, Murphy PM, Anderson LJ.** CX3C chemokine mimicry by respiratory syncytial virus G glycoprotein. Nature immunology. 2001;2:732-8.

29. **Sun D, Luthra P, Xu P, Yoon H, He B.** Identification of a Phosphorylation Site within the P Protein Important for mRNA Transcription and Growth of Parainfluenza Virus 5. J Virol. 2011;85:8376-85.

30. **Ulane CM, Horvath CM.** Paramyxoviruses SV5 and HPIV2 assemble STAT protein ubiquitin ligase complexes from cellular components. Virology. 2002;304:160-6.

31. **Fuentes S, Crim RL, Beeler J, Teng MN, Golding H, Khurana S.** Development of a simple, rapid, sensitive, high-throughput luciferase reporter based microneutralization test for measurement of virus neutralizing antibodies following Respiratory Syncytial Virus vaccination and infection. Vaccine. 2013;31:3987-94.

32. **Johnson TR, Johnson JE, Roberts SR, Wertz GW, Parker RA, Graham BS.** Priming with secreted glycoprotein G of respiratory syncytial virus (RSV) augments interleukin-5 production and tissue eosinophilia after RSV challenge. Journal of Virology. 1998;72:2871-80.

33. **Wright PF, Karron RA, Belshe RB, Thompson J, Crowe JE, Jr., Boyce TG, et al.** Evaluation of a live, cold-passaged, temperature-sensitive, respiratory syncytial virus vaccine candidate in infancy. J Infect Dis. 2000;182:1331-42.

34. **Karron RA, Buonagurio DA, Georgiu AF, Whitehead SS, Adamus JE, Clements-Mann ML, et al.** Respiratory syncytial virus (RSV) SH and G proteins

are not essential for viral replication in vitro: clinical evaluation and molecular characterization of a cold-passaged, attenuated RSV subgroup B mutant. Proc Natl Acad Sci USA. 1997;94:13961-6.

35. **Wright PF, Shinozaki T, Fleet W, Sell SH, Thompson J, Karzon DT.** Evaluation of a live, attenuated respiratory syncytial virus vaccine in infants. J Pediatr. 1976;88:931-6.

36. **Johnson PR, Jr., Feldman S, Thompson JM, Mahoney JD, Wright PF.** Comparison of long-term systemic and secretory antibody responses in children given live, attenuated, or inactivated influenza A vaccine. J Med Virol. 1985;17:325-35.

37. **Johnson PR, Feldman S, Thompson JM, Mahoney JD, Wright PF.** Immunity to influenza A virus infection in young children: a comparison of natural infection, live cold-adapted vaccine, and inactivated vaccine. J Infect Dis. 1986;154:121-7.

38. **Wright PF, Karron RA, Madhi SA, Treanor JJ, King JC, O'Shea A, et al.** The interferon antagonist NS2 protein of respiratory syncytial virus is an important virulence determinant for humans. J Infect Dis. 2006;193:573-81.

39. **Martinez-Sobrido L, Gitiban N, Fernandez-Sesma A, Cros J, Mertz SE, Jewell NA, et al.** Protection against respiratory syncytial virus by a recombinant Newcastle disease virus vector. Journal of Virology. 2006;80:1130-9.

40. **Jones BG, Sealy RE, Rudraraju R, Traina-Dorge VL, Finneyfrock B, Cook A, et al.** Sendai virus-based RSV vaccine protects African green monkeys from RSV infection. Vaccine. 2012;30:959-68.

41. **Tang RS, Spaete RR, Thompson MW, MacPhail M, Guzzetta JM, Ryan PC, et al.** Development of a PIV-vectored RSV vaccine: preclinical evaluation of safety, toxicity, and enhanced disease and initial clinical testing in healthy adults. Vaccine. 2008;26:6373-82.

42. **Nelson CL, Tang RS, Stillman EA.** Genetic stability of RSV-F expression and the restricted growth phenotype of a live attenuated PIV3 vectored RSV vaccine candidate (MEDI-534) following restrictive growth in human lung cells. Vaccine. 2013.

43. **Yang CF, Wang CK, Malkin E, Schickli JH, Shambaugh C, Zuo F, et al.** Implication of respiratory syncytial virus (RSV) F transgene sequence heterogeneity observed in Phase 1 evaluation of MEDI-534, a live attenuated parainfluenza type 3 vectored RSV vaccine. Vaccine. 2013;31:2822-7.

44. **Collins PL, Graham BS.** Viral and host factors in human respiratory syncytial virus pathogenesis. Journal of Virology. 2008;82:2040-55.
45. **Power UF, Plotnicky-Gilquin H, Huss T, Robert A, Trudel M, Stahl S, et al.** Induction of protective immunity in rodents by vaccination with a prokaryotically expressed recombinant fusion protein containing a respiratory syncytial virus G protein fragment. Virology. 1997;230:155-66.

46. **Taylor G, Stott EJ, Bew M, Fernie BF, Cote PJ, Collins AP, et al**. Monoclonal antibodies protect against respiratory syncytial virus infection in mice. Immunology. 1984;52:137-42.

47. **Trudel M, Nadon F, Seguin C, Binz H.** Protection of BALB/c mice from respiratory syncytial virus infection by immunization with a synthetic peptide derived from the G glycoprotein. Virology. 1991;185:749-57.

48. **Routledge EG, Willcocks MM, Samson AC, Morgan L, Scott R, Anderson JJ, et al.** The purification of four respiratory syncytial virus proteins and their evaluation as protective agents against experimental infection in BALB/c mice. The Journal of general virology. 1988;69 (Pt 2):293-303.

CHAPTER 4

PIV5-BASED RSV VACCINES PROTECT COTTON RATS AND AFRICAN GREEN MONKEYS AGAINST RSV CHALLENGE[2]

[2]Phan S.I., Wang D., DiStefano D.J., Citron M.P., Callahan C.L., Indrawati L., Dubey S.A., Heidecker G.J., Govindarajan D., Liang X., He B., Espeseth A.S. To be submitted to *Journal of Virology.*

Abstract

Human respiratory syncytial virus (RSV) is a ubiquitous pathogen of the *Paramyxoviridae* family that commonly infects infants, the elderly, and the immunocompromised. No licensed vaccine exists. In this work, we evaluate two PIV5-based vaccine candidates expressing RSV-F (rPIV5-RSV-F) or RSV-G (rPIV5-RSV-G) for replication, immunogenicity, and protective efficacy in cotton rats and African green monkeys. The vaccine candidates replicated in the upper and lower respiratory tracts of both species without apparent symptoms. The vaccines were immunogenic and protective in cotton rats, conferring complete lower respiratory tract infection after one intranasal vaccine dose. In seronegative African green monkeys, the vaccines elicited high RSV-specific mucosal IgA titers and reduced RSV loads in the upper and lower respiratory tracts. The vaccines also boosted neutralizing antibody titers in seropositive African green monkeys. Overall, our data suggests that PIV5-based RSV vaccine candidates are immunogenic and efficacious, and may be suitable for immunizing RSV seronegative and seropositive populations.

Introduction

Human respiratory syncytial virus (RSV) is a common pathogen of the *Paramyxoviridae* family that routinely infects infants, elderly, and immunocompromised individuals. It is the leading cause of bronchiolitis and pneumonia in children under one year of age, and almost all children will be infected by two years of age. Re-infection throughout life is common (1, 2). There is no licensed vaccine or effective therapeutic, and supportive care is the only treatment. Administration of highly neutralizing immunoglobulin is used in a clinical setting to prevent infection in high-risk infants (3).

Vaccination is the best strategy to control infection, but RSV vaccine development has been fraught with challenges. A formalin-inactivated vaccine developed during the 1960s and tested in children caused enhanced disease in the vaccinees upon natural exposure to RSV (4–7). A number of vaccine candidates have been developed over the last fifty years including live attenuated vaccines, vectored vaccines, subunit vaccines, and virus-like particles (8–11). Each type of vaccine has advantages and drawbacks, and different strategies will need to be used to vaccinate different susceptible populations.

Infants comprise the most susceptible population. The goal of immunizing this group is to prevent severe respiratory complications caused by RSV infection. However, the presence of maternal antibodies and immunological immaturity can dampen the immune response to vaccination (12). Live vaccines are the most attractive approach in infants because they strongly induce innate and adaptive immunity. Furthermore, priming with a replicating vaccine is not associated with vaccine-induced enhanced disease (13, 14).

Elderly adults are also at risk for developing severe RSV disease (2). Vaccination of this group should prevent serious respiratory complications and reduce RSV transmission. Since pre-existing immunity to RSV precludes the use of a live attenuated vaccine, the most effective vaccines for elderly adults are likely subunit or live vectored vaccines. Immune senescence can lead to a sub-optimal vaccine response, so the ideal vaccine candidate should be able to stimulate robust immunity and boost pre-existing antibody levels (15, 16).

Parainfluenza virus 5 (PIV5) has been used as a vector for vaccines against influenza, rabies virus, RSV, and mycobacterium tuberculosis (17–25). PIV5 is a paramyxovirus that has been isolated from a number of animal species but causes no known disease (26–30). It has been associated kennel cough in dogs, but does not cause kennel cough (31–33). However this association led to its inclusion in the kennel cough vaccine for over 40 years without safety concerns for animals or humans. The natural host of PIV5 is unclear, but a study performed by Chen et al. detected PIV5 neutralizing antibodies in 30% of human serum samples. Host pre-existing antibodies against a vaccine vector can be problematic. However, it has been shown that dogs with pre-existing immunity to PIV5 can still mount robust humoral responses to a PIV5-based influenza vaccine (34).

Previous work has shown that two PIV5-based RSV vaccine candidates were immunogenic in BALB/c mice and conferred potent lower respiratory tract protection against RSV challenge. The vaccines consisted of inserting genes encoding the RSV fusion protein (F) or the attachment protein (G) in between the HN and L genes of PIV5 (24). In this study, we evaluated these vaccines in cotton rats and African green monkeys

for replication, immunogenicity, and protective efficacy against RSV infection. A single intranasal dose of either candidate was immunogenic and protective in both models, but the rPIV5-RSV-F candidate was more efficacious, warranting further investigation as an RSV vaccine.

Materials and Methods

Cells and viruses

The recombinant PIV5 vector expressing RSV F or G were constructed as previously described (25). The vaccine viruses were propagated in MDBK cells with Dulbecco's modified Eagle medium (DMEM) containing 2% fetal bovine serum (FBS), 100 IU/mL penicillin, and 100 μg/mL streptomycin (1% P/S). Cell free virus was harvested at 5 to 7 days post infection, flash frozen on liquid nitrogen and stored at -80 °C. RSV strain A2 (ATCC VR-1540) and Long (ATCC VR-26) stocks were grown in Hep2 cells. MDBK cells were maintained in DMEM supplemented with 5% FBS and 1% P/S. The Hep2 cells were cultured in Eagle minimum essential medium (EMEM) containing 10% FBS, 2 mM L-glutamine, 50 μg/ml Gentamicin, 25 μg/ml Amphotericin B, 100 IU/mL penicillin, and 100 μg/mL streptomycin (1% P/S).

Immunization and RSV challenge in cotton rats

Female cotton rats (*Sigmodon hispidus*) of 4 to8 weeks old were purchased from SAGE (Boyertown, PA) and maintained at a Merck animal facility in West Point, PA. The animal studies were approved by the Merck Institutional Animal Care and Use Committee and conducted in accordance with animal care guidelines. To determine the replication of PIV5 in cotton rats, animals were inoculated intranasally with 10^5 PFU of PIV5 in 10 μl or 100 μl volumes, equally divided between two nostrils. At day 4 or day 6,

animals were sacrificed by CO_2 inhalation. The lung (left lobes) and nasal turbinates were removed and homogenized in Hanks Balanced Salt Solution (Lonza) containing SPG buffer (0.2 M sucrose, 3.8 mM KH_2PO_4, 7.2 mM K_2HPO_4, and 5.4 mM monosodium glutamate) on wet ice. Samples were clarified by centrifugation at 2,000 rpm for 10 minutes, aliquoted, flash frozen on liquid nitrogen, and immediately stored frozen at -70^{o}C. The PIV5 vectored vaccine titers were determined by plaque assay in BHK cells. To determine the immunogenicity of PIV5-RSV-F or PIV5-RSV-G, cotton rats received one dose of 10^3, 10^4, 10^5, or 10^6 PFU of vaccine in a 10 µl volume by intranasal administration, equally divided between two nostrils. Serum samples at days 28 were collected for determining the neutralization titers. On day 28, all cotton rats were inoculated intranasally, under isoflurane anesthesia (1-4%), with 100 µl of $10^{5.5}$ PFU of RSV/A/A2. Four days post challenge, animals were sacrificed by CO2 inhalation and lung (left lobes) and nasal turbinates were removed and homogenized in Hanks Balanced Salt Solution (Lonza) containing SPG buffer on wet ice. Samples were clarified by centrifugation at 2,000 rpm for 10 minutes, aliquoted, flash frozen, and immediately stored frozen at -70°C. The RSV titers were determined by plaque assay in Hep2 cells.

Immunization and RSV challenge in African green monkeys

African green monkeys (*Chlorocebus sabaeus*) were domestically bred, raised, and maintained at New Iberia Research Center (NIRC, New Iberia, LA). The animals were prescreened for RSV- and PIV5-specific antibodies, as well as neutralizing antibody titers. The animal studies were approved by the Merck Institutional Animal Care and Use Committee (IACUC) and conducted in accordance with animal care guidelines. To determine the replication of PIV5 in African green monkeys, PIV-5 seronegative animals

(n=3) were anesthetized with Ketamine (10 mg/kg), and inoculated intranasally with 10^2, 10^4, 10^6, or 10^8 PFU of PIV5 in 0.25 ml split evenly between two nostrils. Nasopharyngeal swabs and bronchoalveolar lavage (BAL) were collected at days 3, 5, 7, 10, 14, and 21. The nasopharyngeal samples were collected by gently rubbing two areas of the oropharynx region using a Darcon swab and placing the tips in a solution containing Hanks balanced salt solution (HBSS) with SPG buffer and 0.1% gelatin. For BAL, approximately 5 ml HBSS was infused directly into the lung and aspirated via a sterile French catheter and syringe. Recovered samples were supplemented with a 0.1 volume of 10x SPG and 0.1 volume of 1% gelatin, aliquoted, flash frozen, and stored at -70^{o}C. To determine the immunogenicity of PIV5 vectored vaccines, PIV5 and RSV seronegative African green monkeys, identified by RSV F-specific IgG ELISA and serum neutralization titer, were immunized intranasally with 10^4 or 10^6 PFU of vaccines at day 0 in 0.25 ml evenly divided between two nostrils. The BAL and nasopharyngeal swabs were collected at days 3, 5, 7 and 14 post vaccination as described above, to monitor vaccine virus replication. At day 21, sera and PBMCs were also collected. At day28 post immunization, all monkeys were anesthetized and challenged with 2 x $10^{5.5}$ PFU of RSV A2 strain. The challenge virus was administered by intranasal and intratracheal inoculation, 1 ml at each route. Following challenge, nasopharyngeal swabs and BAL samples were collected at days 3, 5, 7, 10 and 14 post-challenge. Recovered samples were supplemented with 0.1 volume of 10x SPG and 0.1 volume of 1% gelatin, aliquoted, flash frozen and stored at -70^{o}C.

IgG ELISA assay

Immulon® 2HB microtiter plates (NUNC) were coated with 2 μg/ml recombinant RSV F protein and incubated at 4°C overnight. The plates were then washed and blocked for 1 h with phosphate-buffered saline containing 0.05% Tween-20® (PBST) and 3% milk at room temperature. Test samples were serially diluted 4-fold in blocking buffer starting at 1:100 dilution, transferred to the F coated plates, and incubated for 2 h at room temperature. Following three washes with PBST, goat anti-human IgG-HRP diluted to 1:2000 in blocking buffer was added to the plates, and incubated for an additional 1 h at room temperature. Plates were washed again and developed with SuperBlu Turbo TMB (Virolabs) in the dark. The reaction was stopped after 5 minutes and absorbance was read at 450 nm on a VersaMax ELISA microplate reader (Molecular Devices). Titers are reported as the reciprocal of the last dilution that is 2 fold greater than the background.

IgA assay

The IgA titers were quantified by direct binding ELISA on the Meso Scale 169 platform (Meso Scale Discovery, MSD). Briefly, the 96-well standard Meso Scale plates were coated with 0.2 μg/ml recombinant RSV F or ovalbumin proteins at 4°C overnight. The plates were then washed and blocked for 1h with PBST containing 3% milk at room temperature. Nasal samples were serially-diluted 2-fold in HISPEC buffer (Bio-Rad) starting at 1:4 dilution, transferred to the F coated plates, and incubated for 1 h at room temperature. After wash, SULFO-TAG (MSD) conjugated goat anti-human IgA diluted to 1:1000 in HISPEC buffer was added to the plates and incubated for 1 h at room temperature. Plates were washed again, and 1X Read Buffer T (MSD) was added to the plates and immediately read on a Sector S 600 plate reader (MSD). RSV-F-specific ECL

values were background adjusted by subtracting ovalbumin values. Titers are expressed as the reciprocal of the last dilution that was greater than 3-fold of the background.

Neutralization assays

Two-fold serial dilutions of the serum samples were prepared in EMEM containing 2% FBS starting at a 1:4 dilution. Diluted serum was added in duplicate to 96-well plates and mixed with RSV Long strain in a 100-µl total volume. The virus/antibody mixture was incubated for 1 h at 37^{o}C. Following incubation, Hep-2 cells at a concentration of $1.5x10^{4}$ cells per well were added. The plates were incubated for 3 days at 37^{o}C. The cells were then washed and fixed with 80% acetone for 15 min. RSV-infected cells were then immunostained. Briefly, RSV-F and N-specific monoclonal antibodies were added to the test plates with fixed cells and incubated for 1 h at room temperature. After washing, biotinylated goat anti-mouse IgG was added and incubated for 1 h. The plates were washed again and developed by a dual channel near infrared detection (NID) system. Infrared dye-Streptavidin to detect RSV specific signal and two cell stains for assay normalization were added to the 96-well plates and incubated for 1 hour in the dark. Plates were washed and dried in the dark for 20 minutes, and read on the Licor Aerius® Automated Imaging System utilizing a 700 channel laser for cell normalization and an 800 channel laser for detection of RSV specific signal. The 800/700 ratios were calculated and serum neutralizing titers were determined by four parameter curve fit in GraphPad.

IFN-γ ELISPOT assay

Peripheral blood mononuclear cells (PBMC) were isolated from whole blood by Ficoll gradient centrifugation and tested for IFN-γ ELISPOT responses to pools of

synthetic peptides representing RSV proteins F, G, and N (15mers overlapping by 11 amino acids). The F peptides were divided into two pools, F1 (aa1- aa295) and F2 (aa285 to aa574). Ninety-six well plates with PVDF membranes (Millipore) were coated overnight at 4^{o}C with anti-IFN-γ monoclonal antibody (U-Cytech). PBMC were added to the blocked plates at 4x10^{5}/well. Peptide pools were added to the cells at approximately 2 μg/ml final concentration per peptide. After overnight incubation in a 37^{o}C CO2 incubator, bound IFN-γ was detected with biotinylated anti-IFN-γ antibody (U-Cytech), followed by alkaline phosphatase-conjugated streptavidin (BD PharMingen) and NBT/BCIP Substrate (Pierce). Spots were enumerated using a digital imager and automated counting system (AID-AutoImmun Diagnostika), and responses normalized to spot-forming cells (SFC) per 1x10^{6} PBMC. A positive response is defined as an antigen-specific response that is at least 55 spot-forming cells per 1x10^{6} PBMC and at least 3-fold over the corresponding unstimulated (mock) control.

Titration of PIV5 and RSV

Ten-fold serial dilutions of PIV5 in DMEM with 1% BSA were incubated with BHK-21 cells for 1 h at 37 °C, 5% CO2. The inocula were removed, and cells were overlaid with DMEM containing 2% FBS, 1% P/S, and 1% low-melting point agarose. After incubation for 5-7 days at 37°C, 5% CO_2, cells were fixed with 2% formaldehyde and stained with crystal violet to visualize plaques. To titrate RSV, Hep2 cells were incubated with serial dilutions of RSV prepared in Williams Medium E with 2 mM L-glutamine and 50 μg/ml Neomycin. After adsorption for 1 h at 37°C, 5%CO_2, cells were overlaid with Williams Medium E containing 1.6% FBS, 2 mM L-glutamine, 50 μg/ml

Neomycin, and 0.8% methylcellulose. Five days later, cells were fixed with glutaric dialdehyde and stained with crystal violet to visualize plaques.

Statistical analysis

Statistical analysis was performed using GraphPad Prism software version 6 for Macintosh (GraphPad Software, La Jolla, CA). Two-way analysis of variance (ANOVA) followed by Sidak's multiple comparison tests were used to analyze antibody titers and virus loads.

Results

PIV5 replication in cotton rats

While PIV5 has been shown to infect a wide variety of animals, it has not yet been shown to infect cotton rats (32, 35). To determine whether cotton rats were permissive to PIV5 infection, the animals were intranasally inoculated with 10^5 PFU of PIV5 in 10 µl or 100 µl volumes. Different volumes were used to determine whether the inoculation volume impacted viral load in the upper and lower respiratory tracts. Four days post-infection (dpi), 3 to 4 $\log_{10}$ PFU/g of virus was detected in the nasal tissue of both the 10-µl and 100-µl groups. The titers decreased by approximately 1 $\log_{10}$ by six dpi. Virus replication in the lower respiratory tract depended on the inoculation volume. Four days after infection, virus was only detected in the lungs of animals inoculated with the 100-µl volume, with titers reaching 4.5 $\log_{10}$ PFU/g. Six days post-infection, only one animal in the 10-µl group had detectable virus in the lungs, while three out of four animals in the 100-µl group had detectable viral loads. Titers reached 2 $\log_{10}$ PFU/g in animals that had detectable virus in the lungs 6 dpi (Fig. 4.1). Thus, for future studies,

animals were inoculated with 10 μl volumes to mimic intranasal immunization in humans.

Immunogenicity of rPIV5-RSV-F and rPIV5-RSV-G in cotton rats

Immunization with rPIV5-RSV-F or rPIV5-RSV-G elicited the production of RSV antigen-specific antibodies in cotton rats. All vaccine doses (10^3, 10^4, 10^5, and 10^6 PFU) induced antigen-specific antibody responses, but not necessarily in a dose-specific manner. All doses of rPIV5-RSV-F generated consistently high F-specific titers (Fig. 4.2A). However, increasing doses of rPIV5-RSV-G showed a trend toward decreasing G-specific titers, suggesting that the maximum dose may not be the optimal dose (Fig. 4.2B). Only rPIV5-RSV-F was able to generate *in vitro* neutralizing antibodies (Fig. 4.2C).

Protection against RSV challenge in cotton rats

To determine whether the vaccine candidates were able to protect cotton rats against upper and lower respiratory tract RSV infection, cotton rats were challenged with $10^{5.5}$ PFU of RSV/A/A2 21 days post-immunization. Four days after challenge, nasal turbinate and lung samples were harvested to assess RSV titers by plaque assay.

Immunizing cotton rats with the vaccine candidates conferred significant protection against RSV challenge. Naïve cotton rats had RSV titers of 2.2×10^5 PFU/g in the nose and 2.7×10^5 PFU/g in the lungs (Fig.4.3). Cotton rats immunized with rPIV5-RSV-F or rPIV5-RSV-G had 2 to 3 $\log_{10}$ reductions in RSV titers in the upper respiratory tract for all vaccine doses, relative to the PBS group (Fig.4.3A). Animals vaccinated with 10^4 or 10^5 PFU of rPIV5-RSV-F had complete protection against lower respiratory RSV infection (Fig.4.3B). The rPIV5-RSV-G was not as protective as the F candidate, but

animals vaccinated with rPIV5-RSV-G still had 2 to 3 $\log_{10}$ reductions of RSV in the lower respiratory tract (Fig. 4.3).

While increasing doses of rPIV5-RSV-F from 10^3 to 10^5 PFU appeared to protect against RSV challenge in a dose-dependent manner, the 10^6 PFU dose only reduced RSV titers by 1.5 $\log_{10}$ PFU. These results again suggest that increasing the vaccination dose may not always confer better protection against infection. Furthermore, while the rPIV5-RSV-G-vaccinated cotton rats did not have detectable serum neutralizing antibodies, they were still somewhat protected against RSV challenge. These results are consistent with a previously published report in which rPIV5-RSV-G vaccination in mice did not generate *in vitro* neutralizing antibodies, but still reduced RSV titers in the lungs (24).

PIV5 replication in RSV-naive African green monkeys

African green monkeys are known to be permissive to infection with paramyxoviruses such as RSV, human metapneumovirus, Sendai virus, and PIV3 (36–39). To determine whether African green monkeys are permissive to PIV5 infection, groups of three to four PIV5-seronegative, RSV-naïve monkeys were immunized with 10^4 or 10^6 PFU of PIV5, rPIV5-RSV-F, or rPIV5-RSV-G. One group of RSV-experienced monkeys was immunized with 10^6 PFU of rPIV5-RSV-F to serve as a control to compare with another study in RSV-experienced monkeys. Groups were immunized with 10^4 PFU of the vaccine candidates to determine what level of immunogenicity and efficacy could be achieved with a lower dose. In light of the cotton rat studies, it was possible that a lower dose could be more efficacious. BAL and nasopharyngeal swab samples were collected 3, 5, 7, 10, 14, and 21 dpi, and serum was collected 3 days before immunization and 21 days after immunization. The animals were

then challenged with $10^{5.5}$ PFU of RSV A2 28 days after immunization. BAL and nasopharyngeal swab samples were collected at several time points after challenge to determine RSV titers (Fig. 4.4A).

Both vaccine candidates replicated to high titers in both the upper and lower respiratory tracts of the monkeys. Unexpectedly, high levels of virus were also recovered from the PBS controls (Fig. 4.4B and 4.4C). It was later determined that animals from different groups had been co-housed, resulting in the vaccinated animals shedding virus to the mock-vaccinated animals. We therefore used the PIV5-immunized group as the control for further comparisons. Nevertheless, the results were interesting because they showed that there was bona fide PIV5 replication in the contact animals, and PIV5 could replicate to equally high titers in animals that were infected via shedding.

Immunogenicity of rPIV5-RSV-F and rPIV5-RSV-G in RSV-naïve African green monkeys

To examine the humoral immune response to rPIV5-RSV-F and rPIV5-RSV-G, RSV-F and G-specific serum IgG levels were measured by ELISA. Immunization of RSV-naïve African green monkeys with rPIV5-RSV-F or rPIV5-RSV-G elicited the production of high RSV antigen-specific antibody titers by 21 days after immunization. Animals vaccinated with rPIV5-RSV-F had mean IgG titers of 5 $\log_{10}$, and the animals that received the rPIV5-RSV-G candidate had mean IgG titers of 4 $\log_{10}$ (Fig. 4.5A and 4.5B). The vaccine dose did not have a significant impact on IgG titers.

Naïve groups immunized with 10^4 and 10^6 PFU of rPIV5-RSV-F had geometric mean neutralization titers (GMT) of 16 and 8, respectively. Groups that received 10^6 PFU of PIV5, or 10^4 and 10^6 PFU of rPIV5-RSV-G, had no detectable neutralization

titers as expected (Fig. 4.5C). Despite the low levels of serum neutralizing antibodies, significant levels of RSV-antigen-specific IgA were detected in the mucosal secretions of animals that were immunized the rPIV5-RSV-F or G candidates (Fig. 4.6A and 4.6B).

Cell-mediated immune responses were measured 21 days post-vaccination by IFN-γ ELISpot using PBMCs. Low levels of F-specific cell mediated responses were detected in animals that were immunized with 10^6 PFU of rPIV5-RSV-F. No G-specific cell mediated responses were detected in animals that were immunized with rPVI5-RSV-G. However, it should be noted that the assay background for the G-specific responses was high relative to the F-specific responses (Fig. 4.7)

Protection against RSV challenge in African green monkeys

The animals were challenged with $10^{5.5}$ PFU of RSV/A/A2 28 days after immunization. Bronchoalveolar lavage and nasopharyngeal swabs were collected 3, 5, 7, 10, and 14 days post-challenge and viral loads were determined by plaque assay. Animals vaccinated with PIV5 had peak RSV titers of 4 $\log_{10}$ PFU in the nasopharynx and 5.8 $\log_{10}$ PFU in the BAL. The animals cleared virus from the upper respiratory and lower respiratory tracts by 10 and 15 days post-challenge, respectively. Immunization with 10^6 PFU of rPIV5-RSV-F reduced nasopharyngeal titers by as much as 2 $\log_{10}$. BAL viral titers were reduced by approximately 5 $\log_{10}$, and the animals completely cleared the virus from the lower respiratory tract by 7 days post-challenge. Immunization with rPIV5-RSV-G also conferred significant protection against RSV challenge, albeit not as robust as the F candidate. Animals immunized with 10^6 rPIV5-RSV-G had 1 $\log_{10}$ and 3 $\log_{10}$ reductions in RSV titers in the upper and lower respiratory tracts, respectively. These animals cleared virus by 10 days post-challenge (Fig. 4.8).

PIV5 replication in RSV-experienced African green monkeys

To examine whether the vaccine candidates could replicate in an RSV-experienced population, the candidates were tested in RSV-seropositive African green monkeys. RSV-seropositive monkeys were immunized intranasally with 10^2 to 10^6 PFU of PIV5, or 10^6 PFU of rPIV5-RSV-F or rPIV5-RSV-G. BAL and nasopharyngeal swab samples were collected 3, 5, 7, 10, 14, and 21 dpi to determine vaccine virus replication. Serum was collected 28 days post-immunization for analysis of antibody titers (Fig. 9A).

PIV5 and PIV5-RSV vaccine candidate replication kinetics in RSV-experienced monkeys were similar to those observed in RSV-naïve monkeys (Fig. 4.9B-4.9E). In both the BAL and nasopharyngeal swab, the highest viral titers of rPIV5-RSV-F and rPIV5-RSV-G were observed on day 3 post-immunization and decreased over time. There was no detectable virus by 14 days after immunization. Interestingly, rPIV5-RSV-F seemed to be cleared at a faster rate than rPIV5-RSV-G (Fig. 4.9D and 4.9E). The reason is unclear, but we speculate this could be due to pre-existing F-specific neutralizing antibodies clearing the virus.

Immunogenicity of rPIV5-RSV-F and rPIV5-RSV-G in RSV-experienced African green monkeys

To determine whether immunization with the vaccine candidates boosted pre-existing RSV antibody titers, we measured IgG levels by ELISA and performed *in vitro* plaque-reduction assays using pre-and post-immunization serum. PIV5-RSV-F and PIV5-RSV-G boosted pre-existing serum IgG levels against their respective antigens by approximately 40-fold and 25-fold, respectively (Fig.4.10A and 4.10B). PIV5-RSV-F and PIV5-RSV-G increased neutralizing antibody titers against RSV A2 by 50-fold and

12-fold, respectively. Only rPIV5-RSV-F boosted neutralizing antibody titers against RSV B1, a virus from a different subgroup (29-fold increase) (Fig. 4.10C and 4.10D)

Discussion

In this work, we evaluated two PIV5-based vaccines in cotton rat and African green monkey models of RSV infection. The candidates replicated in the upper and lower respiratory tracts of both species, making them useful animal models for evaluating the vaccine candidates. None of the animals immunized with the PIV5-based vaccines exhibited symptoms after vaccination, suggesting that these vaccines were safe.

In cotton rats, a single intranasal dose of either vaccine induced systemic immune responses and reduced RSV loads in the upper and lower respiratory tracts. Both candidates elicited the production RSV-antigen-specific IgG, but only vaccination with the F candidate induced neutralizing antibodies. These results are consistent with the previous mouse study (24). It has been previously shown that G-specific antibodies may not efficiently neutralize virus *in vitro* but still protect animals against RSV infection (10, 40). This is likely a result of differences in receptors used for attachment *in vitro* and *in vivo* (41). Nevertheless, PIV5-RSV-F was slightly more immunogenic and protective against RSV challenge in cotton rats.

In RSV-naïve African green monkeys, a single intranasal immunization with PIV5-RSV-F or PIV5-RSV-G induced high RSV-antigen-specific IgG titers but modest or no neutralizing antibody titers. Interestingly, both candidates still protected against RSV challenge, reducing viral loads and hastening viral clearance in the upper and lower respiratory tracts. The protection may be attributed to the high IgA titers detected in the mucosal secretions of the animals. Low levels of RSV-specific IgA have been identified

as a risk factor for RSV infection in adults over 65 years old (42). Similarly, in an experimental RSV infection of adult volunteers, high levels of mucosal RSV-specific IgA correlated with protection against RSV infection (43). Therefore, although the vaccine candidates did not induce high levels of serum neutralizing antibodies, the local mucosal antibody response can still be protective against RSV infection in an RSV-naïve population.

In RSV-experienced monkeys, intranasal vaccination with the vaccine candidates boosted RSV-antigen-specific antibody titers. Both candidates significantly increased baseline IgG and neutralizing antibody titers, suggesting that these vaccines were immunogenic and can be used to boost antibody responses in RSV-seropositive populations.

In this work, we demonstrate that these PIV5-based RSV vaccine candidates are immunogenic and efficacious in cotton rat and African green monkey models of RSV infection. The results suggest that the candidates may be promising vaccines in both RSV-seropositive and seronegative populations.

Acknowledgements

We thank the excellent technical support provided by Merck Laboratory Animal Services at West Point, PA, and the animal care staff at New Iberia Research Center (New Iberia, LA). We are grateful for the help from Dr. Biao He's lab.

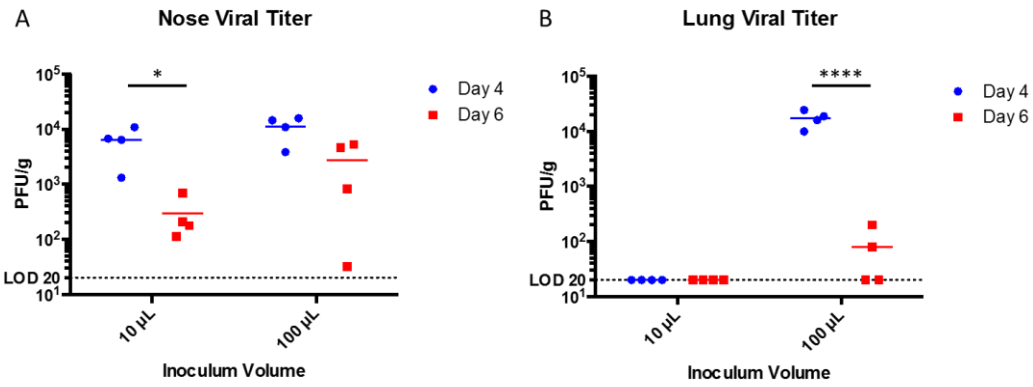

Figure 4.1. PIV5 replication in cotton rats. Cotton rats were infected intranasally with 10^5 PFU of PIV5 in 10 µl or 100 µl volumes. At 4 and 6 days post-challenge, (A) noses and (B) lungs were harvested and viral loads were determined by plaque assay. Each group consisted of 4 cotton rats. Bars represent the geometric mean titer (GMT) of each group. Statistical significance was determined by 2-way ANOVA with Sidak's correction for multiple comparison tests. *$P<0.05$, ****P <0.0001.

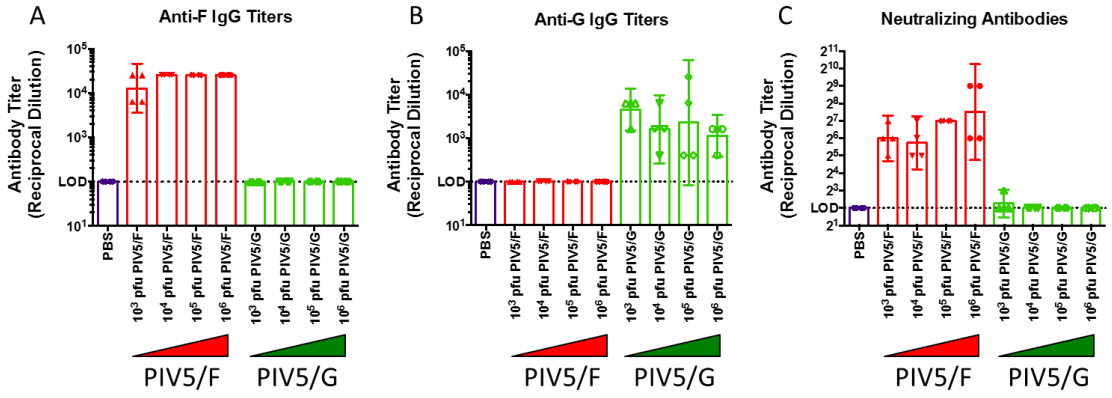

Figure 4.2. Serum antibody titers of cotton rats vaccinated with PIV5-RSV-F or PIV5-RSV-G. Cotton rats were immunized intranasally with 10^3, 10^4, 10^5, or 10^6 PFU of PIV5-RSV-F, PIV5-RSV-G, or PBS. Sera were collected 21 days post-immunization and IgG endpoint titers were determined by ELISA. RSV neutralizing activity was measured by

50% plaque-reduction assay. (A) RSV F-specific IgG titers. (B) RSV-G-specific IgG titers. (C) Serum neutralizing antibody titers. Each group consisted of 4 cotton rats. Graphs represent the GMT of each group. Error bars represent the 95% CI.

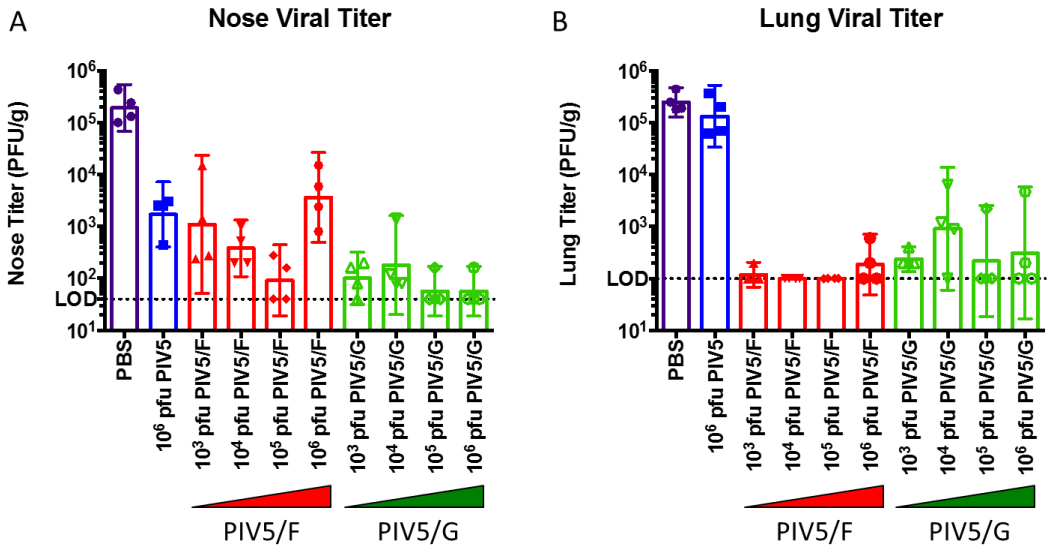

Figure 4.3. Immunization with PIV5-RSV-F or PIV5-RSV-G protected cotton rats against RSV challenge. Cotton rats were immunized intranasally with 10^3, 10^4, 10^5, or 10^6 PFU of PIV5-RSV-F or PIV5-RSV-G, 10^6 PFU of PIV5, or PBS. At 21 days post-immunization, the animals were challenged with $10^{5.5}$ PFU of RSV A2. Four days post-challenge, (A) noses and (B) lungs were harvested and viral loads were determined by plaque assay. Each group consisted of 4 cotton rats. Graphs represent the GMT of each group. Error bars represent the 95% CI.

A

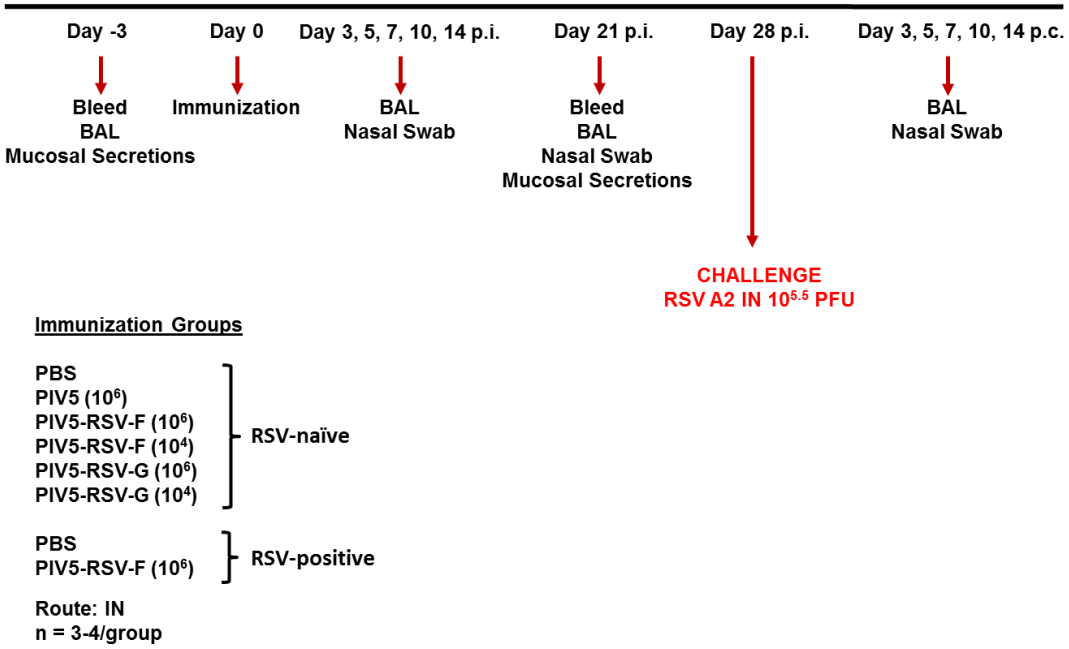
Day -3
Day 0
Day 3, 5, 7, 10, 14 p.i.
Day 21 p.i.
Day 28 p.i.
Day 3, 5, 7, 10, 14 p.c.
Bleed
BAL
Mucosal Secretions
Immunization
BAL
Nasal Swab
Bleed
BAL
Nasal Swab
Mucosal Secretions
BAL
Nasal Swab
CHALLENGE
RSV A2 IN 10^5.5 PFU
Immunization Groups
PBS
PIV5 (10^6)
PIV5-RSV-F (10^6)
PIV5-RSV-F (10^4)
PIV5-RSV-G (10^6)
PIV5-RSV-G (10^4)
RSV-naïve
PBS
PIV5-RSV-F (10^6)
RSV-positive
Route: IN
n = 3-4/group

B

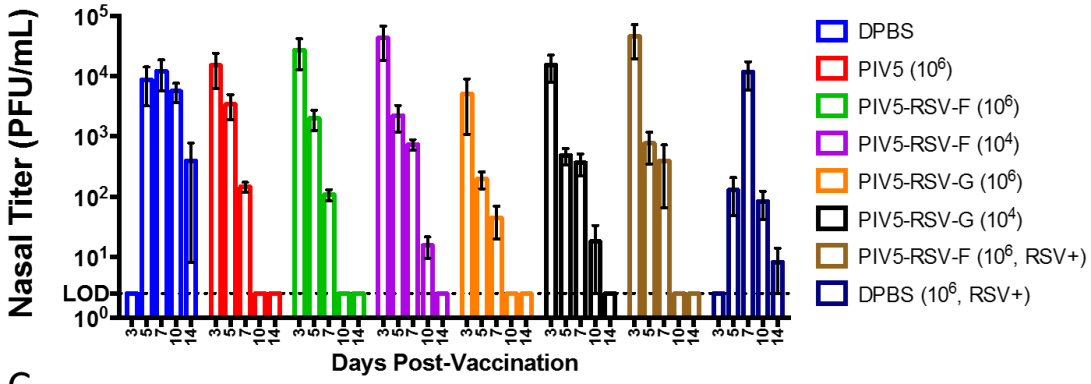
Nasal Titer (PFU/mL)
LOD
Days Post-Vaccination
DPBS
PIV5 (10^6)
PIV5-RSV-F (10^6)
PIV5-RSV-F (10^4)
PIV5-RSV-G (10^6)
PIV5-RSV-G (10^4)
PIV5-RSV-F (10^6, RSV+)
DPBS (10^6, RSV+)

C

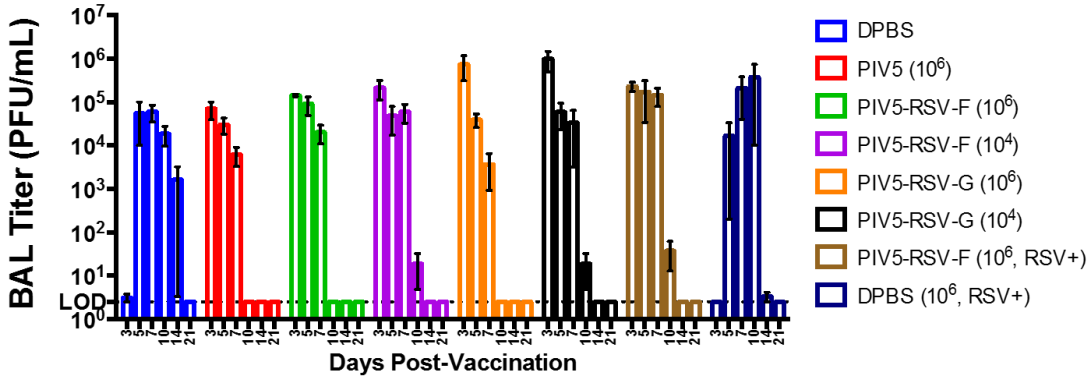
BAL Titer (PFU/mL)
LOD
Days Post-Vaccination
DPBS
PIV5 (10^6)
PIV5-RSV-F (10^6)
PIV5-RSV-F (10^4)
PIV5-RSV-G (10^6)
PIV5-RSV-G (10^4)
PIV5-RSV-F (10^6, RSV+)
DPBS (10^6, RSV+)

Figure 4.4. PIV5 replication in RSV-naïve African green monkeys. (A) Study design. African green monkeys were immunized intranasally with 10^4 or 10^6 PFU of PIV5-RSV-F or PIV5-RSV-G, or 10^6 PFU of PIV5. Negative control groups received PBS. BAL and nasopharyngeal swab samples were collected on days 3, 5, 7, 10, 14, and 21 days post-immunization. Viral loads from each animal at each time point were determined by plaque assay. (B) PIV5 titers in bronchoalveolar lavage (BAL) samples. (C) PIV5 titers in nasopharyngeal swab samples. Each group consisted of 3 to 4 monkeys. All monkeys were PIV5-seronegative and RSV-seronegative except where indicated. Each bar represents the mean of each group. The error bars represent the standard error of the mean.

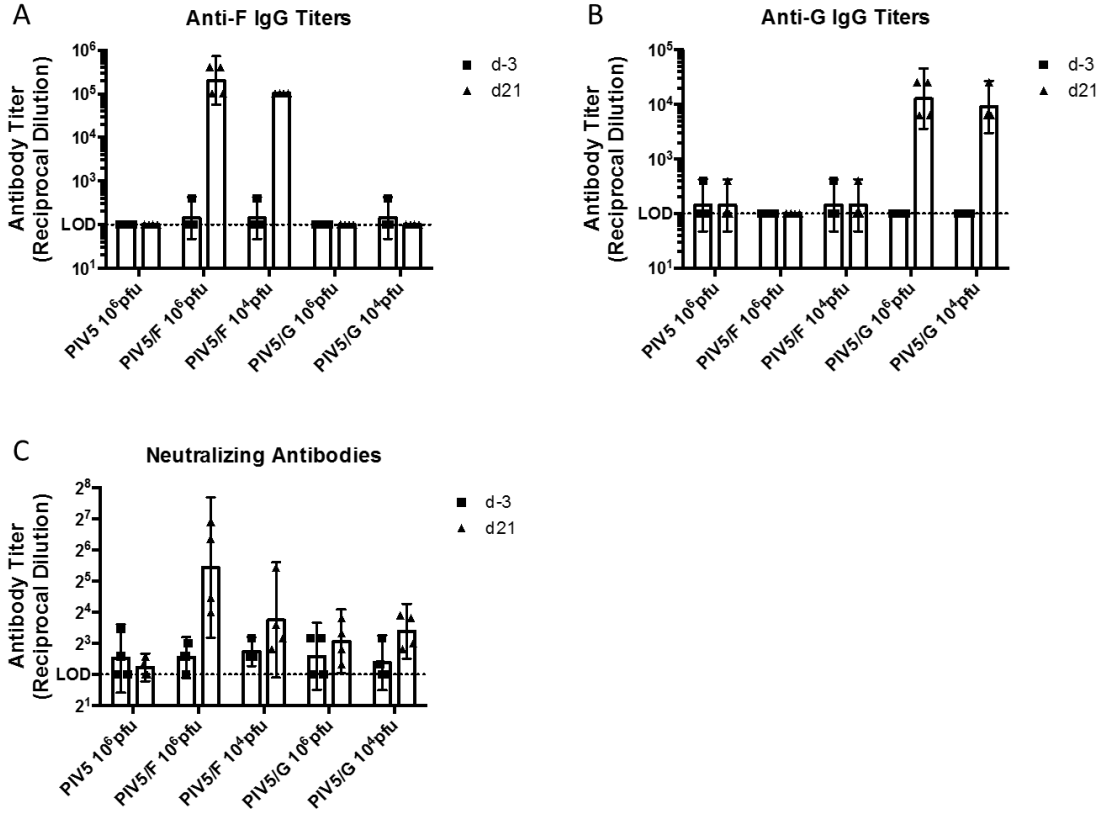

Figure 4.5. Serum antibody responses in RSV-naïve African green monkeys immunized with PIV5-RSV-F or PIV5-RSV-G. African green monkeys were immunized intranasally with 10^4 or 10^6 PFU of PIV5-RSV-F or PIV5-RSV-G, or 10^6 PFU of PIV5. Sera were collected 3 days prior to immunization and 21 days post-immunization. (A) Anti-RSV-F and (B) anti-RSV-G IgG titers were measured by ELISA. (C) Serum neutralization titers were determined by 50% plaque-reduction assay. Each group consisted of 4 PIV5 and RSV-seronegative and monkeys.

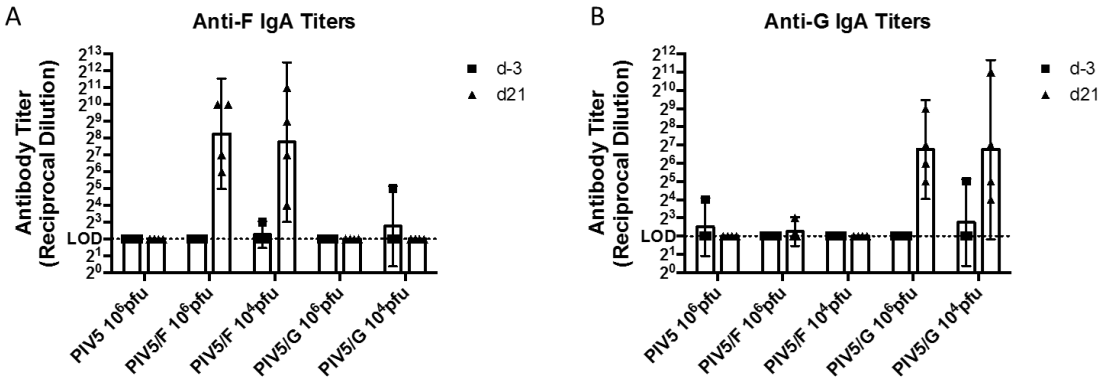

Figure 4.6. Mucosal IgA responses in naïve African green monkeys immunized with PIV5-RSV-F or PIV5-RSV-G. African green monkeys were immunized intranasally with 10^4 or 10^6 PFU of PIV5-RSV-F or PIV5-RSV-G, or 10^6 PFU of PIV5. Mucosal secretions were collected 3 days prior to immunization and 21 days post-immunization. (A) Anti-RSV-F and (B) anti-RSV-G-specific IgA titers were measured by ELISA. Each group consisted of 4 PIV5 and RSV-seronegative monkeys.

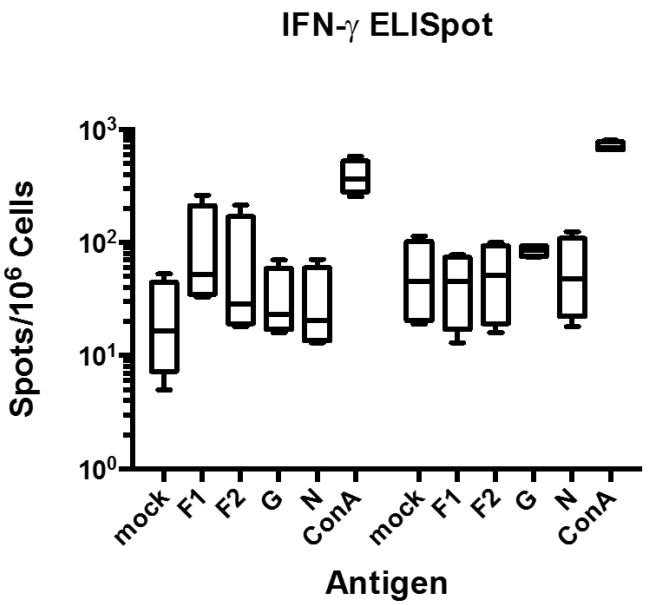

Figure 4.7. Cell-mediated immune responses in PIV5-RSV-F or PIV5-RSV-G-vaccinated African green monkeys. IFN-γ ELISPOT assay. PBMCs were collected from African green monkeys 21 days after intranasal immunization with 10^6 PFU of PIV5-RSV-F, PIV5-RSV-G, or PIV5. Cells were mock-stimulated or stimulated with RSV F, G, N, or concanavalin A (conA) and the number of IFN-γ secreting cells were measured per 10^6 PBMCs. Each group consisted of 4 PIV5 and RSV-seronegative monkeys.

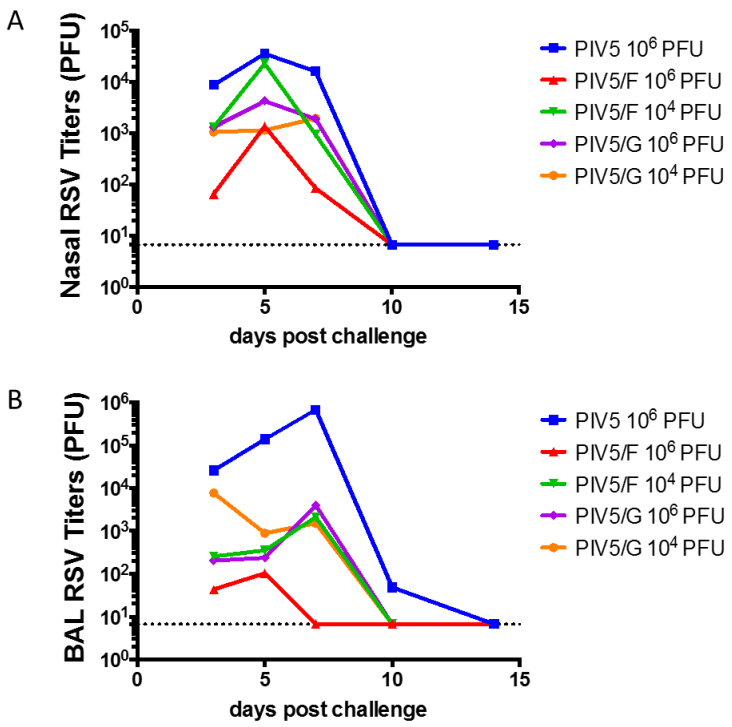

Figure 4.8. Protection against RSV challenge by PIV5-RSV-F or PIV5-RSV-G in vaccinated African green monkeys. African green monkeys were immunized intranasally with 10^4 or 10^6 PFU of PIV5-RSV-F, PIV5-RSV-G, or 10^6 PFU of PIV5. At 28 days post-immunization, animals were challenged with $10^{5.5}$ PFU of RSV A2 intranasally. Nasopharyngeal swabs and BAL samples were collected 3, 5, 7, 10, and 14 days post-challenge and viral loads were determined by plaque assay. Each group consisted of 4 PIV5 and RSV-seronegative monkeys.

A

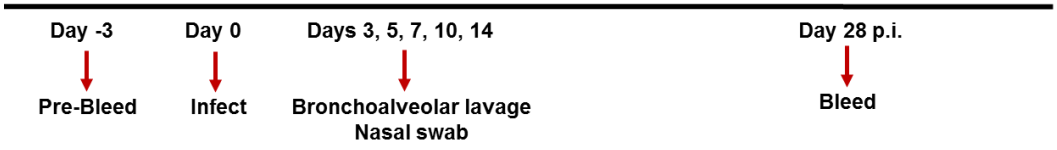

Immunization Groups

PIV5
rPIV5-RSV F
rPIV5-RSV G

Doses:

PIV5	rPIV5-RSV-F/G
IN 10^2 PFU	IN 10^6 PFU
IN 10^4 PFU	
IN 10^6 PFU	
IN 10^8 PFU	

n = 3/group

B

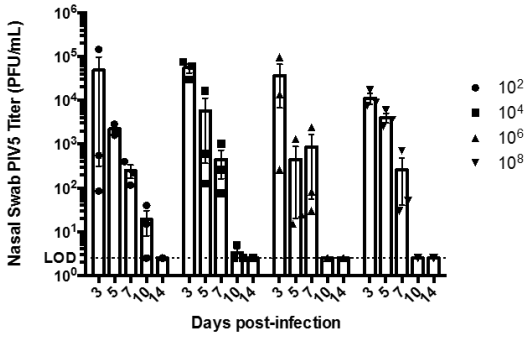

C

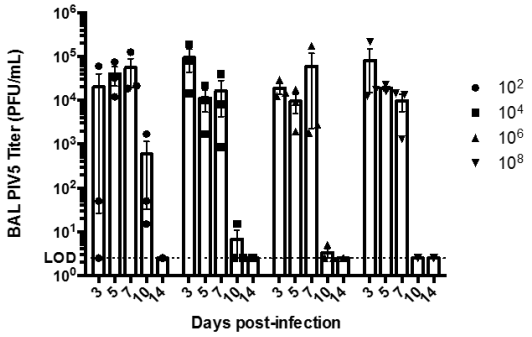

D

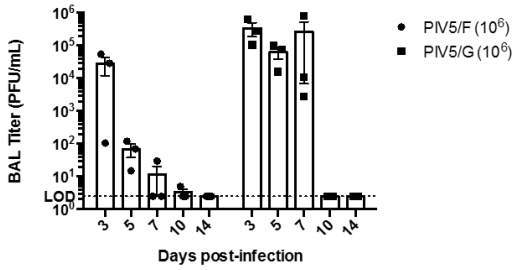

E

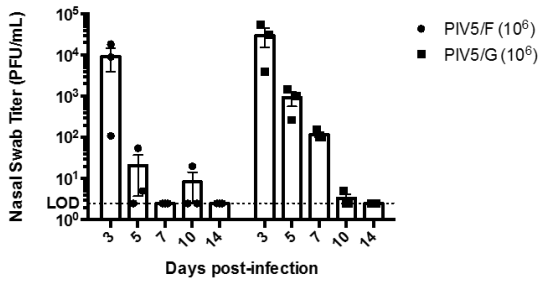

F

	PIV5/F vs. PIV5/G P-values	
	BAL	Nasal Swab
3	**0.0376**	0.2667
5	**0.0002**	**0.0012**
7	**< 0.0001**	**0.0047**
10	> 0.9999	0.9944
14	> 0.9999	> 0.9999

Figure 4.9. PIV5 replication in RSV-experienced African green monkeys. (A) Study design. African green monkeys were immunized intranasally with 10^2, 10^4, 10^6, or 10^8 PFU of PIV5, or 10^6 PFU of PIV5-RSV-F or PIV5-RSV-G. BAL and nasopharyngeal swab samples were collected on days 3, 5, 7, 10, 14, and 21 days post-immunization. Viral loads from each animal at each time point were determined by plaque assay. (B) PIV5 titers in bronchoalveolar lavage (BAL) samples. (C) PIV5 titers in nasopharyngeal swab (NP). (D) PIV5-RSV-F and PIV5-RSV-G titers in BAL samples. (E) PIV5-RSV-F and PIV5-RSV-G titers in NP samples. (F) *P* values for comparing PIV5-RSV-F and PIV5-RSV-G titers at different time points. Values of $P<0.05$ are in bold. Each group consisted of 3 monkeys. All monkeys were PIV5-seronegative and RSV-seropositive. Each bar represents the mean of each group. The error bars represent the standard error of the mean.

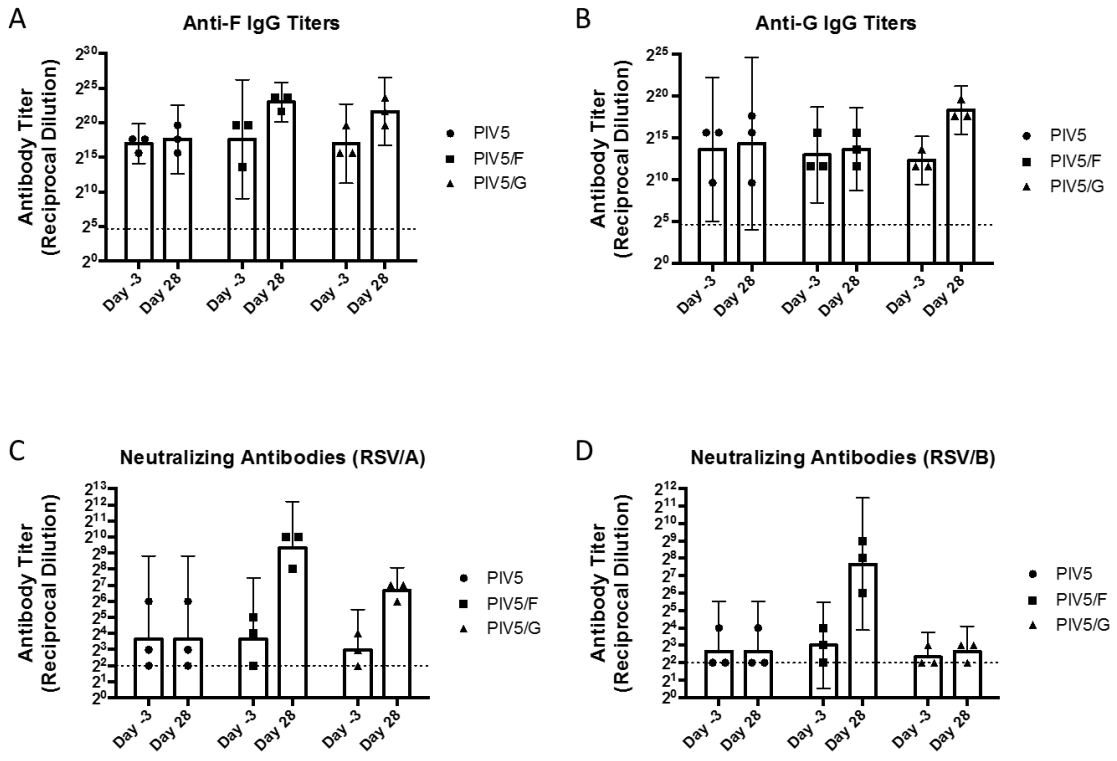

Figure 4.10. Serum neutralizing antibody responses in RSV-experienced African green monkeys immunized with PIV5-RSV-F or PIV5-RSV-G. African green monkeys were immunized intranasally with 10^6 PFU of PIV5-RSV-F, PIV5-RSV-G, or PIV5. Sera were collected 28 days post-immunization. (A) Anti-RSV-F and (B) anti-RSV-G-specific IgG titers were measured by ELISA. (C and D) Neutralizing antibody titers were measured by 50% plaque reduction assay against (C) RSV/A/A2 and (D) RSV/B/B1. Each group consisted of 3 PIV5 seronegative, RSV-seropositive monkeys. Statistical significance was determined by 2-way ANOVA with Sidak's multiple comparison test.

References

1. **Nair H**, **Nokes DJ**, **Gessner BD**, **Dherani M**, **Madhi S a.**, **Singleton RJ**, **O'Brien KL**, **Roca A**, **Wright PF**, **Bruce N**, **Chandran A**, **Theodoratou E**, **Sutanto A**, **Sedyaningsih ER**, **Ngama M**, **Munywoki PK**, **Kartasasmita C**, **Simões EA**, **Rudan I**, **Weber MW**, **Campbell H**. 2010. Global burden of acute lower respiratory infections due to respiratory syncytial virus in young children: a systematic review and meta-analysis. Lancet **375**:1545–1555.

2. **Falsey AR**, **Hennessey PA**, **Formica MA**, **Cox C**, **Walsh EE**. 2005. Respiratory syncytial virus infection in elderly and high-risk adults. N. Engl. J. Med. **352**:1749–59.

3. 2003. Revised indications for the use of palivizumab and respiratory syncytial virus immune globulin intravenous for the prevention of respiratory syncytial virus infections. Pediatrics **112**:1442–6.

4. **Chin J**, **Magoffin RL**, **Shearer LA**, **Schieble JH**, **Lennette EH**. 1969. Field evaluation of a respiratory syncytial virus vaccine and a trivalent parainfluenza virus vaccine in a pediatric population. Am. J. Epidemiol. **89**:449–63.

5. **Fulginiti VA**, **Eller JJ**, **Sieber OF**, **Joyner JW**, **Minamitani M**, **Meiklejohn G**. 1969. Respiratory virus immunization. I. A field trial of two inactivated respiratory virus vaccines; an aqueous trivalent parainfluenza virus vaccine and an alum-precipitated respiratory syncytial virus vaccine. Am. J. Epidemiol. **89**:435–48.

6. **Kapikian AZ**, **Mitchell RH**, **Chanock RM**, **Shvedoff RA**, **Stewart CE**. 1969. An epidemiologic study of altered clinical reactivity to respiratory syncytial (RS) virus infection in children previously vaccinated with an inactivated RS virus vaccine. Am. J. Epidemiol. **89**:405–21.

7. **Kim HW**, **Canchola JG**, **Brandt CD**, **Pyles G**, **Chanock RM**, **Jensen K**, **Parrott RH**. 1969. Respiratory syncytial virus disease in infants despite prior administration of antigenic inactivated vaccine. Am. J. Epidemiol. **89**:422–434.

8. **Karron RA**. 2013. RSV Vaccines in Clinical Trials.

9. **Gomez M**, **Mufson MA**, **Dubovsky F**, **Knightly C**, **Zeng W**, **Losonsky G**. 2009. Phase-I study MEDI-534, of a live, attenuated intranasal vaccine against respiratory syncytial virus and parainfluenza-3 virus in seropositive children. Pediatr. Infect. Dis. J. **28**:655–8.

10. **Power UF**, **Plotnicky-Gilquin H**, **Huss T**, **Robert A**, **Trudel M**, **Ståhl S**, **Uhlén M**, **Nguyen TN**, **Binz H**. 1997. Induction of protective immunity in rodents by vaccination with a prokaryotically expressed recombinant fusion protein containing a respiratory syncytial virus G protein fragment. Virology **230**:155–66.

11. **Quan F-S**, **Kim Y**, **Lee S**, **Yi H**, **Kang S-M**, **Bozja J**, **Moore ML**, **Compans RW**. 2011. Viruslike particle vaccine induces protection against respiratory syncytial virus infection in mice. J. Infect. Dis. **204**:987–95.

12. **Siegrist CA**. 2003. Mechanisms by which maternal antibodies influence infant vaccine responses: review of hypotheses and definition of main determinants. Vaccine **21**:3406–12.

13. **Waris ME**, **Tsou C**, **Erdman DD**, **Day DB**, **Anderson LJ**. 1997. Priming with live respiratory syncytial virus (RSV) prevents the enhanced pulmonary inflammatory response seen after RSV challenge in BALB/c mice immunized with formalin-inactivated RSV. J. Virol. **71**:6935–9.

14. **Anderson LJ**, **Dormitzer PR**, **Nokes DJ**, **Rappuoli R**, **Roca A**, **Graham BS**. 2013. Strategic priorities for respiratory syncytial virus (RSV) vaccine development. Vaccine **31 Suppl 2**:B209–15.

15. **Burns EA**, **Lum LG**, **L'Hommedieu G**, **Goodwin JS**. 1993. Specific humoral immunity in the elderly: in vivo and in vitro response to vaccination. J. Gerontol. **48**:B231–6.

16. **Ely KH**, **Roberts AD**, **Kohlmeier JE**, **Blackman MA**, **Woodland DL**. 2007. Aging and $CD8^+$ T cell immunity to respiratory virus infections. Exp. Gerontol. **42**:427–31.

17. **Tompkins SM**, **Lin Y**, **Leser GP**, **Kramer KA**, **Haas DL**, **Howerth EW**, **Xu J**, **Kennett MJ**, **Durbin RK**, **Durbin JE**, **Tripp R**, **Lamb RA**, **He B**. 2007. Recombinant parainfluenza virus 5 (PIV5) expressing the influenza A virus hemagglutinin provides immunity in mice to influenza A virus challenge. Virology **362**:139–50.

18. **Mooney A**, **Li Z**, **Gabbard JD**, **He B**, **Tompkins SM**. 2012. Recombinant PIV5 vaccine encoding the influenza hemagglutinin protects against H5N1 highly pathogenic avian influenza virus infection when delivered intranasally or intramuscularly. J. Virol. **Epub ahead**.

19. **Mooney AJ**, **Li Z**, **Gabbard JD**, **He B**, **Tompkins SM**. 2013. Recombinant parainfluenza virus 5 vaccine encoding the influenza virus hemagglutinin protects against H5N1 highly pathogenic avian influenza virus infection following intranasal or intramuscular vaccination of BALB/c mice. J. Virol. **87**:363–71.

20. **Li Z**, **Gabbard JD**, **Mooney A**, **Gao X**, **Chen Z**, **Place RJ**, **Tompkins SM**, **He B**. 2013. Single-dose vaccination of a recombinant parainfluenza virus 5 expressing NP from H5N1 virus provides broad immunity against influenza A viruses. J. Virol. **87**:5985–93.

21. **Li Z**, **Mooney AJ**, **Gabbard JD**, **Gao X**, **Xu P**, **Place RJ**, **Hogan RJ**, **Tompkins SM**, **He B**. 2013. Recombinant Parainfluenza Virus 5 Expressing Hemagglutinin

of Influenza A Virus H5N1 Protected Mice against Lethal Highly Pathogenic Avian Influenza Virus H5N1 Challenge. J. Virol., 2012/10/19 ed. **87**:354–362.

22. **Li Z**, **Gabbard J**, **Johnson S**, **Dlugolenski D**, **Phan S**, **Tompkins M**, **He B**. 2015. Efficacy of a parainfluenza virus 5 (PIV5)-based H7N9 vaccine in mice and guinea pigs: antibody titer towards HA was not a good indicator for protection. PLoS One In Press.

23. **Chen Z**, **Xu P**, **Salyards GW**, **Harvey SB**, **Rada B**, **Fu ZF**, **He B**. 2012. Evaluating a Parainfluenza Virus 5-Based Vaccine in a Host with Pre-Existing Immunity against Parainfluenza Virus 5. PLoS One **7**:e50144.

24. **Phan SI**, **Chen Z**, **Xu P**, **Li Z**, **Gao X**, **Foster SL**, **Teng MN**, **Tripp R a.**, **Sakamoto K**, **He B**. 2014. A respiratory syncytial virus (RSV) vaccine based on parainfluenza virus 5 (PIV5). Vaccine **32**:3050–3057.

25. **Chen Z**, **Gupta T**, **Xu P**, **Phan S**, **Pickar A**, **Yau W**, **Karls RK**, **Quinn FD**, **Sakamoto K**, **He B**. 2015. Efficacy of parainfluenza virus 5 (PIV5)-based tuberculosis vaccines in mice. Vaccine **33**:7217–24.

26. **Goswami KK**, **Cameron KR**, **Russell WC**, **Lange LS**, **Mitchell DN**. 1984. Evidence for the persistence of paramyxoviruses in human bone marrows. J. Gen. Virol. **65 (Pt 11**:1881–8.

27. **Hsiung GD**. 1972. Parainfluenza-5 virus. Infection of man and animal. Prog. Med. Virol. Fortschritte der medizinischen Virusforschung. Progrès en Virol. médicale **14**:241–74.

28. **Hull RN**, **Minner JR**, **SMITH JW**. 1956. New viral agents recovered from tissue cultures of monkey kidney cells. I. Origin and properties of cytopathogenic agents S.V.1, S.V.2, S.V.4, S.V.5, S.V.6, S.V.11, S.V.12 and S.V.15. Am. J. Hyg. **63**:204–15.

29. **Tribe GW**. 1966. An investigation of the incidence, epidemiology and control of Simian virus 5. Br. J. Exp. Pathol. **47**:472–479.

30. **Binn LN**, **Eddy GA**, **Lazar EC**, **Helms J**, **Murnane T**. 1967. Viruses recovered from laboratory dogs with respiratory disease. Proc Soc Exp Biol Med **126**:140–145.

31. **Cornwell HJ**, **McCandlish IA**, **Thompson H**, **Laird HM**, **Wright NG**. 1976. Isolation of parainfluenza virus SV5 from dogs with respiratory disease. Vet Rec **98**:301–2.

32. **Rosenberg FJ**, **Lief FS**, **Todd JD**, **Reif JS**. 1971. Studies of canine respiratory viruses. I. Experimental infection of dogs with an SV5-like canine parainfluenza agent. Am J Epidemiol **94**:147–165.

33. **McCandlish IA**, **Thompson H**, **Cornwell HJ**, **Wright NG**. 1978. A study of dogs with kennel cough. Vet. Rec. **102**:293–301.

34. **Chen Z**, **Xu P**, **Salyards GW**, **Harvey SB**, **Rada B**, **Fu ZF**, **He B**. 2012. Evaluating a Parainfluenza Virus 5-Based Vaccine in a Host with Pre-Existing Immunity against Parainfluenza Virus 5. PLoS One, 2012/11/28 ed. **7**:e50144.

35. **Chang PW**, **Hsiung GD**. 1965. Experimental infection of parainfluenza virus type 5 in mice, hamsters and monkeys. J. Immunol. **95**:591–601.

36. **Kakuk TJ**, **Soike K**, **Brideau RJ**, **Zaya RM**, **Cole SL**, **Zhang JY**, **Roberts ED**, **Wells PA**, **Wathen MW**. 1993. A human respiratory syncytial virus (RSV) primate model of enhanced pulmonary pathology induced with a formalin-inactivated RSV vaccine but not a recombinant FG subunit vaccine. J. Infect. Dis. **167**:553–61.

37. **MacPhail M**, **Schickli JH**, **Tang RS**, **Kaur J**, **Robinson C**, **Fouchier RAM**, **Osterhaus ADME**, **Spaete RR**, **Haller AA**. 2004. Identification of small-animal and primate models for evaluation of vaccine candidates for human metapneumovirus (hMPV) and implications for hMPV vaccine design. J. Gen. Virol. **85**:1655–63.

38. **Hurwitz JL**, **Soike KF**, **Sangster MY**, **Portner A**, **Sealy RE**, **Dawson DH**, **Coleclough C**. 1997. Intranasal Sendai virus vaccine protects African green monkeys from infection with human parainfluenza virus-type one. Vaccine **15**:533–40.

39. **Durbin AP**, **Elkins WR**, **Murphy BR**. 2000. African green monkeys provide a useful nonhuman primate model for the study of human parainfluenza virus types-1, -2, and -3 infection. Vaccine **18**:2462–9.

40. **Jorquera PA**, **Oakley KE**, **Powell TJ**, **Palath N**, **Boyd JG**, **Tripp RA**. 2015. Layer-By-Layer Nanoparticle Vaccines Carrying the G Protein CX3C Motif Protect against RSV Infection and Disease. Vaccines **3**:829–49.

41. **Johnson SM**, **McNally BA**, **Ioannidis I**, **Flano E**, **Teng MN**, **Oomens AG**, **Walsh EE**, **Peeples ME**. 2015. Respiratory Syncytial Virus Uses CX3CR1 as a Receptor on Primary Human Airway Epithelial Cultures. PLoS Pathog. **11**:e1005318.

42. **Walsh EE**, **Falsey AR**. 2004. Humoral and mucosal immunity in protection from natural respiratory syncytial virus infection in adults. J. Infect. Dis. **190**:373–8.

43. **Habibi MS**, **Jozwik A**, **Makris S**, **Dunning J**, **Paras A**, **DeVincenzo JP**, **de Haan CAM**, **Wrammert J**, **Openshaw PJM**, **Chiu C**. 2015. Impaired Antibody-mediated Protection and Defective IgA B-Cell Memory in Experimental Infection of Adults with Respiratory Syncytial Virus. Am. J. Respir. Crit. Care Med. **191**:1040–9.

CHAPTER 5

THE GENETIC STABILITY OF PIV5-VECTORED VACCINE CANDIDATES AFTER IN VITRO AND IN VIVO PASSAGE[3]

[3]Phan S.I., Adam C.M., Chen Z., Citron M.P., Liang X., Espeseth S.A., Wang D., He B. Submitted to *Journal of Virology*, 03/10/2016.

Abstract

Human respiratory syncytial virus (RSV) is the leading etiologic agent of lower respiratory tract infections in children, but no licensed vaccine exists. Previously, our laboratory developed two parainfluenza virus 5 (PIV5)-based RSV vaccine candidates that protect mice against RSV challenge. PIV5 was engineered to express either the RSV fusion protein (F) or the RSV major attachment glycoprotein (G) between the HN and L genes of the PIV5 genome (rPIV5-RSV-F or rPIV5-RSV-G). To investigate the stability of the vaccine candidates *in vitro*, they were passaged in Vero cells for eleven generations, and the genome sequences of the resulting viruses were compared with those of the parent viruses. While mutations were observed within clonal populations of the candidates and in the PIV5 backbone of rPIV5-RSV-G, the consensus sequences of the gene insertions had no mutations after *in vitro* passage. We also examined the *in vivo* stability of the vaccine candidates after a single passage in African green monkeys. No mutations were detected in the consensus sequences of viruses collected from the BAL fluid of the animals. Mutations in individual isolates of rPIV5-RSV-G were found in RSV-G and PIV5-L, but plaque isolates of rPIV5-RSV-F had no mutations. The results suggest that foreign gene insertions are stable in PIV5 genome. However, the function of the foreign gene insertion may need to be considered when designing PIV5-based vaccines.

Introduction

Human respiratory syncytial virus (RSV) is a leading cause of viral bronchiolitis and hospitalizations in infants and young children. Globally, an estimated 33.8 million cases of RSV-associated acute lower-respiratory infection occur annually in children under the age of five, resulting in approximately 3 million hospitalizations (1). In the United States, greater than 60% of children are infected with RSV by the age of one, and nearly all children are infected by two years old (2). Furthermore, severe infection during infancy has been implicated in the development of childhood asthma and wheezing (3, 4). Since natural RSV infection does not confer long-lasting immunity, reinfection, although usually mild in healthy individuals, can occur throughout life. Therefore, RSV infection can still cause serious complications in immunocompromised individuals and the elderly (5). For these reasons, vaccines are needed for both young and aged populations.

While many attempts have been made at developing an RSV vaccine for over forty years, no licensed vaccine currently exists (6). The most advanced RSV vaccine candidates to date have been live attenuated or vectored vaccines. One live attenuated candidate, rA2 cp248/404/1030ΔSH, was immunogenic and well-tolerated in RSV-naïve, 1 to 2-month-old infants. However, 34% of the virus isolates recovered from post-vaccination nasal washes demonstrated partial loss of the temperature-sensitive (ts) phenotype. Specifically, loss of 248ts or 1030ts mutations was observed, with 83% of reversions occurring at 1030ts (7). Further examination in *in vitro* studies showed that the two mutations occurred as a result of selective pressure at 35°C, similar to the maximum temperature of the respiratory tract. MEDI-534, a live vectored RSV vaccine candidate, also encountered obstacles related to genome stability. MEDI-534 is a

chimeric, recombinant vaccine consisting of a bovine parainfluenza virus 3 (bPIV3) backbone engineered to express the human PIV3 (hPIV3) fusion protein, hPIV3 hemagglutinin-neuraminidase (HN), and RSV fusion protein (F). In a Phase 1 study conducted in seronegative children, ages 6 to 24 months, all subjects seroconverted in response to hPIV3, but only 50% seroresponded to RSV (8). Sequence analysis of post-vaccination nasal wash samples showed mutations in the poly A sequence downstream of the bPIV3 nucleocapsid gene (N) as well as in the F open reading frame. These variant subpopulations existed at low levels in the administered vaccine, and the mutations were implicated in the down-regulation of F expression and subsequent reduction in the antibody response against F (9). Therefore, genome stability is important for live attenuated and live viral vector-based vaccine candidates.

PIV5 is a non-segmented, negative-sense, RNA virus of the genus *Rubulavirus* in the Paramyxoviridae family (10). Previous work from our lab has shown that PIV5, as a vaccine vector, is safe, efficacious, and able to overcome host pre-existing immunity (11). PIV5-based vaccine candidates against influenza and rabies have conferred protection against infection in various animal models (12–18). Furthermore, in the canine model of H3N2 influenza infection, PIV5 expressing H3 was able to generate protective hemagglutination-inhibition (HAI) titers in PIV5-immunized animals (11). Recently, our laboratory developed PIV5-based RSV vaccine candidates expressing either RSV F or the major attachment glycoprotein (G) between the HN and L genes of PIV5. We showed that the vaccine candidates conferred potent immunity against RSV challenge in mice. Both candidates induced RSV antigen-specific antibodies and reduced RSV lung titers with no evidence of enhanced disease (19).

The genome structure of PIV5 is stable, unlike the genomes of positive-strand RNA viruses (20). Recombinant PIV5 expressing GFP maintained GFP gene expression for more than 10 generations (the duration of the experiment) (21). Sequence variation is also low among PIV5 isolates, and the PIV5 genome remains stable through high multiplicity of infection (MOI) passages in tissue culture cells (22). In this work, we determined the stability of our vaccine candidates after multiple passages in cell culture and a single passage in African green monkeys.

Materials and Methods

Cells and viruses

Vero and BHK21 cells were maintained in Dulbecco's modified Eagle Medium (DMEM) supplemented with 10% fetal bovine serum (FBS), 100 IU/mL penicillin, and 100 μg/mL streptomycin (1% P/S; Mediatech Inc., Manassas, VA, USA). Cells were passed one day prior to infection, achieving approximately 90% confluence by the following day. The rPIV5-RSV-F and rPIV5-RSV-G viruses were generated (19) and grown in MDBK cells as previously described (21).

Serial passages of rPIV5-RSV-F and rPIV5-RSV-G

Vero cells in 6-cm dishes were infected with rPIV5-RSV-F or rPIV5-RSV-G at a MOI = 1. After 5 days, 500 μL of cell supernatant was used to inoculate fresh 6-cm dishes of Vero cells. The remaining cell supernatant was supplemented with 1% BSA and stored at -80°C. Eleven passages were performed.

rPIV5-RSV-G growth curves

Vero cells in 6-well plates were infected with rPIV5-RSV-G P0 or P12 at a MOI=5 or 0.01 and incubated for two hours at 37°C, 5% CO_2. The inocula were

aspirated and replaced with 2 mL of DMEM containing 2% FBS and 1% P/S. One hundred μL samples of supernatant were collected at 0, 12, 24, 36, 48, and 72 hours post-infection for high MOI infection and 0, 24, 48, 72, 96, and 120 hours post-infection for low MOI infection. Each sample was supplemented with 1% BSA and stored at -80°C immediately after collection. Virus titers were determined by plaque assay as described in Chen et al (16)

Nonhuman primate infection and BAL collection

Animal experiments were performed according to protocols approved by the Merck Institutional Animal Care and Use Committee. African green monkeys, seronegative for PIV5 and seropositive for RSV, were anesthetized with Telazol (4-6 mg/kg), supplemented with Ketamine (5 mg/kg) if needed. 10^6 PFU of either rPIV5-RSV-F or rPIV5-RSV-G were administered intranasally in a 1 mL volume, distributed equally between both nares.

Bronchoalveolar lavage (BAL) samples were collected 3, 5, 7, 10, and 14 days post-infection. Briefly, 5 mL of HBSS was delivered into the lung and then aspirated using a tracheal tube and syringe. BAL samples were mixed with 10% SPG and 1% gelatin, flash-frozen in a dry-ice ethanol bath, and stored at -80°C.

rPIV5 RSV-F and rPIV5-RSV-G plaque purification

Passages 0 and 11 of rPIV5-RSV-F and rPIV5-RSV-G were diluted by a factor of 10^4 to 10^6 in DMEM containing 1% BSA. Fifty μL of each dilution were used to infect 6-well plates of BHK21 cells as described above. After 5 days, plaques were selected and cultured in Vero cells with DMEM containing 2% FBS and 1% P/S. After 4 to 5 days, cell supernatants were harvested, supplemented with 1% BSA, and stored at -80°C.

For plaque purification of rPIV5-RSV-F and rPIV5-RSV-G from NHP samples, BAL wash samples from 5 days post-immunization (dpi) were diluted by a factor of 2 to 2 x 10^5 in DMEM containing 1% BSA. Four hundred μL of each dilution was used to infect BHK21 cells, and plaques were cultured as stated above.

RT-PCR and sequencing

Viral RNA was extracted from cell culture supernatant using a QIAamp viral RNA mini kit (Qiagen Inc., Valencia, CA). Reverse transcription (RT) was performed with Superscript III reverse transcriptase (Life Technologies) and random hexamers (Promega, Madison, WI). The cDNA templates and nineteen genome-specific primer pairs were used to amplify overlapping fragments of the viral genome by PCR. These primers were also used to sequence the PCR products. For NHP plaque isolates, viral RNA was extracted as stated above. Genome specific primers and 5 μL of RNA were used for one-step RT-PCR (Life Technologies). Sequence analysis was performed using Sequencher version 5.1 sequence analysis software (Gene Codes Corporation, Ann Arbor, MI). Primer sequences are available upon request.

Statistical analysis

Graphpad Prism software version 5.04 for Windows was used for statistical analysis (Graphpad Software, La Jolla, CA). Unpaired, two-tailed t-test was used to compare virus titers at different time points in rPIV5-RSV-G P0 and P12 growth curves.

Results

Recombinant PIV5-based RSV vaccine viruses retained inserted genes through multiple passages *in vitro*

To determine the stability of the recombinant viruses through serial passages in cell culture, the vaccine viruses were passaged every 5 days in Vero cells, a cell line that has been approved for vaccine production by the WHO and FDA, for a total of 11 passages. Both recombinant viruses retained the RSV gene insertion through serial passages (Fig. 5.1A and 5.1B).

Full-genome sequencing of rPIV5-RSV-F passages 0 (P0) and 11 (P11) showed no differences between the consensus sequence of the initial stock virus and the virus from P11 (Table 5.1). To assess differences within the P0 and P11 virus populations, over 20 plaques at P0 and P11 were isolated and cultured. The gene insertion, including the upstream and downstream intergenic regions, was sequenced. Interestingly, 13% (3 out of 23) of the rPIV5-RSV-F P0 isolates differed from the parent sequence, even though P0 was grown from a single isolate. The mutations were nucleotide substitutions within the RSV-F gene, all of which resulted in amino acid mutations. By P11, 26% (6 out of 23) of the rPIV5-RSV-F isolates differed from the parent sequence. However, all of these mutations were mixed bases within the RSV-F gene. Of the six mutated isolates, only three isolates (13%) actually sustained amino acid mutations. Of note, none of the mixed bases in P11 matched the mutations in the P0 (Table 5.2).

Full-genome sequencing of rPIV5-RSV-G showed that P11 had two mutations, one mutation in the V/P gene, and the other in the 3' untranslated region (UTR) of M. The mutation in the V/P gene caused an amino acid change from lysine to glutamate at

amino acid residue 78 in the conserved N-terminus. The 3' UTR of M had a cytosine (C) to adenine (A) mutation at nucleotide position 4,292 (Table 5.3).

Since two mutations were detected in the PIV5 backbone of rPIV5-RSV-G P11, the regions of interest in all passages were sequenced to determine when the mutations occurred. For the K78E mutation, a minor guanine (G) peak was detected at passage 3, and full conversion from A to G occurred by passage 7 (Fig. 5.2A). In the case of the C-to-A mutation at nucleotide position 4,292, a minor C peak was detected in passage 1. Full conversion from C to A occurred by passage 7 (Fig. 5.2B). To determine whether there were differences in growth between early and late-passage viruses, growth curves were performed using P0 and P12 viruses (P11 was expanded to generate P12). Growth of P0 and P12 were similar at high MOI infection, but P12 grew slightly faster by 24 hpi and to a higher final titer by 72 hpi (~0.5 $\log_{10}$) at low MOI infection (Fig. 5.3).

At the plaque isolate level in rPIV5-RSV-G P0, 4% (1 out of 23) of the isolates were different, with the mutation being a mixed base within the RSV-G gene. This mutation was silent. None of the rPIV5-RSV-G P11 isolates differed from the parent sequence (Table 5.4). Thus, the RSV-G gene and the flanking intergenic regions appeared stable through multiple *in vitro* passages even though the genome sustained mutations elsewhere.

The genome of rPIV5-RSV-F, but not rPIV5-RSV-G, remained stable through *in vivo* passaging

Since *in vitro* passage of the viruses may not accurately reflect stability in vivo, we sought to sequence virus isolates that were recovered from an in vivo infection. African green monkeys were inoculated with either rPIV5-RSV-F or rPIV5-RSV-G, and

BAL washes were collected 5 days post-infection. Serial dilutions of the BAL wash samples were used for plaque assay in BHK cells. After 5 days, plaques were picked, cultured in Vero cells for 5 days, and tissue culture supernatant was used for subsequent RNA isolation, RT-PCR, and sequencing (Fig. 5.4).

No mutations were found in the consensus sequences of rPIV5-RSV-F recovered from the BAL washes of three different animals (Table 5.5). None of the six rPIV5-RSV-F plaque isolates selected for full genome sequencing acquired amino acid residue mutations. Isolate 3 from animal 3 had a silent mutation in PIV5-F (Table 5.6). No mutations were observed upon sequencing the RSV-F gene insertion region of six additional isolates, although isolate 3 from animal 6 did have a silent mutation in RSV-F (Table 5.7). Thus the genome rPIV5-RSV-F appeared stable after *in vivo* passage in a non-human primate model.

The consensus sequences of rPIV5-RSV-G recovered from the BAL of three different animals had no mutations (Table 5.8). Interestingly, out of 6 fully-sequenced rPIV5-RSV-G plaque isolates, one isolate had a A753S mutation in PIV5-L (Table 5.9). After sequencing 11 additional isolates over the RSV-G insertion, 2 isolates were found to have mutations in RSV-G (Table 5.10).

Discussion

The encapsidation of the PIV5 RNA genome by NP results in a stable viral genome that retains foreign gene insertions. In this work, we have examined the stability of inserts within the PIV5 genome over 11 passages *in vitro* and a single passage *in vivo*. At different passages, we determined full-genome consensus sequences as well as sequences of the foreign gene insertion in individual virus clones. The foreign gene

insertions were stable; there was no loss of the insertions after passages *in vitro* or *in vivo*. No mutation that could affect the expression of the inserted genes was observed. The results demonstrate that insertion of a foreign gene into the PIV5 genome is stable. This is different from a bovine PIV3-based RSV vaccine, in which mutations affecting the expression of inserted RSV F were observed in isolates after a single passage in clinical trial subjects (9).

Over 11 *in vitro* passages, the inserts within rPIV5-RSV-F and rPIV5-RSV-G had no mutations in the consensus sequences, demonstrating that PIV5-based vectors are stable. However, examination of the rPIV5 vaccine viruses showed that mutations within clonal populations of each virus exist. For rPIV5-RSV-F, 3 out of 23 clones contained mutations within the RSV F gene at P0. By P11, 6 out of 23 clones contained mutations as a mixture at a given site. These mutations were different from those found in P0, indicating that these initial mutations did not provide a replicative advantage or undergo selection in subsequent passage. Thus, rPIV5-RSV-F is very stable, with no mutations emerging in the consensus sequence of the genome after 11 passages. Interestingly, while no mutations were detected within the RSV-G gene of rPIV5-RSV-G, mutations emerged within the PIV5 backbone. The K78E mutation is within a previously reported RNA binding region of the V/P gene (23). The mutation in the 3' UTR of the M gene may affect the expression of M as well as F, the downstream gene. The RSV-G gene within the PIV5 genome is approximately 900 nucleotides long, about half the length of RSV-F. The absence of mutations within RSV-G after *in vitro* passage is consistent with its smaller size and with RNA viruses being a quasispecies. However, the insertion of G, despite its smaller size, resulted in mutations within the PIV5 backbone. We speculate

that the emergence of mutations within the rPIV5-RSV-G genome may indicate that the RSV-G gene impacted PIV5 genome stability. The RSV-G protein binds to cell surface heparan sulfate and serves as an attachment protein for RSV (24). It is possible that functionality of RSV-G affects the replication of rPIV5-RSV-G in cultured cells.

We also investigated the stability of the vaccine candidates after a single *in vivo* passage in African green monkeys. No mutations were found in the consensus sequence of rPIV5-RSV-F recovered from BAL fluid 5 days after infection. Further examination of individual plaque isolates also revealed no mutations. The rPIV5-RSV-G consensus sequence appeared stable after passage, but 3 out of 17 isolates had mutations in various parts of the genome. One isolate sustained an A753S mutation in L, while 2 isolates had mutations in RSV-G. The A753S mutation was located in the polymerase domain of L, but the 753 residue is not known to be associated with catalytic activity (25). Both mutations in G were found in a hypervariable mucin-like region, with the T125A mutation being a potential O-linked glycosylation site (26, 27). Thus, while rPIV5-RSV-F remained stable through *in vivo* passage, rPIV5-RSV-G acquired mutations in both the PIV5 backbone and the RSV-G insertion. Together, with the *in vitro* data, these results suggest that the RSV-G gene may affect the stability of the rPIV5-RSV-G candidate.

When considering further vaccine design using PIV5 as a vector, it is important to consider the functions of inserted antigens and the potential impact on viral genome stability. Previously, we generated a PIV5-based H5N1 vaccine using the HA of an H5N1 influenza virus that lacks the cleavage site, rendering the HA molecule inactive but maintaining the immunogenicity of the protein (13, 17). A similar approach may be considered for improving the stability of PIV5-based RSV-G vaccine viruses.

Acknowledgements

We would like to thank all members of Biao He's laboratory for their helpful discussion and technical assistance. We would also like to thank the teams at Merck and the New Iberia Research Center for their assistance with the non-human primate studies. This work was supported by an endowment from Fred C. Davison Distinguished University Chair in Veterinary Medicine to B.H.

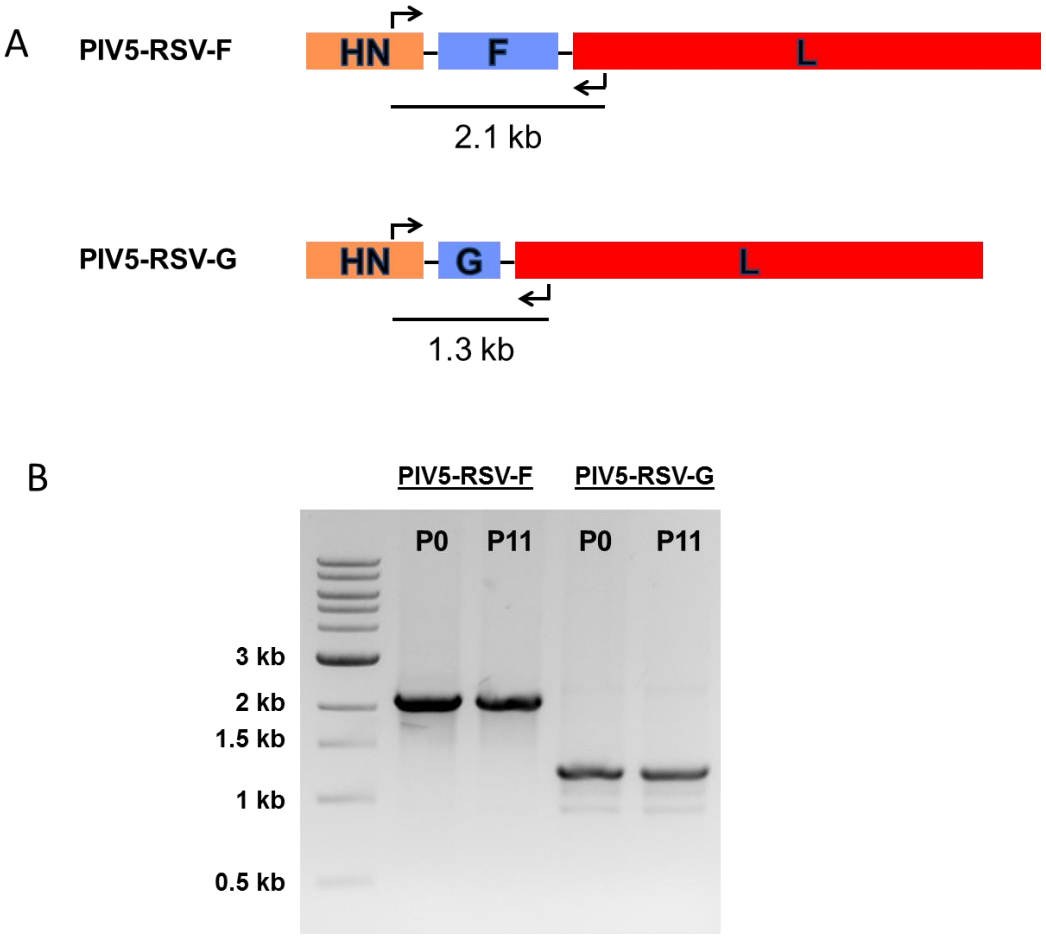

Figure 5.1. Stability of rPIV5-RSV-F and rPIV5-RSV-G through multiple passages in cell culture. (A, B) Vero cells were infected with rPIV5-RSV-F or rPIV5-RSV-G at a MOI of 1. Five hundred µL of infected cell culture supernatant was used to infect fresh Vero cells every 5 days, for a total of 11 passages. Retention of the RSV-F or RSV-G gene was confirmed by performing RT-PCR on cell culture supernatants with primers flanking the 5' and 3' intergenic regions of the gene insertion.

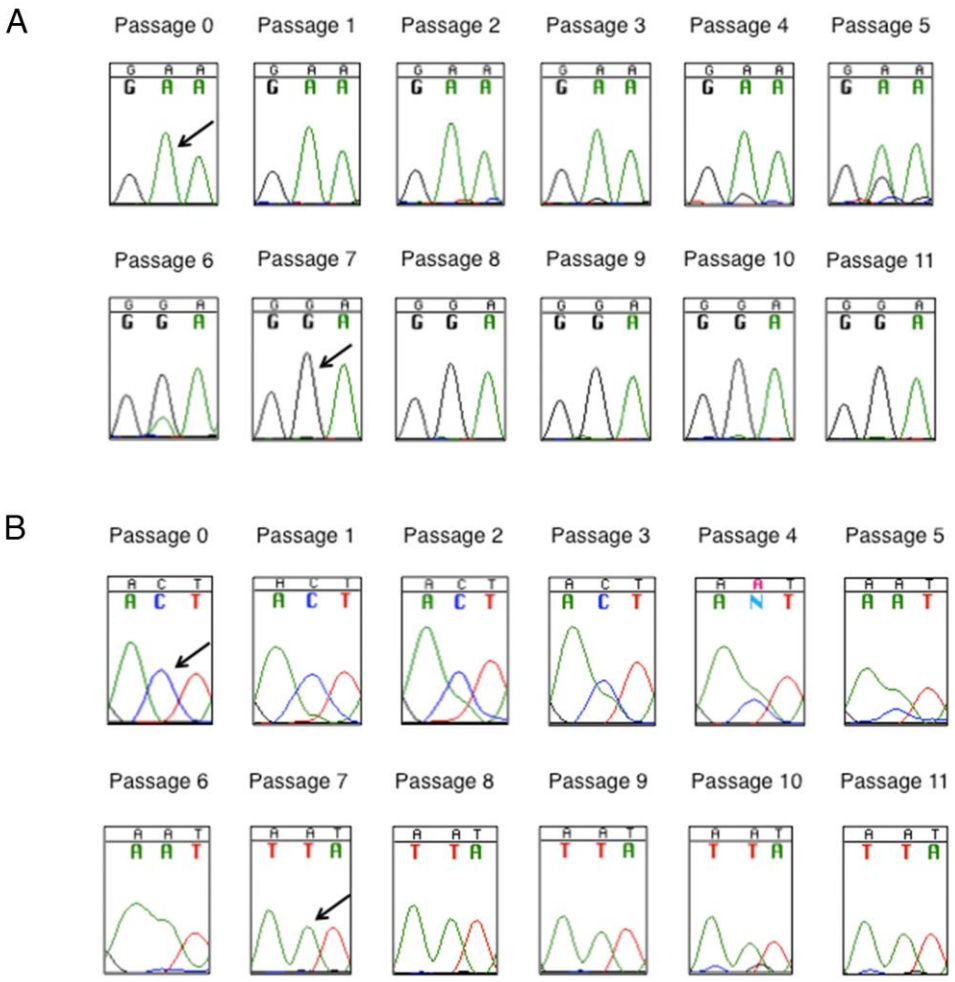

Figure 5.2. Tracking mutations detected in the rPIV5-RSV-G P11 genome. RT-PCR was performed using viral RNA isolated from rPIV5-RSV-G P0 through P11. RT-PCR products were sequenced to determine when the K78E mutation (A) and C-to-A mutation at nucleotide position 4,292 (B) occurred. Chromatogram images were generated using Sequencher v.5.1.

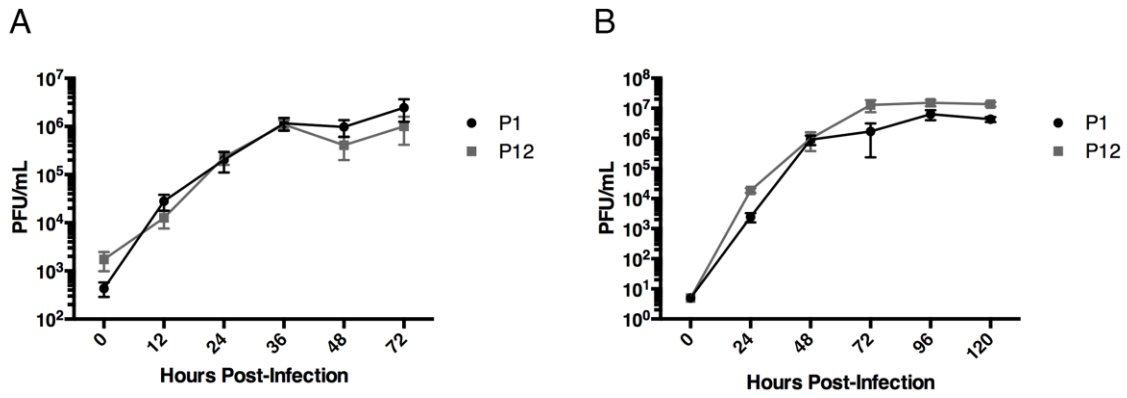

Figure 5.3. Growth Kinetics of rPIV5-RSV-G P1 versus P12. (A) Single-cycle growth curves of rPIV5-RSV-G P0 and P12 in Vero cells. Vero cells were infected with rPIV5-RSV-G P0 or P12 at a MOI = 1. Samples of tissue culture supernatant were collected at 12-hour intervals for 72 hours. (B) Multi-cycle growth curves of rPIV5-RSV-G P0 and P12 in Vero cells. Vero cells were infected with rPIV5-RSV-G P1 or P12 at a MOI = 0.01. Samples of tissue culture supernatant were collected at 24-hour intervals for 120 hours. Samples of three biological replicates were collected at each time point, and plaque assays were performed in BHK21 cells to determine virus titers. Error bars represent the standard error of the mean.

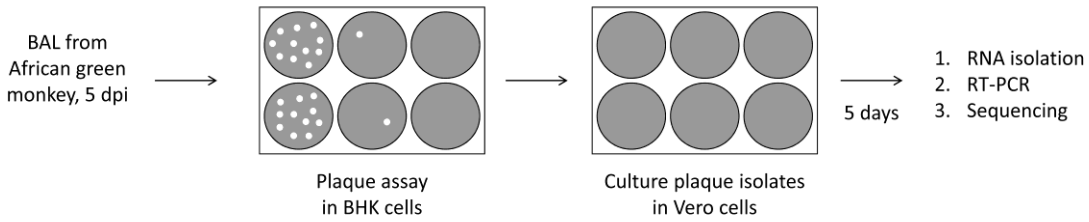

Figure 5.4. Isolation of rPIV5-RSV-F and rPIV5-RSV-G after in vivo passage in African green monkeys. African green monkeys were immunized with $1x10^6$ PFU of rPIV5-RSV-F or rPIV5-RSV-G. BAL washes were collected 5 dpi, and plaque assays were performed in BHK21 cells. 5 days later, plaque isolates were selected and cultured in Vero for 5 days, followed by RNA isolation, RT-PCR, and sequencing of the RT-PCR products.

Table 5.1. Comparison of genomes of rPIV5-RSV-F P0 and P11

P0	P11	Location
None	None	None

Table 5.2. Comparison of insertion sequences of rPIV5-RSV-F P0 and P11 plaque isolates

Mutations	Location
Passage 0 (3/23 isolates)	
V56M	RSV-F
T174A	RSV-F
F114S/Y117H	RSV-F
Passage 11 (6/23 isolates)	
Mixed N569L	RSV-F
Mixed L95L (silent)	RSV-F
Mixed I76N	RSV-F
Mixed F572F (silent)	RSV-F
Mixed F572F (silent)	RSV-F
Mixed K461STOP/MixedF572F (silent)	RSV-F

Table 5.3. Comparison of genomes of rPIV5-RSV-G P0 and P11

P0	P11	Location
K78	E78	V/P
C4292	A4292	3’ UTR of M

Table 5.4. Comparison of insertion sequences of rPIV5-RSV-G P0 and P11 plaque isolates

Mutations	Location
Passage 0 (1/23 isolates)	
I243I (silent)	RSV-G
Passage 11 (0/24 isolates)	
None	

Table 5.5. Comparison of genomes of rPIV5-RSV-F P0 and rPIV5-RSV-F BAL (5 dpi)

P0	BAL Day 5	Location
None	None (A12M001)	None
	None (A12M003)	None
	None (A12M032)	None

Table 5.6. Results of full genome sequencing of rPIV5-RSV-F isolates from BAL (5 dpi)

AGM ID #	Isolate #	Mutation	Location
A12M001	1	None	
A12M001	2	None	
A12M001	3	None	
A12M003	1	None	
A12M032	1	None	
A12M032	3	V128V	PIV5-F

Table 5.7. Results of sequencing insertion region of rPIV5-RSV-F isolates from BAL (5 dpi)

AGM ID #	Isolate #	Mutation	Location
A12M001	4	None	
A12M001	5	None	
A12M001	6	None	
A12M032	4	None	
A12M032	5	None	
A12M032	6	V56V	RSV-F

Table 5.8. Comparison of genomes of rPIV5-RSV-G P0 and rPIV5-RSV-G BAL (5 dpi)

P0	BAL Day 5	Location
None	None (A12M004)	None
	None (A12M015)	None
	None (A12M008)	None

Table 5.9. Results of full genome sequencing of rPIV5-RSV-G isolates from BAL (5 dpi)

AGM ID #	Isolate #	Mutation	Location
A12M004	1	T119T	RSV-G
A12M004	2	None	
A12M015	1	None	
A12M015	2	None	
A12M008	1	A753S	PIV5-L
A12M008	2	None	

Table 5.10. Results of sequencing insertion region of rPIV5-RSV-G isolates from BAL (5 dpi)

AGM ID #	Isolate #	Mutation	Location
A12M004	3	Q77H	RSV-G
A12M004	4	None	
A12M004	5	None	
A12M004	6	None	
A12M015	3	None	
A12M015	4	None	
A12M015	5	None	
A12M015	6	None	
A12M008	3	T125A	RSV-G
A12M008	4	None	
A12M008	5	None	

References

1. **Nair H, Nokes DJ, Gessner BD, Dherani M, Madhi S a., Singleton RJ, O'Brien KL, Roca A, Wright PF, Bruce N, Chandran A, Theodoratou E, Sutanto A, Sedyaningsih ER, Ngama M, Munywoki PK, Kartasasmita C, Simões EA, Rudan I, Weber MW, Campbell H**. 2010. Global burden of acute lower respiratory infections due to respiratory syncytial virus in young children: a systematic review and meta-analysis. Lancet **375**:1545–1555.

2. **Glezen WP, Taber LH, Frank AL, Kasel JA**. 1986. Risk of primary infection and reinfection with respiratory syncytial virus. Am. J. Dis. Child. **140**:543–6.

3. **Escobar GJ, Ragins A, Li SX, Prager L, Masaquel AS, Kipnis P**. 2010. Recurrent Wheezing in the Third Year of Life Among Children Born at 32 Weeks' Gestation or Later. Arch. Pediatr. Adolesc. Med. **164**:915–22.

4. **Wu P, Hartert T V**. 2011. Evidence for a causal relationship between respiratory syncytial virus infection and asthma. Expert Rev. Anti. Infect. Ther. **9**:731–745.

5. **Falsey AR, Walsh EE**. 2000. Respiratory syncytial virus infection in adults. Clin. Microbiol. Rev. **13**:371–84.

6. **Anderson LJ, Dormitzer PR, Nokes DJ, Rappuoli R, Roca a., Graham BS**. 2013. Strategic priorities for respiratory syncytial virus (RSV) vaccine development. Vaccine **31**.

7. **Karron R a, Wright PF, Belshe RB, Thumar B, Casey R, Newman F, Polack FP, Randolph VB, Deatly A, Hackell J, Gruber W, Murphy BR, Collins PL**. 2005. Identification of a recombinant live attenuated respiratory syncytial virus vaccine candidate that is highly attenuated in infants. J. Infect. Dis. **191**:1093–1104.

8. **Bernstein DI, Malkin E, Abughali N, Falloon J, Yi T, Dubovsky F**. 2012. Phase 1 study of the safety and immunogenicity of a live, attenuated respiratory syncytial virus and parainfluenza virus type 3 vaccine in seronegative children. Pediatr. Infect. Dis. J. **31**:109–14.

9. **Yang CF, Wang CK, Malkin E, Schickli JH, Shambaugh C, Zuo F, Galinski MS, Dubovsky F, Tang RS**. 2013. Implication of respiratory syncytial virus (RSV) F transgene sequence heterogeneity observed in Phase 1 evaluation of MEDI-534, a live attenuated parainfluenza type 3 vectored RSV vaccine. Vaccine **31**:2822–2827.

10. **Lamb R, Kolakofsky D**. 2001. Paramyxoviridae: The viruses and their replication, p. . *In* Knipe, D, Howley, P (eds.), Fields Virology4th Editio. Lippincott, Williams, and Wilkins, Philadelphia.

11. **Chen Z, Xu P, Salyards GW, Harvey SB, Rada B, Fu ZF, He B**. 2012. Evaluating a Parainfluenza Virus 5-Based Vaccine in a Host with Pre-Existing Immunity against Parainfluenza Virus 5. PLoS One **7**:e50144.

12. **Li Z, Mooney a., Gabbard JD, Gao X, Xu P, Place RJ, Hogan RJ, Tompkins SM, He B**. 2012. Recombinant Parainfluenza Virus 5 Expressing HA Of Influenza A Virus H5N1 Protected Mice Against Lethal High Pathogenic Avian Influenza H5N1 Challenge. J. Virol. **87**:354–362.

13. **Li Z, Gabbard JD, Mooney A, Gao X, Chen Z, Place RJ, Tompkins SM, He B**. 2013. Single-dose vaccination of a recombinant parainfluenza virus 5 expressing NP from H5N1 virus provides broad immunity against influenza A viruses. J. Virol. **87**:5985–93.

14. **Li Z, Gabbard JD, Mooney A, Chen Z, Tompkins SM, He B**. 2013. Efficacy of parainfluenza virus 5 mutants expressing hemagglutinin from H5N1 influenza A virus in mice. J. Virol. **87**:9604–9.

15. **Li Z, Gabbard J, Johnson S, Dlugolenski D, Phan S, Tompkins M, He B**. 2015. Efficacy of a parainfluenza virus 5 (PIV5)-based H7N9 vaccine in mice and guinea pigs: antibody titer towards HA was not a good indicator for protection. PLoS One In Press.

16. **Chen Z, Zhou M, Gao X, Zhang G, Ren G, Gnanadurai CW, Fu ZF, He B**. 2012. A Novel Rabies Vaccine Based on a Recombinant Parainfluenza Virus 5 Expressing Rabies Virus Glycoprotein. J. Virol. **87**:2986–2993.

17. **Mooney AJ, Li Z, Gabbard JD, He B, Tompkins SM**. 2013. Recombinant parainfluenza virus 5 vaccine encoding the influenza virus hemagglutinin protects against H5N1 highly pathogenic avian influenza virus infection following intranasal or intramuscular vaccination of BALB/c mice. J. Virol. **87**:363–71.

18. **Tompkins SM, Lin Y, Leser GP, Kramer KA, Haas DL, Howerth EW, Xu J, Kennett MJ, Durbin RK, Durbin JE, Tripp R, Lamb RA, He B**. 2007. Recombinant parainfluenza virus 5 (PIV5) expressing the influenza A virus hemagglutinin provides immunity in mice to influenza A virus challenge. Virology **362**:139–50.

19. **Phan SI, Chen Z, Xu P, Li Z, Gao X, Foster SL, Teng MN, Tripp R a., Sakamoto K, He B**. 2014. A respiratory syncytial virus (RSV) vaccine based on parainfluenza virus 5 (PIV5). Vaccine **32**:3050–3057.

20. **Mueller S, Wimmer E**. 1998. Expression of foreign proteins by poliovirus polyprotein fusion: analysis of genetic stability reveals rapid deletions and formation of cardioviruslike open reading frames. J. Virol. **72**:20–31.

21. **He B, Paterson RG, Ward CD, Lamb R a**. 1997. Recovery of infectious SV5 from cloned DNA and expression of a foreign gene. Virology **237**:249–260.

22. **Rima BK, Gatherer D, Young DF, Norsted H, Randall RE, Davison AJ**. 2014. Stability of the parainfluenza virus 5 genome revealed by deep sequencing of strains isolated from different hosts and following passage in cell culture. J. Virol. **88**:3826–36.

23. **Lin GY, Paterson RG, Lamb R a**. 1997. The RNA binding region of the paramyxovirus SV5 V and P proteins. Virology **238**:460–9.

24. **Bourgeois C, Bour JB, Lidholt K, Gauthray C, Pothier P**. 1998. Heparin-like structures on respiratory syncytial virus are involved in its infectivity in vitro. J. Virol. **72**:7221–7.

25. **Poch O, Blumberg BM, Bougueleret L, Tordo N**. 1990. Sequence comparison of five polymerases (L proteins) of unsegmented negative-strand RNA viruses: theoretical assignment of functional domains. J. Gen. Virol. **71 (Pt 5)**:1153–62.

26. **Johnson PR, Spriggs MK, Olmsted R a, Collins PL**. 1987. The G glycoprotein of human respiratory syncytial viruses of subgroups A and B: extensive sequence divergence between antigenically related proteins. Proc. Natl. Acad. Sci. U. S. A. **84**:5625–5629.

27. **Tan L, Coenjaerts FEJ, Houspie L, Viveen MC, van Bleek GM, Wiertz EJHJ, Martin DP, Lemey P**. 2013. The comparative genomics of human respiratory syncytial virus subgroups A and B: genetic variability and molecular evolutionary dynamics. J. Virol. **87**:8213–26.

CHAPTER 6

PIV5 VECTORS EXPRESSING WILD-TYPE OR PRE-FUSION RESPIRATORY SYNCYTIAL VIRUS FUSION PROTEIN PROTECT MICE AND COTTON RATS FROM RSV CHALLENGE[4]

[4]Phan S.I., Zengel J.R., Wei H., Li Z., Kim S., Gilbert B., Boukhvalova M., He B. To be submitted to *Journal of Virology*.

Abstract

Human respiratory syncytial virus (RSV) is the leading cause of pediatric bronchiolitis and hospitalizations. RSV can also cause severe complications in elderly and immunocompromised individuals. There is no licensed vaccine. We previously generated a PIV5-vectored vaccine candidate expressing RSV-F that was immunogenic and protective in mice. Groups have recently demonstrated that antibodies against the pre-fusion conformation of the RSV fusion protein (F) have more potent neutralizing activity than antibodies against the post-fusion conformation. Therefore, to improve on our previously developed PIV5-based RSV vaccine candidate, we engineered PIV5 to express a pre-fusion stabilized F mutant. We also deleted the SH gene from the PIV5 backbone, which has been shown in the past to improve vaccine efficacy. The candidates were tested in BALB/c mice via the intranasal route and induced both humoral and cell-mediated immunity. They also protected against RSV infection in the mouse lung. When administered intranasally or subcutaneously in cotton rats, the candidates were highly immunogenic and reduced RSV loads in both the upper and lower respiratory tracts. PIV5-RSV-F was equally protective when administered intranasally or subcutaneously. In all cases, the pre-fusion F mutant did not induce higher neutralizing antibody titers than wild-type F. These results show that antibodies against both pre- and post-fusion F are important for neutralizing RSV, and should be considered when designing a vectored RSV vaccine. The findings also indicate that PIV5-RSV-F may be administered subcutaneously, which is the preferred route for vaccinating infants who may develop nasal congestion as a result of intranasal vaccination.

Introduction

Human respiratory syncytial virus (RSV) is a leading cause of pediatric bronchiolitis and pneumonia, resulting in over 3 million hospitalizations and 200,000 deaths globally each year in children under 5 years old (1). Disease burden is also significant among elderly and immunocompromised populations. An estimated 3 to 7% of healthy adults over 65 years old and 4 to 10% of high-risk adults develop RSV infections annually, with mortality reaching 8% among hospitalized individuals (2).

RSV vaccine development has been ongoing since the 1960s, when the virus was first discovered. Numerous candidates have been developed and tested, but a vaccine has yet to be licensed. A formalin-inactivated RSV vaccine (FI-RSV) tested during the 1960s failed to protect against infection. Furthermore, it caused enhanced disease in vaccinees upon natural exposure during the following RSV season. The concern of enhanced disease has been a major hurdle for vaccine development (3–6). Many approaches have been used, including live attenuated vaccines, vectored vaccines, subunit vaccines, and virus-like particles (7–10) . Promising live attenuated and vectored vaccine candidates have been developed, which are not known to potentiate disease upon natural RSV infection (11).

A PIV5-vectored RSV vaccine has been recently developed in which the coding sequence of the RSV fusion protein (RSV-F) is inserted between the HN and L genes of PIV5 [PIV5-RSV-F (HN-L)]. The vaccine candidate was immunogenic and highly efficacious at protecting mice against RSV lower respiratory tract infection (12). It has been hypothesized that the vaccine candidate can be improved by modifying the vector or by increasing the antigen expression level. The small hydrophobic (SH) protein of PIV5

plays an important role in blocking TNF-α-mediated apoptosis. Deletion of this gene from PIV5 induces apoptosis in infected cells through an intrinsic pathway, possibly making it a better vector for presenting foreign antigens (13). Previous work has shown that deleting the SH gene from PIV5 improves the efficacy of a PIV5-based vaccine expressing H5 of the H5N1 influenza strain. When tested in mice, the PIV5ΔSH-H5 vaccine increased antibody and cell-mediated immune responses to influenza, and provided better protection against H5N1 infection compared to its SH-containing counterpart (14).

The PIV5-RSV-F vaccine candidate can also be improved by modifying the RSV-F antigen. Recent work has suggested that RSV-F in its pre-fusion conformation induces the production of antibodies with more potent *in vitro* neutralizing activity (15). A stabilized pre-fusion RSV-F mutant called DS-Cav1 was recently crystallized and has been shown to induce higher neutralizing antibody titers than the post-fusion conformation of F (16, 17). Introduction of the DS-Cav1 construct into a chimeric bovine/human PIV3 vector generated a vaccine candidate that was more immunogenic and protective than the same vector expressing post-fusion RSV-F (18).

In this work, we sought to improve on the previous PIV5-RSV-F (HN-L) candidate by deleting the SH gene of PIV5 or by replacing wild-type RSV-F with the DS-Cav1 pre-fusion mutant. We hypothesized that combining both modifications into a vaccine would generate a candidate that is more immunogenic and protective against RSV infection.

Materials and Methods

Cells

Vero and Hep-2 cells were maintained in Dulbecco's Modified Eagle Medium (DMEM) supplemented with 10% fetal bovine serum (FBS), 100 IU/mL penicillin, and 100 μg/mL streptomycin (1% P/S; Mediatech Inc., Manassas, VA, USA). MDBK cells were grown in DMEM containing 5% FBS and 1% P/S. Cells were prepared one day prior to infection, achieving approximately 90% confluence by the following day.

Plasmids and virus rescue

To obtain the DS-Cav1 coding sequence, the mutations described in McClellan et al. were introduced into the wild-type F sequence from RSV/A/A2 by splicing by overlap extension (16). The cDNA clones of PIV5 expressing RSV-F or the DS-Cav1 mutant were constructed using previously described methods (12, 14, 19). Primer sequences are available upon request. Infectious viruses were rescued in BHK cells as previously described (12).

Viruses

Recombinant PIV5 or PIV5ΔSH viruses expressing RSV-F or DS-Cav1 were propagated in MDBK cells as previously described (12, 19). Briefly, MDBK cells were infected at a multiplicity of infection (MOI) of 0.01 in DMEM and 1% BSA. After allowing the inoculum to adsorb for 1-2 h, the inoculum was removed and replaced with DMEM containing 2% FBS and 1% P/S. After 4-5 days of incubation at 37°C, 5% CO_2, the cell medium was collected and centrifuged to remove debris. The supernatant was mixed with a 0.1 volume of 10X SPG buffer, flash-frozen in liquid nitrogen, and stored at -80°C.

RSV/A/A2 used in mouse studies was grown in Vero cells as previously described (12, 20). RSV/A/Tracy and RSV/A/A2 used in cotton rat studies were propagated in HEp-2 cells. FI-RSV Lot#100 was produced in the mid-1960s by Pfizer Inc., and was stored and used on-site at Sigmovir, Inc.

Immunofluorescence assay (IFA)

Direct and indirect immunofluorescence assays were performed to detect total RSV-F, pre-fusion RSV-F, and post-fusion RSV-F in cells infected with PIV5-RSV-F (HN-L), PIV5-RSV-F (SH-HN), PIV5-RSV-pF (SH-HN), PIV5ΔSH-RSV-F, and PIV5ΔSH-RSV-pF. A549 cells seeded onto coverslips were infected with the vaccine candidates. Two days after infection, cells were fixed with 2% formaldehyde in phosphate-buffered saline (PBS) and immunostained with antibodies that bound total RSV-F (palivizumab, site II-specific), post-fusion F (4D7, site I-specific), and pre-fusion F (D25, site φ-specific). Palivizumab and D25 were directly labeled with Zenon® Alexa Fluor 488® and Zenon® allophycocyanin (APC) complexes, respectively, according to the manufacturer's instructions (Thermo Fisher Scientific, Waltham, MA). The 4D7 antibody was indirectly labeled with goat anti-mouse IgG conjugated to Cy3. For permeabilized samples, 0.1% saponin was included in the immunostaining buffers. Following staining, the coverslips were mounted with ProLong Gold antifade reagent and imaged using a NikonA1R confocal microscope (Nikon Instruments Inc., Melville, NY).

Flow cytometry

A549 cells were infected with PIV5-RSV-F (HN-L), PIV5-RSV-F (SH-HN), PIV5-RSV-pF (SH-HN), PIV5ΔSH-RSV-F, and PIV5ΔSH-RSV-pF. Forty-eight hours after infection, the cells were harvested with 10 mM EDTA and immunostained with

palivizumab, D25, and 4D7 antibodies conjugated to Zenon® Alexa Fluor 488® , Zenon® phycoerythrin (PE), or ® Zenon® allophycocyanin (APC). For surface staining, the cells were immunostained with the antibodies and then fixed with 1% formaldehyde. For total staining, the cells were first fixed and permeabilized with BD Cytofix/Cytoperm buffer followed by immunostaining. Since a single cell can present both pre-and post-fusion F, we determined the levels of protein expression based on the percent of RSV-F positive cells that stained positive for pre-fusion RSV-F, post-fusion RSV-F, or both. Flow cytometry was performed using a BD LDR II flow cytometer (Franklin Lakes, NJ).

Plaque assays

PIV5 plaque assays were performed as previously described (21). Briefly, 10-fold serial dilutions were prepared in DMEM with 1% BSA. One hundred μL of each dilution was transferred to 6-well plates of BHK21 cells, in a total infection volume of 1 ml. After adsorption for 1 to 2 h at 37°C, 5% CO_2, the inocula were aspirated, and cell monolayers were overlaid with DMEM containing 10% tryptose phosphate broth (TPB), 2% FBS, 1% P/S, and 1% low melting point agarose. After 5 days, the cells were fixed with 2% formaldehyde, overlays were removed, and the cells were stained with crystal violet to visualize the plaques.

For mouse studies, RSV plaque assays were performed in Vero cells and visualized by immunostaining with RSV-F-specific antibody as previously described (12, 22). For cotton rat studies, plaque assays were performed in HEp-2 cells and visualized by staining with crystal violet.

Mouse studies

All mouse studies were performed according to the protocols approved by the Institutional Animal Care and Use Committee at the University of Georgia. Six to eight-week-old, female, BALB/c mice were anesthetized by intraperitoneal injection of 200 µL of 2, 2, 2-tribromoethanol in tert-amyl alcohol (Avertin). The mice were intranasally immunized with 10^6 PFU of the PIV5-based vaccine candidates or RSV/A/A2 in 100 µl volumes. Mice treated intranasally with 100 µl of PBS served as negative controls. Twenty-one days post-immunization, sera were collected via cheek bleed. Twenty-eight days post-immunization, mice were challenged with 10^6 PFU of RSV/A/A2 in a 100 µl. Four and six days after challenge, mice were humanely sacrificed, and lungs were collected to determine viral burden as previously described (12, 22).

For the cohort used for ELISpot experiments, mice were immunized as described above. Twenty-eight days post-immunization, mice were sacrificed, and spleens were harvested for subsequent splenocyte isolation.

Cotton rat study 1: comparing PIV5-RSV-pF/F (SH-HN) and PIV5ΔSH-RSV-pF/F

All experiments were performed in accordance with guidelines set forth by the National Institutes of Health and the United States Department of Agriculture, using protocols approved by the Baylor College of Medicine Investigational Animal Care and Use Committee. Thirty cotton rats (*Sigmodon Hispidus*) were divided into six groups consisting of 5 animals each. Animals were lightly anesthetized with isoflurane and intranasally immunized with 10^3 PFU of PIV5-RSV-F, PIV5-RSV-pF, PIV5ΔSH-RSV-F, or PIV5ΔSH-RSV-pF in 100 µl. An additional group was intranasally immunized with 10^2 PFU of PIV5ΔSH-RSV-pF. Cotton rats treated with 100 µl of PBS served as the

negative controls (Table 6.1). Sera were collected 21 and 28 days after immunization and four days after challenge for serological studies. Animals were challenged on day 28 with $1.21x10^5$ PFU of RSV/A/Tracy in 100 µl. Four days later, the animals were euthanized by CO_2 asphyxiation, and lungs and noses were lavaged to determine viral burden.

Cotton rat study 2: comparing PIV5-RSV-F (SH-HN) and PIV5ΔSH-RSV-F safety and efficacy using different routes of administration

Cotton rats were maintained and handled according to the National Institutes of Health guidelines and protocols approved by the Sigmovir Institutional Animal Care and Use Committee.

Fifty 6 to 8 week-old inbred female cotton rats were divided into ten groups containing 5 animals each. Animals were anesthetized and immunized according to Table 6.2. Sham-vaccinated groups and the FI-RSV-vaccinated group were boosted 28 days post-primary immunization. All other groups only received a single dose on day 0. Sera were collected 28 and 49 days after primary immunization. Animals were also challenged on day 49. Five days after challenge, the cotton rats were euthanized by CO_2-asphyxiation. Nasal tissue and the left lung section were harvested, homogenized in HBSS and 10% SPG, and used for virus titration. The right lung section was inflated with 10% formalin for histopathology. The lingular lung segments were flash frozen for RNA isolation and qPCR.

Anti-pre-fusion and post-fusion F IgG ELISA

Antibodies against pre-fusion and post-fusion conformations of RSV-F were measured by indirect ELISA. Immulon® 2HB 96-well microtiter plates were coated with

50 µl of purified pre-fusion or post-fusion RSV-F at 2 µg/ml in PBS and incubated overnight at 4°C. Two-fold serial dilutions of serum were made in blocking buffer [3% nonfat dry milk dissolved in PBS containing 0.05% Tween-20® (PBST)]. One hundred microliters of each dilution were transferred to the plates and incubated for two hours at room temperature. The plates were washed with PBST, and secondary antibody was diluted 1:2500 [horseradish-peroxidase (HRP)-conjugated goat anti-mouse IgG or HRP-conjugated chicken anti-cotton rat IgG] in blocking buffer. Fifty microliters of diluted secondary antibody were added to each well, and the plates were incubated for one hour at room temperature. The plates were washed and developed with 100 µl/well of SureBlue Reserve TMB substrate at room temperature. The reaction was stopped with 100 µl/well of 1N HCl after 5 to 7 minutes. The optical density was read at 450 nm using a BioTek Epoch microplate reader. The endpoint antibody titer was defined as the highest serum dilution at which the OD was greater than two standard deviations above the mean OD of the naïve serum.

Cotton rat study 2, anti-RSV-F IgG ELISA: comparing PIV5-RSV-F (SH-HN) and PIV5ΔSH-RSV-F safety and efficacy using different routes of administration

Ninety-six-well ELISA plates were coated with purified RSV F protein extracted from RSV/A/A2-infected HEp-2 cells. Plates were blocked for 1 h, washed, and incubated with four-fold serial dilutions of serum for 1 h at room temperature. After washing, the plates were incubated with rabbit anti-cotton rat IgG (1:4000) for 1 h at room temperature. Following additional washes, the plates were incubated with HRP-conjugated goat anti-rabbit IgG (1:4000) for 1 h at room temperature. The plates were

washed, developed with TMB substrate for 15 minutes, and the reaction was stopped with TMB-Stop solution. The optical density was read at 450 nm.

Mouse study neutralization assays

Serum samples were heat-inactivated at 56°C for 30 minutes. Two-fold serial dilutions of samples were prepared in Opti-MEM I supplemented with 2% FBS, 1% P/S, and 5% guinea pig complement (GPC). The diluted samples were mixed 150 PFU/25 µl of RSV/A/A2 and incubated for 1 h at 37°C, 5% CO_2. The serum-virus mixtures were then transferred to confluent monolayers of Vero cells and allowed to adsorb for 1 h at 37°C, 5% CO_2. The cells were then overlaid with 0.8% methylcellulose dissolved in Opti-MEM I supplemented with 2% FBS, 1% P/S. After incubation for 7 days at 37°C, 5% CO_2, the cells were fixed in 60% acetone/40% methanol and immunostained to visualize plaques. The neutralizing antibody titers were determined based on the highest serum dilution at which 50% neutralization of the input virus control was achieved.

Cotton rat study 1, microneutralization assay: comparing PIV5-RSV-pF/F (SH-HN) and PIV5ΔSH-RSV-pF/F

Two-fold serial dilutions of heat-inactivated serum were prepared and incubated with RSV/A/Tracy or RSV/B/18537 to determine the neutralizing antibody titer. Serum-virus mixtures were transferred to confluent monolayers of HEp-2 cells and incubated at 37°C, 5% CO_2. The cells were then fixed with 10% neutral-buffered formalin and stained with crystal violet. The neutralizing antibody titer was defined as the highest serum dilution at which a 50% reduction in viral cytopathic effect (CPE) was observed.

Cotton rat study 2, neutralization assay: comparing PIV5-RSV-F (SH-HN) and PIV5ΔSH-RSV-F safety and efficacy using different routes of administration

Four-fold dilutions of heat-inactivated serum were prepared in Eagle's Minimum Essential Medium and incubated with 25-50 PFU of RSV/A/A2 for 1 h at room temperature. Serum-virus mixtures were transferred to confluent HEp-2 cell monolayers, allowed to adsorb for 1 h at 37°C 5% CO_2, and overlaid with 0.75% methylcellulose medium. After incubating for 4 days at 37°C, 5% CO_2, cells were fixed and stained with crystal violet to visualize plaques. Neutralizing antibody titer was determined at the 60% reduction endpoint of the virus control using the statistical program "plqard.manual.entry."

ELISpot

Twenty-eight days post-immunization, spleens were harvested from the mice and pressed through 70 μm strainers to isolate splenocytes. After rinsing the strainers with HBSS, the splenocytes were collected by centrifugation and treated with red blood cell lysis buffer (0.15M NH_4Cl, 1M $KHCO_3$, 0.1mM Na_2EDTA; ACK buffer). The cells were then washed with HBSS, resuspended in complete tumor medium (CTM), and diluted to a concentration of $5x10^6$ cells/ml.

The BD Mouse IFN-γ ELISpot Set was used to measure IFN-γ-secreting splenocytes from vaccinated mice. One day prior to performing the assay, ELISpot plates were activated with 70% ethanol, washed with water, and coated with capture antibody overnight at 4°C. The next day, plates were washed and blocked with CTM for at least 2 h at room temperature. The blocking solution was discarded, and peptides were added to the wells (200 ng of peptide/50 μl of CTM/well). The peptides used were RSV-

F (85-93) and GFP (200-208). PMA/ionomycin was used to non-specifically stimulate the cells. Fifty microliters of cells were added to each well, and the plates were incubated for 48 h at 37°C, 5% CO_2. Following incubation, the plates were immunostained according to the manufacturer's instructions and spots were enumerated using an ImmunoSpot® Analyzer.

Quantitative real-time PCR (qPCR)

Total RNA was extracted from lung tissue using the RNeasy kit (Qiagen). To prepare cDNA, 1 μg of total RNA was combined with Superscript II RT (Invitrogen) and oligo dT primer. Real-time PCR reactions were prepared using Bio-Rad iQ™ SYBR Green Supermix and 0.5 μM of primer. The reactions were run on a Bio-Rad iCycler. Baseline cycles and cycle threshold (Ct) were calculated using the PCR Base Line Subtracted Curve Fit mode of the iQ5 software. Relative quantitation of DNA was applied to all samples. Standard curves were generated using serially-diluted cDNA that had the highest levels of the transcript of interest. Ct values were plotted against $\log_{10}$ cDNA dilution factor. The standard curves were used to convert Ct values from experimental samples to relative expression units. The relative expression units were then normalized to level of β-actin mRNA in the corresponding sample.

Histology

Lungs were dissected, inflated with 10% neutral-buffered formalin, and then immersed in the same fixative. The lungs were then embedded in paraffin, sectioned, and stained with hematoxylin and eosin (H&E). Peribronchiolitis, perivasculitis, interstitial pneumonia, and alveolitis were scored in a bind fashion on a severity scale of 0-4. The scores were then converted to a 0-100% histopathology scale.

Statistical analysis

Statistical analysis was performed using Graphpad Prism software version 6 for Macintosh (Graphpad Software, La Jolla, CA). Analysis of variance (ANOVA) followed by Tukey multiple comparison tests were used to analyze antibody titers and challenge virus loads.

Results

Examination of pre-fusion and post-fusion RSV F expression

McLellan et al. recently obtained the crystal structure of pre-fusion stabilized RSV-F mutant called DS-Cav1. This mutant contains substitutions that introduce cysteine modifications and fill cavities in the "head" of the pre-fusion structure (17) (Fig. 6.1A). Four new vaccine candidates were generated by inserting the coding sequence of either wild-type RSV-F or the DS-Cav1 mutant (pF), using previously described methods (Fig. 6.1B) (12, 19). Expression of pre- and post-fusion RSV-F by the vaccine candidates was examined by fluorescence microscopy and flow cytometry. A549 cells were infected with the different candidates and stained 48 h later using antibodies specific to pre-fusion F (D25), post-fusion F (4D7), and total F (palivizumab). Cells infected with candidates encoding wild-type F expressed mixtures of both pre-fusion and post-fusion F (Fig. 6.2C-6.2F, 6.2I and 6.2J, 6.2M and 6.2N). Candidates encoding the DS-Cav1 construct expressed mostly pre-fusion F as expected, but DS-Cav1 expression was lower than wild-type F expression. There appeared to be little-to-no post-fusion F expression when examined by microscopy or flow cytometry (Fig. 6.2G and 6.2H, 6.2K-6.2N). F expression was similar in the wild-type PIV5 backbone and the ΔSH backbone (Fig. 6.2C-6.2F, 6.2I and 6.2J,6.2M and 6.2N). Furthermore, the F constructs localized both

inside the cell and on the cell surface (Fig. 6.2A-6.2N). Thus, wild-type F expressed from PIV5-based vectors consisted of a mixture or pre- and post-fusion conformations, while the majority of DS-Cav1 was expressed in the pre-fusion conformation.

Immunogenicity and protective efficacy of vaccine candidates in mice

To examine the immunogenicity of the vaccine candidates, 6 to 8-week-old BALB/c mice were immunized once with 10^6 PFU of the different candidates, and serum was collected 21 days post-vaccination. Antibodies against pre-fusion and post-fusion F were measured by ELISA. Serum neutralizing antibodies were measured by 50% plaque reduction assay.

All of the vaccine candidates induced similar levels of antibodies that bound to pre-fusion F (Fig. 6.3A). The wild-type constructs induced approximately 32-fold higher levels of post-fusion F-specific antibodies compared the DS-Cav1 counterparts (Fig. 6.3B). All of the candidates induced serum neutralizing antibody titers, but candidates expressing wild-type F induced titers approximately 8 to 32-fold higher than those induced by the DS-Cav1-expressing candidates (Fig. 6.3C). The PIV5ΔSH backbone did not increase the immunogenicity of any of the constructs (Fig 6.3A and 6.3B). Therefore, despite expressing mostly pre-fusion F, candidates encoding the DS-Cav1 construct did not increase levels of pre-fusion F antibodies or neutralizing antibodies in mice.

To examine cell-mediated immune responses induced by the vaccine candidates, ELISpot was performed on splenocytes harvested from a separate cohort of 6 to 8 week-old mice. All of the immunization groups had similar numbers of IFN-γ-secreting cells in response to RSV-F peptide stimulation (Fig. 6.3D-6.3F). Thus, all of the vaccine candidates elicited significant cell-mediated immune responses, regardless of pre-fusion

and post-fusion F expression and regardless of the presence of SH in the vector backbone.

The mice were challenged 28 days post-immunization with RSV/A/A2 to determine the protective efficacies of the different vaccine candidates. None of the mice had detectable challenge virus in the lungs four and six days post-challenge, showing that all of the candidates induced potent lower respiratory tract protection against RSV infection (Fig. 6.4A and 6.4B).

Immunogenicity and protective efficacies of vaccine candidates in cotton rats

The vaccine candidates were further evaluated in cotton rats, a more permissive model for RSV infection (23). Previous findings indicated that PIV5-RSV-F (HN-L) induced potent protection against RSV infection in cotton rats. Therefore, for this study, we intranasally immunized cotton rats with low doses (10^3 PFU) of PIV5-RSV-F (SH-HN), PIV5-RSV-pF (SH-HN), or the ΔSH counterparts to determine if differences in vaccine could be observed at low doses. An additional group was immunized with 10^2 PFU of PIV5ΔSH-pF to determine whether the candidate was efficacious at an even lower dose. Similar to the findings in mice, all candidates elicited similar levels of anti-pre-fusion F IgG (Fig. 6.5A), while the DS-Cav1-expressing candidates induced 8-fold lower anti-post-fusion F IgG titers (Fig. 6.5B). The candidates also induced similar serum neutralizing antibody titers against RSV/A (Fig. 6.5C). The neutralizing antibody titers against RSV/B were significantly lower than the titers against RSV/A (Fig. 6.5D). Only the animals immunized with PIV5-RSV-F (SH-HN) or PIV5ΔSH had significant levels of neutralizing antibodies against RSV/B (Fig. 6.5D).

Cotton rats were challenged 28 days post-immunization with $1.21x10^5$ PFU of RSV/A/Tracy, which is 97% identical to RSV/A/A2. Immunization with the candidates reduced viral loads in the nasal wash fluid by 1.40 to 1.66 $\log_{10}$ PFU (Fig. 6.6A). In the lung lavage fluid, viral loads were reduced by 2 to 3 $\log_{10}$ (Fig. 6.6B). There were no statistical differences in post-challenge viral loads between groups. Thus, all of the candidates were highly effective at inducing humoral immune responses and protecting against RSV challenge. Furthermore, immunization with 10^2 PFU of PIV5ΔSH-pF was as effective as immunizing with 10^3 PFU.

Evaluating efficacies of wild-type F expressing candidates using different routes of administration

Since the DS-Cav1 expressing candidates were no more effective than the wild-type F-expressing candidates at inducing RSV-specific immunity and protection, we sought to evaluate the efficacies of PIV5-RSV-F (SH-HN) and PIV5ΔSH-RSV-F in cotton rats using alternate routes of administration. Cotton rats were intranasally or subcutaneously immunized with 10^5 PFU of the vaccine candidates. The candidates were also administered subcutaneously at 10^6 PFU. A group intranasally immunized with 10^5 PFU RSV/A/A2 was used as a positive control for protection and safety. Mice sham-vaccinated with PBS intranasally or intramuscularly were used as negative controls for protection. An additional FI-RSV-group was included for comparison in safety studies. This group was intramuscularly vaccinated two times, with 28 days between prime and boost vaccinations (Table 2).

Serum samples were collected 28 and 49 days post-immunization for serology studies. High levels of RSV-specific IgG antibodies were detected in all groups

immunized with the vaccine candidates, with titers comparable to the RSV/A/A2-immunized group. The FI-RSV-immunized group had lower F-specific IgG titers overall, with antibody levels increasing between 28 and 49 days post-immunization due to boosting. The antibody titers of the groups immunized with the vaccine candidates were slightly higher 28 days-post immunization than 49 days post-immunization (Fig. 6.7A). The highest average neutralizing antibody titers were observed in the group immunized with RSV/A/A2. Both PIV5-RSV-F (SH-HN) and PIV5ΔSH-RSV-F elicited significant neutralizing antibodies by both intranasal and subcutaneous routes. PIV5-RSV-F (SH-HN) administered intranasally or subcutaneously at 10^5 PFU induced similar levels of neutralizing antibodies. The subcutaneous 10^6 PFU dose of PIV5-RSV-F (SH-HN) did not improve the neutralizing antibody response. For the PIV5ΔSH-RSV-F candidate, 10^5 PFU administered intranasally induced slightly higher neutralizing antibodies than when given via the subcutaneous route. Increasing the subcutaneous dose of PIV5ΔSH-RSV-F to 10^6 PFU induced slightly higher neutralizing antibody titers. Similar to the serum IgG titers, the neutralizing antibody titers were higher at 28 days post-immunization compared to 49 days post-immunization (Fig. 6.7B). Overall, 10^5 or 10^6 PFU of PIV5-RSV-F (SH-HN) given subcutaneously induced similar antibody titers as 10^5 PFU administered intranasally. Deleting SH from the PIV5 backbone did not improve the humoral response to RSV.

The cotton rats were intranasally challenged 49 days post-immunization with 10^5 PFU of RSV/A/A2. Nasal and lung tissue were collected five days post-challenge to determine viral loads. No challenge virus was detected in the nasal tissues of animals vaccinated with RSV/A/A2. Immunization with 10^5 PIV5-RSV-F (SH-HN) intranasally

or subcutaneously reduced nasal viral loads by 3.5 $\log_{10}$. Increasing the subcutaneous dose to 10^6 PFU did not improve protection. Immunization with PIV5ΔSH-RSV-F intranasally also reduced nasal viral loads by 3.5 $\log_{10}$. Subcutaneous administration of the vaccine candidate was less efficacious, reducing nasal viral loads by 2 $\log_{10}$ at the 10^5 PFU dose and 3 $\log_{10}$ at the 10^6 PFU dose. As expected, sham-vaccinated animals or FI-RSV-vaccinated animals had high viral loads in the nose (Fig. 6.8A). In the lung, animals immunized with PIV5-RSV-F (SH-HN) by either route had no detectable virus, comparable to the animals immunized with RSV/A/A2. Animals immunized subcutaneously with PIV5ΔSH-RSV-F also had no detectable virus in the lung. Only one out of five animals immunized intranasally with PIV5ΔSH-RSV-F had any virus detected in the lung (2.5 $\log_{10}$ PFU/g). FI-RSV vaccination conferred modest protection against lower respiratory tract infection (Fig. 6.8B). All of the PIV5-based vaccine candidates provided robust upper and lower respiratory tract protection by both the intranasal and subcutaneous routes. The PIV5-RSV-F (SH-HN) candidate appeared to be slightly more efficacious than the rPIV5ΔSH-RSV-F candidate via the subcutaneous route.

Evaluating the safety of wild-type F expressing candidates using different routes of administration

In addition to testing the efficacies of the vaccine candidates, we examined their safety. Since the FI-RSV vaccine causes post-challenge enhanced disease that can be recapitulated in cotton rats, we sought to determine whether there was any evidence of enhanced disease caused by our vaccine candidates (23). Since enhanced disease is associated with a Th2-biased immune response, cytokine levels were measured in lung tissues five days post-challenge by qPCR (24). Specifically, mRNA levels of IFN-γ, IL-2

and IL-4 were measured. IFN-γ mRNA levels were highest in sham-immunized and FI-RSV-immunized groups. IFN-γ mRNA levels were similarly low between groups immunized with the PIV5-based candidates and the RSV-immunized group (Fig. 6.9A). IL-2 mRNA levels were similar among all groups, but the average IL-2 level from the FI-RSV group was significantly higher (Fig. 6.9B). IL-4 was only significantly elevated in the FI-RSV-vaccinated group, consistent with the histopathology results and the enhanced disease phenotype (Fig. 6.9C and 6.9D).

Hematoxylin and eosin-stained lung sections from the different groups were examined for four hallmarks of pulmonary inflammation: peribronchiolitis, perivasculitis, interstitial pneumonia, and alveolitis. Histopathology was scored on a 0-4 severity scale and converted to a 0-100% scale. The greatest lesions were observed in the FI-RSV-immunized, RSV-challenged group. Pulmonary changes were moderate in groups immunized with PIV5-RSV-F (SH-HN) or PIV5ΔSH-RSV-F (IN or SC), with levels that did not exceed those observed in the RSV-immunized, RSV-challenged group or the sham-immunized, RSV-challenged group (Fig. 6.9D). Based on cytokine profile and the histopathology results, the PIV5-based vaccine candidates did not appear to cause enhanced disease upon challenge with RSV.

Discussion

In this study, we characterized and evaluated recombinant PIV5-based RSV vaccine candidates expressing wild-type or pre-fusion-stabilized RSV-F in a PIV5 or PIV5ΔSH backbone. The candidates were evaluated in mice and cotton rats for immunogenicity, protection against RSV infection, and safety.

RSV-F expression in cells infected with the vaccine candidates demonstrated similar levels of wild-type RSV-F expression and DS-Cav1 expression by both PIV5 and PIV5ΔSH vectors. Wild-type F was expressed as a mixture of pre-fusion and post-fusion conformations, with a bias towards the post-fusion conformation. DS-Cav1 expressed mostly pre-fusion RSV-F. The deletion of SH did not appear to impact viral protein expression.

Recent studies have shown that antibodies against the pre-fusion conformation of RSV-F are responsible for the majority of the neutralizing activity (15). Therefore, we initially hypothesized that candidates expressing the pre-fusion stabilized F construct, DS-Cav1, would induce the best neutralizing antibody response. However, PIV5-RSV-F (SH-HN), which expressed wild-type F, elicited the highest neutralizing antibody titers in the mouse model. This virus induced similar levels of anti-pre-fusion F IgG, but higher amounts of anti-post-fusion F IgG compared to the DS-Cav1-expressing counterpart. While antibodies against pre-fusion F account for the majority of neutralizing activity, antibodies against post-fusion F are also important. Palvizumab and motavizumab, two highly neutralizing antibodies against RSV-F, recognize epitopes that are exposed in both the pre-fusion and post-fusion conformations (25, 26). Therefore, the higher neutralizing antibody titers in PIV5-RSV-F (SH-HN)-vaccinated mice may be due to the increased levels of anti-post-fusion F antibodies. Regardless of *in vitro* neutralizing antibody titers, all of the PIV5-vectored vaccine candidates induced potent lower respiratory tract protection against RSV challenge in mice.

The vaccine candidates were also evaluated in cotton rats, which are more permissive to RSV infection and allowed for examination of upper and lower respiratory

tract protection against challenge. All PIV5 or PIV5ΔSH candidates expressing pre-fusion or post-fusion RSV-F were highly immunogenic and protective when administered via the intranasal route. The greatest reductions in viral load were observed in the lower respiratory tract, but the candidates also reduced upper respiratory virus load by approximately 1.5 $\log_{10}$. Similar to the results of the mouse study, the pre-fusion F-expressing candidates induced lower IgG titers against post-fusion F (18). Overall, there was no evidence of pre-fusion RSV-F being more immunogenic or protective than wild-type RSV-F in the mouse or cotton rat studies.

Liang et al. recently published studies examining immunogenicity and efficacy of live-attenuated chimeric bovine/human PIV3-vectored vaccines expressing wild-type, pre-fusion, or post-fusion RSV-F. When evaluated in the hamster model, vaccine candidates expressing pre-fusion F were no more immunogenic or efficacious than candidates expressing wild-type F. The pre-fusion-F candidates only induced higher *in vitro* neutralizing antibody titers in the absence of guinea pig complement, leading the authors to conclude that these antibodies were more potent (18). In our studies, antibodies from mice immunized with pre-fusion F candidates were only modestly neutralizing in the absence of guinea pig complement, with an average neutralizing titer of 1:4 (data not shown). While these titers were higher than those induced by wild-type F-expressing candidates under these conditions, the biological relevance of these results is unclear since complement-mediated host defense is active in the pulmonary environment. It is unlikely that vaccine-induced antibodies will function in a complement-free system (27). In the Liang et al. study, the pre-fusion F-expressing candidates only outperformed candidates expressing post-fusion F. For subunit vaccines

that generally express only post-fusion F, there is a rationale to develop a pre-fusion stabilized mutant. However, for vectored vaccines that express wild-type F in both the pre-fusion and post-fusion conformations, there is little evidence that stabilized pre-fusion F is a better antigen.

We also examined whether the PIV5ΔSH would induce better immunity over wild-type PIV5 when used as a vaccine vector. Previous research has shown that deleting SH from PIV5 improves the immunogenicity and efficacy of an intranasal PIV5-based H5N1 influenza vaccine (14). In the current RSV studies, the two vectors performed similarly when administered via the intranasal route. When administered via the subcutaneous route, the wild-type PIV5 vector appeared to confer better protection against RSV challenge. These results contrast with other studies performed in our laboratory in which PIV5ΔSH was a better vector for a rabies vaccine in dogs (unpublished data). The discrepancies observed between PIV5 and PIV5ΔSH-vectored RSV, influenza, and rabies vaccines may be due to both the route of administration and the antigen that is being expressed. In the case of the RSV, PIV5 expressing wild-type RSV-F appears to be the best candidate for administration via the subcutaneous route. Subcutaneous immunization with PIV5-RSV-F (SH-HN) was just as effective as intranasal immunization. This route is particularly advantageous for immunizing newborns because problems associated with intranasal vaccination and nasal congestion can be avoided. There is no evidence of post-challenge enhanced disease in any of the cotton rats that received PIV5 or PIV5ΔSH-vectored vaccines.

All of the PIV5-based RSV vaccine candidates evaluated in this study were highly immunogenic, protective, and safe against RSV challenge. Expression of a pre-fusion

stabilized RSV-F antigen did not improve vaccine-induced immune responses or protection, suggesting that expressing wild-type F in live viral vectors may be the best approach. Furthermore, the nature of the antigen and the route of administration should be considered when making modifications to the PIV5 vector. The findings from this study suggest that PIV5-RSV-F (SH-HN) is a promising vaccine candidate that can be administered intranasally or subcutaneously.

Acknowledgements

We would like to thank all members of Biao He's laboratory for the helpful discussion and technical assistance. We would also like to thank Dai Wang from for the RSV-F antibodies and Patricia Jorquera for the RSV and GFP peptides.

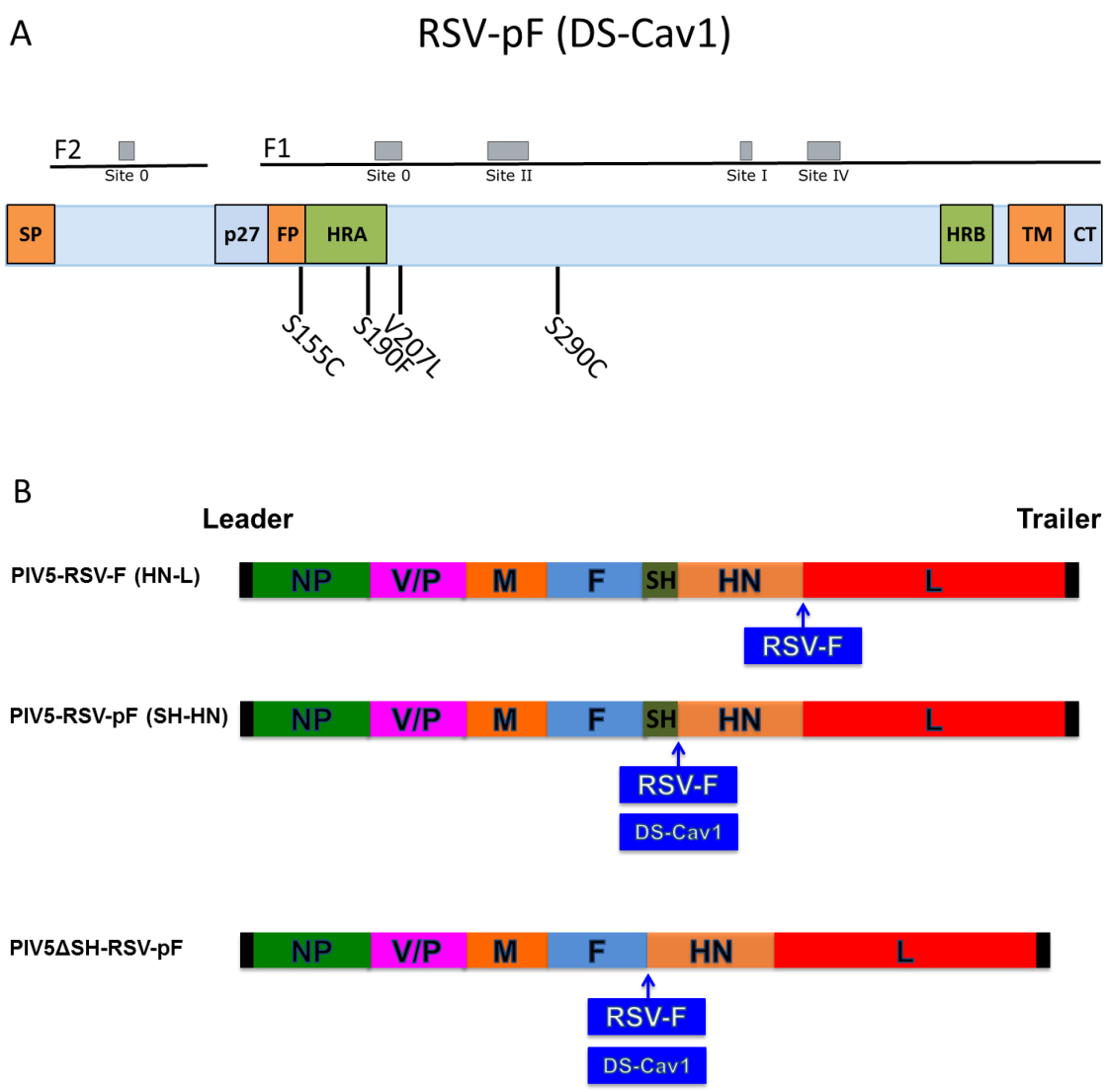

Figure 6.1. Schematics of PIV5-based vaccine candidates. (A) Schematic of substitutions in pre-fusion-stabilized RSV-F (DS-Cav1). (B) Schematic of PIV5-RSV-F (SH-HN), PIV5ΔSH-RSV-F, PIV5-RSV-pF, PIV5ΔSH-RSV-pF. NP, nucleoprotein; V, V protein; P, phosphoprotein; M, matrix protein; F, fusion protein; SH, small hydrophobic protein; HN, hemagglutinin-neuraminidase protein; L, RNA-dependent RNA polymerase; RSV-F, respiratory syncytial virus fusion protein; DS-Cav1, stabilized pre-fusion RSV-F.

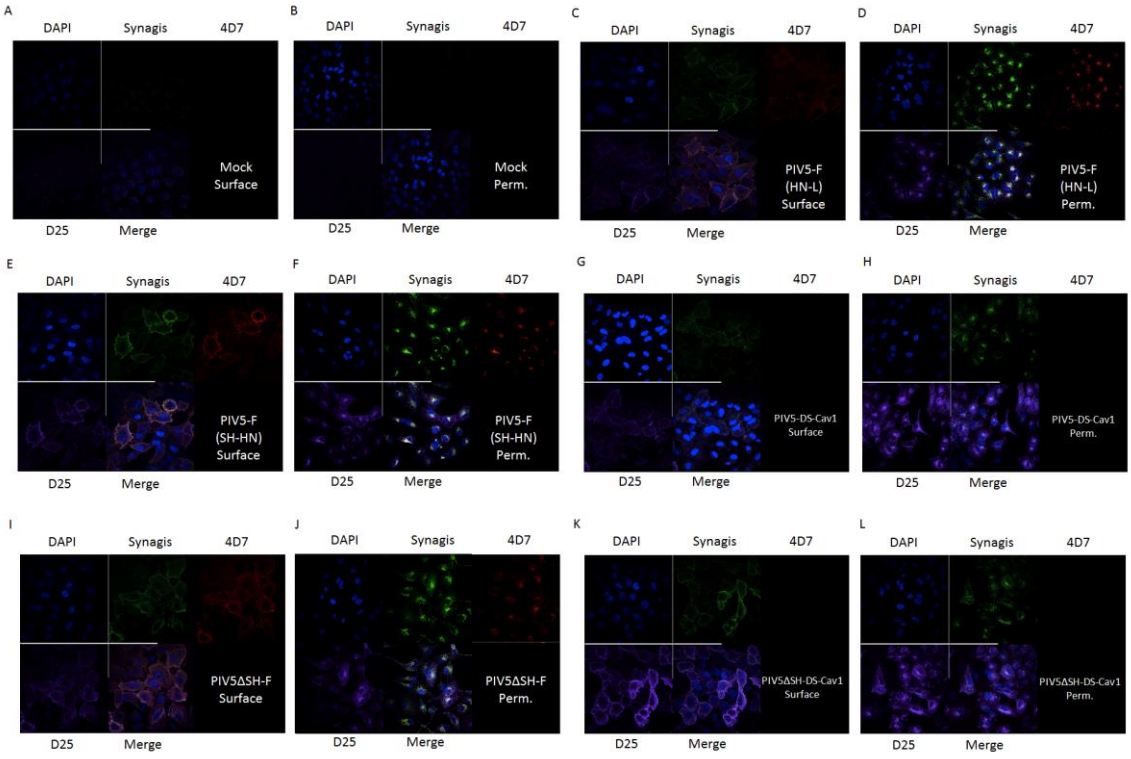
A
DAPI
Synagis
4D7
Mock Surface
D25
Merge
B
DAPI
Synagis
4D7
Mock Perm.
D25
Merge
C
DAPI
Synagis
4D7
PIV5-F (HN-L) Surface
D25
Merge
D
DAPI
Synagis
4D7
PIV5-F (HN-L) Perm.
D25
Merge
E
DAPI
Synagis
4D7
PIV5-F (SH-HN) Surface
D25
Merge
F
DAPI
Synagis
4D7
PIV5-F (SH-HN) Perm.
D25
Merge
G
DAPI
Synagis
4D7
PIV5-DS-Cav1 Surface
D25
Merge
H
DAPI
Synagis
4D7
PIV5-DS-Cav1 Perm.
D25
Merge
I
DAPI
Synagis
4D7
PIV5ΔSH-F Surface
D25
Merge
J
DAPI
Synagis
4D7
PIV5ΔSH-F Perm.
D25
Merge
K
DAPI
Synagis
4D7
PIV5ΔSH-DS-Cav1 Surface
D25
Merge
L
DAPI
Synagis
4D7
PIV5ΔSH-DS-Cav1 Perm.
D25
Merge

M

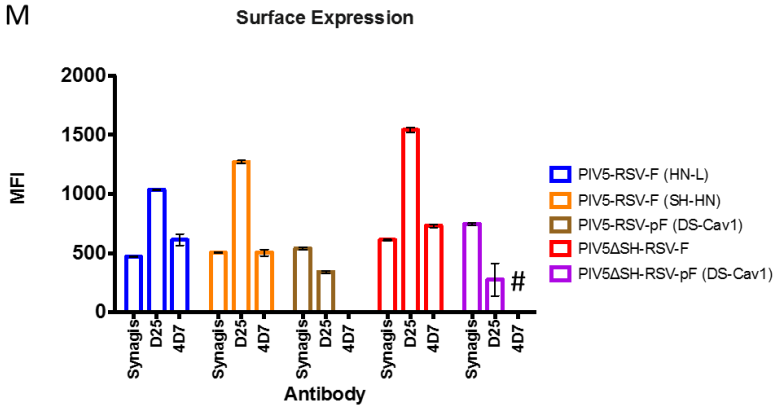
Surface Expression
MFI
2000
1500
1000
500
0
Synagis
D25
4D7
Antibody
#
PIV5-RSV-F (HN-L)
PIV5-RSV-F (SH-HN)
PIV5-RSV-pF (DS-Cav1)
PIV5ΔSH-RSV-F
PIV5ΔSH-RSV-pF (DS-Cav1)

N

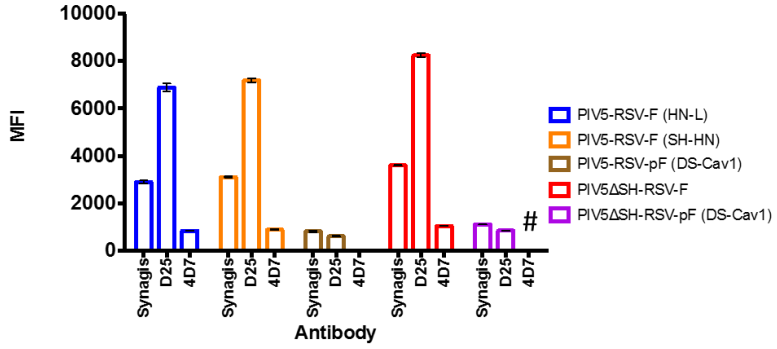
Total Expression
MFI
10000
8000
6000
4000
2000
0
Synagis
D25
4D7
Antibody
#
PIV5-RSV-F (HN-L)
PIV5-RSV-F (SH-HN)
PIV5-RSV-pF (DS-Cav1)
PIV5ΔSH-RSV-F
PIV5ΔSH-RSV-pF (DS-Cav1)

Figure 6.2. Generation and characterization of recombinant PIV5-based vaccine candidates. (A-L) Detection of total RSV-F, post-fusion RSV-F, and pre-fusion RSV-F in infected A549 cells by immunofluorescence assay. Total RSV-F was detected using palivizumab labeled with Alexa Fluor 488 (green). Post-fusion RSV-F was detected with 4D7 antibody labeled with Cy3 (red). Pre-fusion RSV-F was detected using D25 antibody labeled with APC (purple). DAPI (blue) was used as a nuclear stain. Images are representative of three independent experiments. (M, N) Flow cytometry was used to examine (M) surface and (N) total RSV-F, post-fusion RSV-F, and pre-fusion RSV-F expression in A549 cells infected with the vaccine candidates. Antibodies were labeled as in (A-L), except 4D7 was labeled with PE. Graph represents the mean fluorescence intensity (MFI) of cells expressing post-fusion or pre-fusion F. Error bars represent the standard error of the mean. (#) indicates too few positive cells to analyze the MFI.

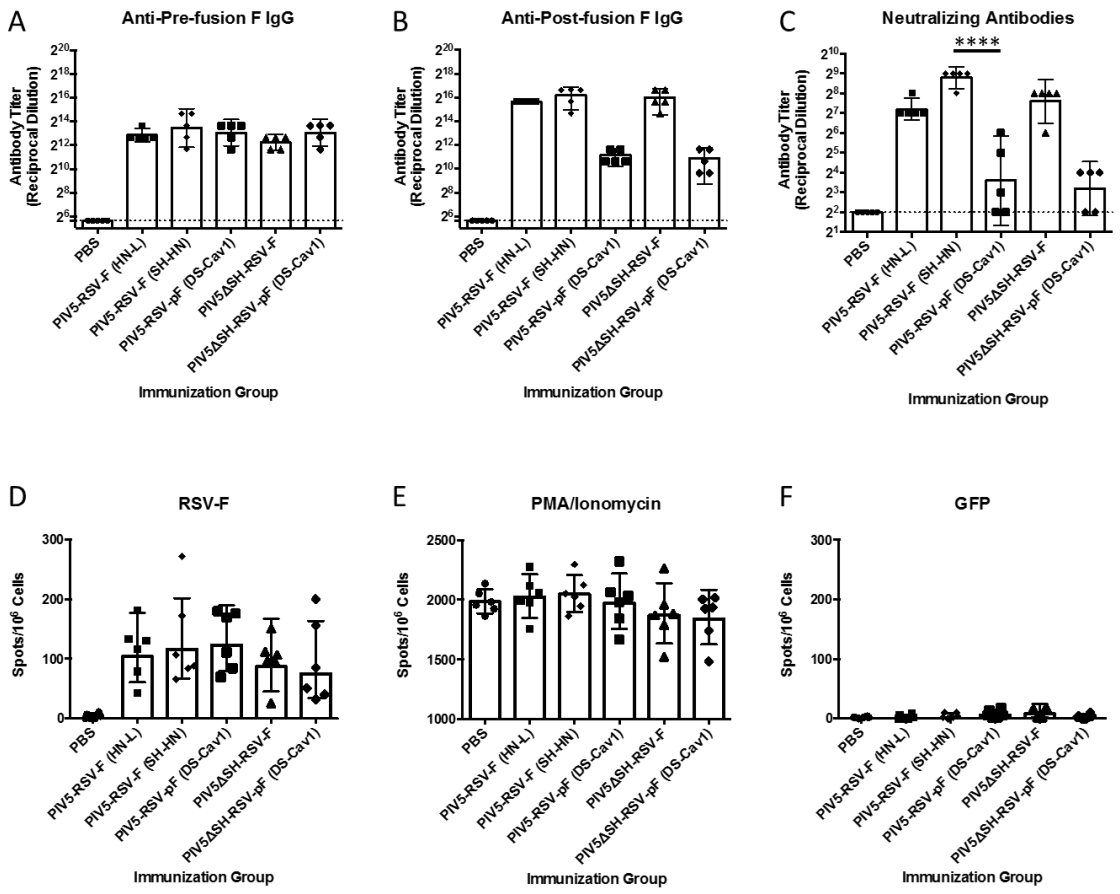

Figure 6.3. Humoral and cell-mediated immune responses in mice immunized with PIV5 or PIV5ΔSH expressing wild-type or pre-fusion RSV-F. Six-to-eight week old BALB/c mice were immunized intranasally with 10^6 PFU of PIV5-RSV-F (HN-L), PIV5-RSV-F (SH-HN), PIV5-RSV-pF (DS-Cav1), PIV5ΔSH-RSV-F, or PIV5ΔSH-RSV-pF (DS-Cav1). Sera were collected 21 days post-immunization. (A and B) Serum IgG antibodies that bound pre-fusion or post-fusion RSV-F were measured by indirect ELISA. (A) Purified pre-fusion-stabilized or (B) post-fusion RSV-F were used as the coating antigens. Two-fold serial dilutions of immune sera were incubated with the immobilized antigens, followed by incubation with HRP-conjugated goat anti-mouse IgG. Plates were developed and optical density was measured at 450 nm. Titers were defined as the reciprocal of the highest dilution at which the absorbance was two standard deviations

above the average absorbance of the PBS sera. (C) Serum neutralizing antibody titers were measured by plaque reduction assay. Two-fold serial dilutions of heat-inactivated immune sera were incubated with 100-150 PFU of RSV/A/A2. Plaques were enumerated 7 days later, and the neutralizing antibody was defined as the reciprocal of the highest dilution at which there was a 50% reduction in input virus. Graphs represent the geometric mean antibody titer of four to five mice per group, and error bars represent the 95% confidence interval (CI). (D) Six to eight-week-old BALB/c mice from a separate cohort were immunized as in (A-C). Splenocytes were collected 27 days post-immunization and cell-mediated immune responses were measured by ELISpot. Cells were stimulated with 200 ng/well of (D) RSV-F peptide, (E) PMA/Ionomycin, or (F) GFP peptide for 48 hours. The number of IFN-γ-secreting cells per $2x10^5$ cells were enumerated. Graphs represent the average number of spots per 10^6 cells in each group of six mice. Statistical significance was determined using one-way ANOVA and Tukey's test for multiple comparisons. ****, $P < 0.0001$.

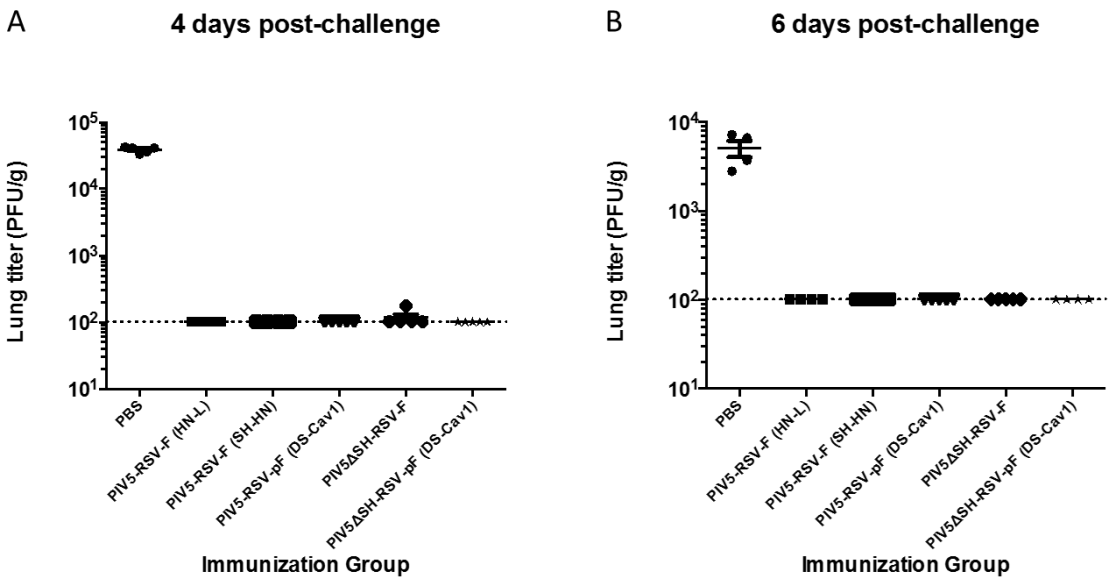

Figure 6.4. Protection in mice immunized with PIV5 or PIV5ΔSH expressing wild-type or pre-fusion RSV-F. Six to eight-week-old BALB/c mice were immunized intranasally with 10^6 PFU of PIV5-RSV-F (HN-L), PIV5-RSV-F (SH-HN), PIV5-RSV-pF (DS-Cav1), PIV5ΔSH-RSV-F, or PIV5ΔSH-RSV-pF (DS-Cav1). The mice were challenged 28 days post-immunization with 10^6 PFU of RSV/A/A2. (A) Four and (B) six days later, lungs were harvested to assess viral load by plaque assay in Vero cells. Graphs represent the average lung titer from four to five mice per group. Error bars represent the standard error of the mean.

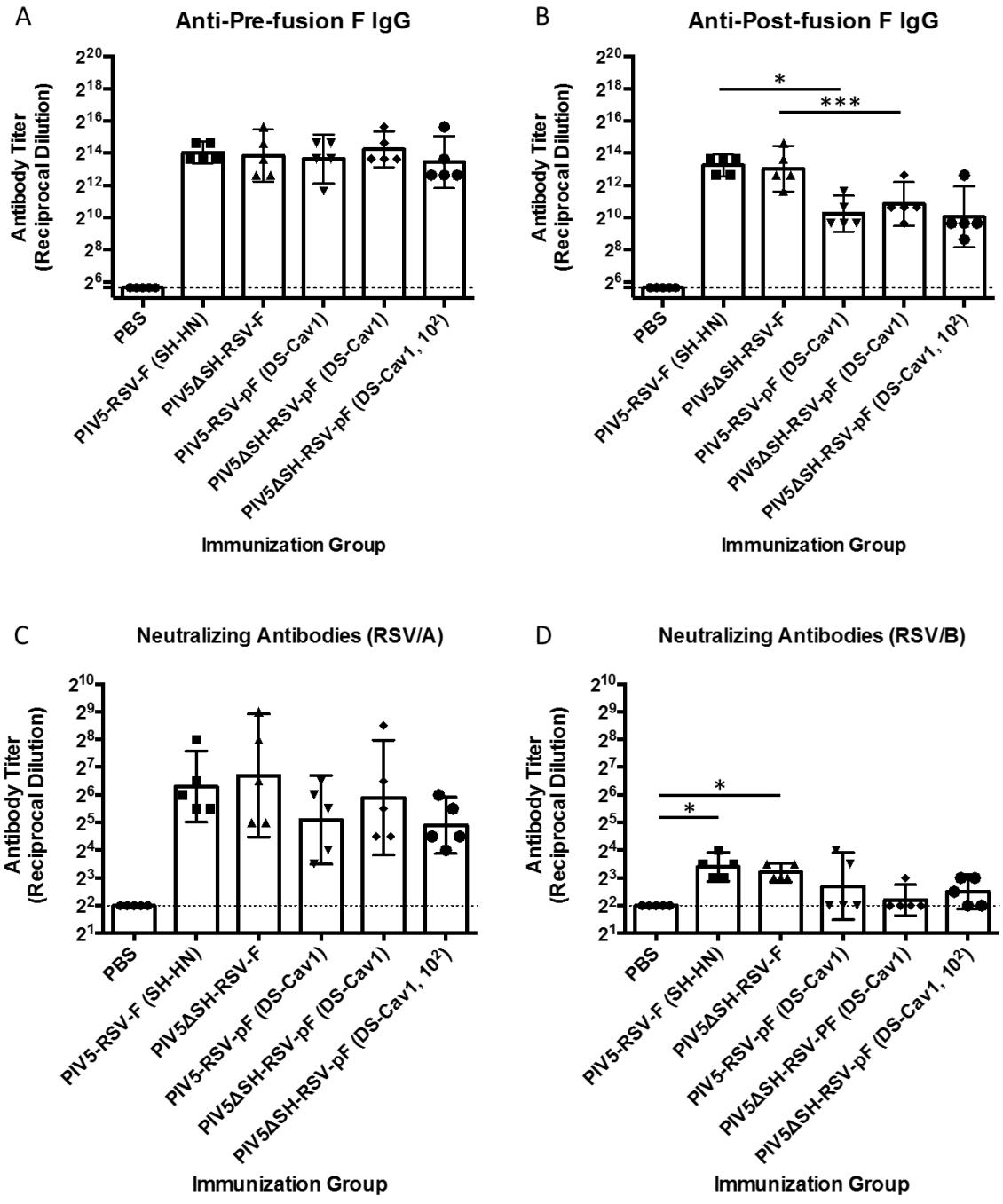
A
Anti-Pre-fusion F IgG
Antibody Titer (Reciprocal Dilution)
Immunization Group
PBS
PIV5-RSV-F (SH-HN)
PIV5ΔSH-RSV-F
PIV5-RSV-pF (DS-Cav1)
PIV5ΔSH-RSV-pF (DS-Cav1)
PIV5ΔSH-RSV-pF (DS-Cav1, 10²)
B
Anti-Post-fusion F IgG
*
***
C
Neutralizing Antibodies (RSV/A)
D
Neutralizing Antibodies (RSV/B)

Figure 6.5. Humoral responses in cotton rats immunized with PIV5 or PIV5ΔSH expressing wild-type or pre-fusion RSV-F. Cotton rats were intranasally immunized with PIV5-RSV-F (SH-HN), PIV5-RSV-pF (DS-Cav1), PIV5ΔSH-RSV-F, or PIV5ΔSH-RSV-pF (DS-Cav1). Groups received 10^2 or 10^3 PFU of vaccine virus as indicated. Using serum collected 28 dpi, IgG antibodies against (A) pre-fusion or (B) post-fusion RSV-F were measured by ELISA using chicken anti-cotton rat IgG conjugated to HRP. Serum neutralizing antibody titers against RSV/A/Tracy and were measured in sera collected 28 dpi. The neutralizing activity of the sera were measured against (C) RSV/A/Tracy and (D) RSV/B/18537. The neutralizing antibody was defined as the reciprocal of the serum dilution at which there was a 50% reduction in viral CPE. Graphs represent the geometric mean antibody titer from five cotton rats per group. Error bars represent the 95% CI. Statistical significance was determined using one-way ANOVA and Tukey's test for multiple comparisons. *, $P < 0.05$; ***, $P < 0.001$.

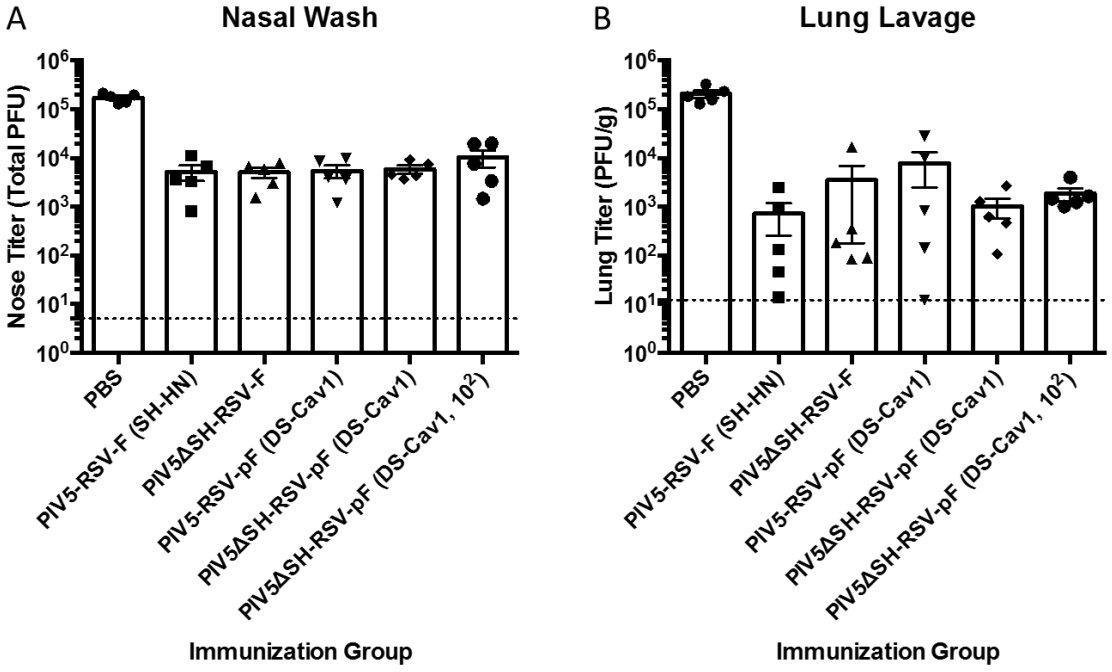

Figure 6.6. Protection in cotton rats immunized with PIV5 or PIV5ΔSH expressing wild-type or pre-fusion RSV-F. Cotton rats were intranasally immunized with PIV5-RSV-F (SH-HN), PIV5-RSV-pF (DS-Cav1), PIV5ΔSH-RSV-F, or PIV5ΔSH-RSV-pF (DS-Cav1). Groups received 10^2 or 10^3 PFU of vaccine virus as indicated. Animals were challenged with 1.21×10^5 PFU of RSV/A/Tracy 28 days post-immunization. Four days later, (A) nose and (B) lungs were lavaged to determine virus titer by plaque assay in HEp-2 cells. Graphs represent the average lung titer from five rats per group. Error bars represent the standard error of the mean.

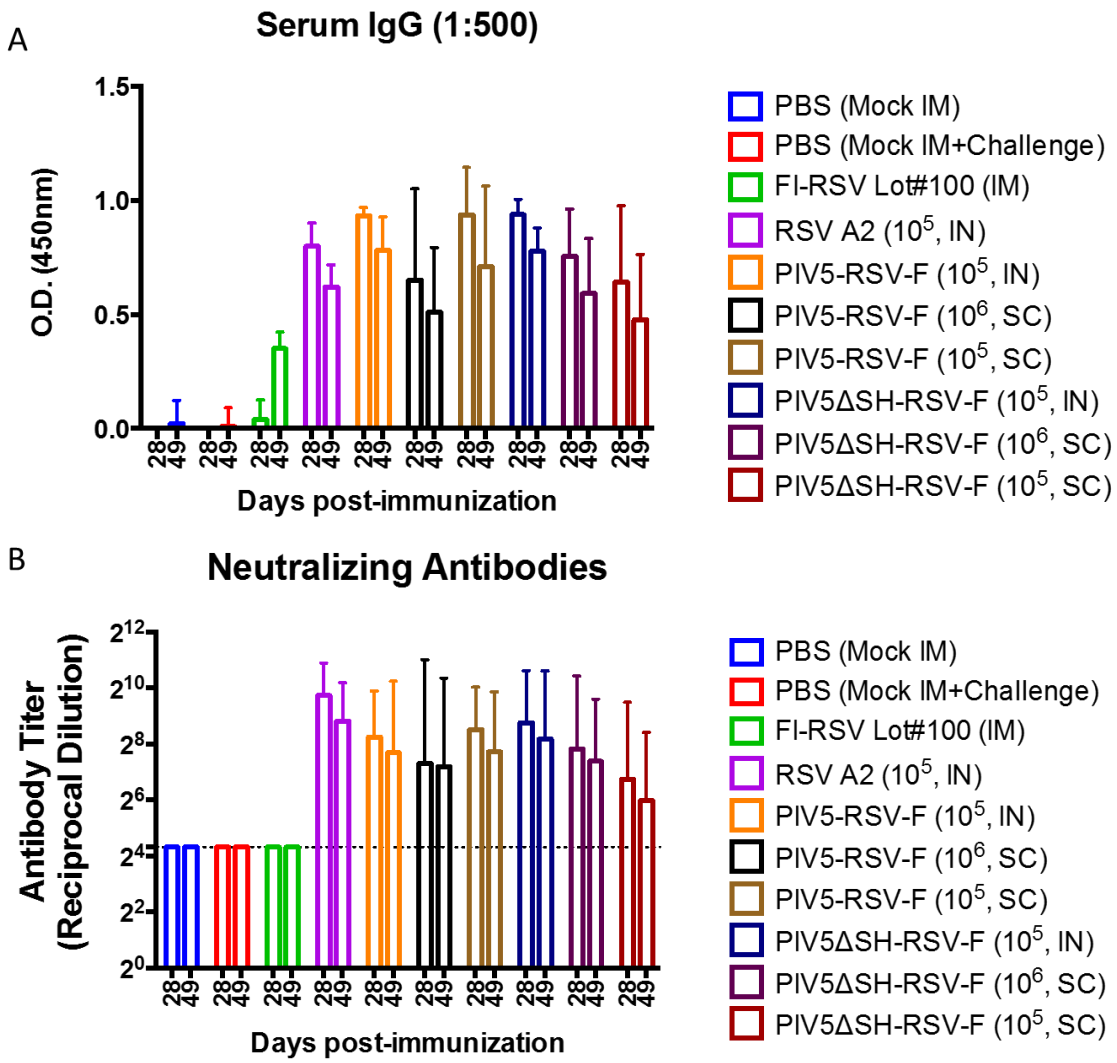

Figure 6.7. Humoral responses in cotton rats immunized with PIV5 or PIV5ΔSH expressing wild-type RSV-F using different routes of administration. Cotton rats were immunized with RSV/A/A2, PIV5-RSV-F (SH-HN), or PIV5ΔSH-RSV-F. Animals received 10^5 PFU intranasally or 10^5 to 10^6 PFU subcutaneously as indicated. Animals vaccinated with FI-RSV were immunized intramuscularly. (A) Serum samples from day 28 post-immunization were diluted 1:500 and anti-post-fusion RSV-F IgG was measured by ELISA. IgG levels are shown as the absorbance at 450 nm. Graphs represent the average IgG measurement from five animals per group. Error bars represent the standard

error of the mean. (B) Serum neutralizing antibody titers were measured against RSV/A/A2. The neutralizing antibody was defined as the reciprocal of the highest dilution at which there was a 60% reduction in viral CPE. Graphs represent the geometric mean neutralizing antibody titer from five cotton rats per group. Error bars represent the 95% CI.

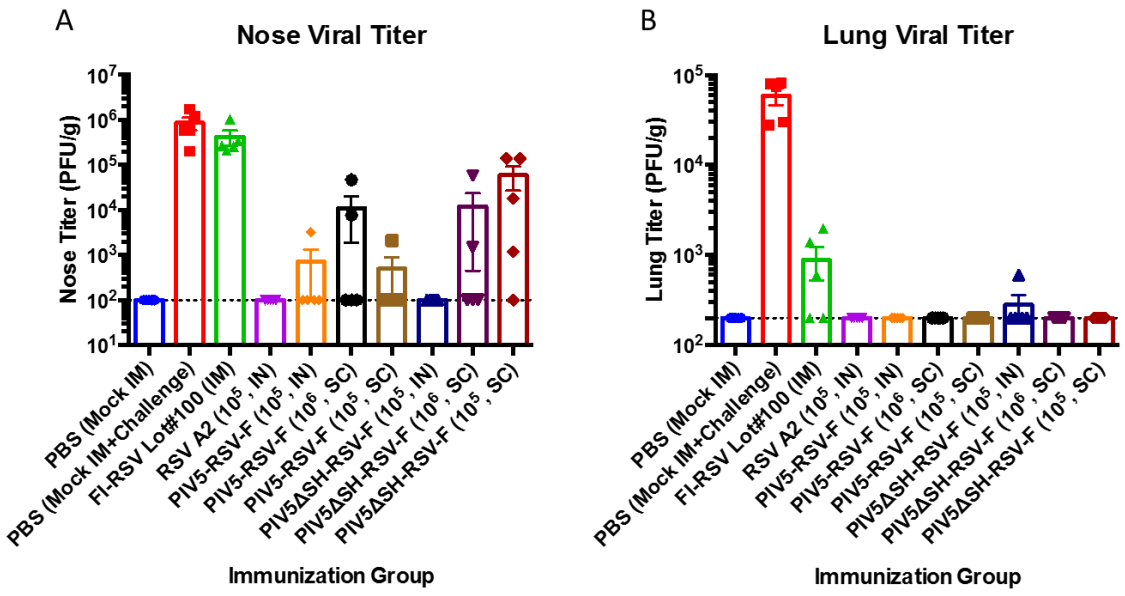

Figure 6.8. Protection in cotton rats immunized with PIV5 or PIV5ΔSH expressing wild-type RSV-F using different routes of administration. Cotton rats were immunized with RSV/A/A2, PIV5-RSV-F (SH-HN), or PIV5ΔSH-RSV-F. Animals received 10^5 PFU intranasally or 10^5 to 10^6 PFU subcutaneously as indicated. Animals vaccinated with FI-RSV were immunized intramuscularly. Animals were challenged with 10^5 PFU of RSV/A/A2 49 days post-immunization. Five days later, (A) nose and (B) lung tissues were harvested to determine viral loads by plaque assay in HEp-2 cells. Graphs represent the average nose and lung titers from five rats per group. Error bars represent the standard error of the mean.

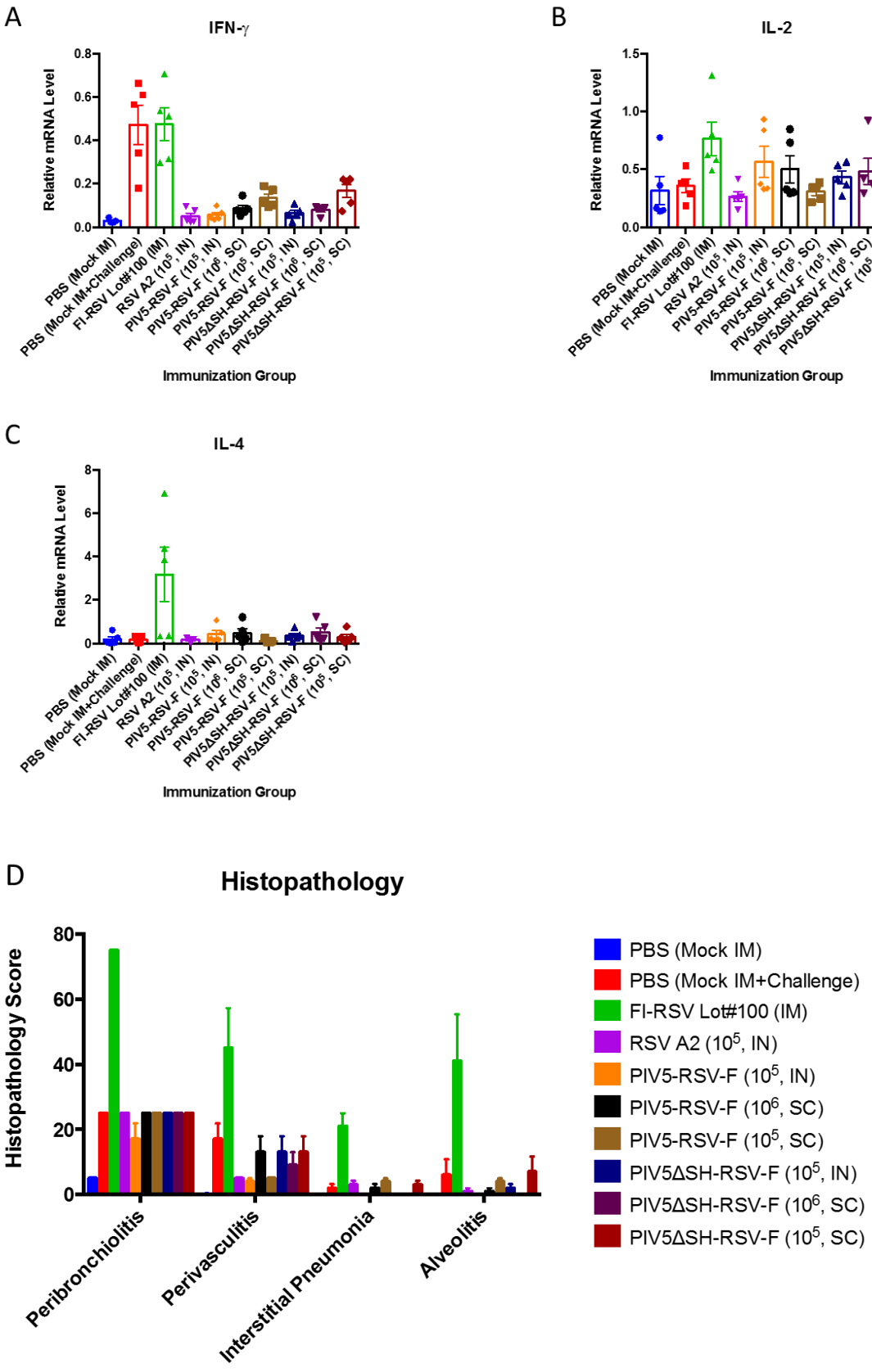
A
IFN-γ
Relative mRNA Level
0.0
0.2
0.4
0.6
0.8
PBS (Mock IM)
PBS (Mock IM+Challenge)
FI-RSV Lot#100 (IM)
RSV A2 (10^5, IN)
PIV5-RSV-F (10^5, IN)
PIV5-RSV-F (10^6, SC)
PIV5-RSV-F (10^5, SC)
PIV5ΔSH-RSV-F (10^5, IN)
PIV5ΔSH-RSV-F (10^6, SC)
PIV5ΔSH-RSV-F (10^5, SC)
Immunization Group
B
IL-2
Relative mRNA Level
0.0
0.5
1.0
1.5
PBS (Mock IM)
PBS (Mock IM+Challenge)
FI-RSV Lot#100 (IM)
RSV A2 (10^5, IN)
PIV5-RSV-F (10^5, IN)
PIV5-RSV-F (10^6, SC)
PIV5-RSV-F (10^5, SC)
PIV5ΔSH-RSV-F (10^5, IN)
PIV5ΔSH-RSV-F (10^6, SC)
PIV5ΔSH-RSV-F (10^5, SC)
Immunization Group
C
IL-4
Relative mRNA Level
0
2
4
6
8
PBS (Mock IM)
PBS (Mock IM+Challenge)
FI-RSV Lot#100 (IM)
RSV A2 (10^5, IN)
PIV5-RSV-F (10^5, IN)
PIV5-RSV-F (10^6, SC)
PIV5-RSV-F (10^5, SC)
PIV5ΔSH-RSV-F (10^5, IN)
PIV5ΔSH-RSV-F (10^6, SC)
PIV5ΔSH-RSV-F (10^5, SC)
Immunization Group
D
Histopathology
Histopathology Score
0
20
40
60
80
Peribronchiolitis
Perivasculitis
Interstitial Pneumonia
Alveolitis
PBS (Mock IM)
PBS (Mock IM+Challenge)
FI-RSV Lot#100 (IM)
RSV A2 (10^5, IN)
PIV5-RSV-F (10^5, IN)
PIV5-RSV-F (10^6, SC)
PIV5-RSV-F (10^5, SC)
PIV5ΔSH-RSV-F (10^5, IN)
PIV5ΔSH-RSV-F (10^6, SC)
PIV5ΔSH-RSV-F (10^5, SC)

Figure 6.9. Post-challenge pulmonary cytokine levels and lung histology of cotton rats immunized with PIV5 or PIV5ΔSH expressing wild-type RSV-F. Cotton rats were immunized with RSV/A/A2, PIV5-RSV-F (SH-HN), or PIV5ΔSH-RSV-F. Animals received 10^5 PFU intranasally or 10^5 to 10^6 PFU subcutaneously as indicated. Animals vaccinated with FI-RSV were immunized intramuscularly. Animals were challenged with 10^5 PFU of RSV/A/A2 49 days post-immunization. (A-C) Five days post-challenge, lung tissue was collected for RNA isolation and qPCR. Levels of (A) IFN-γ, (B) IL-2, and (C) IL-4 mRNA were normalized to β-actin mRNA levels in each sample. Graphs represent the average relative mRNA levels from five rats per group. (D) Five days post-challenge, lungs were harvested and fixed in 10% neutral-buffered formalin. Lung sections were stained with hematoxylin and eosin. The sections were scored on a scale of 0 to 4 for peribronchiolitis, perivasculitis, interstitial pneumonia, and alveolitis. The scores were then converted to a 0 to 100% histopathology scale. Graphs represent the average score from five rats per group. Error bars represent the standard error of the mean.

Table 6.1. Study design for cotton rat study 1: comparing PIV5-RSV-pF/F (SH-HN) and PIV5ΔSH-RSV-pF/F

Treatment	Treatment Dose (in 100 µl)	Immunization Day	Route	RSV Challenge (in 100 µl)
PBS (mock)	n/a	0	IN	PBS
sPIV5-RSV-F (SH-HN)	10^3 PFU	0	IN	$1.21x10^5$ PFU
PIV5ΔSH-RSV-F	10^3 PFU	0	IN	$1.21x10^5$ PFU
PIV5-RSV-pF (SH-HN)	10^3 PFU	0	IN	$1.21x10^5$ PFU
PIV5ΔSH-RSV-pF	10^3 PFU	0	IN	$1.21x10^5$ PFU
PIV5ΔSH-RSV-pF	10^2 PFU	0	IN	$1.21x10^5$ PFU

Table 6.2. Study design for cotton rat study 2: comparing PIV5-RSV-F (SH-HN) and PIV5ΔSH-RSV-F safety and efficacy using different routes of administration

Treatment	Treatment Dose (in 100 µl)	Immunization Days	Route	RSV Challenge (in 100 µl)
PBS (mock)	n/a	0, 28	IM	PBS
PBS (mock)	n/a	0, 28	IM	10^5 PFU
FI-RSV Lot#100	1:100 in PBS	0, 28	IM	10^5 PFU
RSV/A/A2	10^5 PFU	0	IN	10^5 PFU
PIV5-RSV-F (SH-HN)	10^5 PFU	0	IN	10^5 PFU
PIV5-RSV-F (SH-HN)	10^6 PFU	0	SC	10^5 PFU
PIV5-RSV-F (SH-HN)	10^5 PFU	0	SC	10^5 PFU
PIV5ΔSH-RSV-F	10^5 PFU	0	IN	10^5 PFU
PIV5ΔSH-RSV-F	10^6 PFU	0	SC	10^5 PFU
PIV5ΔSH-RSV-F	10^5 PFU	0	SC	10^5 PFU

References

1. **Nair H**, **Nokes DJ**, **Gessner BD**, **Dherani M**, **Madhi S a.**, **Singleton RJ**, **O'Brien KL**, **Roca A**, **Wright PF**, **Bruce N**, **Chandran A**, **Theodoratou E**, **Sutanto A**, **Sedyaningsih ER**, **Ngama M**, **Munywoki PK**, **Kartasasmita C**, **Simões EA**, **Rudan I**, **Weber MW**, **Campbell H**. 2010. Global burden of acute lower respiratory infections due to respiratory syncytial virus in young children: a systematic review and meta-analysis. Lancet **375**:1545–1555.

2. **Falsey AR**, **Hennessey PA**, **Formica MA**, **Cox C**, **Walsh EE**. 2005. Respiratory syncytial virus infection in elderly and high-risk adults. N. Engl. J. Med. **352**:1749–59.

3. **Chin J**, **Magoffin RL**, **Shearer LA**, **Schieble JH**, **Lennette EH**. 1969. Field evaluation of a respiratory syncytial virus vaccine and a trivalent parainfluenza virus vaccine in a pediatric population. Am. J. Epidemiol. **89**:449–63.

4. **Fulginiti VA**, **Eller JJ**, **Sieber OF**, **Joyner JW**, **Minamitani M**, **Meiklejohn G**. 1969. Respiratory virus immunization. I. A field trial of two inactivated respiratory virus vaccines; an aqueous trivalent parainfluenza virus vaccine and an alum-precipitated respiratory syncytial virus vaccine. Am. J. Epidemiol. **89**:435–48.

5. **Kapikian AZ**, **Mitchell RH**, **Chanock RM**, **Shvedoff RA**, **Stewart CE**. 1969. An epidemiologic study of altered clinical reactivity to respiratory syncytial (RS) virus infection in children previously vaccinated with an inactivated RS virus vaccine. Am. J. Epidemiol. **89**:405–21.

6. **Kim HW**, **Canchola JG**, **Brandt CD**, **Pyles G**, **Chanock RM**, **Jensen K**, **Parrott RH**. 1969. Respiratory syncytial virus disease in infants despite prior administration of antigenic inactivated vaccine. Am. J. Epidemiol. **89**:422–434.

7. **Karron RA**, **Buchholz UJ**, **Collins PL**. 2013. Live-attenuated respiratory syncytial virus vaccines. Curr. Top. Microbiol. Immunol. **372**:259–84.

8. **Gomez M**, **Mufson MA**, **Dubovsky F**, **Knightly C**, **Zeng W**, **Losonsky G**. 2009. Phase-I study MEDI-534, of a live, attenuated intranasal vaccine against respiratory syncytial virus and parainfluenza-3 virus in seropositive children. Pediatr. Infect. Dis. J. **28**:655–8.

9. **Power UF**, **Plotnicky-Gilquin H**, **Huss T**, **Robert A**, **Trudel M**, **Ståhl S**, **Uhlén M**, **Nguyen TN**, **Binz H**. 1997. Induction of protective immunity in rodents by vaccination with a prokaryotically expressed recombinant fusion protein containing a respiratory syncytial virus G protein fragment. Virology **230**:155–66.

10. **Quan F-S**, **Kim Y**, **Lee S**, **Yi H**, **Kang S-M**, **Bozja J**, **Moore ML**, **Compans RW**. 2011. Viruslike particle vaccine induces protection against respiratory syncytial virus infection in mice. J. Infect. Dis. **204**:987–95.

11. **Anderson LJ**, **Dormitzer PR**, **Nokes DJ**, **Rappuoli R**, **Roca A**, **Graham BS**. 2013. Strategic priorities for respiratory syncytial virus (RSV) vaccine development. Vaccine **31 Suppl 2**:B209–15.

12. **Phan SI**, **Chen Z**, **Xu P**, **Li Z**, **Gao X**, **Foster SL**, **Teng MN**, **Tripp R a.**, **Sakamoto K**, **He B**. 2014. A respiratory syncytial virus (RSV) vaccine based on parainfluenza virus 5 (PIV5). Vaccine **32**:3050–3057.

13. **Lin Y**, **Bright AC**, **Rothermel TA**, **He B**. 2003. Induction of apoptosis by paramyxovirus simian virus 5 lacking a small hydrophobic gene. J. Virol. **77**:3371–83.

14. **Li Z**, **Gabbard JD**, **Mooney A**, **Chen Z**, **Tompkins SM**, **He B**. 2013. Efficacy of parainfluenza virus 5 mutants expressing hemagglutinin from H5N1 influenza A virus in mice. J. Virol. **87**:9604–9.

15. **Magro M**, **Mas V**, **Chappell K**, **Vázquez M**, **Cano O**, **Luque D**, **Terrón MC**, **Melero JA**, **Palomo C**. 2012. Neutralizing antibodies against the preactive form of respiratory syncytial virus fusion protein offer unique possibilities for clinical intervention. Proc. Natl. Acad. Sci. U. S. A. **109**:3089–94.

16. **McLellan JS**, **Chen M**, **Leung S**, **Graepel KW**, **Du X**, **Yang Y**, **Zhou T**, **Baxa U**, **Yasuda E**, **Beaumont T**, **Kumar A**, **Modjarrad K**, **Zheng Z**, **Zhao M**, **Xia N**, **Kwong PD**, **Graham BS**. 2013. Structure of RSV fusion glycoprotein trimer bound to a prefusion-specific neutralizing antibody. Science **340**:1113–7.

17. **McLellan JS**, **Chen M**, **Joyce MG**, **Sastry M**, **Stewart-Jones GBE**, **Yang Y**, **Zhang B**, **Chen L**, **Srivatsan S**, **Zheng A**, **Zhou T**, **Graepel KW**, **Kumar A**, **Moin S**, **Boyington JC**, **Chuang G-Y**, **Soto C**, **Baxa U**, **Bakker AQ**, **Spits H**, **Beaumont T**, **Zheng Z**, **Xia N**, **Ko S-Y**, **Todd J-P**, **Rao S**, **Graham BS**, **Kwong PD**. 2013. Structure-based design of a fusion glycoprotein vaccine for respiratory syncytial virus. Science **342**:592–8.

18. **Liang B**, **Surman S**, **Amaro-Carambot E**, **Kabatova B**, **Mackow N**, **Lingemann M**, **Yang L**, **McLellan JS**, **Graham BS**, **Kwong PD**, **Schaap-Nutt A**, **Collins PL**, **Munir S**. 2015. Enhanced Neutralizing Antibody Response Induced by Respiratory Syncytial Virus Prefusion F Protein Expressed by a Vaccine Candidate. J. Virol. **89**:9499–510.

19. **He B**, **Paterson RG**, **Ward CD**, **Lamb RA**. 1997. Recovery of infectious SV5 from cloned DNA and expression of a foreign gene. Virology **237**:249–260.

20. **Collins PL**, **Hill MG**, **Camargo E**, **Grosfeld H**, **Chanock RM**, **Murphy BR**. 1995. Production of infectious human respiratory syncytial virus from cloned cDNA confirms an essential role for the transcription elongation factor from the 5’ proximal open reading frame of the M2 mRNA in gene expression and provides a capability for vaccine . Proc. Natl. Acad. Sci. U. S. A. **92**:11563–7.

21. **Chen Z**, **Zhou M**, **Gao X**, **Zhang G**, **Ren G**, **Gnanadurai CW**, **Fu ZF**, **He B**. 2012. A Novel Rabies Vaccine Based on a Recombinant Parainfluenza Virus 5 Expressing Rabies Virus Glycoprotein. J. Virol. **87**:2986–2993.

22. **Johnson TR**, **Johnson JE**, **Roberts SR**, **Wertz GW**, **Parker R a**, **Graham BS**. 1998. Priming with secreted glycoprotein G of respiratory syncytial virus (RSV) augments interleukin-5 production and tissue eosinophilia after RSV challenge. J. Virol. **72**:2871–80.

23. **Boukhvalova MS**, **Prince GA**, **Blanco JCG**. 2009. The cotton rat model of respiratory viral infections. Biologicals **37**:152–9.

24. **Graham BS**, **Henderson GS**, **Tang YW**, **Lu X**, **Neuzil KM**, **Colley DG**. 1993. Priming immunization determines T helper cytokine mRNA expression patterns in lungs of mice challenged with respiratory syncytial virus. J. Immunol. **151**:2032–40.

25. **Swanson KA**, **Settembre EC**, **Shaw CA**, **Dey AK**, **Rappuoli R**, **Mandl CW**, **Dormitzer PR**, **Carfi A**. 2011. Structural basis for immunization with postfusion respiratory syncytial virus fusion F glycoprotein (RSV F) to elicit high neutralizing antibody titers. Proc. Natl. Acad. Sci. U. S. A. **108**:9619–24.

26. **McLellan JS**, **Yang Y**, **Graham BS**, **Kwong PD**. 2011. Structure of respiratory syncytial virus fusion glycoprotein in the postfusion conformation reveals preservation of neutralizing epitopes. J. Virol. **85**:7788–96.

27. **Watford WT**, **Ghio AJ**, **Wright JR**. 2000. Complement-mediated host defense in the lung. Am. J. Physiol. Lung Cell. Mol. Physiol. **279**:L790–8.

CHAPTER 7

CONCLUSIONS

RSV is an important viral pathogen that causes serious lower respiratory tract infections in infants, the elderly, and immunocompromised individuals. No licensed vaccine exists, and treatments are limited. In this work, we describe the development and evaluation of PIV5-vectored RSV vaccines. PIV5 has been used as viral vector to develop vaccine candidates against a number of different pathogens. Therefore, we hypothesized that PIV5 would be a safe and efficacious viral vector for developing RSV vaccines. To address this hypothesis, we examined the following specific aims:

Specific aim 1: To develop vaccine candidates against RSV using PIV5 as a vector to express RSV surface glycoproteins. The working hypothesis is that PIV5-expressing RSV-F or RSV-G will be able to elicit RSV antigen-specific humoral responses and provide protection against RSV infection in various animal models.

***Specific aim 1a*:** To evaluate the efficacies of PIV5 expressing RSV-F or RSV-G as vaccines to prevent RSV infection in mice. The data in chapter 3 shows that PIV5 was able to express RSV-F and RSV-G, and that intranasal immunization of mice with these PIV5-vectored vaccines induced the production of RSV antigen-specific antibodies. The PIV5-RSV-F candidate also elicited the production of neutralizing antibodies. Examination of IgG subtypes and lung sections suggested that the vaccines did not cause enhanced disease relative to RSV-immunized mice. Importantly, the vaccines induced potent protective immunity against lower respiratory tract RSV infection.

***Specific aim 1b*:** To evaluate the efficacies of the above vaccines in cotton rats, a more relevant model for RSV vaccine evaluation. Since the PIV5-RSV-F and PIV5-RSV-G were efficacious vaccines in mice, we hypothesized that they would also safely confer protection against RSV infection in cotton rats. The data in chapter 4 indicates that the vaccines replicated in the upper and lower respiratory tracts of cotton rats without apparent signs of disease. Both candidates were immunogenic and conferred complete lower respiratory tract protection against RSV infection after a single intranasal dose.

***Specific aim 1c*:** To examine the replication and evaluate the efficacies of the above vaccines in RSV-experienced and RSV-naïve non-human primates. Since the PIV5-vectored vaccines delivered promising results in rodent models of RSV infection, we hypothesized that they would also be efficacious in nonhuman primate models that mirror different target populations for RSV vaccines. The data in chapter 4 demonstrates that the vaccines replicate well in RSV seropositive and seronegative African green monkeys without causing any obvious signs of disease. Seronegative monkeys developed modest neutralizing antibody titers, but robust mucosal IgA titers. The immunity generated in seronegative monkeys was sufficient to reduce RSV replication in the upper and lower respiratory tracts. The vaccines were also able to boost baseline antibody titers in seropositive monkeys. These results suggest that the PIV5-vectored RSV vaccines may be used in both seronegative and seropositive target populations.

Specific aim 1d: To determine the sequence stability of the vaccine candidates *in vitro* and *in vivo*. In light of earlier studies involving the serial passage of PIV5 expressing EGFP, the working hypothesis is that the PIV5 expressing RSV-F or RSV-G will remain stable through *in vitro* and *in vivo* passage. In chapter 5, we examined the *in*

vitro stability of the candidates by passing them in Vero cells for eleven generations and compared the genome sequences of the resulting viruses with those of the parental viruses. Mutations were observed in clonal populations of the vaccine candidates and in the PIV5 backbone of PIV5-RSV-G. There were no mutations in the consensus sequences of the inserted genes for both candidates. The *in vivo* stability of the candidates was examined after a single passage in African green monkeys. No mutations were observed in the consensus sequences of the viruses recovered from the BAL fluid. These results indicate that RSV gene insertions were stable in the PIV5 genome.

Specific aim 2: To improve the PIV5-RSV-F vaccine candidate by engineering RSV-F to be more immunogenic and/or by modifying the PIV5 vector to enhance RSV-F presentation. The working hypothesis is that expressing pre-fusion mutants of RSV-F and/or deleting the SH gene from the PIV5 backbone will improve the current vaccine candidate by eliciting highly neutralizing antibodies and by enhancing apoptosis, respectively. In chapter 5, we engineered and inserted a pre-fusion-stabilized RSV-F mutant between the PIV5 SH and HN genes and examined whether it increased the immunogenicity and efficacy of the wild-type F-expressing counterpart. We also deleted the SH gene from PIV5 to examine whether the modification improved vaccine efficacy. All of the candidates were immunogenic and protective in mice, but the pre-fusion F candidates elicited lower neutralizing antibody titers than the wild-type F candidates. When the vaccines were evaluated in cotton rats, they were similarly immunogenic and protective when administered intranasally. Subcutaneous administration of the PIV5-RSV-F (SH-HN) candidate conferred better protection than the ΔSH counterpart. These results suggest that expressing pre-fusion F and/or deleting SH did not improve vaccine

efficacy. The findings of the subcutaneous vaccination study also indicate that PIV5 expressing RSV-F is safe and highly efficacious when administered by this route. This has exciting implications for vaccinating young infants, as it provides a method to circumvent potential problems associated with intranasal vaccine-induced nasal congestion.

Taken together, the results of these vaccine studies suggest that PIV5 is a promising vector for RSV vaccines. The PIV5-RSV vaccines were safe, immunogenic, and protective in all of the pre-clinical animal models that were tested.This work also furthers our understanding of PIV5 stability and the role of SH in determining vaccine efficacy.

Future studies will be needed to examine the durability of the immune responses generated by the PIV5-RSV vaccines. Previous work with a PIV5-vectored rabies vaccine in dogs has shown protective antibody levels up to one year after immunization. Our studies showed that cotton rats had significant RSV-specific antibodies 49 days after immunization, but it is important to determine how long the PIV5-RSV vaccines confer protection against RSV infection. The durability of the immune responses may also differ depending on the route of vaccine administration. A prime-boost vaccine regimen may need to be implemented to prolong the protective immune response.

PIV5-RSV vaccine tropism and persistence should also be studied. The vaccines have been shown to infect the respiratory tract, but the specific tissue cell types or immune cell types that are infected have not been examined. Additional studies are also needed to study the tropism of the vaccines when they are administered subcutaneously. It will be important to determine how long the vaccines persist and where they persist

after immunization. The host immune response controls and clears the vaccine viruses, as live virus is undetectable in the BAL washes of nonhuman primates two weeks post-immunization. However, the mechanism of this process has not yet been studied in detail, and other potential vaccine virus reservoirs should be examined. These studies will improve our understanding of the immunobiology of PIV5-based vaccines and may help determine if the vector requires additional modification. This work provides a rationale to pursue the use of a PIV5-vectored RSV vaccine in a clinical setting. The PIV5-RSV vaccines were safe, immunogenic, and did not potentiate enhanced disease in animal models. Moving forward, important considerations must be made regarding target vaccination groups and relevant endpoints to be measured. Our goal is to protect infants and the elderly against medically-attended RSV infection, and our studies suggest that a PIV5-vectored RSV vaccine may be a viable solution.

APPENDIX A

THE ROLE OF AKT IN RSV PHOSPHOPROTEIN FUNCTION

Phan S.I.*, Fuentes S.M.*, Foster S.L., Tran K., Barrozo E., Teng M.N., He B. To be submitted to *Journal of Virology*. *Authors contributed equally.

Abstract

The respiratory syncytial virus (RSV) phosphoprotein (P) is a heavily phosphorylated component of the viral RNA-dependent RNA polymerase (RdRp). Phosphorylation of P is thought to be important in regulating viral RNA synthesis, but the precise role is unclear. Since the RSV genome does not encode a kinase, host kinases are required for phosphorylation of viral proteins. It has previously been shown that the host kinase, Akt1, plays an important role in the replication of negative-sense RNA viruses. In this work, we show that Akt is important in RSV growth. Akt phosphorylates RSV-P *in vitro*, and the inhibition of Akt activity results in decreased viral replication. We identified several sites in P that were phosphorylated by Akt and examined their functional roles in a minigenome system. Recombinant viruses with mutations at these sites were also rescued to examine the effects of these mutations on virus growth. Threonine at position 210 was found to be critical to RSV replication and survival.

Introduction

Respiratory syncytial virus (RSV) is a prototypical *Pneumovirus* of the *Paramyxoviridae* family. Its RNA-dependent RNA polymerase (RdRp) consists of the nucleocapsid (N), phosphoprotein (P), large polymerase (L), and M2-1 proteins. The N protein encapsidates the viral RNA (vRNA), protecting it from degradation by cellular nucleases (1, 2). The P protein interacts with N, L, and M2-1, stabilizing the RdRp complex and facilitating docking of the complex on the encapsidated vRNA (3–6). It also serves as a chaperone for soluble N, sequestering it in preparation for encapsidating the vRNA (2). L is the catalytic polymerase (7). M2-1 is an anti-termination factor that is important for processivity during transcription of long mRNAs (8). The RSV P protein is critical for vRNA synthesis. It is the most heavily phosphorylated RSV protein, but the role of P phosphorylation in RSV transcription and replication is not completely understood (9, 10).

Since bacterially-purified, unphosphorylated P is inactive in transcription, it suggests that phosphorylation is required for the function of P (11). Lu et al. previously identified phosphorylation sites in two clusters: one cluster consisting of S116, S117, and S119 in the oligomerization domain, and the other cluster consisting of S232 and S237 in the C-terminal domain of the protein. Phosphorylation of these sites was not required for virus replication *in vitro*, but played a role in efficient virus growth both *in vitro and in vivo* (10). Phosphorylation of S116, S117, and S119 was also required for M2-2 to mediate inhibition of RSV genome transcription (12). Asenjo et al. identified phosphorylation sites at S54 and S108, both of which are important for P function.

Phosphorylation of S54 may play a role in viral uncoating, whereas phosphorylation of S108 may be important for the interaction between P and M2-1 (13, 14).

Since P does not have intrinsic catalytic activity, and no RSV proteins are known to phosphorylate P, it is believed that host kinases are responsible for phosphorylating P. Specifically, it has been shown that casein kinase II (CKII) can phosphorylate P at S232 and S237 (15, 16). However, the number of host kinases that phosphorylate P *in vivo* is unknown.

In this study, we have found that Akt phosphorylates P through the use of an *in vitro* kinase assay. Akt is a serine/threonine-specific kinase that is a member of the AGC subfamily and plays important roles in cell cycle progression, cell survival, proliferation, metabolism, and migration (17, 18). Due to its diverse roles in many cellular processes, it has been the focus of anti-cancer drug development. As a result, there are many commercially available Akt inhibitors, some of which have undergone clinical trials (19). In this work, we discuss a role for Akt in RSV growth and propose a new role for re-purposing Akt inhibitors to control RSV infection. These results show that Akt activity is important for RSV growth.

Materials and Methods

Cells

A549 cells were maintained in Dulbecco's Modified Eagle Medium (DMEM) supplemented with 10% fetal bovine serum (FBS),100 IU/ml penicillin, and 100 μg/ml streptomycin (1% P/S, Mediatech, Inc., Manassas, VA). BSR-T7 cells were maintained in DMEM with 10% FBS, 10% tryptose phosphate broth (TPB), 1% P/S and 400 μg/ml G418 sulfate antibiotic (Mediatech, Inc.). Cell lines were grown at 37°C, 5% CO_2 and

passaged 1 day prior to transfection or infection to achieve 80-90% confluence by the following day.

Viruses

Recombinant RSV subgroup A2 (rA2), RSV expressing *Renilla* luciferase (rA2-Rluc), and rA2 P mutants were propagated and titered in Vero cells. Vero cells were infected with virus in Opti-MEM I reduced serum medium (Opti-MEM) supplemented with 2% FBS and 1% P/S at a multiplicity of infection (MOI) of 0.1. Cells were monitored for syncytia formation, and virus was collected 3 to 4 days post-infection as described previously (20, 21).

All other RSV infections were performed as indicated in the figure legends. Briefly, virus was diluted in Opti-MEM containing 2% FBS and 1% P/S to infect cells at the indicated MOI. After adsorbing for 1-2 h, the inoculum was removed and replaced with fresh Opti-MEM supplemented 2% FBS and 1% P/S.

Plasmids

Plasmids used to rescue rA2 viruses have been described previously (21). The plasmids for the RSV minigenome system were a gift from Dr. Martin Moore. Codon-optimized genes encoding the minigenome reporter, N, M2-1, and L were cloned in pcDNA3.1. The gene encoding P was cloned in pCaggs.

The Akt1 dominant-negative (DN) mutant construct, pMT2-AH-AKT1 (PH-AKT) contained the PH domain of Akt (amino acids 1-147) and a Myc tag as described in Khwaja, et al (22). The kinase-dead Akt1 DN mutant (AAA-Akt1) described previously by Srinivas, et al. contained three alanine mutations and an HA tag. The

K179A mutation was located in the ATP binding site of Akt. Mutations T308A and S473A were located in the Akt activation sites (23).

Bacterial protein expression plasmids were generated by cloning the P gene from rA2 into the pET15b vector (Novagen, Madison, WI) downstream of the T7 promoter and histidine tag. P mutants were made by PCR mutagenesis using pET15b-RSV P as a template. For protein expression in mammalian cell lines, expression plasmids were made by cloning the P gene into pCaggs (pCaggs-P). FLAG-tagged Akt1 was cloned into pCaggs as well.

Akt inhibitors, siRNA, and dominant-negative mutants

Akt inhibitor IV, Akt 1/2 isotype-selective inhibitor, and casein kinase II inhibitor (EMD Millipore, Billerica, MA) were dissolved in DMSO and used at the concentrations indicated in the figure legends. DMSO was used as a negative control for all experiments involving inhibitors.

Small interfering RNA (siRNA) targeted against Akt1, Akt2, and Akt3 isoforms and a non-target control were purchased from Dharmacon (Lafayette, CO). A549 cells in 24-well plates were transfected with 100 nM of the various siRNAs using Oligofectamine reagent (ThermoFisher) according to the manufacturer's protocol. After incubating the transfected cells overnight at 37°C, 5% CO_2, the culture medium was changed to Opti-MEM with 2% FBS and 1% P/S. Two days after transfection, the cells were infected with rA2-Rluc at an MOI of 1. For immunoprecipitation experiments, A549 cells in 6-cm dishes were transfected with 1 μM of siRNA as described above and infected with rA2 at an MOI of 1.

Akt1 dominant-negative mutants AAA-Akt1 and PH-Akt were transfected into A549 cells with Lipofectamine and Plus reagent (ThermoFisher) according to manufacturer's instructions. Six μg of DNA per 6-cm dish were used for immunoprecipitation experiments. Four hundred ng of DNA were transfected per well of a 24-well plate for luciferase assays.

Luciferase assays

A549 cells in 24-well plates were transfected with Akt-specific siRNA or Akt1 dominant-negative mutant and then infected with rA2-RLuc as described above. One day post-infection, cells were lysed and luciferase activity was measured using the Renilla luciferase assay system from Promega (Madison, WI). Luminescence was measured using a Glomax 96 Microplate Luminometer (Promega, Madison, WI). The remaining cell lysates were diluted 1:1 in protein loading buffer [2% sodium dodecyl sulfate (SDS), 62.5 mM Tris-HCl (pH 6.8), 2% dithiothreitol (DTT)], heated, and resolved on an SDS-PAGE gel. (Should this be in another section?) Akt isoforms were detected by immunoblotting with mouse monoclonal anti-Akt1 (2H10), rabbit anti-Akt2, or rabbit anti-Akt3 antibodies (Cell Signaling Technology, Danvers, MA). Expression of the Akt DN mutants was detected by immunoblotting with anti-Myc (PH-AKT) or anti-HA antibodies (AAA-Akt1).

RSV minigenome system and dual-luciferase assay

The RSV minigenome assay was performed as previously described with modifications (24). Briefly, BSR-T7 cells in 24-well plates were transfected with plasmids encoding the RSV minigenome reporter (200 ng), N (100 ng), P/P mutant (5-80 ng), M2-1 (100 ng), L (50 ng), and Renilla luciferase (1 ng) using JetPRIME reagent

(Polyplus, Illkirch, France) according to manufacturer's guidelines. Plasmid amounts were normalized between wells using empty vector. Forty-eight hours post-transfection, cells were lysed in 100 μl of Passive Lysis Buffer (Promega, Madison, WI) on an orbital shaker for 15-20 minutes. Clarified lysates (40 μl) were transferred to a white 96-well plate, and the dual-luciferase assay was performed according to manufacturer's instructions. Luminescence was measured using a Glomax 96 Microplate Luminometer (Promega, Madison, WI). Relative luciferase activity was calculated as the ratio of firefly luciferase activity to *Renilla* luciferase activity. Each condition was assayed in quadruplicate, and leftover lysates were used to examine P expression by Western blot.

Immunoprecipitation and co-immunoprecipitation

To determine whether Akt and P interacted, BSR-T7 cells in 10-cm dishes were transfected with pCaggs-Akt1-FLAG (2 μg), pCaggs-P (7 μg), or both using Lipofectamine and Plus reagent. One day post-transfection, cells were starved for 30 minutes in either cysteine and methionine-deficient DMEM or phosphate-deficient DMEM. Cells were metabolically labeled with DMEM containing ^{35}S-Met and ^{35}S-Cys for 4 h at 37°C, 5% CO_2. Cells were lysed with whole cell extract buffer (WCEB; 50 mM Tris-HCl [pH 8], 280 mM NaCl, 0.5% NP-40, 0.2 mM EDTA, 2 mM EGTA, 10% glycerol, 1X protease inhibitor cocktail, 0.1 mM phenylmethylsufonyl fluoride) and lysates were cleared by centrifugation. Proteins were co-immunoprecipitated using mouse anti-Akt1 antibody (clone 2H10) or rabbit anti-P serum (raised against N-terminal sequence IKGKFTSPKDPKKKC) and Sepharose G beads at 4°C. After washing with WCEB, the proteins were resolved on a 15% SDS-PAGE gel and visualized with a Storm 860 Molecular Imager (GE Healthcare Life Sciences, Piscataway, NJ).

To identify phosphorylation sites in P during RSV infection, A549 cells were infected with rA2 at an MOI of 1. The next day, cells were lysed with WCEB, and clarified lysates were immunoprecipitated with monoclonal anti-P antibody (clone D6). Proteins were resolved on a 15% SDS-PAGE gel and visualized with Coomassie Blue stain. The P band was excised and prepared for mass spectrometry as described in the mass spectrometry methods.

To examine the effect of Akt inhibition on P phosphorylation, A549 cells were infected with rA2 or rA2 mutants at an MOI of 1. One day post-infection, cells were starved for 30 minutes in either cysteine and methionine-deficient DMEM or phosphate-deficient DMEM. Cells were metabolically labeled with DMEM containing ^{35}S-Met and ^{35}S-Cys or ^{33}[P] orthophosphate with or without Akt inhibitor for 4-6 h at 37°C, 5% CO_2. Cells were lysed with whole cell extract buffer (WCEB; 50 mM Tris-HCl [pH 8], 280 mM NaCl, 0.5% NP-40, 0.2 mM EDTA, 2 mM EGTA, 10% glycerol) and lysates were cleared by centrifugation. Proteins were immunoprecipitated with rabbit anti-RSV P serum (raised against N-terminal sequence IKGKFTSPKDPKKKC) and Sepharose G beads overnight at 4°C. After washing with WCEB, the proteins were resolved on a 15% SDS-PAGE gel and visualized with a Typhoon 9700 Phosphorimager (GE Healthcare Life Sciences, Piscataway, NJ).

Protein purification

The pET15b-P/P mutant plasmids were transformed in BL21(DE3)/pLysS competent cells. The bacteria were grown overnight on Luria Bertani (LB) agar plates with ampicillin (AMP; 100 μg/mL) and chloramphenicol (CAM; 34 μg/mL) selection. A single colony was selected for each construct and cultured in 3 mL of LB overnight at

37°C with AMP and CAM. The following morning, the culture was used to inoculate a 250 mL flask of LB containing AMP and CAM. The culture was grown at 37°C until it reached an OD_{600} of 0.5-0.6 and then induced with 1mM isopropyl β-D-1 thiogalactopyranoside (IPTG) for 4 hours. The bacteria were pelleted by centrifugation, resuspended in binding buffer (50 mM Tris-HCl [pH 8], 0.05% Tween-20, 200 mM NaCl, 5 mM imidazole) and sonicated on ice. The lysate was clarified by centrifugation at 20,000 x g for 45 minutes at 4°C. The clarified lysate was loaded onto a Polyprep chromatography column (BioRad, Hercules, CA) containing 1 mL of Ni-NTA His-Bind® resin (EMD Millipore). After washing with wash buffers containing increasing concentrations of imidazole, the protein was eluted with elution buffer (50 mM Tris-HCl [pH 8], 0.05 Tween-20, 200 mM NaCl, 400 mM imidazole) followed by concentration and buffer exchange with 50 mM Tris-HCl [pH 8], 150mM NaCl. The protein fractions were analyzed by SDS-PAGE followed by Coomassie Blue staining.

***In vitro* kinase assay**

For Figure 3C, increasing concentrations of purified P or P S86A (1.65 μg, 3.3 μg, and 4.95 μg) were mixed with active Akt1 (400 ng, Upstate Biotechnology), 10 μCi of [γ-^{32}P]-ATP, and 1X kinase buffer (Cell Signaling Technologies). The reactions were incubated for 2 h at 30°C and terminated by the addition of protein loading buffer. The samples were resolved on a 10% SDS-PAGE gel and visualized using a Storm 860 Molecular Imager.

For Figure 7C, the *in vitro* kinase assay was carried out in the same manner, except with 3 μg of purified P or P mutant and 250 ng of active Akt1 (EMD Millipore). The gel was visualized using a Typhoon 9700 Phosphorimager.

Mass spectrometry

To identify Akt phosphorylation sites in P, a cold *in vitro* kinase assay was performed with active Akt1 (4 μg), P (16 μg), ATP (200 mM), and 1X kinase buffer. The proteins were separated on a 10% SDS-PAGE gel and stained with Coomassie Blue. The P band was excised into 1 mm^2 cubes, destained, and dehydrated using 100 mM NH_4HCO_3 in 50% acetonitrile. Disulfide bonds were reduced with 100 mM DTT in 25 mM NH_4HCO_3 and alkylated with 55 mM iodoacetamide in 25 mM NH_4HCO_3. The protein was subjected to in-gel tryptic digestion (12.5 ng/mL trypsin in NH_4HCO_3), and the peptides were extracted with 5% formic acid in 50% acetonitrile. Samples were sent to the Yale Cancer Center Mass Spectrometry Resource and W.M. Keck Foundation Biotechnology Resource Laboratory for TiO_2 enrichment and liquid chromatography-tandem mass spectrometry (LC-MS/MS). The Mascot database was used to identify the peptides (25).

Statistical analysis

Statistical analysis was performed using GraphPad Prism software version 6 for Macintosh (GraphPad Software, La Jolla, CA). Analysis of variance (ANOVA) followed by Dunnett's correction for multiple comparisons or Student's t-test was used where indicated.

Results

Akt is involved in RSV protein expression

Previous studies by Sun et al. have shown that Akt plays a role in RNA synthesis of non-segmented, negative-sense RNA viruses (26). To determine whether Akt is important for RSV protein expression, A549 cells were transfected with siRNA against

various Akt isoforms and then infected with rA2-Rluc. Western blotting of cell lysates was performed to confirm Akt knockdown. Luciferase activity was significantly reduced in cells transfected with Akt-specific siRNA, with the greatest reduction observed in cells treated with siRNA against Akt1 (Fig. A.1A). These results show that Akt is important for RSV protein synthesis.

Akt contains two domains: a pleckstrin homology (PH) domain and a kinase domain (17, 18). To examine which domain is important for RSV protein synthesis, A549 cells were transfected with plasmids encoding dominant-negative Akt mutants and then infected with rA2-Rluc. The PH domain mutant contains only the PH domain of Akt. The kinase domain mutant contains amino acid substitutions in the ATP binding pocket (K179A) and the activation site (T308A and S473A). While expression of the PH domain mutant reduced luciferase activity by 10%, the kinase domain mutant had greater than a 40% reduction in luciferase activity, suggesting that the kinase domain plays a more prominent role in RSV protein expression (Figure A.1B).

RSV P is a target of Akt

Since Akt was found to be important for RSV protein expression, the target of Akt during viral RNA synthesis was examined. RSV nucleoprotein (N), phosphoprotein (P), large protein (L), and M2-1 are proteins known to be involved in RNA synthesis. The heavily phosphorylated P protein is thought to regulate viral RNA transcription and replication (10), but the precise role of its phosphorylation is unknown.

It has been previously shown that P phosphorylation is reduced in infected cells in the presence of Akt IV inhibitor, suggesting that P is a target of Akt (26). To examine whether Akt interacts with P, BSR-T7 cells were transfected with plasmids encoding Akt,

P, or empty vector. Co-immunoprecipitation experiments were performed using radiolabeled cell lysates, and Akt and P were found to interact when pulled down with either an anti-FLAG antibody (Akt) or an anti-P antibody (Fig. A.2).

Serine 86 is not important for RSV growth

To determine whether Akt phosphorylated P, a radioactive *in vitro* kinase assay was performed using purified Akt and P protein. After resolving the samples by SDS-PAGE, Akt was found to directly phosphorylate P (Fig. A.3A and A.3B). Mass spectrometry analysis of the phosphorylated P protein band showed that serine at position 86 (S86) was found to be a major phosphorylation site (Fig.A.3C). An *in vitro* kinase assay with Akt demonstrated that the S86A mutant had reduced phosphorylation compared to wild-type P (Fig. A.3D). S86 was also found to be phosphorylated in A549 cells infected with rA2, showing that phosphorylation at this site also occurred outside the *in vitro* kinase assay system (Fig. A.3E). However, when a growth curve was performed with a recombinant rA2 mutant encoding the S86A mutation, the S86A virus grew similarly to rA2 (Fig. A.4). These results suggest that phosphorylation at the S86 site is not important for RSV growth.

Examination of additional phosphorylation sites in RSV P

Since mutating S86 had no effect on virus growth, we sought to examine other phosphorylated sites in RSV P. The *in vitro* kinase assay and mass spectrometry were repeated using Akt and purified RSV P encoding the S86A mutation (Fig. A.5). Serine at position 30 was phosphorylated, but a recombinant virus encoding S30A also grew similarly to wild-type rA2 (Fig. A.6). Thus, the process was repeated again, but this time with an RSV P encoding T29A, S30A, and S86A mutations (Fig. A.7A and A.7B).

Threonine at position 29 was also mutated because it formed a TS*P motif with S30. Akt phosphorylates R-X-X-S/T motifs, but substrates have been found that do not contain this motif (17, 18). The mass spectrometry results yielded phosphorylation at sites S94, S99, T183, T210, S211, S215, T219, and S220 (Fig. A.7C, Table A1).

Examination of the purified RSV P T210A mutant in an *in vitro* kinase assay showed no significant reduction in phosphorylation, suggesting that T210 was not the major phosphorylation site of RSV P. A significant reduction in phosphorylation was only observed when T29A, S30A, S86A, and T210A mutations were combined (Fig. A.7D and A.7E). When mutant viruses encoding S30A, S86A, S211A, or S220A mutations were used to infect A549 cells, the S86A, S211A, and S220A mutants had reduced P phosphorylation relative to wild-type RSV. However, all mutants showed similar reductions in P phosphorylation in the presence of Akt IV inhibitor, showing that none of these sites of RSV P were major phosphorylation targets of Akt (Fig. A.8A and A.8B).

We also examined the effects of mutating these phosphorylation sites to alanine on RSV transcription and replication using a minigenome system. We found that the T210A mutant had a dramatic reduction in minigenome activity, while S211A and S220A had moderately reduced and increased activity, respectively (Table A1, Fig. A.8C). These mutants had equivalent expression levels compared to wild-type P (Fig. A.8D). Mutant viruses encoding the S211A and S220A mutations grew similarly to wild-type RSV. Consistent with the minigenome data, a T210A mutant virus could not be rescued, showing that this site was critical for RSV transcription and/or replication (Table A1).

Discussion

In a previous publication, we demonstrated that Akt played an important role in the life cycles of non-segmented, negative-sense RNA viruses (26). In this work, we report that Akt is important for RSV RNA synthesis, but the mechanism of action may not be the direct phosphorylation of P by Akt. Inhibition of Akt by siRNA, small molecule inhibitor, or DN mutant reduced RSV protein expression. *In vitro* studies showed that RSV P was a phosphorylation target of Akt. Multiple rounds of *in vitro* kinase assays using purified Akt, wild-type RSV P, and RSV P mutants followed by LC-MS/MS identified several phosphorylation sites in P. The effects of mutating these sites to alanine on RSV transcription and replication were assessed using a minigenome system. When possible, the mutations were also incorporated into rA2 to examine the effects on virus growth.

Residue S86 of P was phosphorylated in both *in vitro* kinase assay and in infected cells. Furthermore, it was found to be conserved in the phosphoproteins of other pneumoviruses. However, upon incorporating the S86A mutation into a recombinant virus, there was no difference in growth when compared to wild-type rA2. Furthermore, the S86A mutant virus had reduced P phosphorylation in the presence of Akt IV inhibitor, suggesting that it was not the major target of Akt phosphorylation *in vitro*. This is not the first instance in which a phosphorylated site in P was found to be dispensable for growth *in vitro*. Lu et al. found that the casein-kinase II-mediated phosphorylation sites of P were not required for virus replication *in vitro*, but were important for virus budding *in vitro* and growth *in vivo* (10). Thus, although S86 was phosphorylated, it is unlikely to be important for RSV transcription and replication.

Of the sites examined, mutating T210 to alanine dramatically reduced minigenome activity, and a virus encoding the T210A mutation could not be rescued. Mutating T210 to glutamic acid or serine also greatly reduced minigenome activity, suggesting that T210 is crucial for RSV P function. However, the precise role that T210 plays in virus transcription and replication is unclear. One possibility is that T210 is important for the structure or organization of RSV P. However, since T210 is located in a disordered region of RSV P outside the oligomerization domain, it is not likely to play a role in P's ability to form a tetramer (27). Alternatively, T210 may play a role in P's ability to interact with other viral proteins. Asenjo et al. reported that a P T210A mutant was defective in a minigenome system and demonstrated reduced binding to NP. Interestingly, the P T210D mutant was also defective in the minigenome system but bound to N similarly to wild-type RSV P (28). Thus, the observed reduction in minigenome activity may be independent of P-N binding.

In this study, we found that Akt played an important role in RSV growth. Akt directly phosphorylated P, but it is unclear whether this interaction was the mechanism by which Akt mediated its effect. Residue P T210 was phosphorylated by Akt and found to be critical for RSV transcription and replication. However, analysis of various T210 mutants could not definitively show that the addition of a phosphate at T210 was the determining factor in P function. Further investigation is required to elucidate the role of T210 in P function.

Acknowledgements

We would like to thank all members of the Biao He lab for their technical support and helpful discussion. We would also like to thank Dr. Martin Moore for the plasmids used in the minigenome assay.

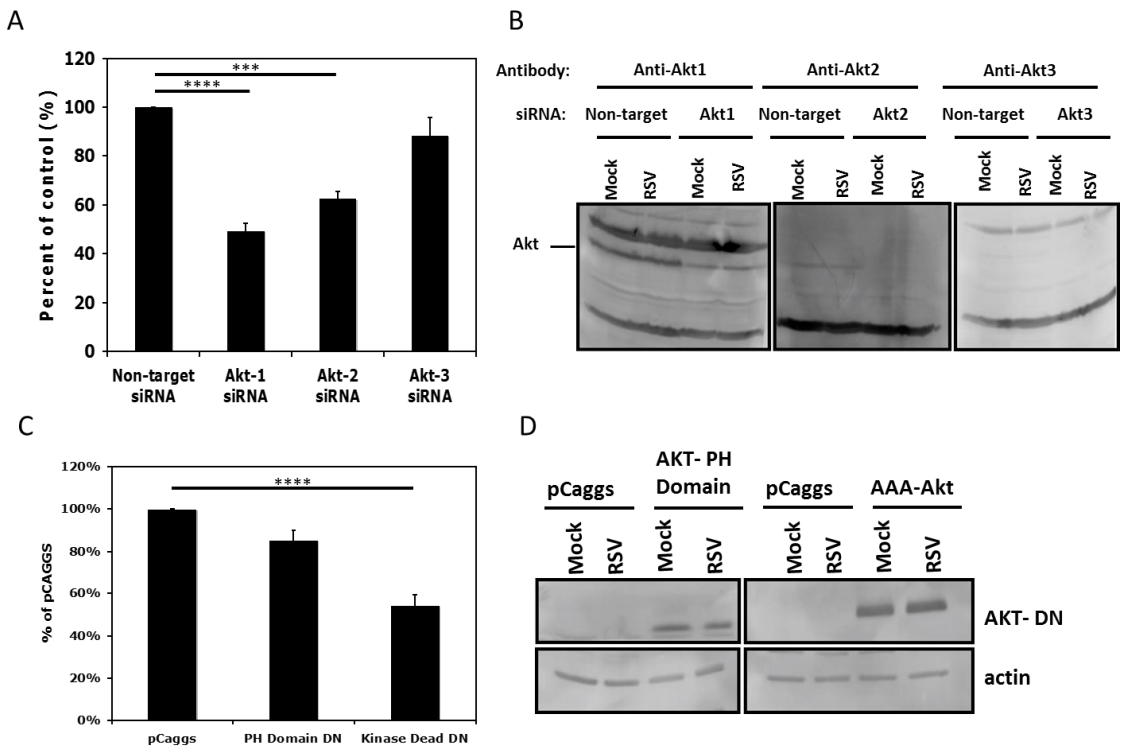

Figure A1. Inhibition of Akt by siRNA or dominant-negative mutant. (A) A549 cells were transfected with non-target, Akt1, Akt2, or Akt3-specific siRNA. Two days post-transfection, cells were infected with rA2-RLuc at an MOI of 1. One day post-infection, cells were lysed, and *Renilla* activity was measured by luciferase assay. Luciferase activity is expressed as a percentage of the activity of the non-target siRNA-treated sample. Graph is an average of three independent experiments. (B) Western blot of cell lysates was used to confirm Akt knockdown. (C) A549 cells were transfected with Akt dominant-negative mutants, followed by infection with rA2-RLuc one day later. *Renilla* activity was measured by luciferase assay 1 day post-infection. Graph is an average of four independent experiments. Luciferase activity is expressed as a percentage of luciferase activity in pCaggs-transfected sample. (D) Expression of Akt dominant-

negative mutants was confirmed by Western blot. Error bars represent the standard error of the mean (SEM). Statistics were performed using one-way ANOVA with Dunnett's correction for multiple c***, $P < 0.001$; ****, $P < 0.0001$.omparisons.

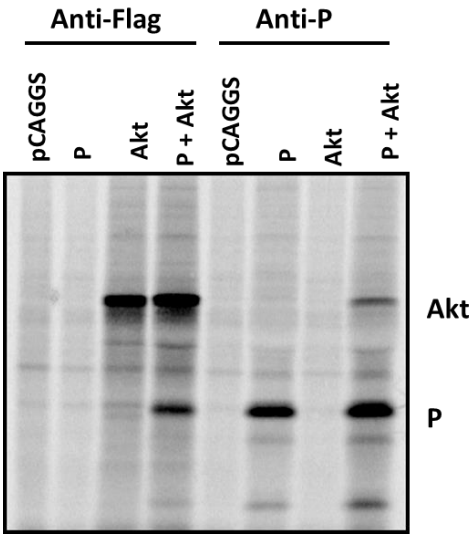

Figure A2. Akt and P interaction. BSR-T7 cells were transfected with pCaggs-Akt1-FLAG, pCaggs-P, or pCaggs, One day post-transfection, cells were labeled with ^{35}S, and proteins were immunoprecipitated from cell lysate using anti-FLAG or anti-P antibodies. Immunoprecipitation products were resolved on a 15% SDS-PAGE gel and visualized by phosphorimaging.

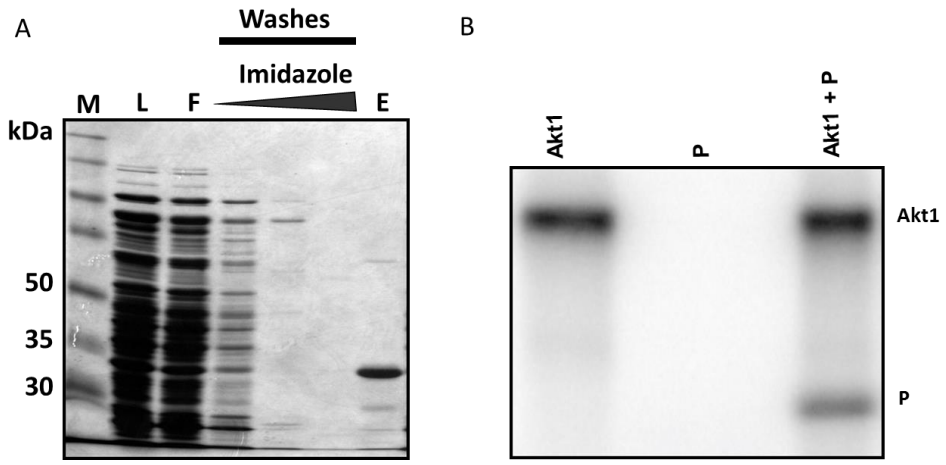

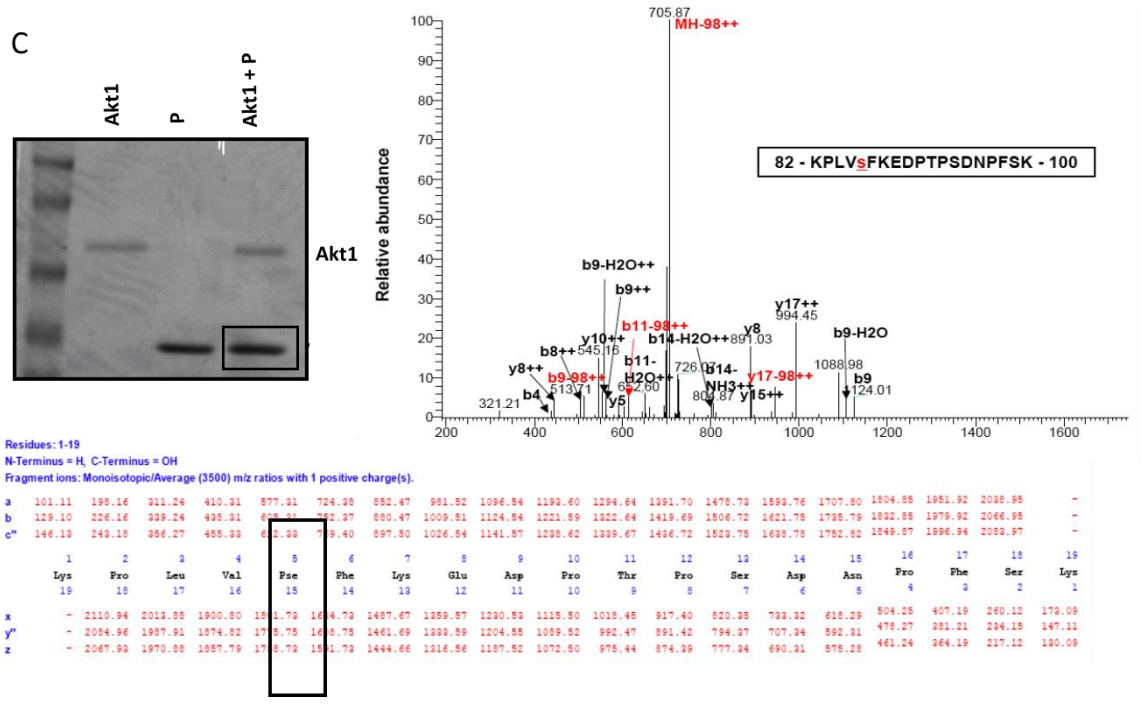

a	101.11	198.16	311.24	410.31	577.31	724.38	852.47	981.52	1096.54	1193.60	1294.64	1391.70	1478.73	1593.76	1707.80	1804.85	1951.92	2038.95	-	
b	129.10	226.16	339.24	438.31	605.31	752.37	880.47	1009.51	1124.54	1221.59	1322.64	1419.69	1506.72	1621.75	1735.79	1832.85	1979.92	2066.95	-	
c''	146.13	243.18	356.27	455.33	622.33	769.40	897.50	1026.54	1141.57	1238.62	1339.67	1436.72	1523.75	1638.78	1752.82	1849.87	1996.94	2083.97	-	
	1	2	3	4	5	6	7	8	9	10	11	12	13	14	15	16	17	18	19	
	Lys	Pro	Leu	Val	Pse	Phe	Lys	Glu	Asp	Pro	Thr	Pro	Ser	Asp	Asn	Pro	Phe	Ser	Lys	
	19	18	17	16	15	14	13	12	11	10	9	8	7	6	5	4	3	2	1	
x	-	2110.94	2013.88	1900.80	1833.73	1686.73	1487.67	1359.57	1230.53	1115.50	1018.45	917.40	820.35	733.32	618.29	504.25	407.19	260.12	173.09	
y''	-	2084.96	1987.91	1874.82	1775.75	1628.75	1461.69	1333.59	1204.55	1089.52	992.47	891.42	794.37	707.34	592.31	478.27	381.21	234.15	147.11	
z	-	2067.93	1970.88	1857.79	1758.73	1611.73	1444.66	1316.56	1187.52	1072.50	975.44	874.39	777.34	690.31	575.28	461.24	364.19	217.12	130.09	

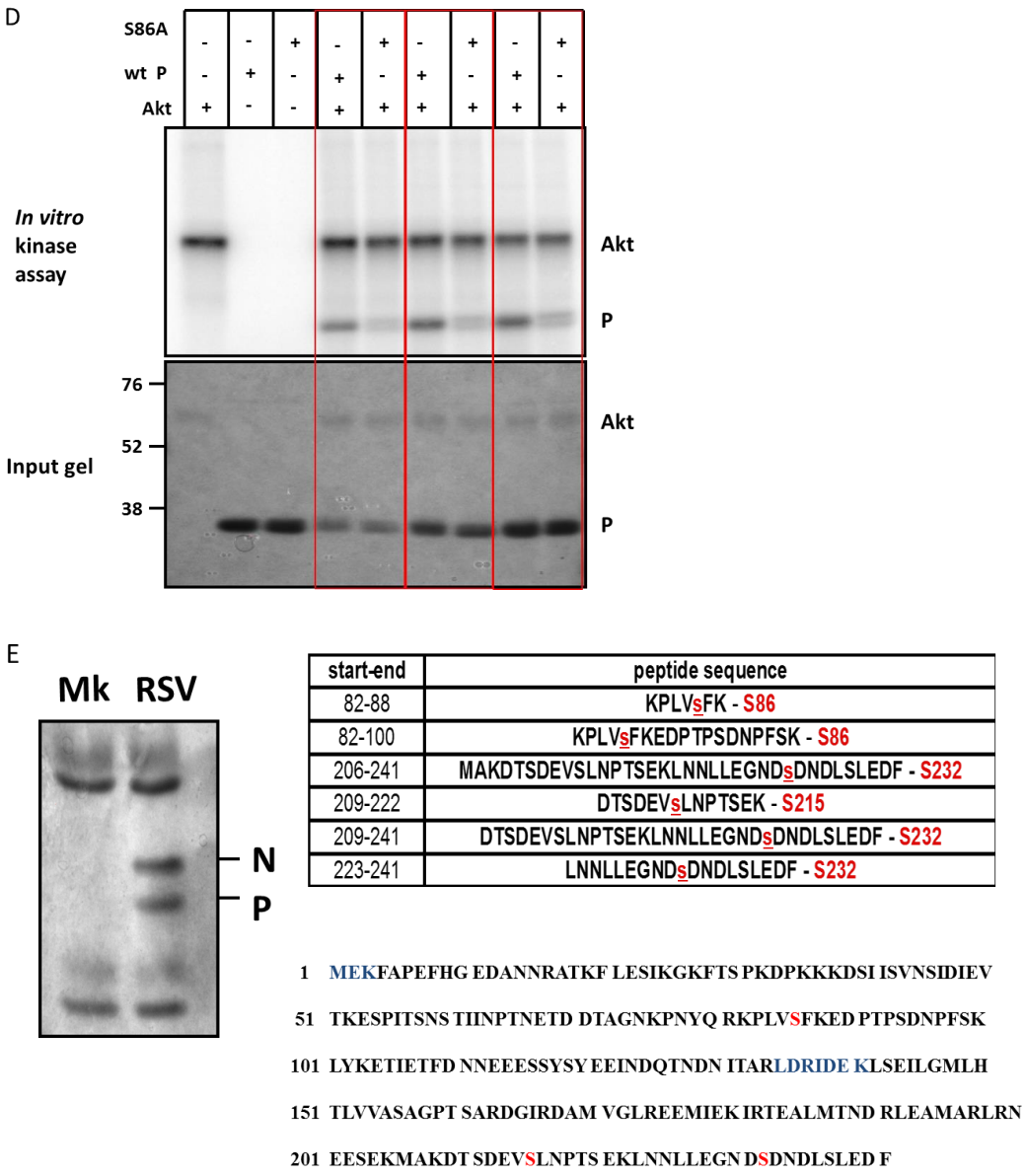

Figure A3. Identification of phosphorylation sites in P. (A) Purification of bacterially expressed P. The P gene of rA2 was cloned into pET15b vector and expressed in *E. coli*. His-tagged P was purified from bacterial lysate using Ni^{2+} affinity chromatography as described in Materials and Methods. Protein fractions were analyzed by SDS-PAGE followed by Coomassie Blue staining. M, marker; U, uninduced bacterial lysate; F,

column flow-through; E, elution. *In vitro* kinase assay. (B) Purified P was incubated with active Akt1 in the presence of [γ-^{32}P] ATP for 2 hours at 30°C. Proteins were resolved by on a 10% SDS-PAGE gel and visualized by phosphorimaging. (C) Mass spectrometry analysis of Akt-phosphorylated P. A cold *in vitro* kinase assay was performed with bacterially purified P incubated with or without active Akt1 in the presence of 5'-ATP for 2 hours at 30°C. Proteins were separated by SDS-PAGE and stained with Coomassie Blue. The P bands were excised and prepared for LC-MS/MS as described in Materials and Methods. MS/MS spectra from the generated peptides were analyzed, and phosphopeptides were identified using the Mascot database. MS/MS spectrum shown is for the only phosphopeptide found. Based on intact mass (+80 amu), the peptide contains a phosphorylation site. Y-ions and b-ions, some with neutral loss of -98 (H_3PO_4) covering all phosphorylation sites, verify S86 as a phosphorylation site. (D) Serine at position 86 was mutated to alanine (S86A) and purified from *E. coli* as described in (A). A radioactive *in vitro* kinase assay was performed as described in (B) with active Akt1 and increasing amounts of wild-type P or S86A mutant (1.65 μg, 3.3 μg, or 4.95 μg). (E) Identification of phosphorylated sites in P purified from infected cells. A549 cells were infected with rA2 at an MOI of 1. One day post-infection, cells were lysed and proteins were immunoprecipitated with monoclonal anti-P antibody. Immunoprecipitated proteins were resolved on a 15% SDS-PAGE gel and stained with Coomassie blue. The P band was excised and processed for LC-MS/MS. (E) Schematic showing phosphorylated peptides and amino acids covered by LC-MS/MS analysis. The phosphorylated serine residues are highlighted in red. Residues in blue were not covered.

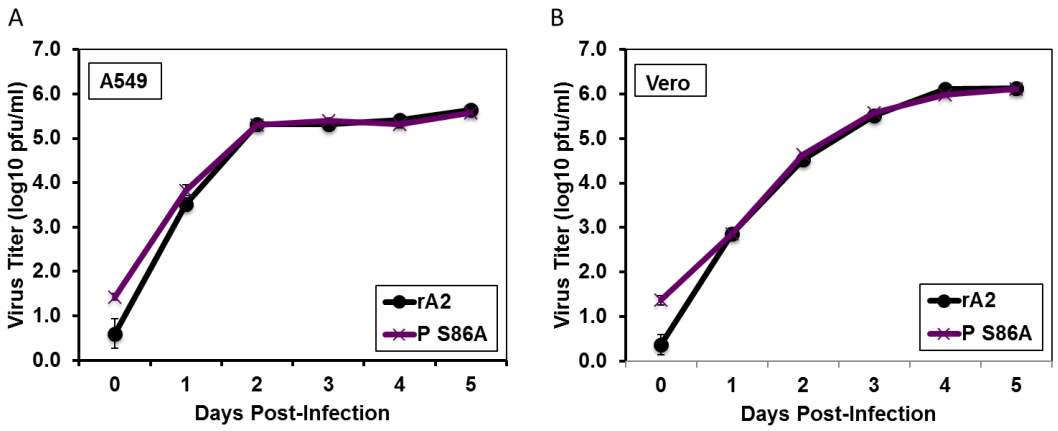

*Figure A4. Growth kinetics of rA2 P S86A mutant. (*A) A549 or (B) Vero cells were infected with either rA2 or rA2 P S86A at an MOI of 0.01. Samples of supernatant were collected every 24 h for 5 days and quantified by plaque assay in Vero cells. Growth curves were performed in triplicate. Error bars represent SEM.

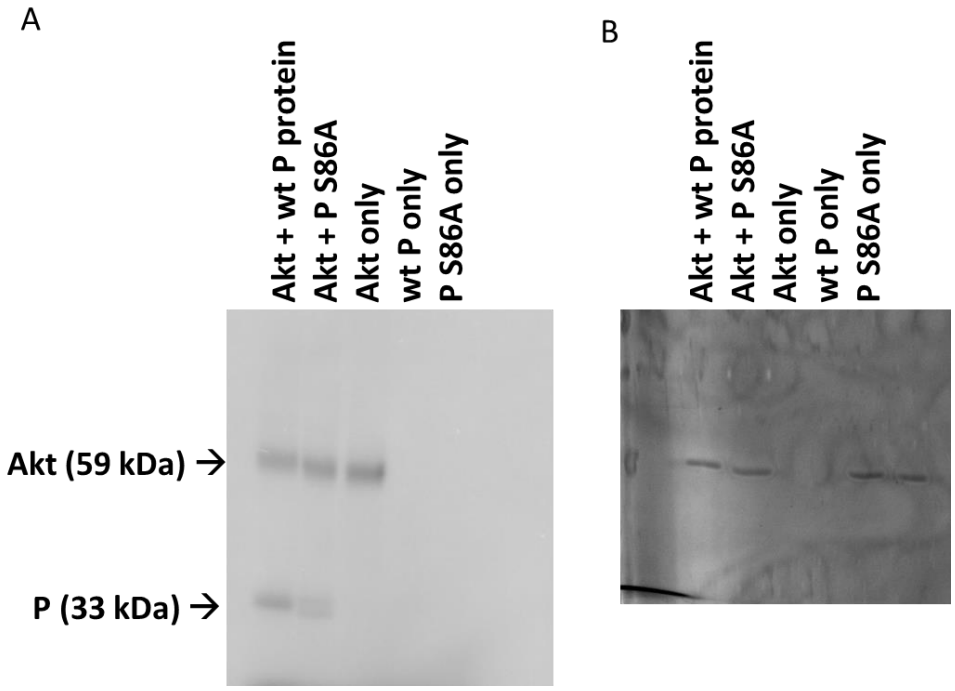

Figure A5. Identification of phosphorylation sites in P S86A. A cold *in vitro* kinase assay was performed with bacterially-purified P S86A with or without active Akt1 in the

presence of 5'-ATP for 2 hours at 30°C. Proteins were separated by SDS-PAGE and stained with Coomassie Blue. The P bands were excised and prepared for LC-MS/MS as described in Materials and Methods.

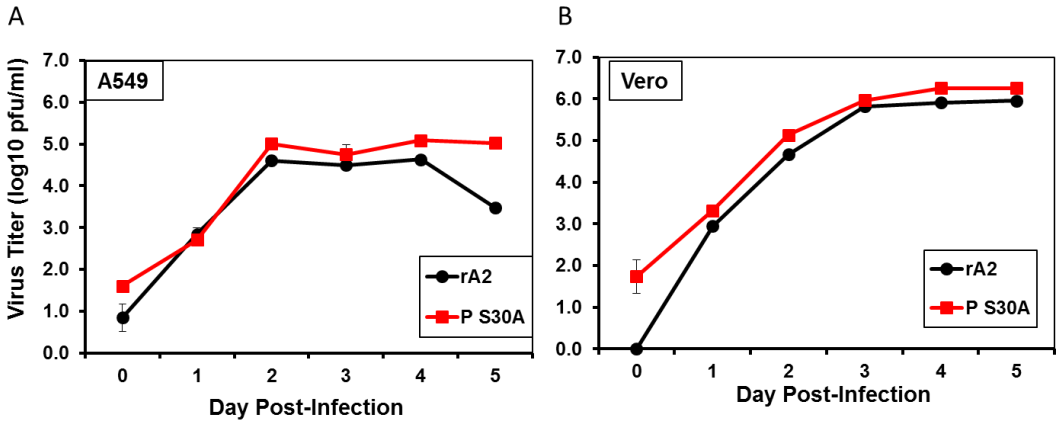

Figure A6. Growth kinetics of rA2 P S30A mutant. (A) A549 or (B) Vero cells were infected with either rA2 or rA2 P S30A at an MOI of 0.01. Samples of supernatant were collected every 24 h for 5 days and quantified by plaque assay in Vero cells. Growth curves were performed in triplicate. Error bars represent SEM.

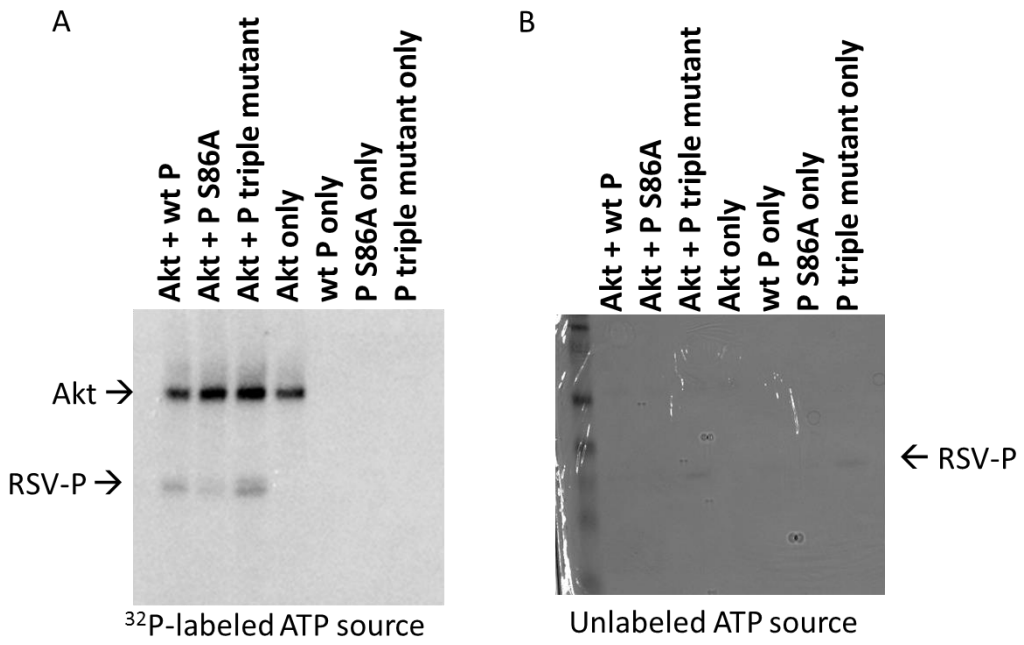

C RSV-P-triple mutant sequence:

MEKFAPEFHG EDANNRATKF LESIKGKFAA PKDPKKKDSI ISVNSIDIEV
TKESPITSNS TIINPTNETD DTAGNKPNYQ RKPLVAFKED PTPSDNPFSK
LYKETIETFD NNEEESSYSY EEINDQTNDN ITARLDRIDE KLSEILGMLH
TLVVASAGPT SARDGIRDAM VGLREEMIEK IRTEALMTND RLEAMARLRN
EESEKMAKDT SDEVSLNPTS EKLNNLLEGN DSDNDLSLED F

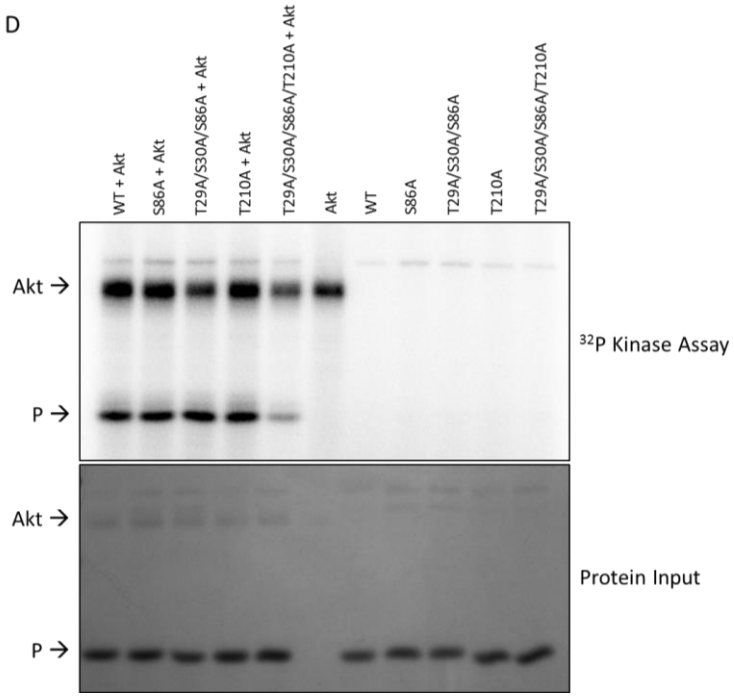

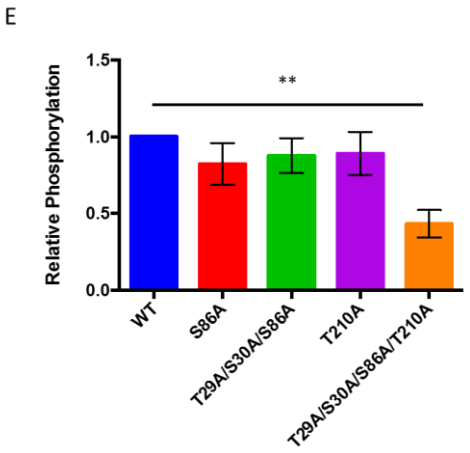

Figure A7. Identification of phosphorylation sites in P T29A/S30A/S86A. (A) A radioactive *in vitro* kinase assay was performed as described in Materials and Methods with active Akt1, wild-type P, P S86A, or P T29A/S30A/S86A mutants. (B) A cold *in vitro* kinase assay was performed as described in Materials and Methods with active Akt1, wild-type P, P S86A, or P T29A/S30A/S86A mutants. (C) The P band was excised and processed for LC-MS/MS as described in Materials and Methods. Red residues represent T29A, S30A, and S86A mutations in the triple mutant. Blue residues represent phosphorylation sites identified by mass spectrometry. Purple residues represent additional phosphorylation sites from a custom database based on the triple mutant sequence. Green sites represent the sites previously identified as dispensable by Jin et al. (D) A radioactive *in vitro* kinase assay was performed as described in Materials and Methods with active Akt1, wild-type P, P S86A, P T29A/S30A/S86A, T210A, or P T29A/S30A/S86A/T210A mutants. (E) Relative phosphorylation of P and P mutants in (D). Graph represents three independent experiments. Error bars represent the SEM. Statistical analysis was performed using one-way ANOVA with Dunnett's correction for multiple comparisons. **, $P < 0.01$.

A

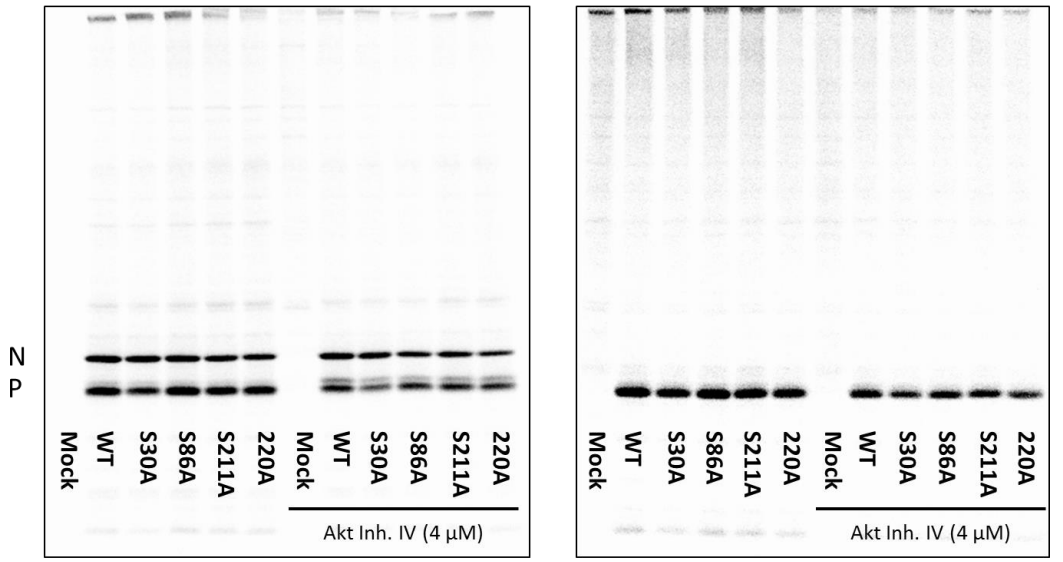
N
P
Mock
WT
S30A
S86A
S211A
220A
Mock
WT
S30A
S86A
S211A
220A
Akt Inh. IV (4 μM)
Mock
WT
S30A
S86A
S211A
220A
Mock
WT
S30A
S86A
S211A
220A
Akt Inh. IV (4 μM)

^{35}S ^{33}P

\

B

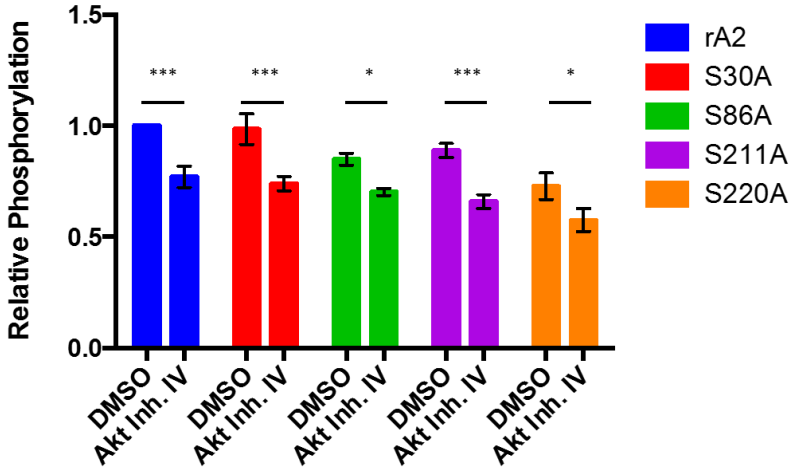
Relative Phosphorylation
1.5
1.0
0.5
0.0
***
***
*
***
*
rA2
S30A
S86A
S211A
S220A
DMSO
Akt Inh. IV
DMSO
Akt Inh. IV
DMSO
Akt Inh. IV
DMSO
Akt Inh. IV
DMSO
Akt Inh. IV

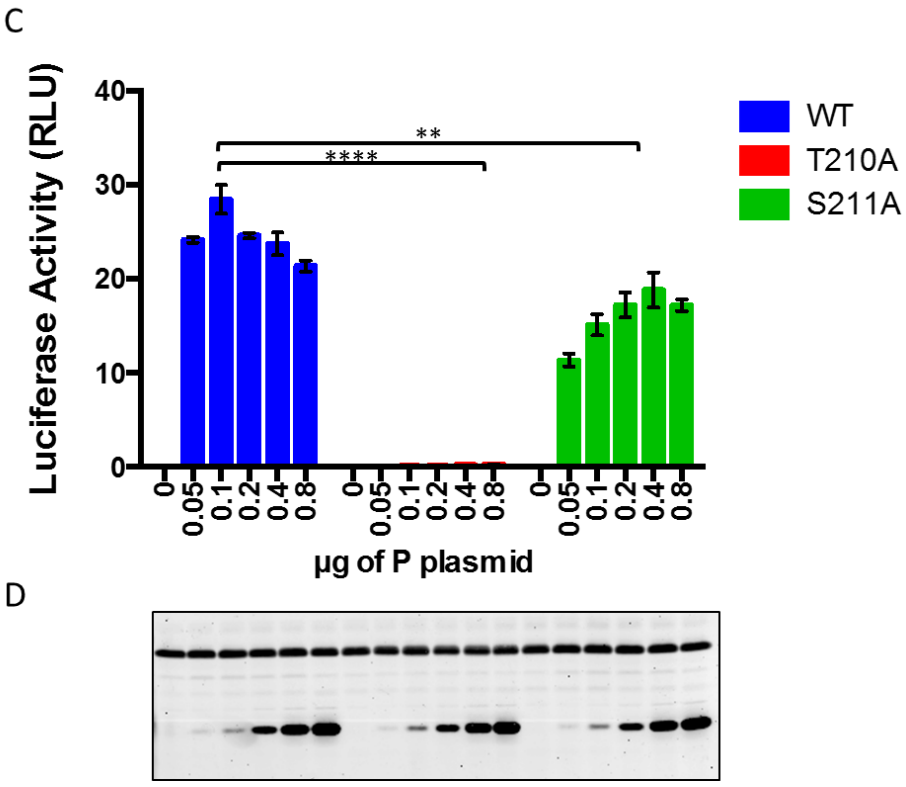

Figure A8. Minigenome activity of P mutants. (A) A549 cells were infected with rA2 or rA2 P mutant viruses at an MOI of 1 in the presence or absence of Akt IV inhibitor (4 µM). One day post-infection, cells were metabolically labeled with ^{35}S or ^{33}P for 4-6 h. Cells were lysed and co-immunoprecipitation was performed using anti-P rabbit sera. (B) Relative phosphorylation of P was measured as a ratio of $^{33}P/^{35}S$ band intensity, with the phosphorylation of wild-type P set to 1. Graph represents 3 independent experiments. Error bars represent the SEM. Statistical analysis was performed using two-tailed Student's t-test without correction for multiple comparisons. (C) Minigenome activity of P, P T210A, and P S211A. BSR-T7 cells were transfected with increasing amounts of plasmids encoding P, P T210A, or P S211A along with other plasmids of the minigenome system as described in the Materials and Methods. Firefly luciferase was the minigenome

reporter and *Renilla* luciferase served as the transfection control. Relative luciferase activity was reported as the ratio of firefly to *Renilla* activity. Error bars represent the SEM of four replicates. (D) Expression of P, P T210A, P S211A, and α-tubulin were detected by Western blot. *, $P < 0.05$; **, $P < 0.01$; ***, $P < 0.001$; ****, $P < 0.0001$.

Table A1. Minigenome activity of P mutants and growth of rA2-P mutant viruses

Phosphorylation Site	Alanine Mutant (Minigenome)	Growth of Mutant Virus
S86	No change	Normal Titer
T29	No change	N/A
S30	No change	Normal Titer
S94	No change	N/A
S99	No change	N/A
T183	No change	N/A
T210	11%	No Rescue
S211	68%	Normal Titer
S215	No change	N/A
T219	No change	N/A
S220	115%	Normal Titer

References

1. **Fields BN**, **Knipe DM**, **Howley PM**. 2015. Fields virology. Wolters Kluwer Health/Lippincott Williams & Wilkins, Philadelphia.

2. **Ruigrok RWH**, **Crépin T**, **Kolakofsky D**. 2011. Nucleoproteins and nucleocapsids of negative-strand RNA viruses. Curr Opin Microbiol **14**:504–10.

3. **Castagné N**, **Barbier A**, **Bernard J**, **Rezaei H**, **Huet J-C**, **Henry C**, **Da Costa B**, **Eléouët J-F**. 2004. Biochemical characterization of the respiratory syncytial virus P-P and P-N protein complexes and localization of the P protein oligomerization domain. J Gen Virol **85**:1643–53.

4. **Slack MS**, **Easton AJ**. 1998. Characterization of the interaction of the human respiratory syncytial virus phosphoprotein and nucleocapsid protein using the two-hybrid system. Virus Res **55**:167–76.

5. **Tran T-L**, **Castagné N**, **Bhella D**, **Varela PF**, **Bernard J**, **Chilmonczyk S**, **Berkenkamp S**, **Benhamo V**, **Grznarova K**, **Grosclaude J**, **Nespoulos C**, **Rey FA**, **Eléouët J-F**. 2007. The nine C-terminal amino acids of the respiratory syncytial virus protein P are necessary and sufficient for binding to ribonucleoprotein complexes in which six ribonucleotides are contacted per N protein protomer. J Gen Virol **88**:196–206.

6. **Mason SW**, **Aberg E**, **Lawetz C**, **DeLong R**, **Whitehead P**, **Liuzzi M**. 2003. Interaction between human respiratory syncytial virus (RSV) M2-1 and P proteins is required for reconstitution of M2-1-dependent RSV minigenome activity. J Virol **77**:10670–6.

7. **Morin B**, **Kranzusch PJ**, **Rahmeh AA**, **Whelan SPJ**. 2013. The polymerase of negative-stranded RNA viruses. Curr Opin Virol **3**:103–10.

8. **Fearns R**, **Collins PL**. 1999. Role of the M2-1 transcription antitermination protein of respiratory syncytial virus in sequential transcription. J Virol **73**:5852–64.

9. **Brandt C**, **Power UF**, **Plotnicky-Gilquin H**, **Huss T**, **Nguyen T**, **Lambert PH**, **Binz H**, **Siegrist C a**. 1997. Protective immunity against respiratory syncytial virus in early life after murine maternal or neonatal vaccination with the recombinant G fusion protein BBG2Na. J Infect Dis **176**:884–91.

10. **Lu B**, **Ma C-H**, **Brazas R**, **Jin H**. 2002. The major phosphorylation sites of the respiratory syncytial virus phosphoprotein are dispensable for virus replication in vitro. J Virol **76**:10776–84.

11. **Barik S**, **McLean T**, **Dupuy LC**. 1995. Phosphorylation of Ser232 directly regulates the transcriptional activity of the P protein of human respiratory syncytial virus: phosphorylation of Ser237 may play an accessory role. Virology **213**:405–1

12. **Asenjo A**, **Villanueva N**. 2016. Phosphorylation of the human respiratory syncytial virus P protein mediates M2-2 regulation of viral RNA synthesis, a process that involves two P proteins. Virus Res **211**:117–125.

13. **Asenjo A**, **González-Armas JC**, **Villanueva N**. 2008. Phosphorylation of human respiratory syncytial virus P protein at serine 54 regulates viral uncoating. Virology **380**:26–33.

14. **Asenjo A**, **Calvo E**, **Villanueva N**. 2006. Phosphorylation of human respiratory syncytial virus P protein at threonine 108 controls its interaction with the M2-1 protein in the viral RNA polymerase complex. J Gen Virol **87**:3637–42.

15. **Mazumder B**, **Adhikary G**, **Barik S**. 1994. Bacterial expression of human respiratory syncytial viral phosphoprotein P and identification of Ser237 as the site of phosphorylation by cellular casein kinase II. Virology **205**:93–103.

16. **Mazumder B**, **Barik S**. 1994. Requirement of casein kinase II-mediated phosphorylation for the transcriptional activity of human respiratory syncytial viral phosphoprotein P: transdominant negative phenotype of phosphorylation-defective P mutants. Virology **205**:104–11.

17. **Manning BD**, **Cantley LC**. 2007. AKT/PKB signaling: navigating downstream. Cell **129**:1261–74.

18. **Bellacosa A**, **Testa JR**, **Moore R**, **Larue L**. 2004. A portrait of AKT kinases: human cancer and animal models depict a family with strong individualities. Cancer Biol Ther **3**:268–75.

19. **Feltes TF**, **Cabalka AK**, **Meissner HC**, **Piazza FM**, **Carlin DA**, **Top FH**, **Connor EM**, **Sondheimer HM**. 2003. Palivizumab prophylaxis reduces hospitalization due to respiratory syncytial virus in young children with hemodynamically significant congenital heart disease. J Pediatr **143**:532–540.

20. **Phan SI**, **Chen Z**, **Xu P**, **Li Z**, **Gao X**, **Foster SL**, **Teng MN**, **Tripp R a.**, **Sakamoto K**, **He B**. 2014. A respiratory syncytial virus (RSV) vaccine based on parainfluenza virus 5 (PIV5). Vaccine **32**:3050–3057.

21. **Collins PL**, **Hill MG**, **Camargo E**, **Grosfeld H**, **Chanock RM**, **Murphy BR**. 1995. Production of infectious human respiratory syncytial virus from cloned cDNA confirms an essential role for the transcription elongation factor from the 5’ proximal open reading frame of the M2 mRNA in gene expression and provides a capability for vaccine . Proc Natl Acad Sci U S A **92**:11563–7.

22. **Khwaja A**, **Rodriguez-Viciana P**, **Wennström S**, **Warne PH**, **Downward J**. 1997. Matrix adhesion and Ras transformation both activate a phosphoinositide 3-OH kinase and protein kinase B/Akt cellular survival pathway. EMBO J **16**:2783–93.

23. **Srinivas H**, **Xia D**, **Moore NL**, **Uray IP**, **Kim H**, **Ma L**, **Weigel NL**, **Brown PH**, **Kurie JM**. 2006. Akt phosphorylates and suppresses the transactivation of retinoic acid receptor alpha. Biochem J **395**:653–62.

24. **Hotard AL**, **Shaikh FY**, **Lee S**, **Yan D**, **Teng MN**, **Plemper RK**, **Crowe JE**, **Moore ML**. 2012. A stabilized respiratory syncytial virus reverse genetics system amenable to recombination-mediated mutagenesis. Virology **434**:129–36.

25. **Perkins DN**, **Pappin DJ**, **Creasy DM**, **Cottrell JS**. 1999. Probability-based protein identification by searching sequence databases using mass spectrometry data. Electrophoresis **20**:3551–67.

26. **Sun M**, **Fuentes SM**, **Timani K**, **Sun D**, **Murphy C**, **Lin Y**, **August A**, **Teng MN**, **He B**. 2008. Akt plays a critical role in replication of nonsegmented negative-stranded RNA viruses. J Virol **82**:105–14.

27. **Asenjo A**, **Villanueva N**. 2000. Regulated but not constitutive human respiratory syncytial virus (HRSV) P protein phosphorylation is essential for oligomerization. FEBS Lett **467**:279–84.

28. **Asenjo A**, **Mendieta J**, **Gómez-Puertas P**, **Villanueva N**. 2008. Residues in human respiratory syncytial virus P protein that are essential for its activity on RNA viral synthesis. Virus Res **132**:160–73.

APPENDIX B

ATM PLAYS AN IMPORTANT ROLE IN THE RSV LIFE CYCLE

Phan S.I.*, Fuentes S.M.*, Foster S.L., Barrozo E., Nassiri S., Tripp R.A., Teng M.N., Hogan R.J., He B. To be submitted to *Journal of Virology*. *Authors contributed equally.

Abstract

Human respiratory syncytial virus (RSV) is the leading cause of pediatric respiratory disease and hospitalizations. It also causes severe illness in elderly and immunocompromised populations. No licensed vaccine or effective therapeutic currently exists. RSV encodes viral proteins that are phosphorylated by host kinases. Previously, we reported that host kinases play critical roles in the RSV life cycle and can be targeted for anti-RSV drug development. In this work, we identified ataxia telangiectasia mutated (ATM), a host kinase, that played a critical role in the RSV life cycle. The role of ATM in the virus cycle was highly dependent on the *in vitro* system used to examine ATM-RSV interactions. Treatment of cells with an ATM inhibitor and siRNA targeting ATM reduced RSV growth in cell culture. Pre-treatment of cells with an ATM inhibitor had no effect on virus growth or viral gene expression, which indicated that ATM plays a role in virus assembly or egress. Understanding the interactions between RSV proteins and host kinases may lead to development of novel antiviral strategies.

Introduction

Respiratory syncytial virus is the most important etiologic agent of pediatric viral respiratory infection and remains a major cause of morbidity and mortality among infants, immunocompromised subjects, and the elderly (1). In addition, RSV infection has been associated with wheezing and asthma later in life. Unlike infection by other respiratory viruses, RSV does not induce long-lasting protective immunity against subsequent infection. Thus, individuals can be infected multiple times throughout life. Currently, there is no vaccine for RSV, nor are there effective curative treatments for severe RSV disease, although aerosolized ribavirin and prophylactic immunoglobulin therapy are used in the clinical setting. However, the high cost of palivizumab prophylaxis compounded with the need for monthly injections during RSV season raises the question of cost-effectiveness relative to the health benefits. Therefore, there is a pressing need for safe and effective therapeutic interventions for RSV.

RSV is classified in the family *Paramyxoviridae* in the order *Mononegavirales*, and is the prototypical member of the Pneumovirus genus (1). The non-segmented, negative-sense (NNS) RNA genome of RSV is 15,222 nucleotides long and contains a linear array of 10 transcription units from which 11 proteins are translated. RSV enters cells by direct fusion of its envelope with the plasma membrane. Transcription of the genome by the viral RNA-dependent RNA polymerase (RdRP) occurs solely in the cytoplasm. As the infection progresses, the viral RdRP replicates the viral genome, that is bound by N protein and assembled into encapsidated ribonucleoprotein (RNP) complexes. Accumulation of viral proteins and encapsidated viral genomes initiates the assembly and budding of infectious RSV. It is thought that the viral RNP first associates

with the M protein, which traffics the complex to cytoplasmic tails of the viral glycoproteins, which are localized to lipid raft domains in the plasma membrane (2–4). The budding process requires the N, P, M, and F proteins (4, 5). Unlike other paramyxoviruses, RSV does not require its attachment protein to complete this process. RSV lacking G, either by specific mutation or spontaneous deletion, can replicate in cell culture (6–8).

RSV M2-1, M, and P are phosphorylated (9). The M2-1 protein is an anti-termination factor, and its phosphorylation is essential for its function (9–11). The roles of phosphorylation of M and P are less certain, although recent evidence indicates that M phosphorylation regulates virion assembly (12). Since RSV does not encode a viral kinase, host kinases are responsible for phosphorylation of viral proteins. Previously, we have reported that inhibiting host kinase Akt1 blocks RSV replication, likely through a P-mediated mechanism (13). In this work, we identified ATM as a host kinase that plays a role in life cycle of RSV.

Materials and Methods

Cells, viruses and plasmids

A549, Hep-2, 293T, and Vero cells were grown in Dulbecco's Modified Eagle Medium (DMEM) supplemented with 10% fetal bovine serum (FBS), 100 IU Penicillin and 100 µg/mL of Streptomycin (1% P/S) and maintained at 37°C and 5% CO_2. GM16666 and GM16667 cell lines were maintained in DMEM supplemented with 15% FBS and 100 µg/mL of hygromycin B at 37°C and 10% CO_2. RSVeGFP and rA2-Rluc were made by cloning the eGFP or Renilla luciferase genes between the leader sequence and NS1 gene of recombinant RSV A2 strain. The viruses were grown in Vero cells. All

infections were done in Opti-MEM medium supplemented with 2% FBS and 1% P/S. Virus titers were determined in Vero cells by plaque assay as described previously. Briefly, Vero cells in 24-well plates were infected with serial dilutions of the virus. One hour post-infection, a 0.8% methylcellulose/2% FBS/1% P/S/Opti-MEM overlay was added to the plates. Plates were incubated at 37°C and 5% CO_2 for 5-7 days until plaques were visible. Plaques were immuno-stained using mouse anti-RSV G antibody and goat anti-mouse IgG conjugated to alkaline phosphatase secondary antibody. Plaques were visualized by the addition of Vector Black solution (Vector Laboratories). The pCaggs-ATM plasmid was generated by cloning the full-length coding sequence of ATM into the pCaggs vector. The pCaggs vector has been described previously (14). Codon optimized pCDNA3.1- M, G, and F were a gift from Dr. Martin Moore (Emory University).

Reagents

Goat anti-RSV was obtained from Maine Biotechnology (cat no. PAB7133P) and used at 1:1000 for Western Blot (WB) or at 1:50 for immunoprecipitation (IP). Rabbit anti-ATM (Ab3) was obtained from Calbiochem (EMD Millipore, cat no. PC116) and used at 1:1000 for WB or 1:50 for IP.

ATM inhibitor (KU-55933) was obtained from Calbiochem (EMD4Biosciences, USA) and dissolved in DMSO. Unless otherwise specified, the inhibitor was added to cells in Opti-MEM supplemented with 2% FBS and 1% P/S after the infection media was removed. Different concentrations were used for the experiments as described in figures.

Transfections and luciferase assay

On-TARGETplus SMART pool ATM siRNA and ATM and On-TARGETplus Non-targeting pool siRNA were obtained from Dharmacon (ThermoScientific, USA).

A549 cells in 96-well plates were transfected in 100 μl of Opti-MEM with 200 nM ATM siRNA and 0.8 μl Oligofectamine (Life Technologies) per well. One day post-transfection, 50 μl of Opti-MEM/30% FBS were added to the cells. Two days post-transfection, cells were infected with rA2-Rluc at an MOI of 0.1, 1, or 3 in Opti-MEM/2% FBS/1% P/S. Cells were lysed in Renilla lysis buffer 1-2 days post-infection (dpi). A Renilla luciferase assay (Promega, Madison, WI, cat no. E2820) was performed according to the manufacturer's instructions.

For experiments measuring RSV growth in ATM-deficient (GM16666) and ATM-corrected (GM16667) cell lines, cells were infected with rA2-Rluc at an MOI of 1 or 0.1. Cells were lysed 1-2 dpi and assayed for luciferase activity as described above. There were five replicates per condition.

For experiments examining the effect of ATM over-expression on RSV growth, 293T cells in 96-well plates were transfected according to manufacturer's instructions with 100 ng/well of pCaggs-ATM or empty vector using JetPRIME reagent. One day later, cells were infected in quadruplicate with rA2-Rluc at an MOI of 1. Cells were lysed 1, 2, and 3 dpi and assayed for luciferase activity as described above.

Digital microscopy of live cells

A549 cells were infected with RSVeGFP virus at an MOI of 0.1 or 1 in Opti-MEM/ 2% FBS/ 1% P/S. After one hour of adsorption, the infection media was removed and replaced with media containing inhibitor. Pictures were taken at different time points post-infection as indicated using an EVOS fluorescent microscope (Advanced Microscopy Group, Bothell, WA).

Cell viability assay

A549 cells in opaque wall, 96-well plates were treated with DMSO or increasing concentrations of ATM inhibitor diluted in 100 μl of Opti-MEM/ 2% FBS/1% P/S. One-day post treatment, media was removed and a CellTiter-Glo Luminescent viability assay (Promega, cat no. G7571) was performed on the cells. This assay measures ATP levels as an indication of metabolically-active cells. Briefly, 100 μl of CellTiter-Glo reagent were added to the cells, mixed in an orbital shaker for 2 minutes, and incubated at room temperature for 10 min before reading luminescence using a GloMax-96 luminometer (Promega).

Virus growth

To look at virus growth kinetics after inhibitor treatment, A549 or Hep-2 cells in 6-well plates were infected in triplicate with rA2 or RSVΔG at an MOI of 0.1 or 1 in Opti-MEM/2% FBS/1% P/S. After one-hour adsorption, infection media was removed and replaced with media containing DMSO or the inhibitors at the concentration indicated. Media was collected at different time points post-infection and titers determined by plaque assay.

To look at the effect of pretreatment of cells with ATM inhibitor on virus growth, A549 cells in 6-well plates were treated in triplicate with DMSO or ATM inhibitor in Opti-MEM/2% FBS/1% P/S for 1 hour at 37°C and 5% CO_2. Cells were washed 3 times with phosphate-buffered saline (PBS) before infecting at an MOI of 1. One day post-infection, media was collected and used for a plaque assay.

To look at cell-associated viral titers, cells were infected and media collected as described above. Cells were washed with PBS and scraped into Opti-MEM

supplemented with 2% FBS, 1% P/S, 100 mM HEPES, and 50 mM $MgSO_4$. Cells were frozen 3 times by incubating in dry-ice followed by thawing at 37°C. Cell debris was pelleted by centrifugation and supernatant was used for plaque assay.

Radio-immunoprecipitation

A549 cells in 6-cm plates were infected with rA2 at an MOI of 1 in Opti-MEM/2% FBS/1% P/S for 1 hour at 37°C and 5% CO_2. Infection media was removed and replaced with Opti-MEM/2% FBS/1% P/S. Thirty-six hours post-infection, the cells were starved for 30 min in methionine and cysteine-deficient DMEM or phosphate-deficient DMEM. Cells were labeled for 6-8 hours with ^{35}S-Met and ^{35}S-Cys in starvation media. Cells were lysed with 0.75 M NaCl RIPA buffer (20 mM Tris-HCl pH 7.4, 150 mM NaCl, 0.2% Triton-X100, 0.1% SDS, 5 mM iodoacetamide) containing a protease inhibitor cocktail. Lysate was passed through a QIAshredder column (QIAgen) and debris precipitated at 14,000 rpm for 30 min at 4°C. Proteins in the supernatant were immunoprecipitated with 10 μl of goat anti-RSV antibody (Maine Biotechnology) and Sepharose G beads for 3 hours at 4°C. Bead-bound proteins were washed three times with RIPA buffer containing 0.75 M NaCl, 0.3 M NaCl, or 0.15 M NaCl, respectively, and denatured with SDS protein loading buffer (2% SDS, 62.5 mM Tris-Cl pH 6.8, 2% DTT). Proteins were separated in 15% SDS-PAGE and visualized using a Typhoon 9700 Phosphorimager (GE Healthcare Life Sciences, Piscataway, NJ).

Virus release assay

A549 cells in 6-well plates were infected with rA2 at an MOI of 1 in triplicate. One-day post-infection, 500 μl of media was collected for a plaque assay. The rest of the media from each sample triplicate was combined, and cell debris pelleted by

centrifugation at 3,000 rpm for 5 min. Supernatants were incubated with 10% Polyethylene glycol-8000 for 90 min at 4°C with gentle rotation. The virus was then precipitated at 3,250 x g for 20 min. The resulting pellet and the cells in the plate were lysed in 500 μl of 2X SDS protein loading buffer. Proteins were separated in a 10% SDS-PAGE (Bio-Rad), transferred to a PVDF membrane, and immunoblotted with goat anti-RSV or mouse anti-P (D6 clone) and rabbit anti-actin. Proteins were visualized using an ECL Advance Western Blotting detection kit (GE Healthcare) and a Kodak Image Station 440 system.

Statistical analysis

Statistical analysis was performed using GraphPad Prism software version 5.04 for Windows (GraphPad Software, La Jolla, CA). An nnpaired, two-tailed t-test was used to compare Renilla luciferase activities in siRNA-treated cells infected with rA2-Rluc (Figure 1A). Multiple two-tailed t-tests followed by Holm-Sidak multiple comparison tests were used to compare growth curve data (Figures 2 and 7). Ordinary one-way ANOVA followed by Dunnett's multiple comparison test was used to analyze cell viability in Figure 1D and virus titers in Figure 4A. Ordinary one-way ANOVA and Sidak's multiple comparison tests were used to compare virus titers in Figure 5.

Results

Inhibition of ATM reduces RSV protein expression and titers

An siRNA screening of host kinases that were important for RSV replication led to identification of ATM as a potential inhibitory kinase for RSV replication (data not shown). To confirm these results, A549 cells were transfected with ATM siRNA and infected with rA2 48 hours later, when the siRNA's impact was its peak. There was no

difference in the viral protein expression one day post-infection. However, two days post-infection, the RSV protein expression was reduced to 70%, 72%, and 84% in the cells infected at an MOI of 0.1, 1, and 3, respectively (Fig. B.1A). We further confirmed these results with a commonly used ATM inhibitor, KU-55933, and RSV expressing GFP. A549 cells infected at an MOI of 1 were treated with ATM inhibitor after infection media was removed. Cells treated with ATM inhibitor at a 2.5 μM concentration showed no visible reduction of number of cells expressing GFP 1 day post-infection (dpi) and only minimal reduction 2 dpi. Cells treated with 7.5 μM of ATM inhibitor had a notable reduction of number of cells expressing GFP at 2 dpi (Fig. B.1B). When the cells were infected at an MOI of 0.1, both concentrations of the inhibitor showed a significant reduction in the number of cells expressing GFP by 3 dpi (Fig B.1C). The effect of the ATM inhibitor on cell viability was tested, and the maximum concentration used in this experiment (7.5 μM) had a 12% reduction in viable cells in the sample compared to the DMSO control (Fig. B.1D).

The effect of the ATM inhibitor on RSV titers was analyzed in Figure B2. In A549 cells infected at high MOI, the ATM inhibitor reduced RSV titers relative to DMSO by 1 dpi with a maximum 15-fold reduction at 2 dpi (Fig. B.2A). Similar results were seen in Hep-2 cells with a maximum 10-fold reduction seen at 3 dpi (Fig. B.2B). The ATM inhibitor also reduced viral titers in A549 and Hep-2 cells after low MOI infections (Fig. B.2C and B.2D). From these results, we concluded that inhibition of ATM by siRNA or small molecule inhibitor reduced RSV growth. Intriguingly, the impact of ATM inhibitor and siRNA was more pronounced in low MOI infection and at later time points after infection.

ATM is involved in a late step in RSV cycle

To investigate in which step of RSV life cycle ATM plays a role, the effects of ATM inhibitor on viral entry, viral protein synthesis, and virus release were examined. A549 cells were treated with ATM inhibitor for 1 hour prior to infection. The inhibitor was removed, and the cells were then infected at an MOI of 1. One-day post-infection media was collected to determine viral titers. Pretreatment of A549 cells with the ATM inhibitor did not reduce viral titers (Fig. B.3A), suggesting that ATM did not play a role in viral entry. To measure viral protein synthesis, A549 cells were infected at an MOI of 1. Eighteen hours post-infection, the cells were labeled with ^{35}S-Cys and ^{35}S-Met followed by immunoprecipitation with anti-RSV antibody. Treatment with the ATM inhibitor did not reduce protein synthesis (Fig. B.3B). These results suggest that the ATM inhibitor affects a step after viral entry and early protein expression.

To determine the role of ATM in virus release, A549 cells were infected with rA2 at an MOI of 1. One day later, media and cells were collected separately to measure virus titers and viral proteins. Viral titers in the media were reduced after ATM inhibitor treatment (Fig. B.4A). G protein in the media was also reduced after ATM inhibitor treatment (Fig. B.4C). In contrast, there was no reduction in the levels of viral proteins in the cell at this time point (Fig. B.4B). These results confirm that ATM plays a role in virus release. This result is consistent with the observation that there was no reduction of GFP-positive cells initially when cells were infected with low MOI of RSV-GFP (Fig. B.1B-B.1D).

ATM affects a step in virus egress

RSV can remain cell-associated after budding. To determine whether ATM reduces viral titers by increasing the amount of cell-associated virus, A549 and Hep-2 cells were infected at an MOI of 0.1 and media and cell-associated virus were collected at 3 dpi as described in the Materials and Methods. In A549 cells, there was a 6-fold reduction in virus in the media after ATM treatment, while there was a 10-fold reduction in cell-associated virus (Fig. B.5A). In Hep-2 cells, there was a 6-fold reduction in virus in the media and a 4-fold reduction in cell-associated virus after ATM inhibitor treatment (Fig. B.5B). These results suggest that the reduction in titers after ATM inhibitor treatment is not due to an increase in cell-associated virus.

Absence of ATM increased RSV protein expression

A study published by Fang et al. demonstrated that silencing ATM in A549 cells using shRNA increased RSV replication (15). Since these results contradicted the findings of our siRNA and ATM inhibitor studies, we examined RSV growth in ATM-deficient and ATM-corrected cell lines. The immortalized cell lines were derived from skin fibroblasts of a patient with ataxia telangiectasia. The ATM-corrected cell line expressed ATM from an episomal plasmid, while the ATM-deficient cell line carried an empty vector (16). The cells were infected with rA2-Rluc at an MOI of 1 or 0.1, and luciferase activity was measured in the cell supernatant and the cell lysate 1-2 days later. Luciferase activity was significantly higher in the cell lysates of ATM-deficient cells 1 and 2 dpi (Fig. B.6). These results showed that RSV protein expression increased in the absence of ATM.

Overexpression of ATM increased RSV protein expression

In light of the conflicting results in the different *in vitro* systems, we sought to examine the role of ATM overexpression in the RSV life cycle. 293T cells were transfected with pCaggs-ATM and then infected with rA2-Rluc one day later. Luciferase activity was measured in the cell lysates 1-3 dpi and normalized to cell viability measurements. ATM overexpression resulted in increased rA2-Rluc activity 2 and 3 dpi (Fig. B.7). These results indicated that increasing ATM expression increased RSV protein expression at later time points.

Discussion

ATM is a serine/threonine kinase that plays important roles in many cellular processes such DNA repair and cell cycle regulation. It plays a critical role in the DNA repair pathway by sensing DNA damage. Previously, it has been shown that ATM is important for replication of many DNA viruses such as HPV (17, 18). ATM primarily localizes in the nucleus, but some ATM localizes in the cytoplasm to serve as a key regulator of cellular responses to stress such as chemical agents (19, 20). ATM can regulate activities of mTOR and PI3K-AKT pathways (21, 22).

It has been previously reported that ATM negatively regulates RSV growth *in vitro*. Fang et al. proposed a model in which RSV-induced oxidative stress triggers the DNA-damage response through ATM, resulting in the production of type I and type III IFNs and suppression of viral replication (15). Our results suggest that the role of ATM in the RSV life cycle may be more complex and highly system-dependent.

Inhibition of ATM via siRNA knockdown or with a small molecule inhibitor decreased RSV growth, suggesting that ATM plays a positive role in RSV replication

(Figure 1 and 2). ATM inhibitor did not affect the entry of RSV (Figure 3A) and did not affect viral gene expression (Figure 3B and Figure 4). It also did not reduce the number of RSV- infected cells at an early time point (Figure 1). At late time points of low MOI infection, when secondary infection occurred, ATM inhibitor did have an effect on viral gene expression (Figure 1) with a reduced amount of RSV released in the presence of ATM inhibitor. Overexpression of ATM in 293T cells increased RSV protein expression at late time points (Figure 7). This suggests that ATM plays a positive role in late-stage RSV growth, contrary to a previously published report.

In ATM-deficient cell lines, RSV protein expression was significantly increased 1 and 2 dpi (Figure 6). These results were consistent with the findings of Fang et al. in ATM-silenced cells and suggest that ATM is plays a negative role in RSV growth. Taken together, these findings suggest that the role of ATM in the RSV life cycle is unclear and dependent on the system used to examine the ATM-RSV interaction.

The discrepancies in the findings may be due to the inherent differences between the two systems. The ATM-silenced cells have undergone multiple rounds of selection and have little-to-no ATM expression. These cells likely adapted to having no ATM and may have developed compensatory mutations. Studies using siRNA, small-molecule inhibitors, or transient overexpression reflect the impact of acute ATM perturbation on RSV growth. Further investigation is required to clarify the role of ATM in the RSV life cycle.

Acknowledgements

We would like to thank Dr. Marty Moore for the RSV plasmids. We thank Peter Collins for recombinant RSVs. We also appreciate the helpful discussion and technical

assistance from all members of Biao He's laboratory. The work was supported by R01AI081977 from NIH.

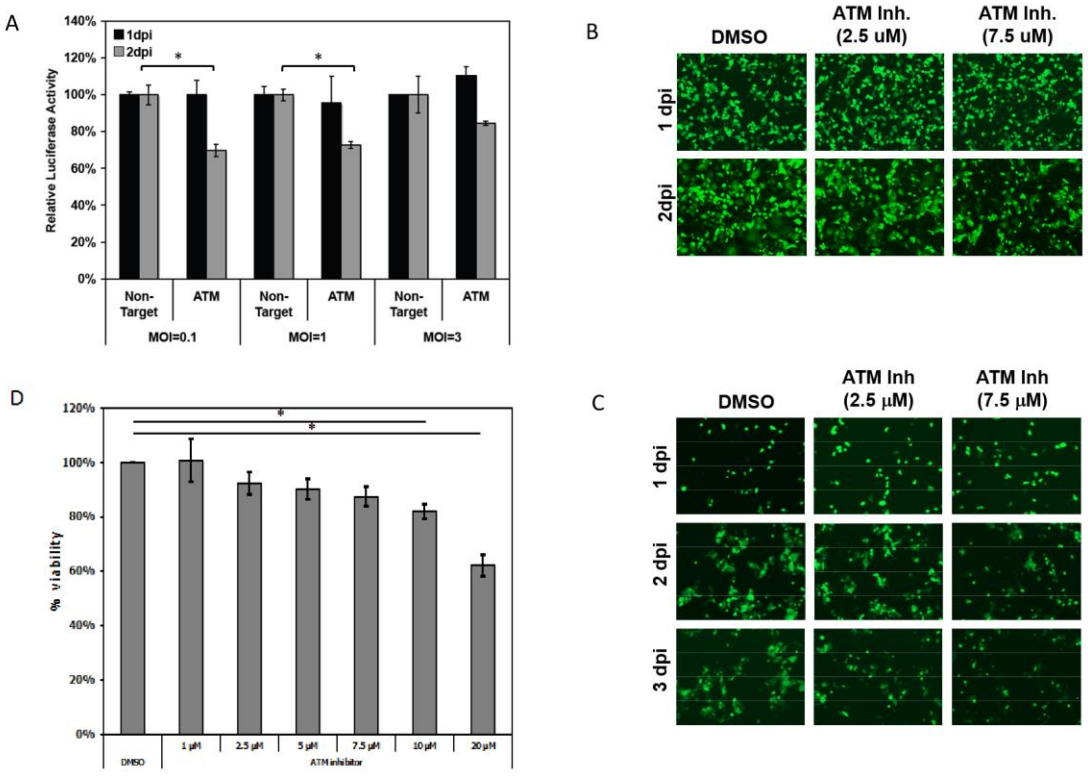

Figure B1. ATM plays a role in the RSV life cycle. (A) A549 cells in 96 well plates were transfected with 200 nM Non-target or ATM siRNA per well as described in Materials and Methods. Two days post-transfection, the cells were infected with rA2-Rluc at an MOI of 0.1, 1, or 3. One or two days post-infection, the cells were lysed with Renilla lysis buffer, and a luciferase assay was performed. (B-C) A549 cells were infected with RSVeGFP at an MOI of 1 (B) or 0.1 (C) and treated with DMSO or ATM inhibitor (2.5 μM or 7.5 μM) after infection as described in Materials and Methods. Pictures were taken at 1 and 2 dpi using an EVOS fluorescent microscope. (D) A549 cells in 96-well plates were treated with DMSO or increasing concentrations of the ATM inhibitor. Toxicity was measured 24 hours later using the CellTiter-Glo system from Promega. Results are presented as the average of three independent experiments. Error bars

represent the SEM. (A) Statistical significance was determined using unpaired, two-tailed t-test. (D) Statistical significance was determined by one-way ANOVA followed by Dunnett's multiple comparison test. *, $P< 0.05$

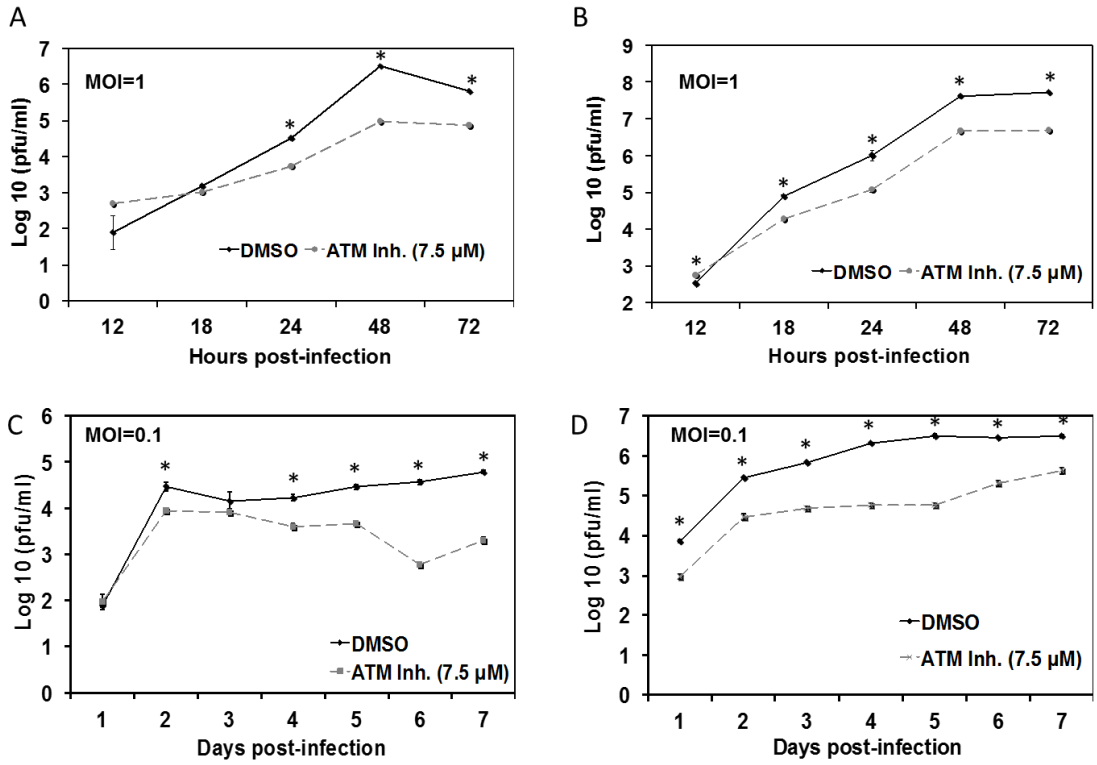

Figure B2. ATM inhibitor reduces RSV titers. A549 (A, C) or Hep-2 cells (B, D) were infected at an MOI of 1 (A, B) or 0.1 (C, D). Infection media was removed after 1 hour and replaced with media containing DMSO or ATM inhibitor (7.5 μM). Media samples were collected at the time-points indicated and titers determined with a plaque assay. Error bars represent the SEM. Statistical significance was determined using multiple t-tests followed by Holm-Sidak multiple comparison tests. *, $P< 0.05$

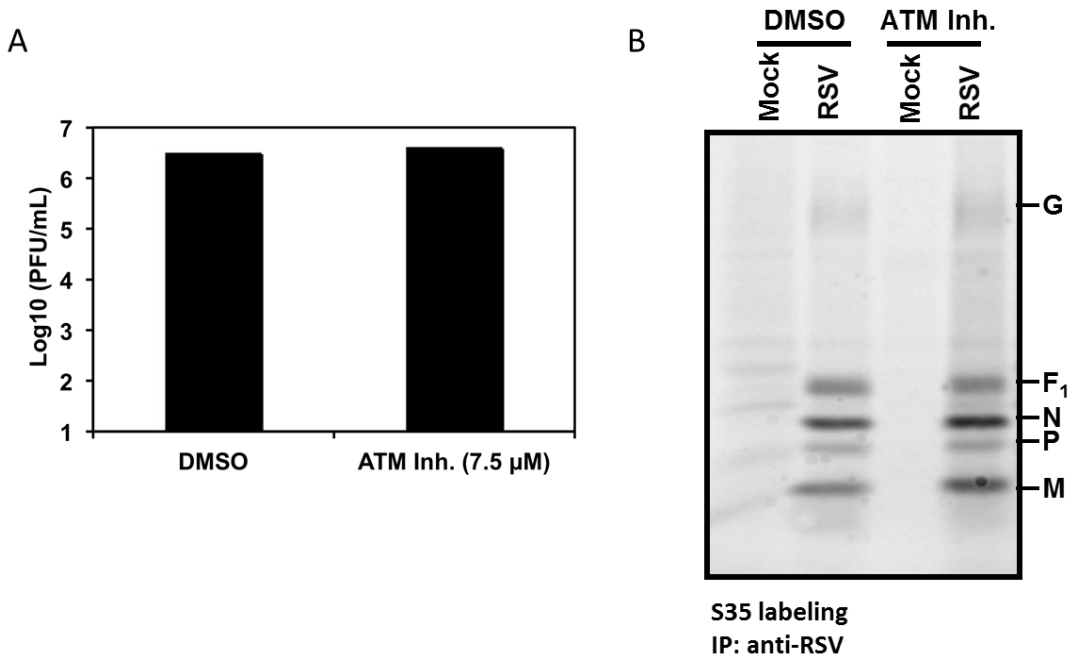

Figure B3. ATM does not inhibit RSV entry or protein expression. (A) A549 cells in 6-well plates were pretreated with media containing ATM inhibitor (7.5 µM) for 1 hour at 37°C, 5% CO2. Media containing inhibitor was removed, and cells were washed 3 times with PBS before replacing with 2% FBS/P/S/ Opti-MEM. One-day post-infection, media was collected and titers determined with a plaque assay. (B) A549 cells in 6-cm plates were infected with rA2 at an MOI of 1. One-day post-infection, the cells were starved for 30 min in media deficient in Met and Cys and labeled for 6 hours with S35-labeled Met and Cys. Cells were lysed with RIPA buffer and proteins immunoprecipitated with goat-anti-RSV antibody. Proteins were separated in 15% SDS-PAGE. Proteins were visualized using a Typhoon Scanner.

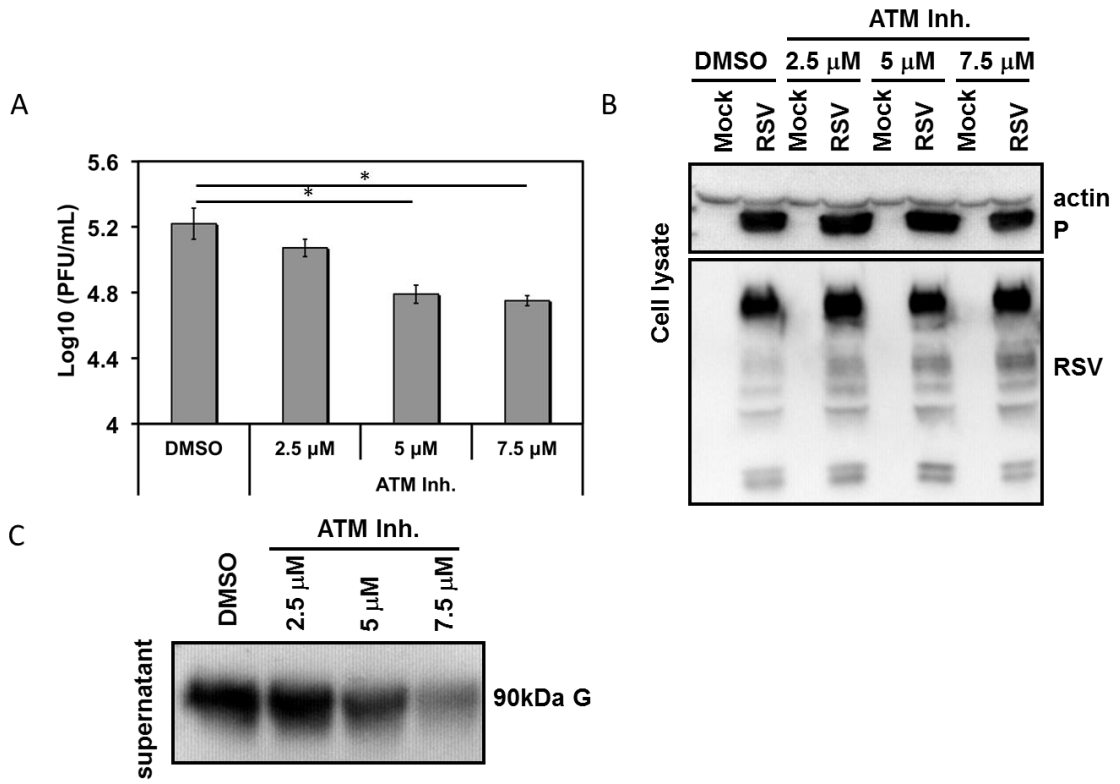

Figure B4. ATM inhibitor reduces RSV particles in media. A549 cells in 6-well plates were infected with RSV at an MOI of 1 in 2% FBS/P/S/Opti-MEM. Infection media was removed, cells were washed with PBS and then replaced with media containing DMSO or ATM inhibitor (7.5 μM). (A) One-day post-infection, 500 μl of the media was collected for plaque assay. Error bars represent the SEM. (B) The rest of the media were combined and cell debris removed by centrifugation at 3,000 rpm for 5 min. Supernatants were incubated with 10% PEG-8000 for 90 min at 4°C with gentle rotation. The virus was then precipitated with at 3250 X g for 20 min. Pellet was lysed with 500 μl of SDS protein loading buffer containing DTT and boiled for 5 min at 95°C. Proteins were separated in a 10% SDS-PAGE, transferred to a PVDF membrane, and visualized by immunoblotting with goat anti-RSV antibody. (C) Cells in the plate were lysed with 500 μl of SDS protein loading buffer containing DTT and boiled for 5 min at 95°C.

Proteins were separated in a 10% SDS-PAGE, transferred to a PVDF membrane, and visualized by immunoblotting with goat anti-RSV, mouse anti-P (D6) or rabbit anti-actin antibodies. Statistical significance was determined by one-way ANOVA followed by Dunnett's multiple comparison test. *, $P< 0.05$

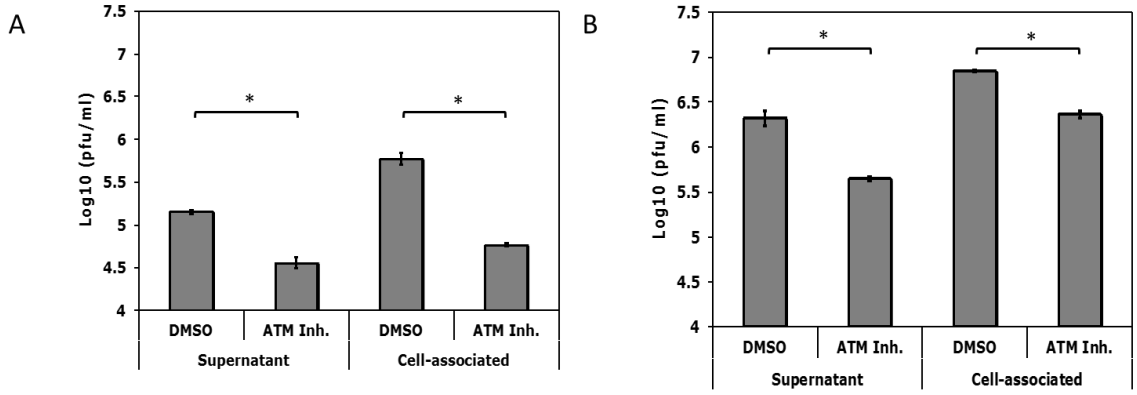

Figure B5. ATM inhibitor affects virus assembly and release. (A) A549 or (B) Hep-2 cells in 6 well plates were infected with rA2 at an MOI of 0.1. Media was collected at 3 dpi and used for plaque assay. Cells were washed with PBS and scraped off the plate into Opti-MEM containing 2% FBS, 1% P/S, 100 mM HEPES, 50 mM MgSO4. Cells were frozen/thawed 3 times, cell debris was pelleted, and supernatant used for plaque assay. Statistical significance was determined by one-way ANOVA followed by Sidak's multiple comparison test. *, $P< 0.05$

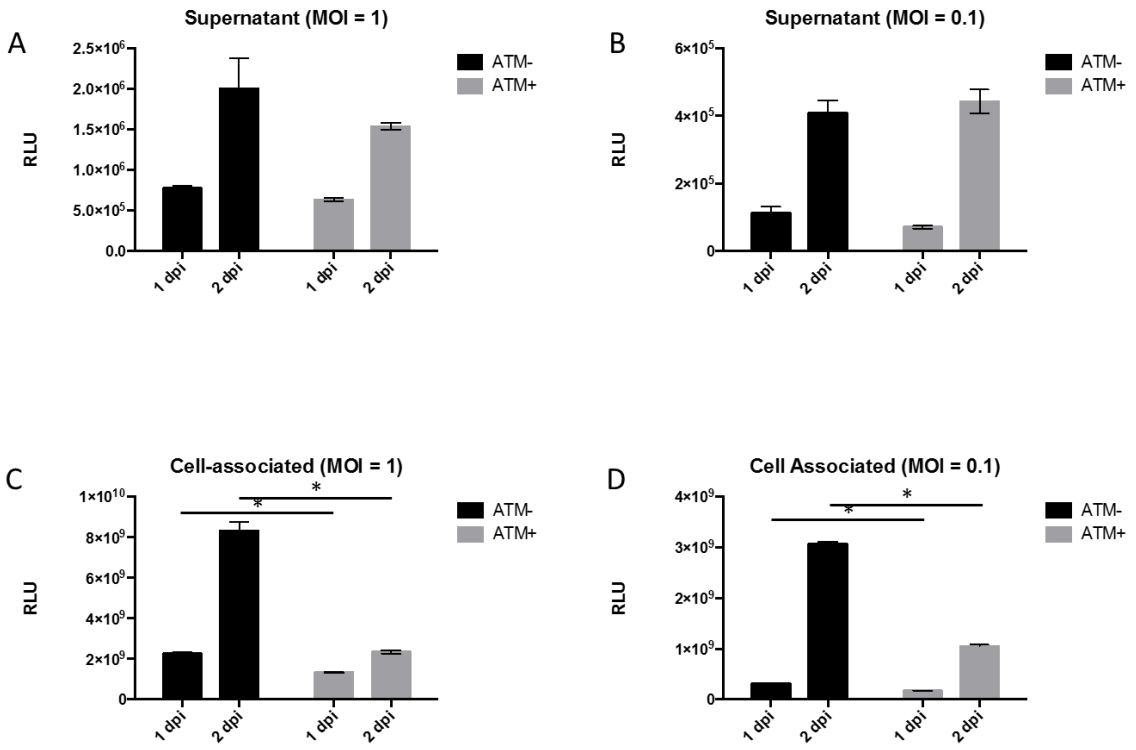

Figure B6. Absence of ATM increased RSV protein expression. ATM-deficient (GM16666) and ATM-corrected (GM16667) skin fibroblast cells in 96-well plates were infected with RA2-Rluc at an MOI of 1 or 0.1. Cells were lysed 1 and 2 dpi, and luciferase activity was measured in both the (A, B) cell supernatant or the cell lysate (C, D). Five replicates were assayed for each condition. Graphs represent the mean Renilla luciferase activity. Error bars represent the SEM. Statistical significance was determined by unpaired, 2-tailed *t*-test, $*P < 0.05$.

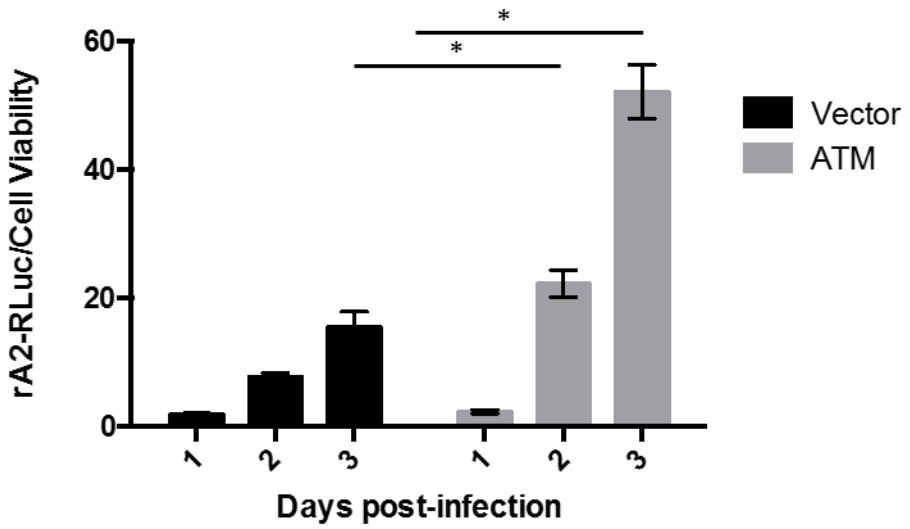

Figure B7. Overexpression of ATM increased RSV protein expression. 293T cells in 96-well plates were transfected with pCaggs or pCaggs-ATM. One day later, the cells were infected with RA2-Rluc at an MOI of 1. Cells were lysed and luciferase activity was measured 1, 2, and 3 dpi. Samples were assayed in quadruplicate. Graphs represent the mean Renilla luciferase activity normalized to cell viability. Error bars represent the SEM. Statistical significance was determined by unpaired, 2-tailed *t*-test, $*P < 0.05$.

References

1. **Fields BN**, **Knipe DM**, **Howley PM**. 2015. Fields virology. Wolters Kluwer Health/Lippincott Williams & Wilkins, Philadelphia.

2. **Fleming EH**, **Kolokoltsov AA**, **Davey RA**, **Nichols JE**, **Roberts NJ**. 2006. Respiratory syncytial virus F envelope protein associates with lipid rafts without a requirement for other virus proteins. J Virol **80**:12160–70.

3. **Brown G**, **Rixon HWM**, **Sugrue RJ**. 2002. Respiratory syncytial virus assembly occurs in GM1-rich regions of the host-cell membrane and alters the cellular distribution of tyrosine phosphorylated caveolin-1. J Gen Virol **83**:1841–50.

4. **Brown G**, **Jeffree CE**, **McDonald T**, **Rixon HWM**, **Aitken JD**, **Sugrue RJ**. 2004. Analysis of the interaction between respiratory syncytial virus and lipid-rafts in Hep2 cells during infection. Virology **327**:175–85.

5. **Teng MN**, **Collins PL**. 1998. Identification of the respiratory syncytial virus proteins required for formation and passage of helper-dependent infectious particles. J Virol **72**:5707–16.

6. **Teng MN**, **Whitehead SS**, **Collins PL**. 2001. Contribution of the respiratory syncytial virus G glycoprotein and its secreted and membrane-bound forms to virus replication in vitro and in vivo. Virology **289**:283–96.

7. **Techaarpornkul S**, **Barretto N**, **Peeples ME**. 2001. Functional analysis of recombinant respiratory syncytial virus deletion mutants lacking the small hydrophobic and/or attachment glycoprotein gene. J Virol **75**:6825–34.

8. **Techaarpornkul S**, **Collins PL**, **Peeples ME**. 2002. Respiratory syncytial virus with the fusion protein as its only viral glycoprotein is less dependent on cellular glycosaminoglycans for attachment than complete virus. Virology **294**:296–304.

9. **Lambert DM**, **Hambor J**, **Diebold M**, **Galinski B**. 1988. Kinetics of synthesis and phosphorylation of respiratory syncytial virus polypeptides. J Gen Virol **69 (Pt 2)**:313–23.

10. **Collins PL**, **Hill MG**, **Cristina J**, **Grosfeld H**. 1996. Transcription elongation factor of respiratory syncytial virus, a nonsegmented negative-strand RNA virus. Proc Natl Acad Sci **93**:81–85.

11. **Cuesta I**, **Geng X**, **Asenjo A**, **Villanueva N**. 2000. Structural phosphoprotein M2-1 of the human respiratory syncytial virus is an RNA binding protein. J Virol **74**:9858–67.

12. **Bajorek M**, **Caly L**, **Tran KC**, **Maertens GN**, **Tripp RA**, **Bacharach E**, **Teng MN**, **Ghildyal R**, **Jans DA**. 2014. The Thr205 phosphorylation site within respiratory syncytial virus matrix (M) protein modulates M oligomerization and virus production. J Virol **88**:6380–93.

13. **Sun M**, **Fuentes SM**, **Timani K**, **Sun D**, **Murphy C**, **Lin Y**, **August A**, **Teng MN**, **He B**. 2008. Akt plays a critical role in replication of nonsegmented negative-stranded RNA viruses. J Virol **82**:105–14.

14. **Niwa H**, **Yamamura K**, **Miyazaki J**. 1991. Efficient selection for high-expression transfectants with a novel eukaryotic vector. Gene **108**:193–9.

15. **Fang L**, **Choudhary S**, **Tian B**, **Boldogh I**, **Yang C**, **Ivanciuc T**, **Ma Y**, **Garofalo RP**, **Brasier AR**. 2015. Ataxia telangiectasia mutated kinase mediates NF-κB serine 276 phosphorylation and interferon expression via the IRF7-RIG-I amplification loop in paramyxovirus infection. J Virol **89**:2628–42.

16. **Ziv Y**, **Bar-Shira A**, **Pecker I**, **Russell P**, **Jorgensen TJ**, **Tsarfati I**, **Shiloh Y**. 1997. Recombinant ATM protein complements the cellular A-T phenotype. Oncogene **15**:159–67.

17. **Moody CA**, **Laimins LA**. 2009. Human papillomaviruses activate the ATM DNA damage pathway for viral genome amplification upon differentiation. PLoS Pathog **5**:e1000605.

18. **Gillespie KA**, **Mehta KP**, **Laimins LA**, **Moody CA**. 2012. Human papillomaviruses recruit cellular DNA repair and homologous recombination factors to viral replication centers. J Virol **86**:9520–6.

19. **Sun Y**, **Connors KE**, **Yang D-Q**. 2007. AICAR induces phosphorylation of AMPK in an ATM-dependent, LKB1-independent manner. Mol Cell Biochem **306**:239–45.

20. **Armata HL**, **Golebiowski D**, **Jung DY**, **Ko HJ**, **Kim JK**, **Sluss HK**. 2010. Requirement of the ATM/p53 tumor suppressor pathway for glucose homeostasis. Mol Cell Biol **30**:5787–94.

21. **Alexander A**, **Kim J**, **Walker CL**. 2010. ATM engages the TSC2/mTORC1 signaling node to regulate autophagy. Autophagy **6**:672–3.

22. **Alexander A**, **Cai S-L**, **Kim J**, **Nanez A**, **Sahin M**, **MacLean KH**, **Inoki K**, **Guan K-L**, **Shen J**, **Person MD**, **Kusewitt D**, **Mills GB**, **Kastan MB**, **Walker CL**. 2010. ATM signals to TSC2 in the cytoplasm to regulate mTORC1 in response to ROS. Proc Natl Acad Sci U S A **107**:4153–8.